SCREENING FOR NEW CIRCADIAN CLOCK COMPONENTS IN *DROSOPHILA*

Thesis submitted for the degree of

Doctor of Philosophy

at the University of Leicester

by

Renata Van Der Maas de Azevedo

Department of Genetics

University of Leicester

September 2010

Screening for New Circadian Clock Components in *Drosophila*

Renata Van Der Maas de Azevedo

Abstract

The endogenous circadian clock adjusts the physiology and behaviour of an organism to advantageous periods of the day, and represents an adaptation to daily environmental cycles, such as light and temperature. Locomotor activity in *Drosophila melanogaster* represents a robust behavioural rhythm used to study the clock. This clock is located in the lateral and dorsal neurons of the fly and in the suprachiasmatic nuclei (SCN) of the hypothalamus in the mammal. The molecular bases of underlying circadian timing mechanisms in insects and mammals are conserved. Although we have a basic knowledge of the *Drosophila* molecular clock circuits functioning, many questions regarding the nature of the protein complexes that subserve circadian pacemakers, the connections between the oscillator and the overt rhythms and the entrainment signals to the clock remain unanswered.

To identify new *D. melanogaster* circadian components I used three different approaches. The first is based on immunoprecipitation of protein complexes using tagged CYC, a dedicated clock protein, to pull down its partners. The second employs a comparative approach with the mammalian circadian SCN proteome and the third uses a tap-tagging design which is used to screen the proteome. Expression studies of candidate proteins, and behavioural analyses using mutants and transgenes to disrupt and silence some of these factors, have revealed a number of candidate genes that may affect aspects of clock function. Two novel genes involved in glutamate metabolism are particularly compelling, and appear to contribute to the circadian mechanism by mediating the neurons that are important for light input. A further synaptic gene may be involved in setting the clock pacemaker.

I DEDICATE THIS THESIS TO MY HUSBAND, JOAO GESTO, WHO HAS GIVEN ME A LOT OF LOVE AND SUPPORT DURING MY PHD. ONE LIFE IS NOT ENOUGH TIME TO LOVE HIM…

Acknowledgements

I am heartily thankful to my supervisor, Prof. Bambos Kyriacou, whose encouragement, guidance and support from the initial to the final level enabled me to develop and conclude my PhD project and dissertation. It is very good to have a genius supervisor who is always available. I would like to thank the project collaborators Michael Hastings at the MRC Laboratory of Molecular Biology, and Kathryn Lilley at Dept. of Biochemistry, Cambridge Centre for Proteomics, both in Cambridge. My sincere thanks also go to my thesis committee members, Dr. Ezio Rosato and Dr. Andrew Bottrill, for their encouragement and insightful comments. I am very thankful to Alexandre Peixoto, who has encouraged me to start this adventure and for all his support and friendship. Also for leaving his lab door always open for me.

I would like to show my gratitude to my colleagues who have contributed immensely to my personal and professional time in Leicester. I am especially thankful to Karen Smith, who has helped me a lot during these 4 years. She is the sweetest person in UK. I am very grateful to the best friends I have made in Leicester, Mobina Khericha, Monserrath Felix and Supryia Bhutani. They had made my life pleasant during these years and we shared lots of good moments. I am sure we are friends for life. Also, I would like to thank my old friends back home who have supported me emotionally through my time here.

I will be forever grateful to my family, the Azevedo's and the Gesto's, for all the love and support they have given me. Although it was very difficult to be physically far from them, I always felt their presence and love. I want to specially thank my parents who inspired, encouraged and fully supported me morally throughout my life. I have no words to thank the love of my life, Joao Gesto. He is indispensable in every step I take, and during the PhD it was not any different.

Finally, and most importantly of all, I would like to acknowledge Programa Alban and EUCLOCK for providing me with financial support, without which this adventure would not have been possible.

List of Tables

List of Figures

List of Contents

Chapter 1: Introduction

1.1 Basic Attributes of Circadian Clocks

The word 'circadian' derives from the Latin words *circa* (about) and *dian* (day). Given that we live in a cyclic environment created by the rotation of the Earth, it is not surprising that daily rhythms in physiology, metabolism and behaviour are found in a diverse array of organisms including animals, plants, fungi, and even some prokaryotes. These rhythms are driven by self-sustaining endogenous circadian clocks, as they persist in the absence of environmental time cues (Pittendrigh, 1967). As shown in figure 1.1, circadian clocks can be dissected into three components: input pathways, the clock itself and output pathways.

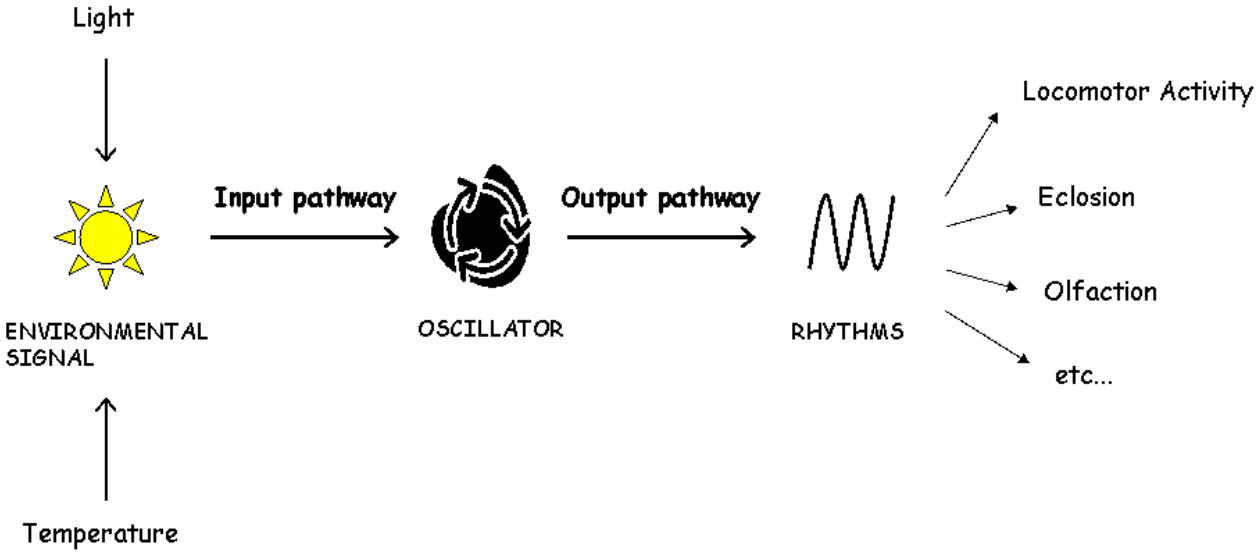

Figure 1.1 - Basic mechanism of the circadian clock. It involves input pathways (light and temperature), a central driving oscillator comprising of the core clock genes and output pathways (behavioural rhythms).

Clocks can be synchronized or entrained by environmental stimuli or *zeitgebers* (time givers), most notably the daily changes in light intensity and temperature. The

abundance of many core circadian gene products oscillates with a period of about 24 hours, controlling a number of rhythmic outputs in *Drosophila* (Williams and Sehgal, 2001; Taghert and Shafer, 2006).

The periods of circadian rhythms are temperature compensated, showing little variation when the organism is submitted to different temperatures. This mechanism is very important given that organisms must be synchronized to the environment despite daily and seasonal variations of temperature (Pittendrigh, 1954).

1.2 Clock Outputs

An elementary question in circadian biology is how circadian oscillators regulate rhythms in behaviour, physiology and metabolism. In *Drosophila*, the circadian clock is manifested as a number of rhythmic phenotypes, including eclosion (the emergence of the adult from the pupal case), locomotor activity (Konopka and Benzer, 1971), olfactory physiology (Krishnan *et al*., 1999) and egg-laying rhythms (Allemand and David, 1984). However, rhythms in locomotor activity have been the most extensively characterized output in flies.

Five independent microarray studies have been used as an efficient method to identify transcripts that cycle in abundance in *Drosophila* heads (Ceriani *et al*., 2002; Claridge-Chang *et al*., 2001; Lin *et al*., 2002; McDonald and Rosbash, 2001; Ueda *et al*., 2002b). These genes are believed to be under clock control, since their rhythmic expression is abolished in arrhythmic Clk^{JRK} flies. A number of mutants have been identified that specifically abrogate a single rhythmic output, suggesting that a number of distinct output signalling pathways are employed. For example, the *Drosophila lark* eclosion-rhythm mutant, isolated from a behavioural screen, exclusively affects one pacemaker output pathway (Newby and Jackson, 1993).

Heterozygous *lark* mutant flies eclose early in an LD cycle, but do not alter the circadian control of locomotor activity (McNeil *et al*., 1998; Huang *et al*., 2007). LARK, predicted to be an RNA binding protein, exhibits oscillation during 24 hours and is highly expressed during the day, when the eclosion behaviour is suppressed. Moreover, *lark* mutants are lethal when homozygous, suggesting that it plays a vital role in development (Newby and Jackson, 1993).

An additional example of a *Drosophila* mutation that influences a specific circadian output is $ebony^{01}$. The *ebony* RNA was shown to exhibit robust circadian cycling in two independent studies (Claridge-Chang *et al*., 2001; Ueda *et al*., 2002b). These results suggest that ebony protein functions in a clock output pathway. The mutation on this downstream clock gene, seems to have no apparent impact on the circadian rhythm of adult eclosion, but affects locomotor activity rhythms (Newby and Jackson, 1991).

Another output gene, *takeout*, affects the circadian control of feeding metabolism along with locomotor activity (Sarov-Blat *et al*., 2000). An important and extensively studied output gene in *Drosophila* is the neuromodulator, pigment dispersing factor, *pdf* (Renn *et al*., 1999). A *pdf* mutant that does not express this peptide has a high frequency of arrhythmic locomotor activity but normal cycling of the core clock gene *period* in individual clock neurons in the brain (described in section 1.4).

1.3 *Drosophila* Central Oscillator

The central oscillator of *Drosophila melanogaster* has been very well characterised over the past couple of decades (Rosato *et al*., 2006). It is composed of at least two intracellular feedback loops in gene expression (see figure 1.2): a *Per/Tim* loop and a *Clk* loop.

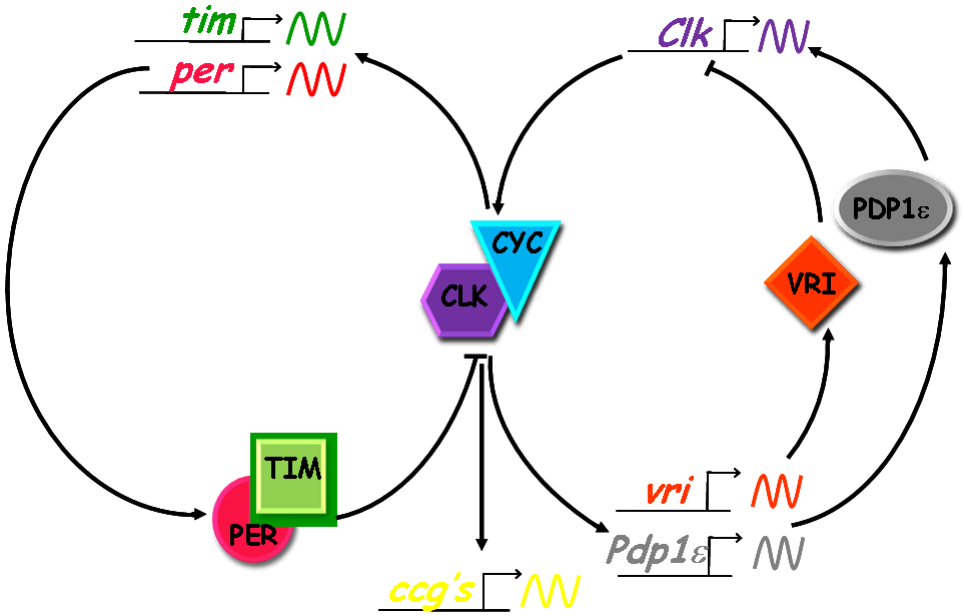

Figure 1.2 - Model of the two interlocked feedback loops. *tim*: *timeless*. ***per*:** *period*. ***Clk*:** *clock*. **CYC:** cycle. ***vri*:** *vrille*. ***Pdp1ε*:** *Par domain protein-1ϵ*. **ccg's:** clock controlled genes. The CLK/CYC transcriptional activation complex interconnects two feedback loops on gene expression and mediates downstream output processes by promoting the expression of clock controlled genes.

1.3.1 The PER-TIM Feedback Loop

In 1971 the first clock gene, called *period* (*per*), was identified by Konopka and Benzer after the isolation of three EMS mutagenized *Drosophila* lines. All these mutations were mapped to the same locus on the X-chromosome and led to aberrant eclosion and locomotor activity. Mutants for this gene have either a 19 h rhythm (per^S) or a 29 h rhythm (per^L) or they are completely arrhythmic (per^{01}) in constant darkness (figure 1.3).

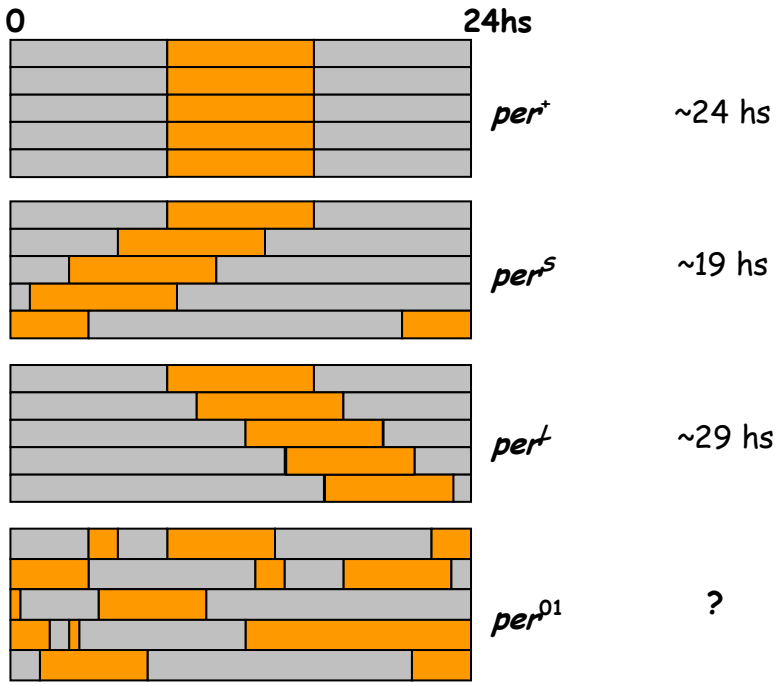

Figure 1.3 - Representation of the locomotor activity pattern of *Drosophila per* mutants in constant darkness. *per*$^{+}$: wild-type flies with period of activity of about 24 hours. *per*^{S}: short period mutants with 19 hours rhythm. *per*^{L}: long period mutants with 29 hours rhythm. *per*^{01}: arrhythmic mutants. The horizontal bars represent 5 consecutive days. The rest phase is represented in gray and the activity phase in orange.

The *per*^{S} allele is a missense mutation that results in a serine-to-asparagine change in the region of the PER protein that interacts with a kinase called Doubletime (DBT) (Rothenfluh *et al*., 2000a; Yu *et al*., 1987). The long period allele *per*^{L} is also a single nucleotide substitution in the third exon of *per* causing a valine-to-aspartic acid amino acid substitution (Baylies *et al*., 1987; Colot *et al*., 1988; Yu *et al*., 1987). Finally, the arrythmicity in *per*^{01} mutants is explained by the presence of a nonsense mutation at codon 464 that changes a glutamine into a stop codon (Yu *et al*., 1987).

After 1984 when the *period* gene was cloned (Bargiello *et al*., 1984; Reddy *et al*., 1984), it was shown that both *period* mRNA and the protein (PER) cycle with a

period of about 24 hours in fly heads. Interestingly, the peak of the protein occurs few hours later than the transcript suggesting that PER is negatively regulating its own transcription (Hardin *et al.*, 1990) (figure 1.4).

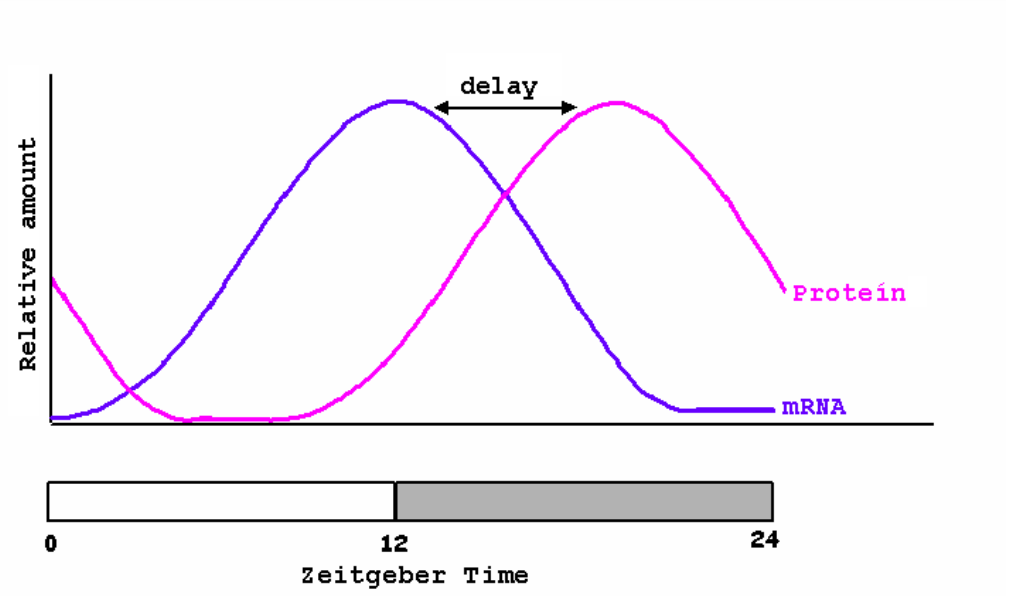

Figure 1.4 – The PER/*per* cycle. Relative levels of *per* and *tim* mRNA and of the proteins encoded by these genes, PER and TIM respectively, during 24 hours**.** White bar represents the day and gray bar represents the night. (Figure modified from Dunlap, 1999).

In 1994 a second mutation called *timeless* (*tim)* was isolated (Sehgal *et al.*, 1994). The cloning and characterization of this gene revealed that *tim* and *per* mRNA cycle in phase with each other (Myers *et al.*, 1995; Sehgal *et al.*, 1994). It was found that the proteins PER and TIM, interact in the cytoplasm to form a heterodimer (Gekakis *et al.*, 1995) via their PAS domains (Huang *et al.*, 1993) and are translocated back into the nucleus late at night (Curtin *et al.*, 1995; Siwicki *et al.*, 1988; Zeng *et al.*, 1996). The translocation of the PER-TIM heterodimer has recently been questioned by fluorescence resonance energy transfer (FRET) studies which indicate that the proteins dissociate before their movement to the nucleus (Meyer *et al.*, 2006).

The elucidation of the feedback mechanism became possible with the identification of two other clock genes: *Clock* (*Clk*) and *cycle* (*cyc*), two basic-helix-loop-helix/PAS domain transcription factors (Allada *et al*., 1998; Darlington *et al*., 1998; Rutila *et al*., 1998). The PAS domain (P=PERIOD, A=ARNT, S=SINGLE-MINDED) is known to be involved in protein-protein interactions and the basic Helix-Loop-Helix (bHLH) domain responsible for DNA binding.

To initiate the negative feedback loop, CLK-CYC heterodimers bind to regulatory elements called E-boxes (conserved *CACGTG* sequences), activating the transcription of *per* and *tim* (Kyriacou and Rosato, 2000). Cytoplasmic PER is phosphorylated by the mammalian casein kinase 1ϵ homolog DOUBLE-TIME (DBT) (Price *et al*., 1998), and then targeted by F-Box/WD40 protein Slimb (SLIMB) for degradation in the proteasome (Grima *et al*., 2002; Ko *et al*., 2002). This degradation would explain the accumulation phase difference between *period* mRNA and its encoded product (Price *et al*., 1998). On the other hand, PER is stabilized by the protein phosphatase 2A (PP2A), which removes phosphates that were added to PER, and by the formation of PER-TIM dimer. However, the nuclear localization of PER-TIM heterodimers depends on the phosphorylation of TIM by Shaggy (SGG), the *Drosophila* homologue of the vertebrate *Glycogen synthetase kinase* (*Gsk3β*), and PER by casein kinase 2 (CK2) (Akten *et al*., 2003; Lin *et al*., 2002; Martinek *et al*., 2001; Sathyanarayanan *et al*., 2004).

Finally, PER-TIM complexes bind to CLK-CYC removing them from the E-box and inhibiting *per* and *tim* transcription during the late evening and early morning (Chang and Reppert, 2003; Darlington *et al*., 1998; Lee *et al*., 1999), representing the typical negative feedback loop responsible for the determination of the circadian rhythms in flies (figure 1.5). Recent studies suggest that PER-TIM complexes

dissociate before their movement to the nucleus, but can re-associate once PER and TIM translocate into the nucleus (Shafer *et al*., 2002; Meyer *et al*., 2006). It is believed that PER alone can inhibit the functioning of the CLK-CYC activity (Rothenfluh *et al*., 2000b), although the repression is more efficient when TIM is present. In contrast, TIM alone is not capable to act as an efficient repressor (Ashmore *et al*., 2003; Chang and Reppert, 2003).

DBT continues to phosphorylate CLK and PER, promoting their degradation during early morning. TIM is also found to be degraded in the presence of light promoted by the blue light photoreceptor cryptochrome (CRY) (Hunter-Ensor *et al*., 1996; Lee *et al*., 1996; Myers *et al*., 1996), mediated by the F box protein Jetlag (JET) (Koh *et al*., 2006), which serves to entrain the circadian oscillator to environmental light-dark cycles.

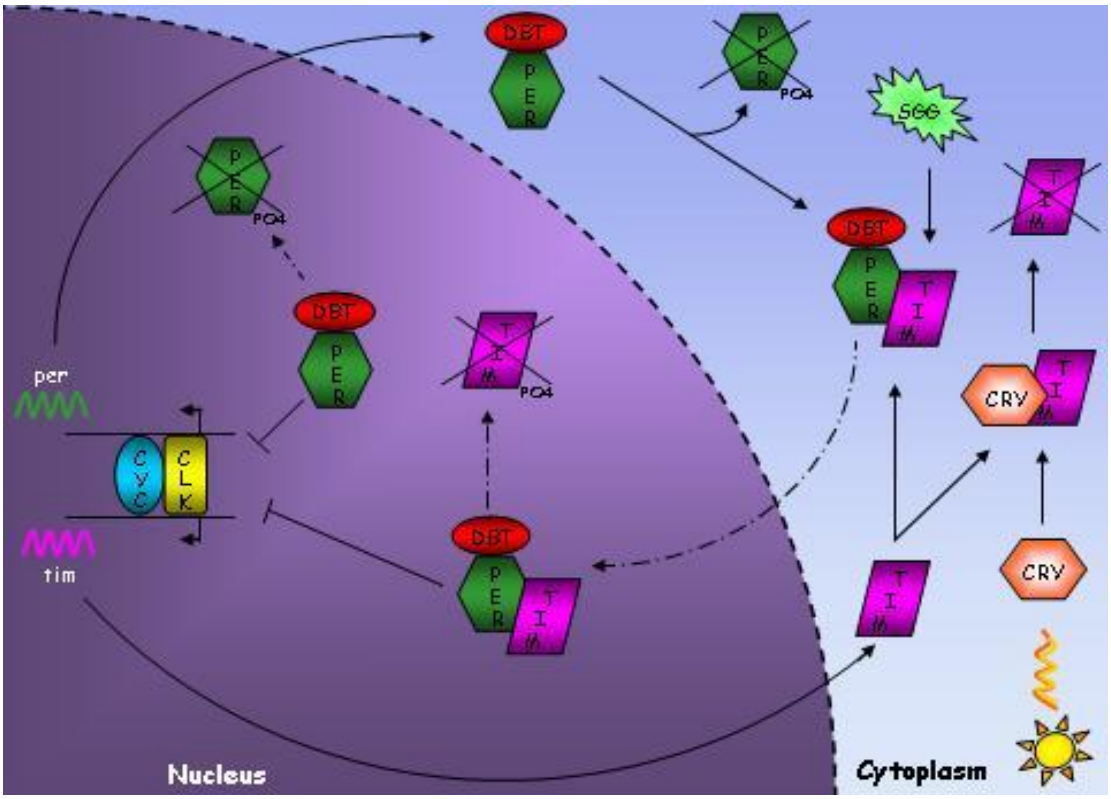

Figure 1.5 - Model of the *Drosophila melanogaster* PER-TIM feedback loop. CLK and CYC form a heterodimer that binds to E-box elements of *per* and *tim* and

activates their transcription during the day and early evening. PER and TIM proteins accumulate, form a PER–TIM complex, and translocate into the nucleus to repress their own transcription during the late night. The delay in PER accumulation is due to phosphorylation induced by DBT. Light induced TIM degradation is mediated by the blue light photoreceptor CRY.

1.3.2 The CLK Feedback Loop

The abundance of *Clk* cycles indicating that its transcription is also rhythmically regulated (Glossop *et al.*, 1999). However, this robust mRNA cycling does not result in cycling CLK protein. The levels of CLK protein remain constant during the day (Houl *et al.*, 2006; Yu *et al.*, 2006), probably because its turnover and the *Clk* mRNA cycling are happening in anti-phase (Zheng and Sehgal, 2008). Indeed, the regulation of CLK in a circadian manner occurs at the level of phosphorylation (Kim and Edery, 2006; Yu *et al.*, 2006).

It has been shown that the transcription of two other basic-leucine zipper (bZIP) genes, *vrille* (*vri*) (Blau and Young, 1999) and *Par domain protein-1ε* (*Pdp1ε*) (Lin *et al.*, 1997) is also activated by the CLK-CYC complex. The CLK negative feedback loop starts when CLK-CYC heterodimers bind to E-boxes activating simultaneously *vri* and *Pdp1ε* transcription (McDonald and Rosbash, 2001). First, VRI accumulates in parallel with its mRNA, inhibiting the transcription of *Clk* when binding to its *Vri/Pdp1ε* boxes (V/P boxes). PDP1ε accumulates in a delayed fashion and competes for access to V/P boxes, acting as a transcriptional activator of *Clk* (Cyran *et al.*, 2003). Finally, CLK binds to CYC starting a new cycle of the CLK loop. The CLK loop also controls rhythmic transcription of the clock controlled genes (*ccg's),* including that of the photoreceptor cryptochrome.

A transcriptional regulator belonging to the basic helix–loop–helix ORANGE family, *clockwork orange* (*cwo*), was identified by both microarray studies (Lim *et*

al., 2007) and an RNA interference screen (Matsumoto *et al*., 2007) to be rhythmically expressed under CLK regulation. *cwo* is activated by CLK-CYC heterodimer through the E-box region and feeds back, repressing CLK-CYC activity. This negative transcriptional feedback loop helps to maintain a circadian oscillation with high amplitudes (Kadener *et al*., 2007; Lim *et al*., 2007; Matsumoto *et al*., 2007; Richier *et al*., 2008).

1.4 Organization of the *Drosophila* Circadian Pacemaker System

Although in insects and mammals there is a master clock located in the brain, there are also independent photoreceptive peripheral clocks in almost all other tissues of the body (Glossop and Hardin, 2002). The master clock is located in the suprachiasmatic nucleus (SCN) of the hypothalamus in the mammal (Ralph *et al*., 1990), and in *D.melanogaster*, its location has been established in the fly brain, at the neuronal level (figure 1.6).

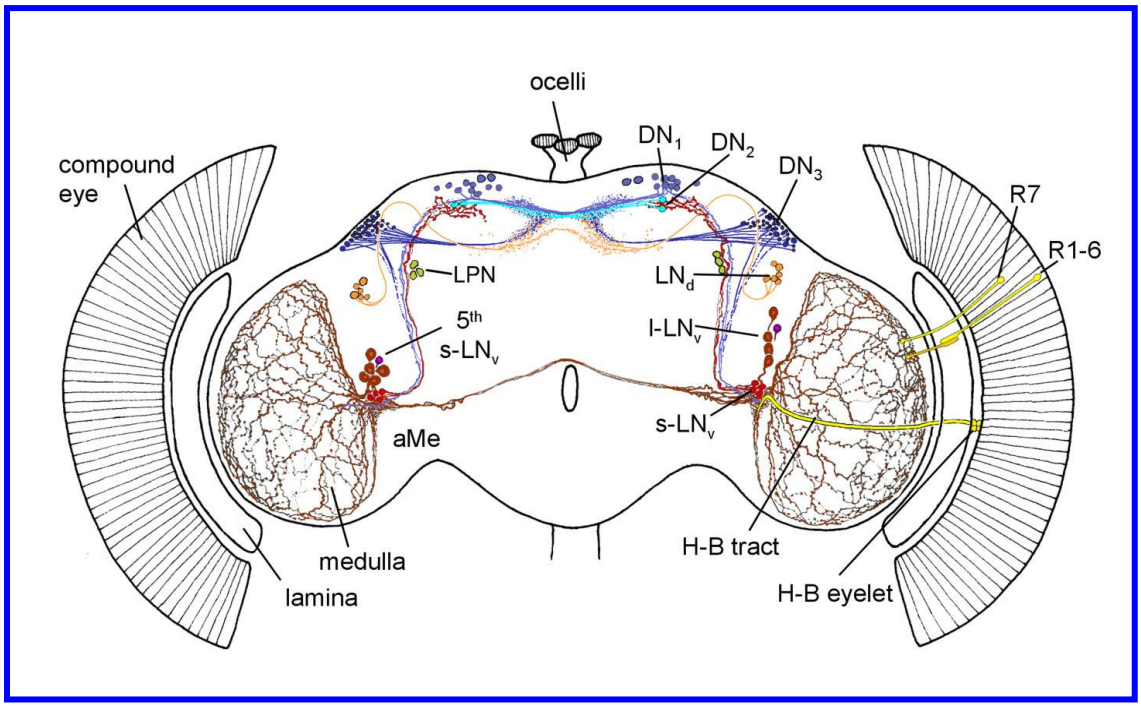

Figure 1.6 - Circadian oscillators in *Drosophila* brain. The Lateral Neurons (LN_D, l-LN_V, s-LN_V are shown in orange/red, the Dorsal Neurons (DN1, DN2, DN3) in blue.

H-B: extra-retinal photoreceptor cells of the Hofbauer-Buchner eyelets found in the posterior border of the compound eye, between retina and lamina. The compound eyes (the main external photoreceptors perceiving the light signals for the circadian clock) and ocelli (another external photoreceptor) are also indicated in the figure. (Helfrich-Forster *et al*., 2007).

In addition to the circadian oscillators in the brain, other clocks have been isolated in numerous tissues from *Drosophila* (Hardin, 1994). The analysis of *per* RNA cycling revealed that *per* is rhythmically expressed in peripheral tissues like antennae (Tanoue *et al*., 2004), Malpighian tubules (Giebultowicz *et al*., 2000; Hege *et al*., 1997), and photoreceptors (Cheng and Hardin, 1998). Another peripheral clock has recently been identified which is responsible for circadian cuticle deposition in the furca in the epidermis of adults (Ito *et al*., 2008). Circadian physiology is therefore not a passive response by the periphery to centrally coded driving signals, but is based on the synchronisation and sustainment of semi-autonomous peripheral clocks by a central pacemaker. These local clocks are in turn responsible for driving local, tissue-specific circadian programmes based on rhythmic gene expression (Plautz *et al*., 1997).

There are approximately 150 circadian clock neurons, clustered in six major defined groups of cells within the adult fly brain (figure 1.7). These clusters were classified based on their size and position (figure 1.6) and were determined by cytological staining for *per* and *tim* RNAs and proteins (Helfrich-Forster, 2005). The clock neurons are divided into two main groups, the lateral neurons (LNs) and the dorsal neurons (DNs). All these cells are placed symmetrically in both brain hemispheres. The lateral neurons can be subdivided into three cell clusters: 5 small ventral lateral neurons (s-LN_Vs), 4 – 6 large ventral lateral neurons (l-LN_Vs) and 5 -8 dorsal lateral neurons (LN_Ds). The dorsal neurons are also divided into three groups based on their relative positions and are called the DN1s (approximately 14-16 in

number), the 2 DN2s and the large group (more than 40) of DN3s (Helfrich-Forster, 2003). Amongst the DN1s, two are anterior in location (DN1a) and the other cells have a posterior position (DN1p). Recent observations suggested the inclusion of another group of neurons to this list, the lateral posterior neurons (LPNs) (Shafer *et al.*, 2006).

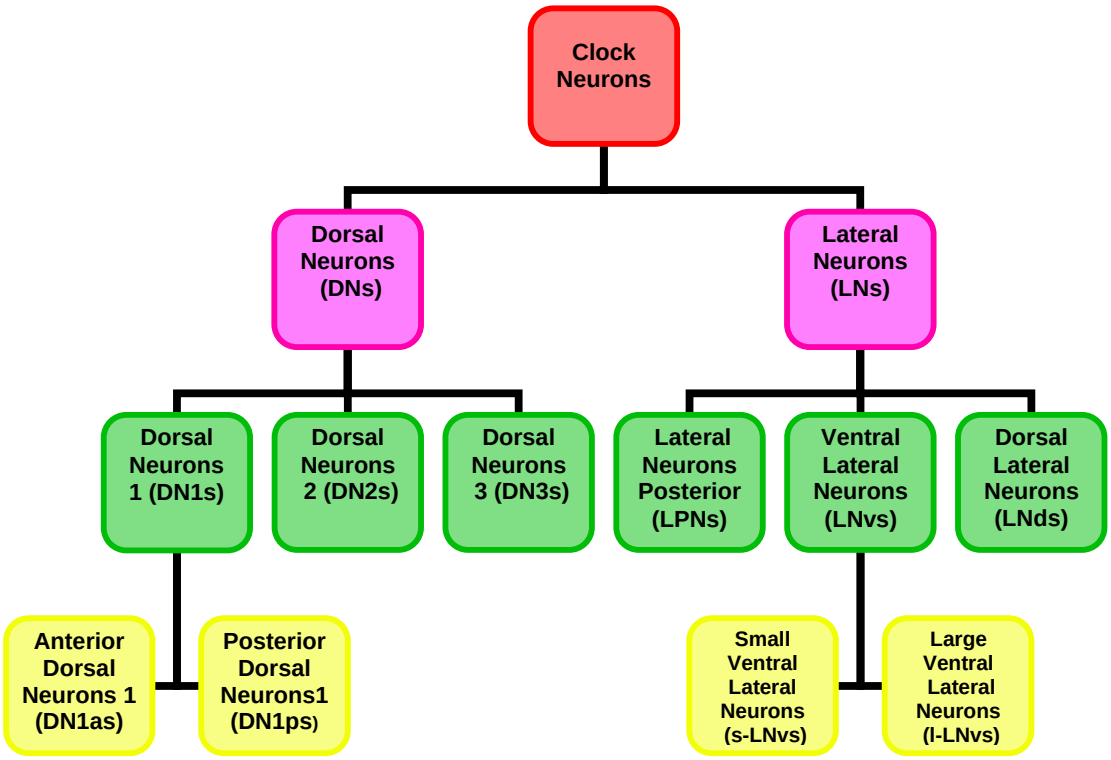

<u>Figure 1.7</u> - Diagrammatic representation of the classification of known clock neurons in the fly brain.

Different groups of cells can have distinct functions, and within a group not necessarily all the neurons have the same role. It has been demonstrated that the s-LN_vs, PDF-expressing neurons, control the locomotor anticipation to lights-on, while the LN_ds and DN_1s control the locomotor anticipation of lights off (Grima *et al.*,

2004; Stoleru *et al*., 2004). These cellular groups, known as "M" (morning) cells and "E" (evening) cells, seem to operate under a certain hierarchy to control the behavioural output (Stoleru *et al*., 2005). It has been shown that the PDF-expressing sLNvs are necessary and sufficient to drive locomotor activity rhythms in DD, since the oscillations in these cells are robust and self-sustained (Grima *et al*., 2004; Veleri *et al*., 2003). This finding was supported by *disco* mutants that lack the lateral neurons and consequently are not able to maintain rhythmicity in constant darkness (Helfrich-Forster *et al*., 2007). The other dorsal neurons and the large ventral lateral neurons are implicated in entrainment to LD conditions (Veleri *et al*., 2003). Recently, it has been established that in regimes of constant light, the clock in evening cells is dominant (Murad *et al*., 2007; Stoleru *et al*., 2007). It is evident from the studies described above that the network of neurons involved in circadian behaviour is complex.

The various clusters of neurons can communicate with each other, manifesting circadian rhythms of locomotor activity (Nitabach, 2005; Peng *et al*., 2003). To have a better understanding on how the clock neurons operate and communicate within the brain, it is necessary to elucidate their connections. Since clock products are mainly located within the cell bodies, the use of antibodies against them is not valuable. However, the study of neurotransmitters released by clock cells and transported to the synapses is very useful to describe the connections between these cells. The function of the neuropeptide Pigment Dispersing Factor (PDF) has been extensively studied. PDF peptide, an orthologue of the crustacean Pigment Dispersing Hormone (PDH) (Helfrich-Forster, 2005), is believed to be essential for normal functioning of the circadian clock as uncovered by mutants and cell ablation studies (Renn *et al*., 1999). In the *Drosophila* central nervous system, PDF expression is limited to the large ventral lateral neurons (l-LNvs) and four out of the five small ventral lateral neurons

(s-LNvs). The PDF receptor (PDFR, also called HAN), independently identified by three groups, is a G-protein coupled receptor (GPCR) (Hyun *et al*., 2005; Lear *et al*., 2005; Mertens *et al*., 2005). Most *Drosophila* clock neurons are receptive to PDF (Shafer *et al*., 2008), which is required for normal clock synchronization and phase adjustment (Lin *et al*., 2004; Peng *et al*., 2003). While levels of *pdf* mRNA and protein do not oscillate, PDF rhythmically accumulates at the terminals of the ventral lateral neurons and this cycling is lost in circadian mutants (Park *et al*., 2000). It is likely that PDF is rhythmically processed, transported or secreted (reviewed in Helfrich-Forster *et al*., 2000). Conversely, rhythmic genetic variants have been identified in the absence of cycling PDF, showing that cycling is not essential for maintenance of circadian rhythms (Kula *et al*., 2006).

Another neuropeptide was implicated as a candidate circadian transmitter in the *Drosophila* brain. The neuropeptide IPNamide (IPNa) was found to be specifically expressed by the DN1a subclass of clock neurons (Shafer *et al*., 2006). Indeed, it is already known that circadian locomotor activity of *Drosophila* is controlled by multiple neuropeptides (Taghert *et al*., 2001).

1.5 Entrainment of the Circadian Clock

Daily rhythms are controlled by endogenous circadian clocks that must maintain synchrony with the environment by external cues. Light and temperature are considered to be the strongest and the most pervasive factors that feed information to the core oscillator of the clock.

1.5.1 Entrainment by Light

Circadian rhythms can be entrained by light in two distinct ways: by constant exposure to day-night cycles and by pulses of light. In constant darkness, a pulse of

light in the early subjective night delays the phase whereas if it occurs in the second half of the subjective night a phase advance can be observed (Sharma and Chandrashekaran, 2005). On the other hand, if the pulse of light is administrated when the organism expects to see light, during the subjective day, the rhythm is not reset. Substantial studies have been made to identify the molecules involved in the light dependent phase shifting in *Drosophila* (Hardin, 2005).

Circadian clocks are entrained by light to follow the daily solar cycle. In *Drosophila*, there are two main light input pathways to entrain the circadian oscillator: the canonical visual system and through a dedicated blue-light photoreceptor Cryptochrome (CRY) (Ishikawa *et al*., 1999; Stanewsky *et al*., 1998). The *Drosophila* CRY is similar to photolyases (flavoproteins that repair DNA damage caused by UV-B radiation) (reviewed by Todo, 1999) and plant cryptochromes (involved in blue-light photoreception) (Emery *et al*., 1998).

In *Drosophila*, CRY is not only expressed in the clock neurons but also in the peripheral tissues (Emery *et al*., 2000a). CRY expression within the brain was dissected to the l-LNvs, about half of the LNds, the two anterior DN1s and some of the posterior DN1s. Thus, the different classes of neurons are heterogeneous with respect to CRY expression (Yoshii *et al*., 2008).

Studies revealed that the clocks of flies overexpressing *cry* are highly sensitive to light, whereas flies carrying *cry* mutation (cry^b flies) show reduction in sensitivity (Stanewsky *et al*., 1998). The circadian behaviour of wild-type flies is dramatically affected by constant light (LL), resulting in arrhythmic behaviour (Konopka *et al*., 1989). Unlike wild- type flies, cry^b mutants seem to be insensitive to constant light, and remain behaviourally rhythmic (Emery *et al*., 2000b). Other photoreceptors are

also involved, since cry^b flies do entrain to light-dark cycles and TIM can be degraded in the oscillator cells of these mutants (Helfrich-Forster *et al*., 2001).

When stimulated by light, CRY interacts with TIM (Ceriani *et al*., 1999) promoting TIM phosphorylation and further degradation via the proteasome (figure 1.4). CRY is also degraded by light (Lin *et al*., 2001). The CRY-TIM interaction involves an F box protein called JETLAG (Koh *et al*., 2006). JETLAG (JET), a putative component of an ubiquitin ligase complex, associates with TIM in a light-dependent way in the presence of CRY. This interaction results in the ubiquitination and degradation of TIM (Peschel *et al*., 2009).

Drosophila has two natural *timeless* alleles that encode different forms of TIM. The *s-tim* variant produces a 23 amino acid N-terminal truncation and is more photoresponsive. On the other hand, *ls-tim* encodes both long and short forms of TIM and is less light sensitive (Sandrelli *et al*., 2007). Yeast two-hybrid assays revealed a dramatic reduction in the strength of L-TIM/CRY when compared to S-TIM/CRY interactions (Peschel *et al*., 2009). Flies carrying jet^c mutation, characterized by a single nucleotide substitution in the leucine- rich repeat (LRR) region of JET, behave rhythmically when constantly exposed to light. However, this behaviour is exclusively observed when less light sensitive L-TIM protein is expressed (Peschel *et al*., 2006).

It was revealed that besides CRY, external photoreceptors in the compound eye and ocelli, and internal photoreceptors in the 2 Hofbauer-Buchner (H-B) eyelets are important to the light entrainment of clock neurons (Helfrich-Forster, 2004). These components of the visual system are believed to be linked to the circadian clock by neuronal connections through the small and large ventral lateral neurons which project into the optic lobes (Helfrich-Forster *et al*., 2002). The lack of one of these photoreceptors makes the mechanism less sensitive but able to keep the phase in LD

cycles. The photoreceptors of *Drosophila* visual system are the G protein coupled receptor (GPCR) rhodopsins. Rhodopsin is activated by absorption of light triggering its conversion into metarhodopsin, which in turn binds to G-proteins. The Phospholipase C (PLC) encoded by *norpA* is then activated and results, by an unknown mechanism, in the activation of two calcium permeable channels called the Transient Receptor Potential (TRP) and TRP-Like channel (TRPL) (reviewed by Hardie and Raghu, 2001; Hardie, 2001; Pak and Leung, 2003). It is believed that this cascade of events forms an essential part of the transduction of light information by the eyes to the clock. In addition, it seems that cry^b flies are able to entrain to light-dark cycles, through the canonical opsin-based pathway (Stanewsky *et al*., 1998), confirming that CRY is not the only light input pathway into the circadian clock. Supporting this idea, it was shown that flies lacking all known external and internal visual structures ($glass60^j$) and cryptochrome (cry^b) are not capable of entraining behavioural circadian rhythms (Helfrich-Forster *et al*., 2001). However, recent results from our laboratory have challenged this assumption (personal communication Breda C, 2010).

1.5.2 Entrainment by Temperature

In natural conditions, temperature shows circadian variations with low temperatures associated with the night (dark) and high temperatures are found during the day (light). Although it is known that temperature is an important *zeitgeber* (Wheeler *et al*., 1993), the whole mechanism by which temperature regulates the clock seems to be very complex and has not yet been completely dissected. Though constant light induces arrhythmicity in wild type flies (Konopka *et al*., 1989), it was demonstrated that under these conditions temperature cycles can generate robust

activity rhythms (Matsumoto *et al*., 1998). These rhythms can be driven even by temperature cycles of just 3°C (Wheeler *et al*., 1993).

A novel mutant, *no-circadian temperature entrainment* (*nocte*), was identified during temperature cycles screens using a *per-luciferase* (*luciferase* reporter gene which lies under the control of the *per* promoter) construct. Although the mutant *nocte* is able to entrain to standard light-dark cycles, the same does not occur with temperature entrainment (Glaser and Stanewsky, 2005).

It was demonstrated that temperature changes regulate the splicing of an intron within the 3` untranslated region (UTR) of *per,* which then determines the position of the evening locomotor activity peak. In winter conditions (short photoperiods and low temperature) the splicing is enhanced, causing an early accumulation of PER followed by the advance in the evening peak of activity (Majercak *et al*., 1999; Majercak *et al*., 2004). This is apparently ecologically beneficial since it would ensure that the bulk of the fly's activity would take place during the middle of the day in winter, when the temperatures are warmer. On the other hand, in summer conditions (represented by high temperatures and long photoperiods) *per* splicing is inhibited, shifting the peak of activity towards dawn and dusk. This is advantageous to the flies since a 'siesta' happens at the warmer temperatures of the day, avoiding midday desiccation.

In *Drosophila*, the phototransduction cascade is mediated by phospholipase C (PLC) encoded by the *norpA* gene. The mutant $norpA^{P41}$ generates an extremely high level of 3' splicing and show an early accumulation of PER at both low and high temperatures. Thus, it seems that *norpA* is a component of the input of temperature information to the circadian clock (Collins *et al*., 2004; Majercak *et al*., 2004), in conjunction with its well established function in the phototransduction pathway as described in section 1.5.1.

1.6 Mammalian Circadian Clock

One of the most surprising general conclusions from recent molecular genetic research is that the circadian timing mechanisms of the two major higher eukaryotic models, the fly and the mouse, employ the same clock molecules in similar ways. The remarkable evolutionary conservation is most spectacularly illustrated by the first clock mutation in the fly, the short 19 hr variant within the *period* gene in which a serine residue was mutated (Yu *et al*., 1987). In a human disorder, Familial Advanced Sleep Phase Syndrome, whose sufferers also show a short period phenotype and subsequently fall asleep and awake relatively early under 24 h cycles, the molecular lesion responsible was localised to one of the human *period* genes, and involved a substitution of the corresponding serine (Toh *et al*., 2001). This astonishing conservation provides an example of the significant progress made in unravelling the complexities of the circadian clockwork by juxtaposition of these two major model systems. This synergy means that an advance in one system can generate a hypothesis to be tested in the other.

The master clock is located in the suprachiasmatic nuclei (SCN) of the hypothalamus in the mammal. The SCN is composed of about 20,000 neurons, the core oscillatory machinery is contained within single cells: most, if not all, SCN neurons are circadian clocks. Their individual rhythms are synchronised across the assemblage, although they are not simultaneous, being held in precise phase-relationships. The factors and mechanisms responsible for this network synchrony are not known, although peptidergic signalling is clearly important (Harmar *et al*., 2002). This population of oscillators is synchronised to solar time by photic cues conveyed through a specialised retinal innervation, mediated by glutamatergic signalling. In turn, neural, paracrine and endocrine outputs of the SCN co-ordinate subordinate

oscillators in other brain regions and in peripheral tissues such as liver (Yamazaki *et al*., 2000; Yoo *et al*., 2004). The identity of these output factors and the mechanisms on which they operate are unclear, but have obvious relevance to understanding how the system operates.

The molecular clockwork of all circadian organisms examined to date consists of interacting positive and negative transcriptional/ post-translational feedback loops. These loops are highly conserved between *Drosophila*, mouse and humans, and are sustained by the positive bHLH/PAS transcription factors CLOCK and BMAL1 (the mammalian homolog of *cyc*) (Reppert and Weaver, 2002). These proteins heterodimerise and bind to E-box enhancer sequences, located in promotor regions of many clock and clock-controlled (output) genes, including the core components *Period (Per1, Per2)* and *Cryptochrome (Cry1, Cry2)* genes in the mouse. The protein products of *Per/Cry* form multimeric complexes that are translocated to the nucleus where they act as negative factors, inhibiting their own transcription by direct interaction with BMAL1. *Per/Cry* expression is reactivated to initiate the next circadian cycle when PER/CRY proteins are cleared from the nucleus.

An auxiliary loop starts when CLOCK/BMAL1 heterodimer activate the transcription of *Rev-Erbα* (believed to be the mammalian analogue of *Drosophila vrille*) and *Rorα*. REV-ERBα and RORα compete to bind to RORE sequences present in *Bma1l* promoter. RORα activates the transcription of *Bmal1*, whereas REV-ERB represses this process. Disappearance of REV-ERB removes this repression and thereby allows *Bmal1* expression to peak at the end of circadian night, thus creating a rhythm of *Bmal1* expression with a phase opposite to those of *Per* and *Cry* (Preitner *et al*., 2002; Ueda *et al*., 2002a).

The generation of the approximately 24 h molecular clock is governed through post-translational modification of clock proteins. CASEIN KINASE 1ε (CK1ε) phosphorylates PER proteins, subjecting them to ubiquitination and degradation in both organisms (Kloss *et al*., 1998; Lowrey *et al*., 2000). Mutations to CK1ε in flies and mammals affect PER stability and therefore alter circadian period (Price *et al*., 1998; Ralph *et al*., 1990)

1.7 Proteomics Application to Circadian Molecular Biology

Circadian timing is a pervasive feature of most, if not all, eukaryotes, and so represents a fundamental biological mechanism. Recent findings show that up to 10% of mRNAs in any one tissue are under circadian regulation, but that only a fraction of these cycling transcripts are shared between different tissues (Akhtar *et al*., 2002). This means that potentially most, if not all, mammalian genes may be under circadian transcriptional control in one organ or another. Post-genomic analyses of normal physiology without reference to the temporal dimension are therefore incomplete and inadequate.

In the past few years the circadian transcriptome has been studied in several model organisms, yet transcriptomics provide an incomplete characterisation of the mechanisms underlying circadian regulation. Five groups used the microarray strategy to identify output genes in *Drosophila* heads (Ceriani *et al*., 2002; Claridge-Chang *et al*., 2001; Lin *et al*., 2002; McDonald and Rosbash, 2001; Ueda *et al*., 2002b). Each study identified > 100 transcripts that cycle within a 24hr period in the fly head and the overlap among all lists represents a small fraction of the total number of cycling genes, probably explained by the differences in the chosen methods.

The study of the hepatic proteome in mouse revealed that up to 20% of soluble proteins in the mouse liver are under circadian control and surprisingly, almost half of

the cycling proteins do not have cycling transcripts (Reddy *et al*., 2006). Moreover, in the mouse SCN between 11% to 38% of circadian proteins have cycling transcripts (Deery *et al*., 2009). Conversely, many cycling proteins will have steady state RNAs. This findings show the importance of posttranscriptional mechanisms as circadian control points.

If we are fully to understand how circadian time is generated and signalled to the organism, it is now necessary to exploit these initial breakthroughs with a study of the cycling proteome. In addition, new proteomic approaches will be critical to characterising the composition and functions of the protein complexes that drive the core oscillation and its outputs, via transcription and temporally-regulated degradation of clock relevant factors. Thus, protein expression, location, identification of components of the complex, and post-translational modifications, must be studied in a time-dependent fashion.

1.8 Aims

1.8.1 General Aim

The aim of this project is to extend our understanding of the fundamental molecular processes that underpin circadian timing. The approach was initially to apply proteomic and genomic technologies to elucidate the critical molecular components of the circadian clockwork. I worked in a team that employs a comparative approach, using the two model organisms that have provided the most significant advances in this field: fruit-flies and mice. Consequently, the project provides a state-of-the-art paradigm for post-genomic analysis of complex phenotypes. My own part of this project was to develop the fly work.

1.8.2 Specific Aims

For a better understanding about the *Drosophila* clockwork it is important to define the protein complexes that subserve circadian pacemaking. For such matter, CYC, a core clock component, was tagged by StrepII or Halo tags to pull down its partners in co-immunoprecipitation (coIP) assays (Chapter 3).

Two different approaches were used in order to screen the circadian proteome of *Drosophila*. The first was based on a protein tagging paradigm to identify new circadian factors. Flies carrying a protein trap vector (CPTI lines), randomly inserted by a piggyBac transposon-based strategy, were used in locomotor activity experiments under constant light and darkness (Chapter 4). Behavioural analyses of the identified candidates, using mutants and transgenes to disrupt these factors, highlighted the importance of two novel genes involved in glutamate metabolism: *Got1* and *Gs2* (Chapter 4). These were further investigated in molecular and more complex behavioural experiments to verify their importance in the modulation of circadian light input (Chapter 5). The second approach to reveal new *Drosophila* circadian factors used the known mouse SCN circadian proteome (Deery *et al*., 2009). Functional analyses were done on the fly orthologues to investigate their contribution to the circadian timing mechanism in *Drosophila* (Chapter 6).

Chapter 2: Materials and Methods

2.1 Looking for Protein Complexes in *Drosophila* Oscillators

2.1.1 Cloning the Transgenes

2.1.1.1 Bacterial Strains

The bacterial strains used for cloning were:

- DH5α
- StrataClone SoloPack competent cells (Stratagene)

2.1.1.2 Vectors

The plasmids used for the cloning experiments were:

- pBluescript II KS+: cloning vector containing CYC full length cDNA and obtained as a gift from Dr. Ezio Rosato.
- pUAST: cloning vector of 8.9kb was designed to direct GAL4-dependent transcription of a gene of choice. The sequence is subcloned into a polylinker situated downstream of five tandemly arrayed, optimized GAL4 binding sites (Brand and Perrimon, 1993).
- Halo Tag® pHT2 (Promega): is a 4.9kb cloning vector that contains the ORF for the original Halo Tag® protein. This vector allows the fusion of proteins at either the N- or C- terminus.
- pSC-B-amp/kan (Stratagene): is a 4.3kb blunt PCR cloning vector.

2.1.1.3 PCR Cloning

The cloned DNA fragments were firstly amplified by PCR reactions performed on the DYAD™ DNA Engine Peltier Thermal Cycler (MJ Reasearch) with the following temperature cycles: an initial denaturation at 98°C for 30 s, 35 cycles of

98°C for 10 s, the optimal annealing temperature according to the set of primers for 20 s, and an extension at 72°C for 30 s, and a final extension of 72°C for 6 min. The volume and concentration of the reagents used for the PCR reactions are listed in table 2.1. The enzyme "Phusion™ Hot Start High-Fidelity DNA polymerase" (Finnzymes) was used to increase the specificity of the PCR amplification by preventing non-specific extension of DNA at ambient temperature. All the primers used are listed in table 2.2 and were synthesized by Sigma. The amplified DNAs were visualised in 1-2% agarose gel, containing 0.05 μg/100ml ethidium bromide. The Running buffer used was 1X TBE and 2μl of 5X Loading dye (250 ml 5X TBE, 31.25g Ficoll and 0.25g Bromophenol Blue) were added to the samples. The molecular weight markers used were ϕX 174 RF DNA HaeIII (Thermo Scientific) and λ HindIII (Invitrogen).

Table 2.1 - PCR reaction components

PCR Components	Volume used in 10 μl
10mM dNTPs	0.16 μl
5X PCR Buffer	2 μl
Forward primer (10μM)	1 μl
Reverse primer (10μM)	1 μl
Phusion Hot Start DNA polymerase (2 U/μl)	0.2 μl
DNA	2 μl
dH_2O	Make up to 10 μl

Table 2.2 – List of primers and their annealing temperatures.

Primer Name	Primer Sequence (5'- 3')	Annealing Temperature
CT-Cyc1	GAATTCATGGAAGTTCAGG	38℃
CT-Cyc2	GCGGCCGCCTTCGCATCGATAAGCC	52℃
CT-Cas1	GCGGCCGCCGTGCCACCCTCGTGATTGG	66℃
CT-Cas2	CCAGCACCTCCAGCACCTGCTCCTGCAGCAC CTCCTGCACCAGCTAAGAACACGG	32℃
CT-Cas3	GGAGGTGCTGGTGCAGGAGCTGCAGGTGGA ATGGGATCCGAAATCGG	48℃
CT-Cas4	CTCGAGGCGGACGGACGACC	50℃
CT-Halo1	ATTCGCCCGTGAGACC	62℃
CT-Halo2	CTCGAGTTAGCCGGCCAGCCC	52℃
CT-Strep2	CTCGAGTTACTTCTCAAATTGTGGATGTGACC ATCCACCTGCAGCTCCT	52℃
NT-Halo1	GAATTCATGGGATCCGAAATCGG	52℃
NT-Halo2	TCTGGCCATTCGTCCCACG	71℃
NT-Cas1	CATACATGAACTGGCTGCACC	65℃
NT-Cas2	CCTCCAGCACCTGCTCCTGCAGCACCTCCTGC ACCAGCGCCGGCCAGCCC	46℃
NT-Cas3	GGTGCTGGAGGTGCTGGTGCAGGAGCTGCAG GTGGAATGGAAGTTCAGG	38℃
NT-Cas4	GCGGCCGCCTTCGCATCGATAAGCC	52℃
NT-Cyc1	GAGCAGCTATCCTCACTGG	60℃
NT-Cyc2	GCGGCCGCTTATAAGAACACGGAATTCTTGG	62℃
NT-strep3	GAATTCATGTGGTCACATCCACAATTTGAGA AGGCTGGTGCAGGAGGT	50℃
pUAST-FW	GCTCCCATTCATCAGTTCCA	60℃
pUAST-RV	TAAACAAGCGCAGCTGAACA	58℃

2.1.1.4 Ligation

The PCR products were initially ligated to the StrataClone vector according to the "StrataClone PCR Cloning Kit "instruction manual (table 2.3). The reactions were incubated for 5 min at room temperature. After bacterial transformation and plasmid DNA preparation (see subsequent items for details), the DNA was digested and ligated to pUAST vector (table 2.4). These ligation reactions were incubated at 4°C overnight or at room temperature for 4 h.

Table 2.3 - "StrataClone PCR Cloning Kit " Ligation.

Component	Volume used in 6 μl
StrataClone Cloning Buffer	3 μl
PCR product	2 μl
StrataClone Vector Mix	1 μl

Table 2.4 - Ligation Reaction Mix.

Component	Volume used in 25 μl
T4 DNA ligase	1 μl
10X T4 ligase reaction buffer	2,5 μl
Vector (75-100 ng)	x μl
Insert DNA	y μl
dH_2O	Make up to 25 μl

2.1.1.5 Bacterial Transformation

Plasmid DNA (2 μl) was mixed with 100 μl DH5α or StrataClone *E. coli* chemically competent cells and then left on ice for 20 min. The cells were heat shocked by placing them in a 42°C water bath for 45 s, then immediately transferred back onto ice for 2 min. Transformed cells were allowed to recover for 1 h by incubating at 37ºC and 250 rpm in 1ml of Luria-Bertani (LB) broth (1% bacto-tryptone, 0.5% bacto-yeast extract, 1% NaCl). The cultures were then spun down, approximately 0.9 ml of the supernatant was removed, and the cells were gently re-suspended in the remaining supernatant. Finally, the cells were plated onto LB agar containing 100 μg/mL ampicillin and X-gal 2% and incubated overnight at 37ºC without shaking.

2.1.1.6 Inoculation

White colonies were inoculated onto 5 ml of LB with 100 μg/mL ampicillin and incubated at 37ºC overnight. On the next day, the cultures were twice centrifuged for 2 min at maximum speed in 1.5 ml tubes and the pellets were used for plasmid DNA preparation.

2.1.1.7 Plasmid DNA Preparation

Mini plasmid preps were made using "Qiagen DNA Spin Mini-prep Kit" following the manufacture's protocol.

2.1.1.8 Digestion

To confirm the presence of the insert or to clone a DNA fragment into a vector, 5 μl and 25 μl, respectively of the mini preps were digested at the optimal temperature for the respective restriction enzymes for 1 hour (table 2.5). All the restriction endonuclease enzymes used were obtained from "New England Biolabs" (NEB), except PasI which was bought from "Fermentas". 1-2% agarose gels were used to visualise the products of the digestions. DNA from agarose gels was recovered by cutting out the band of interest, and then using the "QIAquick extraction gel kit" (QIAGEN) according to the manufacture instructions.

Table 2.5 - Restriction enzymes and their respective optimal temperature.

Restriction Enzyme	Optimal Temperature
BstEII	60°C
Bsu36I	37°C
EcoRI	37°C
NaeI	37°C
NotI	37°C
PasI	55°C
RsrII	37°C
XhoI	37°C

2.1.1.9 Sequencing

All the cloning steps were verified by sequencing (samples were sent to Macrogen) and a map file of the transgene was made to double check the sequence (see appendix 1). The sequences edition and analyses were performed using GCG and Chromas 2.33.

2.1.2 DNA amplification - Polymerase Chain Reaction (PCR)

For each construct injected, flies with the insert in different chromosomes were obtained and then tested by PCR to confirm the presence of the construct.

The PCR reactions followed the details described in item 2.1.1.3. The strategy used to check the presence of the construct was the utilization of a primer annealing with the tag (Halo or StrepII) and another primer hybridizing to pUAST sequence. The primers (showed in Table 2.2) used in each reaction were:

C-terminus Halo Tag: NT-Cas1 and pUAST-FW

N-terminus Halo Tag: pUAST-RV and NT-Halo2

N-terminus Strep TagII: pUAST-RV and Cyc1-RV.

2.1.3 Western Blotting

The constructs were tested in Western Blot assays to check if the tags could be detected by specific antibodies.

2.1.3.1 Protein Extraction of *Drosophila* Heads

The collected flies were frozen in liquid nitrogen and stored in 1.5 ml tubes at -80ºC. The heads were separated from the rest of the body by vortexing the tubes. With the help of a sieve, the heads were collected, put in new tubes and kept in dry ice. The extraction buffer (table 2.6) was added to the samples, which were then homogenised using a sterile plastic pestle. The samples were centrifuged at 13.000 rpm for 10 min at 4ºC and the supernatant was separated in new tubes. After repeating this procedure one more time, the supernatant containing the proteins was retained. To quantify the proteins, 1 µl of sample was added to 800 µl of water and 200 µl of Bradford's Reagent (Sigma). The optical density (OD) was measured at 595 nm using a Spectrophotometer (Eppendorf), and the samples were equalised to 0.3A using extraction buffer before loading onto an SDS-polyacrylamide gel.

Table 2.6 - Extraction Buffer Components.

Components (Stock)	Volume used in 2 ml
10% TritonX-100	10 µl
0.5 M EDTA	4 µl
1M DTT	2 µl
200 mM PMSF	10 µl
10µg/ml Aprotinin	2 µl
10µg/ml Leupeptin	1 µl
10µg/ml Pepstatin	10 µl
1M Sodium β-glycerophosphate	10 µl
4M NaCl	50 µl
100mM HEPES pH7.5	400 µl
dH_20	1.5 ml

2.1.3.2 SDS-Polyacrylamide Gel Electrophoresis (SDS-PAGE)

Appropriate amounts of 3X loading buffer (188mM Tris HCl pH 6.8, 6% v/v SDS, 30% v/v Glycerol, 15% v/v βMercaptoethanol, 0.03% w/v Bromophenol Blue) were added to the samples and they were heated for 5 min at 95^{o}C prior to loading onto a denaturing SDS Polyacrylamide Gel Electrophoresis (SDS-PAGE). A pre-stained broad range molecular weight marker (BioRad Laboratories or New England Biolabs) was loaded along with the samples. The acrylamide gel is divided into stacking and resolving gel (tables 2.7 and 2.8). The first gel to be prepared is the resolving gel, which is covered with water until polymerised. Then the water layer is removed and the stacking gel added and the comb inserted. The gels were run using 1X running buffer (2.5mM Tris, 0.25M Glycine, 0.1% v/v SDS) at constant 250 volts for approximately three hours.

Table 2.7 - Components of the stacking gel portion of a polyacrylamide gel.

Components (Stock)	Volume used in ~10ml
1M Tris HCl pH 6.8	1 ml
20% SDS	50 µl
25% APS	20 µl
TEMED	10 µl
30% Acrylamide	1.5 ml
dH_20	7.3 ml

Table 2.8 - Components of the 6% resolving gel portion of a polyacrylamide gel.

Components (Stock)	Volume used in ~30ml
2M Tris HCl pH 8.8	6 ml
20% SDS	150 µl
25% APS	240 µl
TEMED	36 µl
30% Acrylamide	6 ml
dH_20	17.55 ml

The SDS-PAGE was blotted at constant 50mA overnight at 4°C onto a nitrocellulose membrane (Whatman® Protran®) using transfer buffer (composed of 40mM Tris, 40mM Glycine, 0.375% SDS, 20% Methanol).

2.1.3.3 Immunodetection

The nitrocellulose membranes were washed in milk buffer (table 2.9) for 1 h on a shaking platform at room temperature to prevent binding of primary antibody to any non-specific proteins. After blocking, the membrane was incubated with 50 ml of milk buffer containing the primary antibody at 4°C overnight. The membranes were washed three times for 15 min each in 1X TBST buffer (table 2.9) and then incubated in milk buffer with the secondary antibody for 1 hour at 4°C. Finally, the membranes were washed again three times for 15 min in 1X TBST to remove any unbound secondary antibody.

To detect the transgenes the primary antibodies used were: 1:1000 rabbit polyclonal anti-Halo® tag (Promega), 1:1000 mouse monoclonal anti-Strep tagII (Novagen) and 1:4000 monoclonal anti-Strep TagII Horseradish Peroxidase (HRP) – conjugated (Novagen). The secondary antibodies used were: 1:6000 anti-rabbit Horseradish Peroxidase (HRP) (Sigma) and 1:6000 anti-mouse Horseradish Peroxidase (HRP) (Sigma).

Table 2.9 - 1X TBST and milk buffer components.

1X TBST		**Milk Buffer**	
Components	**Volume in 1 L**	**Components**	**Volume in 250 ml**
NaCl	8,15 g	1X TBST	125 ml
10% Tween	5 ml	Non-fat powdered milk	6.25 g
1M Tris HCl pH 7.5	10 ml		
dH_20	Make up to 1 L		

2.1.3.4 Chemiluminescence

Solutions A and B (table 2.10) were mixed together and poured over a piece of Clingfilm. Each side of the nitrocellulose was soaked in this solution for approximately 30 seconds and then transferred face down onto another piece of Clingfilm (avoiding having bubbles). Within a dark room, X-Ray photographic film (Fujiflim) was placed on top of the membrane inside a light-proof cassette and exposed for between 30 sec and 1 h depending on the strength of the reaction. Finally, the films were developed using an automated developer system.

Table 2.10 - Components of solution A and B.

Solution A		**Solution B**	
Component	**Volume in 5.43 ml**	**Component**	**Volume in 8.1 ml**
1M Tris-HCl pH 8.5	0.5 ml	1M Tris-HCl pH 8.5	0.5 ml
250 mM Luminol (Sigma)	50 µl	30% Hydrogen peroxide (H_2O_2)	3.1µl
90 mM p-coumaric acid (Sigma)	22 µl	dH_20	4.5ml
dH_20	4.43 ml		

2.1.4 Immunoprecipitation

HaloLink Resin (Promega) was used to immobilize the Halo tag fusion proteins. The manufacture protocol was followed to equilibrate the resin, bind the Halo tag protein covalently to a solid Sepharose surface and wash away nonspecific proteins. After all these steps, the resin carrying the attached Halo tag protein was boiled in SDS loading buffer and the supernatant was analysed by SDS-PAGE (as described in section 2.1.3.2).

2.2 Clock Mutants Screening - CPTI flies

2.2.1 Media and Growth Conditions

The CPTI flies were grown in vials on sugar food (231.5 g sugar, 50 g agar, 41 g dried yeast, 5 l water, 50 ml 20% Nipagen in ethanol) and were maintained at 18ºC (their life cycle is approximately 20 days at this temperature). The flies were subjected to 12 hours of light and 12 hours of darkness (LD12:12).

2.2.2 Locomotor Activity Experiments

2.2.2.1 Experimental Set-up

For the locomotor activity experiments, individual male flies (1-4 days old) were placed in small glass tubes filled with sugar food (about 2 cm) and sealed with a black cap at one end and a cotton plug at the other. These tubes were placed individually in channels of monitors (TriKinetics Inc) used to record the locomotor activity of single flies. Each monitor has 32 independent channels able to detect motion as the flies walk back and forth within the tube interrupting an infrared beam. The monitors were housed in light boxes equipped with light emitting diodes (LEDs) programmed to turn on and off using timers according to the experimental light regime. The CPTI flies were entrained for 1-2 days in LD (12:12) conditions, followed by 5-7 days in DD, re-entrained for 1-2 days in LD (12:12) and finally placed in LL conditions for 5-10 days. The light boxes positioned inside incubators (Scientific Laboratories Supplies Ltd) were maintained at 25^{o}C during the whole experiment.

2.2.2.2 Data Collection and Analysis

The locomotor activity monitors were connected to a PC using a Power Supply Interface Unit (TriKinetics Inc) and the data from them was collected using

the DAMSystem2.1.3 software (TriKinetics Inc).

The period (τ) of each individual fly was calculated by Autocorrelation and also by using Python 22 to perform a high resolution spectral analysis using the CLEAN algorithm (Rosato *et al*., 2006). In the autocorrelation analysis, the data (collected in 30 min bins) is shifted point by point and compared to itself to create a series of correlation coefficients (thus called autocorrelation). A rhythmic fly with a 24 h period will have the most significant correlation every 48 bins apart. The 95% confidence limits are given by 2/root N, where N is the number of data points. For the spectral analysis, Monte Carlo simulations were performed by generating 100 randomisations on the data for each fly to give the 95% and 99% confidence limits. Flies with a detectable peak above the 99% confidence limit were included in the computation of the average period of a genotype and all others were considered to be arrhythmic. A fly to be classified as rhythmic had to show both a significant autocorrelation and spectral analysis with a similar period. The data obtained after CLEAN/autocorrelation was assembled together and further processed using BeFly, a collection of macros generated in the laboratory by Edward Green.

The average activity histogram (actogram) was plotted using Microsoft Excel® 2003 and the flies that died during the experiment were excluded from the analysis.

2.3 Glutamate and the Circadian Clock

2.3.1 Locomotor activity experiments

A number of CPTI lines were implicated in glutamate metabolism and were followed up extensively in chapter 5. The locomotor activity experiments were performed and the data was analysed according to section 2.2.2. The flies used in these experiments and their ID numbers are listed in chapter 5.

2.3.2 Determination of *tim* and *jetlag* alleles

The determination of *tim* alleles was performed by PCR reactions using DNA extracted from individual flies. Forward allele specific primers (*s-tim 5'* and *ls-tim 5'*) were used in combination with a common reverse primer *(Tim 3')* and a control of PCR efficiency was amplified with primers *Control 5'* and *Control 3'* (table 2.11). The PCR reactions were carried out with an initial denaturation of 92° C for 2 min, 35 cycles with 92° C for 30 s, 55° C for 30 s, 72° C for 1 min and a final extension of 72° C for 8 min. The reagents used in the PCR reactions are listed in table 2.13.

To check for *jetlag* mutations, DNA from individual flies was amplified with *Jet 5'* and *Jet 3'* primers (table 2.11) according to the cycling conditions described above, but using a different annealing temperature (64° C). The PCR products were purified by E.Z.N.A.® Cycle-Pure Kit following the manufacture's instructions and then sequenced using *Jet5'* primer by PNACL DNA Sequencing Service.

Table 2.11 – Primers to genotype *tim* and *jet al*leles.

Primer Name	Primer Sequence (5'- 3')	Annealing Temperature
ls-tim 5'	TGGAATAATCAGAACTTT**GA**	55°C
s-tim 5'	TGGAATAATCAGAACTTT**AT**	55°C
Tim 3'	AGATTCCACAAGATCGTGTT	55°C
Control 5'	CATTCATTCCAAGCAGTATC	55°C
Control 3'	TATTCATGAACTTGTGAATC	55°C
Jet 5'	CGCGTACTCAAGCTGTCC	64°C
Jet 3'	CACGCCATAGTCGGAGAT	64°C

Table 2.12 - Standard components of the PCR reactions.

PCR Components	Concentration
DNA	Up to 1μg
5X PCR Buffer	1X
Forward primer (10μM)	10 pmoles
Reverse primer (10μM)	10 pmoles
Taq DNA Polymerase	1Unit
dH_2O	Make up to 20 μl

2.3.3 Western Blot to check TIM cycling in LL

Westerns Blots to check TIM stability in LL were performed as described in section 2.1.3. Flies were entrained for 3 days in LD 12:12 at 25° C and heads were collected in the first day of LL at four time points: CT 1, CT7, CT13 and CT19. The antibody used to detect TIM was a gift from Francois Rouyer and tubulin antibody was used to correct for loading errors (table 2.13).

Table 2.13 – List of primary and secondary antibodies used in Western Blots along with their source and working concentrations.

Antibody	Source	Animal in which it was raised	Working Concentration
α-TIM	Prof. Rouyer	Rat	1:2.000
α-Tubulin	Sigma-Aldrich	Mouse	1:40.000
α–Rat	Sigma-Aldrich	Goat	1:10.000
α-Mouse	Sigma-Aldrich	Goat	1:6.000

2.3.4 Phase shift experiments

For the phase shift experiments different flies were entrained for three days to LD 12:12 cycles and a light pulse of 10 min was administrated. Then, the flies were maintained in DD for several days. A group of control flies of the same genotype was equally maintained but did not receive a light pulse. In the delay experiments, the pulse was administrated at ZT15 and in the advance experiments the flies were pulsed at ZT21. The analysis of the data was performed using Befly (created by Edward Green), which uses an automated cross-correlation function to measure the degree of phase shift. Cross-correlation analysis examines the correlation between the individual 30 min activity bins of the experimental data series against the individual activity bins of the control data series. For example, bin 1 of the experimental series is correlated with bin 1 of the control series, bin 2 with bin 2, etc until the end of the data sets. The control series is then moved by one bin and the two data sets are again cross correlated. This will continue until the control data set has been moved down the entire experimental data set. The direction of the movement is dependent upon whether a phase advance or phase delay is expected. If a phase delay is expected, the control data set is moved down by one bin. A correlogram is then produced by plotting the cross-correlation against an axis of 30 min time lags. The phase difference between the control and experimental data sets can then be calculated by extrapolating the highest cross-correlation value onto the time lag axis. The automated method was validated by calculating phase shifts manually (which is extremely laborious) and gives similar phase shifts.

2.4 Identification of *Drosophila* homologues of mammalian genes

2.4.1 Finding *Drosophila* candidates

Cycling proteins from mouse suprachiasmatic nucleus (SCN) were obtained from 2D gels (Deery *et al*., 2009). To find their respective *Drosophila* homologues, the mouse cycling protein's IDs were submitted to NCBI (http://www.ncbi.nlm.nih.gov/), and their sequences were blasted (Blastx) against *Drosophila* database. The *Drosophila* genes chosen to be used for further studies are related to synaptic processes and are shown in table 2.14.

Table 2.14 - *Drosophila* homologues of cyclic synaptic proteins from mammalian SCN.

Mouse SCN protein (ID)	Drosophila homologue	CG number
vesicle-fusing ATPase (1171774)	NSF2	CG33101
vesicle-fusing ATPase (1171774)	NSF1	CG1618
synapsin II (8567410)	Synapsin (Syn)	CG3985
N-ethylmaleimide sensitive fusion protein (54611730)	Snap	CG6625
14-3-3 zeta (1841387)	14-3-3ζ	CG17870

2.4.2 Mutants and RNAi analysis

2.4.2.1 Locomotor Activity

The locomotor activity of a number of mutants for the synaptic genes and UAS-RNAi lines followed the details in section 2.2.2 and the flies used are listed in chapter 6.

2.4.3 Immunnocytochemistry (ICC)

2.4.3.1 Brain dissection

Flies were collected at the appropriate time points and fixed in 4% Paraformaldehyde (PFA) by incubating for approximately 2 h on a rotating wheel in a dark room. They were then washed for 15 min in Phosphate Buffer Saline (PBS)

which is composed of 140mM NaCl, 2.7mM KCl, 10mM Na_2HPO_4, 1.8mM KH_2PO_4. The brains of these flies were dissected under a microscope with the help of fine forceps. A small Petri dish containing a few drops of PBS on a layer of silicon was placed under the microscope. A fly was placed in the drop of PBS and the head of the fly was held with the forceps in the right hand and the body in the left hand. The body was removed and discarded and the head retained in the right hand. The proboscis of the fly was the first to be removed and discarded. The right forceps were then used to hold one eye through the hole created by the removal of the proboscis and the left forceps were also inserted into that hole to hold the other eye. By gently applying pressure, the two eyes were pulled apart in opposite directions to reveal the brain underneath. Before continuing, it was ensured that the cuticle and connective tissue was removed from the surface of the brain to minimise non-specific fluorescence.

2.4.3.2 Incubation with buffers and preparation of slides

The dissected brains were transfered to a 1.5ml eppendorf, using 10ml pasture pipette with a 10ul tip, and were washed three times for 20 min each in 1xPBS/1% TritonX to permeabilize the membrane. The brains were blocked against non-specific binding of the primary antibody for 1 h with blocking solution (1xPBS/0.5% TritonX, 10% heat inactivated goat serum). After blocking, the brains were incubated in the primary antibody diluted in 1xPBS/0.5% TritonX, which contained 0.1% sodium azide. The presence of sodium azide prevents the contamination of the antibody solution with bacteria and thereby allows the re-use of the antibody. The brains were incubated in primary antibody for 1 week at 4°C. They were then washed three times for 20 mins each in 1xPBS/0.5% TritonX. After washing, they were incubated for 2.5 h at 4°C in the appropriate secondary antibody (raised against the animal in which the primary antibody was generated) diluted in 1xPBS/ 0.5% TritonX. The fluorophores

conjugated to the secondary antibody are light-sensitive, therefore the brains were kept in the dark. The secondary antibody was removed and the brains were washed three times for 20 min each in 1xPBS/0.5% TritonX. Table 2.15 lists the antibodies used for the immunocytochemistry experiment conducted.

Table 2.15 - List of primary and secondary antibodies used for ICC.

Antibody	Source	Animal in which it was raised	Fluorophore	Working Concentration
α –TIM	Prof. Rouyer	Rat	-----	1:200
α–PDF	Developmental Studies Hybridoma Bank	Mouse	-----	1:600
α–Rat	Sigma-Aldrich	Goat	Alexa Fluor594	1:200
α –Mouse	Sigma-Aldrich	Goat	AlexaFluor488	1:200

Once the protein of interest had been labelled with the appropriate antibody, the brain was mounted onto slides (VWR) with a drop of mounting medium which comprises of 80% glycerol and 3% propyl gallate and covered with a coverslip of 0.1 mm thickness (VWR). The slides were stored in the dark at 4°C. They were visualised as described below.

2.4.3.3 Visualisation of brains

The slides containing brains stained for the different antibodies were visualised on the laser scanning Olympus FV1000 Confocal microscope. Wherever possible, two images were taken for each brain – one for the right and one for the left hemisphere. The 60X objective was used to create Z-series for each brain. The same microscopic settings were used in all slides to quantify the signal. The laser gain was 1, amplifier offset was 7% (for Alexa 488) and 5% (for Alexa 594) and laser intensity

was 2%. Sequential scans were used to avoid bleed-through and Kalman filter to scan twice the same image.

2.4.3.4 Quantification of signal

When quantifying the signal of TIM across different time points the microscopic settings mentioned above were kept constant not only for all the brains of a time point but also for all the time points. The mean pixel intensity of cytoplasmic and nuclear TIM was quantified using ImageJ Version1.42g (available freely at http://rsb.info.nih.gov/ij/), with the cellular region of interest determined by PDF expression.

Chapter 3: Looking for Protein Complexes in Drosophila Oscillators

3.1 Introduction

A number of genes that are components of the molecular circuitry of the *Drosophila* circadian oscillator have been revealed by genetic analysis (Hall, 2003). The *Drosophila* oscillator is composed by two intracellular feedback loops interlocked by CLK/CYC transcription. The current model of circadian timing proposes that transcriptional activation of circadian genes by CLK/CYC complexes fluctuates as a result of the periodic nuclear entry of complexed negative factors (PER, TIM) which associate with CLK/CYC. For a better understanding about the clockwork it is necessary to identify the nature of the protein complexes that subserve circadian pacemakers. In this work, the strategy chosen for such matter was the use of co-immunoprecipitation (coIP) with a transgene in which CYC is tagged by the Strep tagII or Halo tag. To target the pacemaker tissues the transgenes need to be expressed in a $glass^{60j}$ background. The $glass^{60j}$ mutant flies lack visual photoreceptors which provides the majority of clock gene products in the head, however are perfectly rhythmic since the pacemaker cells are unaffected by the mutation (Veleri *et al.*, 2003).

The Halo Tag protein is a genetically-modified hydrolase that covalently binds hydrolase substrates like the Halo Link Resin, which is a solid support for direct capture of the Halo Tag protein. The resin consists of a Halo Tag ligand bound to Sepharose® beads that specifically and rapidly binds Halo Tag fusion proteins. The covalent nature of the Halo Tag bond gives stability during dilution and stringent

washing, minimizing the loss of the Halo Tag fusion proteins from the surface (Los *et al*., 2008).

The Strep TagII constitutes an eight amino acid-peptide (WSHPQFEK) that binds specifically to streptavidin and occupies the same pocket where biotin is normally complexed. The bond between Strep TagII and a derivate of streptavidin, the Strep.Tactin® (Novagen) protein, is nearly 100 times higher than for streptavidin. To co-capture Strep TagII associated proteins, Strep Tag II binds to the Strep.Tactin® coupled resin, and after unbound proteins are washed away, the purified target protein is competitively eluted with 2.5 mM desthiobiotin, a reversibly analog of biotin (Voss and Skerra, 1997).

3.2 Methods

In order to define the nature of the protein complexes that subserve circadian pacemakers, four different transgenes, in which CYC was tagged with the Strep tagII or Halo tag, were created. The constructs were cloned into the pUAST vector that carry the UAS sequence along with Strep tagII or Halo tag at either N- or C- terminus of CYC, with a glycine/alanine linker (AG linker) separating the tag from *cyc* (figure 3.1). The expression of the tagged gene was directed to pacemaker cells by *tim-Gal4*.

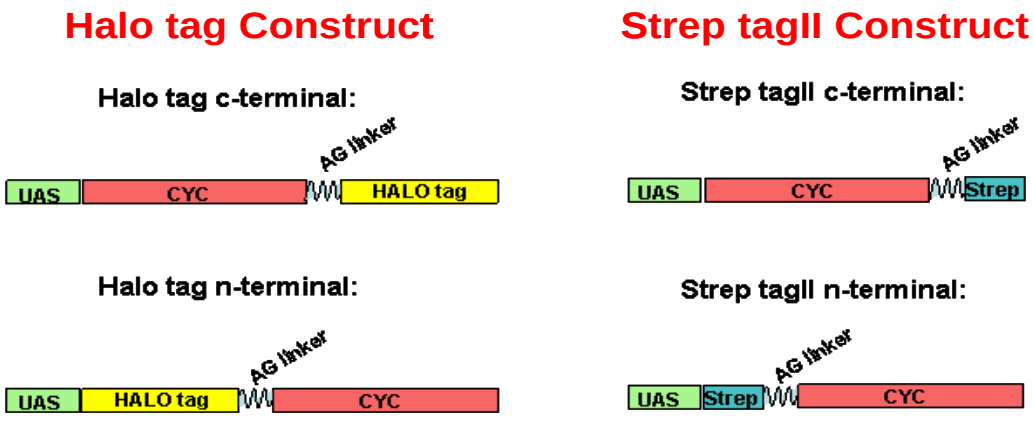

Figure 3.1 - Representative scheme of the four cloned transgenes.

3.3 Results

3.3.1 Cloning Scheme

The cloning of the tag constructs was very laborious and it was performed following a number of steps in which different fragments were inserted into pUAST vector at a time. The pUAST vectors containing the entire and final constructs were checked by sequencing (see appendix 1) prior to their injection into the flies.

3.3.1.1 C-terminus Halo Tag Construct

The final C-terminal Halo Tag transgene inserted in pUAST was obtained after following the steps here described (figure 3.2):

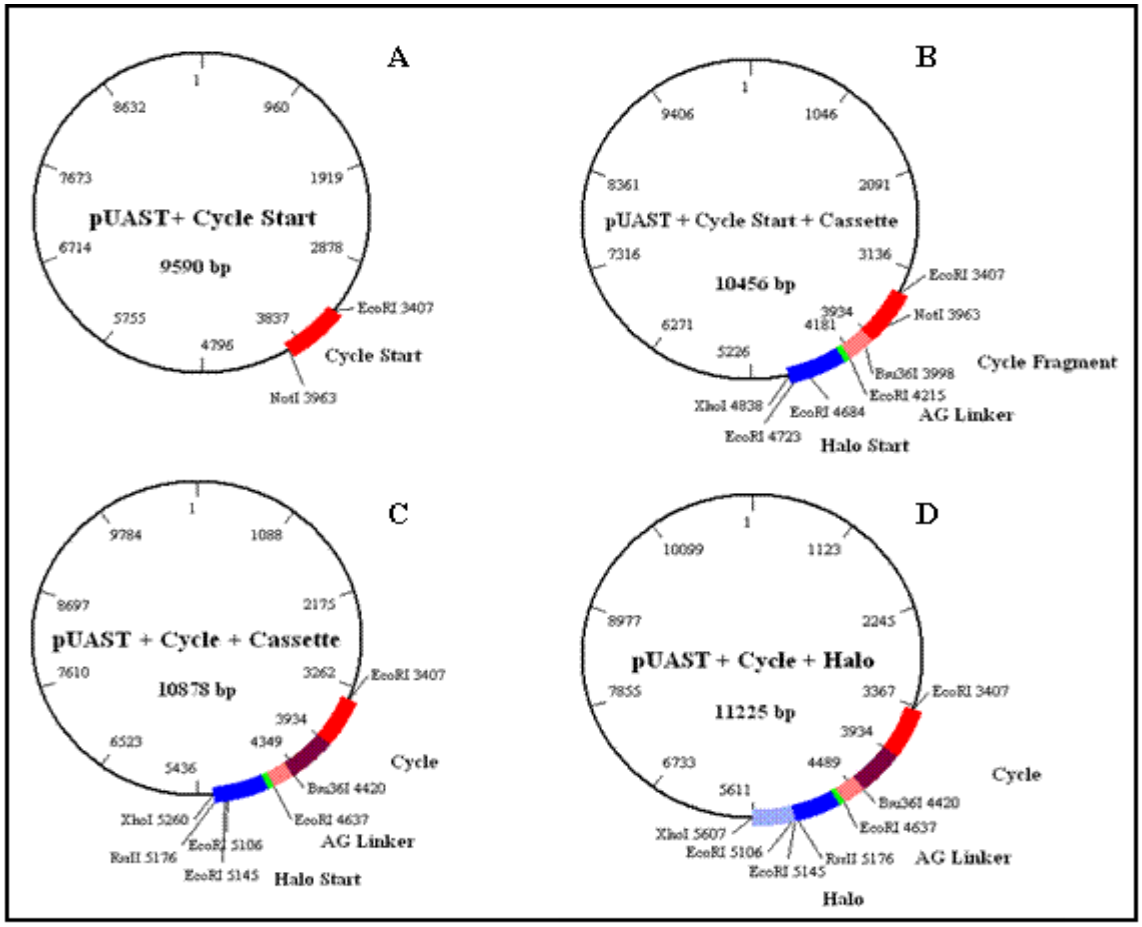

Figure 3.2 - Cloning scheme of C-terminal Halo Tag construct. Red: 5' end of *cycle*. **Pink:** 3' end of *cycle*. **Magenta:** middle part of *cycle*. **Green:** AG Linker. **Dark blue:** 5' end of Halo Tag. **Light blue:** 3' end of Halo Tag.

A. Initially, a fragment containing the first 548 nucleotides of *cyc* (present in pBluescript II KS+) was amplified by PCR, using the primers CT-Cyc1 and CT-Cyc2. The initial portion of *cyc* sequence was cloned into the StrataClone vector, which along with pUAST was double digested by EcoRI and NotI. Finally, *cyc* start was cloned onto pUAST.

B. The 3' end of *cyc* sequence, excluding the stop codon, was amplified by the primers CT-Cas1 (that hybridizes to *cyc* and includes a NotI site at the 5` end) and CT-Cas2. The first fraction of the Halo Tag was also amplified by PCR using the primers CT-Cas3 and CT-Cas4 (complementary to a Halo fragment sequence with the XhoI site added into the 5` end of the primer). The product of both reactions were mixed and used as a template for a new amplification, this time using the primers CT-Cas1 and CT-Cas4, generating the called cassette (figure 3.3). The cassette in the StrataClone vector, and pUAST + *cyc* start (from A) were digested with NotI and XhoI. Then, the cassette was cloned into pUAST + *cyc* start.

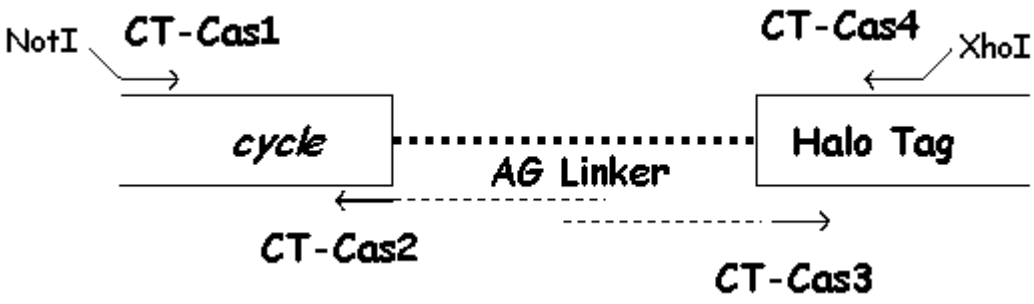

Figure 3.3 - Scheme of C-terminus Halo Tag cassette amplification by PCR.

C. To clone the missing middle part of *cyc* into pUAST + *cyc* start + cassette (from B), both were digested with PasI and Bsu36I.

D. The last step was the cloning of the Halo Tag end fragment into pUAST+ *cyc* + cassette (from C). For that, both were double digested with RsrII and XhoI.

3.3.1.2 N-terminus Halo Tag Construct

The N-terminal Halo Tag transgene was cloned into pUAST after performing various steps (figure 3.4):

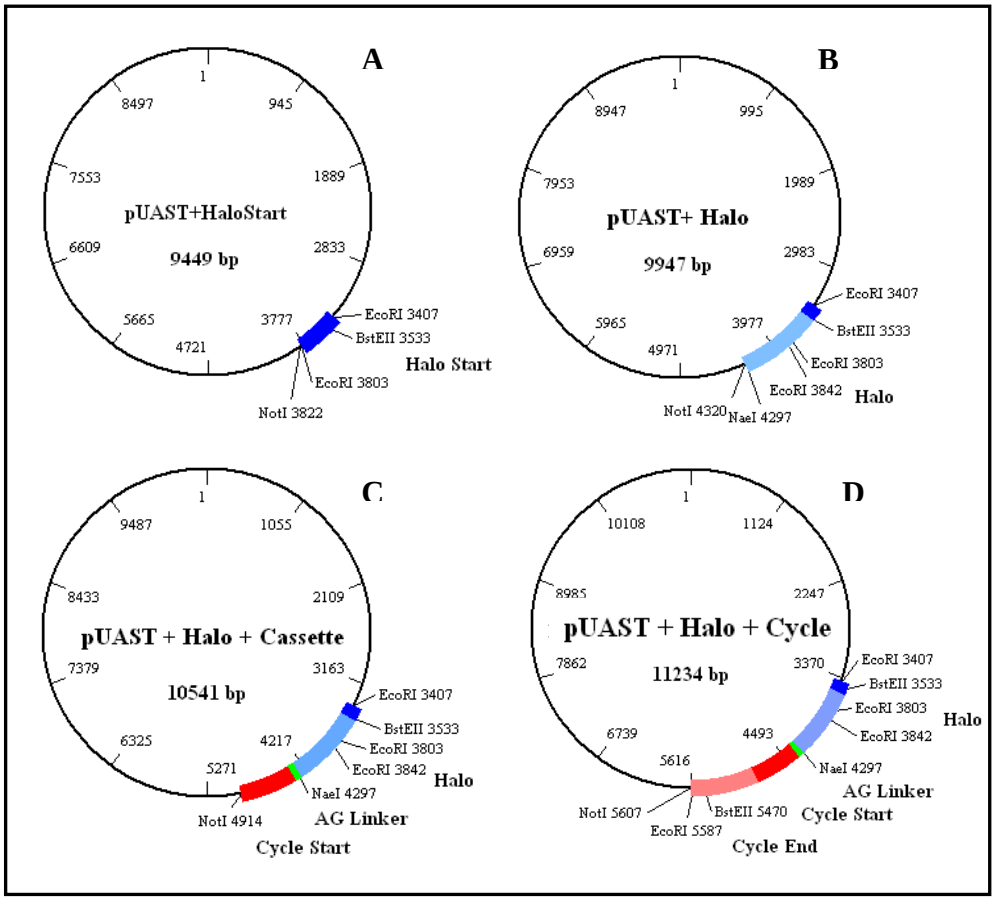

Figure 3.4 - Cloning scheme of N-terminal Halo Tag construct. Red: 5' end of *cycle*. **Pink:** 3' end of *cycle*. **Green:** AG Linker. **Dark blue:** 5' end of Halo Tag. **Light blue:** 3' end of Halo Tag.

A. The Halo Tag start was obtained via PCR with pTH2 as a template, and using NT-Halo1 and NT-Halo2 primers. Halo Tag start in StrataClone vector and pUAST were EcoRI digested. To check if the fragments were inserted in the correct orientation (since only one enzyme was used to clone them), another digestion was performed with the enzymes XhoI and BstEII. Depending on the direction that the fragment was inserted, the products would have different sizes, making it easy to distinguish the correct clone to select.

B. The missing fragment of Halo Tag and pUAST + Halo Tag start were cut by BstEII and NotI.

C. The cassette was obtained by three consecutives PCR reactions (figure 3.5). First using NT-Cas1 and NT-Cas2 and amplifying Halo Tag end + part of the AG linker. The second reaction, utilized NT-Cas3 and NT-Cas4 to amplify the other part of AG linker and *cyc* start. After this, NT-Cas1 and NT-Cas4 were used to amplify the cassette. StrataClone vector containing the cassette and pUAST + Halo Tag (from B) were digested with NaeI and NotI.

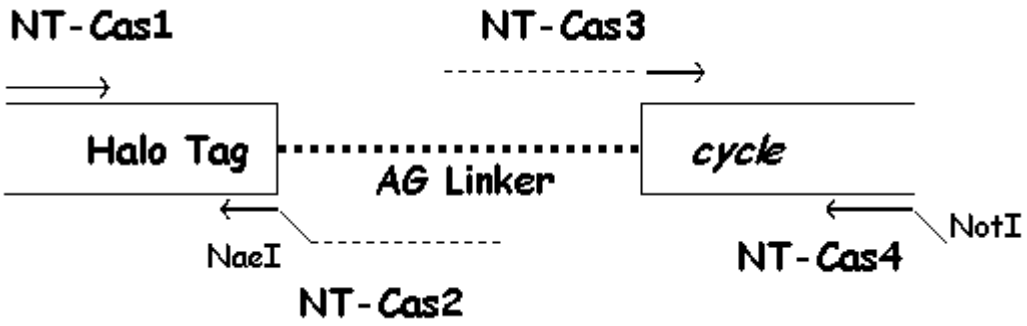

Figure 3.5 - Scheme of N-terminus Halo Tag cassette amplification by PCR.

D. As the last step, another PCR was carried out with the primers NT-Cyc1 and NT-Cyc2 generating *cyc* end as a product. *cyc* end in StrataClone vector along with pUAST + Halo + cassette were digested with PasI and NotI.

3.3.1.3 C-terminus Strep TagII Construct

To obtain the C-terminal Strep TagII construct in pUAST a similar cloning strategy as the previously described was used (figure 3.6):

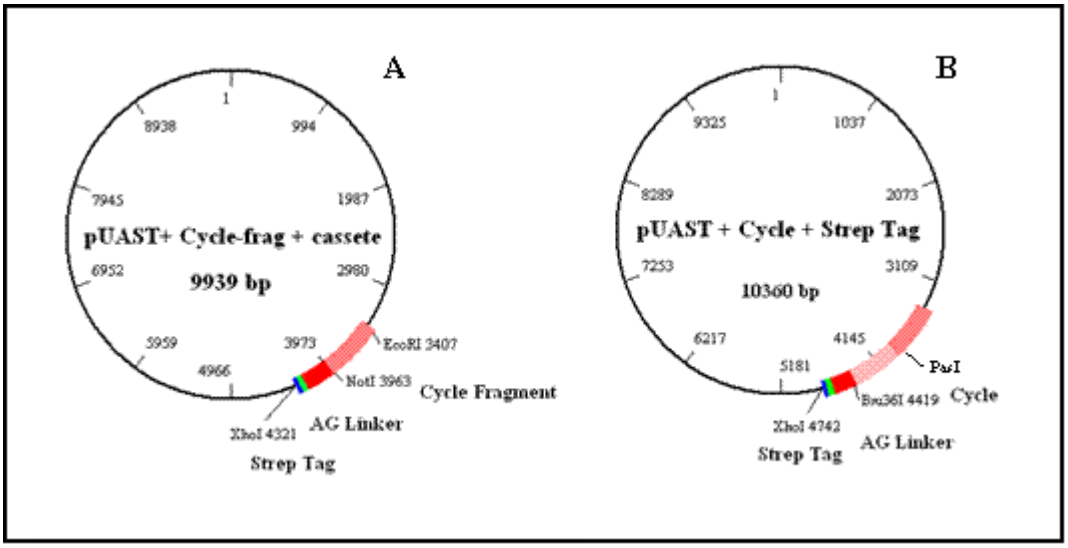

Figure 3.6 - Cloning scheme of C-terminal Strep TagII construct. **Red:** 3' end of *cycle*. **Dark Pink:** 3' end of *cycle*. **Light Pink:** middle part of *cycle*. **Green:** AG Linker. **Blue:** Strep TagII.

A. The C-Halo Tag cassette in SrataClone vector (see item 3.3.1.1 B) was used as a template in a PCR reaction to create a cassette containing Strep tag II instead (figure 3.7). A primer hybridizing to *cyc* sequence (CT-Cas1) and a primer binding to the final part of AG linker followed by Strep TagII and XhoI sequences (CT-Strep2) were

used in the PCR. The new cassette was cloned into pUAST + cyc Start, after digesting both of them with NotI and XhoI.

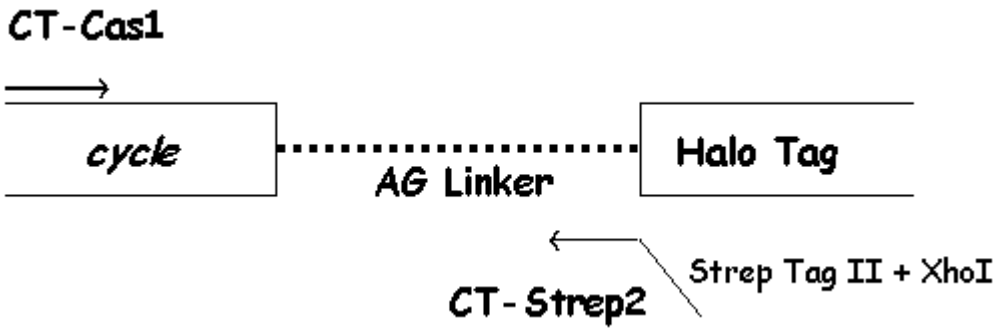

Figure 3.7 - Scheme of C-terminus Strep TagII cassette amplification by PCR.

B. To insert the missing part of *cyc*, pBluescript II KS+ containing *cyc* and pUAST + cyc fragment + cassette (from A) were cut with PasI and Bsu36I.

3.3.1.4 N-terminus Strep TagII Construct

The N-terminal Strep TagII cloning was completed after performing the steps described below (figure 3.8):

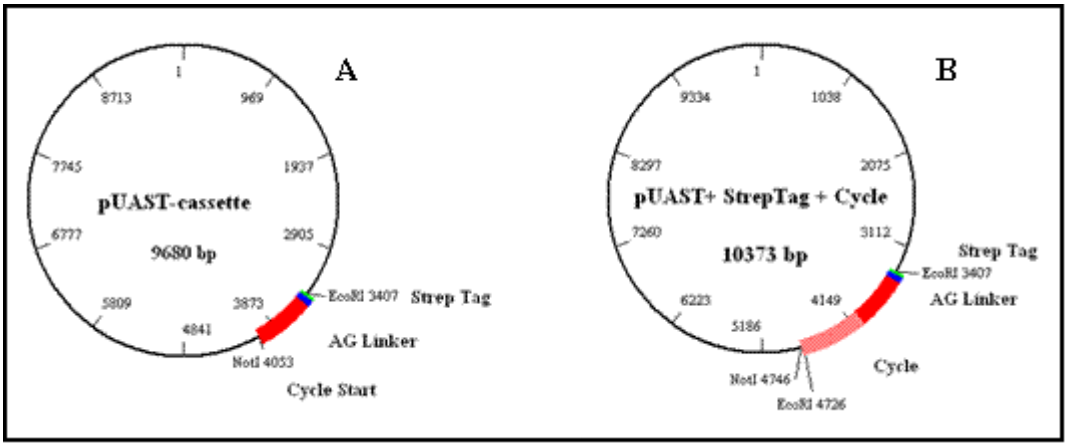

Figure 3.8 - Cloning scheme of N-terminal Strep TagII construct. Red: 5' end of *cycle*. **Pink:** 3' end of *cycle*. **Blue:** AG Linker. **Green:** Strep TagII.

A. To make the N-Strep Tag cassette (figure 3.9) a PCR reaction was performed using the N- Halo cassette as template (see 3.3.1.2 C) and the primers NT-Strep3 (that binds at the start of AG linker and has EcoRI and Strep TagII at the 5` end) and NT-Cas4 (that binds to *cyc* and has a NotI site). The N- Strep Tag cassette was inserted into the pUAST vector, after cutting both with the enzymes EcoRI and NotI.

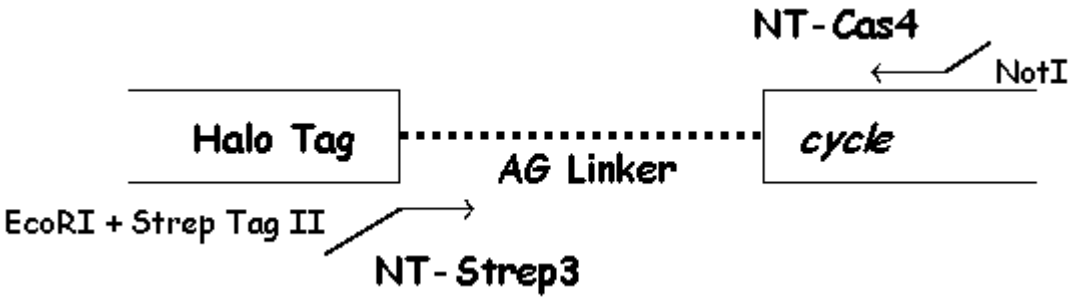

Figure 3.9 - Scheme of N-terminus Strep TagII cassette amplification by PCR.

B. Finally, the end of *cyc* sequence already digested with PasI and NotI (from 3.3.1.2 D) was cloned into pUAST + cassette (from A), previously cut with the same enzymes.

All the constructs, except C-terminus Strep TagII were sent to be injected into w^{1118} flies by BestGene (http://www.thebestgene.com/).

3.3.2 Checking the Constructs by PCR

To confirm that the injected flies had the construct, a PCR using a set of primers strategically located was performed. Figure 3.10 shows the 1.5% agarose gel where the samples were loaded. The expected band for N-Strep TagII amplicon has ~ 590 nucleotides, as seen in lanes 1 to 6. The N-Halo Tag product corresponds to ~ 600 nucleotides and was loaded in slots 9 to 17. In lanes 20 to 29, the C-Halo Tag band of

~ 410 nucleotides can be visualized. The negative controls without DNA did not amplify any band, as showed in lanes 8, 19 and 31. The same negative result was obtained when Canton S flies were used (slots 7, 18 and 30). The reactions loaded in slots 16 and 27 lack a band, suggesting that these amplifications didn't work.

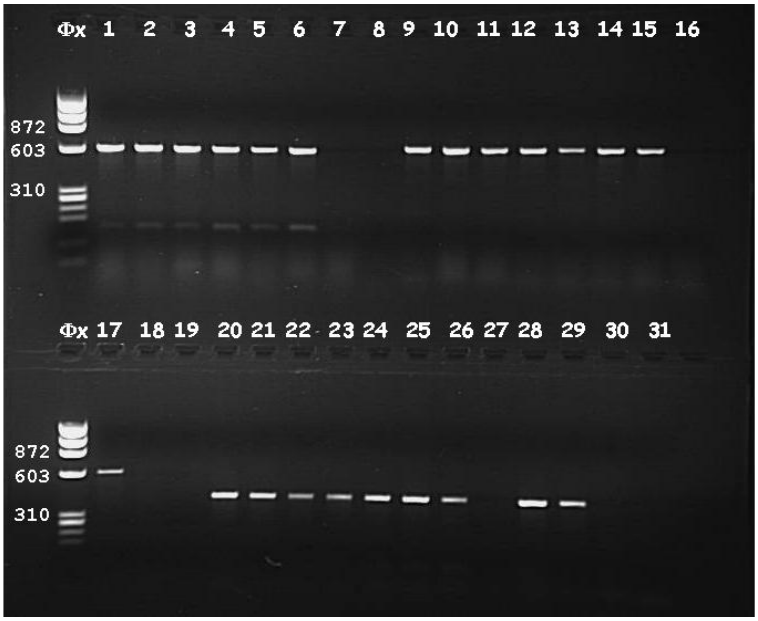

Figure 3.10 - Constructs identification by PCR. The PCR products were resolved on a 1.5% agarose gel. The numbers above each lane represent each fly tested. **ΦX:** ϕX HaeIII. **1 to 6:** N-terminal Strep TagII. **7:** Canton S. **8:** water control (no DNA). **9 to 17:** N-terminal Halo Tag. **18:** Canton S. **19:** water control (no DNA). **20 to 29:** C-terminal Halo Tag. **30:** Canton S. **31:** water control (no DNA).

3.3.3 Locomotor Activity of Flies Carrying the Transgenes

It has been shown in the laboratory that wild-type flies' locomotor behaviour shows a rhythmic profile in constant darkness (DD). In order to check whether the injection of the tagged constructs had disturbed the flies' activity profile some locomotor activity tests were performed under DD conditions and the results are represented in table 3.1.

Table 3.1 – Flies with the tagged construct behave rhythmically.

Genotype	N	Period ± SEM (h)	% Rhythmic
w; UAS Strep AG cyc; + (STREP N)	14	22.8 ± 0.1	71.4
w; UAS Strep AG cyc/Cyo; + (STREP N)	14	23.7 ± 0.1	100
w; UAS Halo AG cyc; + (HALO N)	10	23.2 ± 0.1	90
w; UAS Halo AG cyc/Cyo; + (HALO N)	15	23.4 ± 0.09	93.3
w; UAS cyc AG Halo; + (HALO C)	15	23.6 ± 0.09	80
w; UAS cyc AG Halo/Cyo; + (HALO C)	16	23.9 ± 0.1	100

Every fly carrying one copy of the N-terminus Strep tag construct showed rhythmic locomotor activity (figure 3.11) and the average period was $\tau = 23.7 \pm 0.1$ (table 3.1). In fact, as shown in figure 3.11, even the presence of two copies of the transgene did not disturb the locomotor behaviour of these flies, that continued to move rhythmically with a period of $\tau = 22.8 \pm 0.1$ (table 3.1). However, the period was significantly shorter when compared to Canton S flies by ANOVA ($F_{1,23}= 6.03$, $p= 0.022$).

As observed in figure 3.11, both homozygous and heterozygous flies for the N-terminus Halo tag transgene behaved like wild-type flies with period of activity of $\tau= 23.2 \pm 0.1$ and $\tau= 23.4 \pm 0.09$, respectively (table 3.1).

Finally, the activity test with flies containing the C-terminus Halo tag insert revealed that their locomotor profile was not altered, despite the number of copies that they have (figure 3.11). Both genotypes showed a normal behavioural period: $\tau= 23.9 \pm 0.1$ when only one copy of the Halo C transgene was present and $\tau= 23.6 \pm 0.09$ when flies were homozygous (table 3.1).

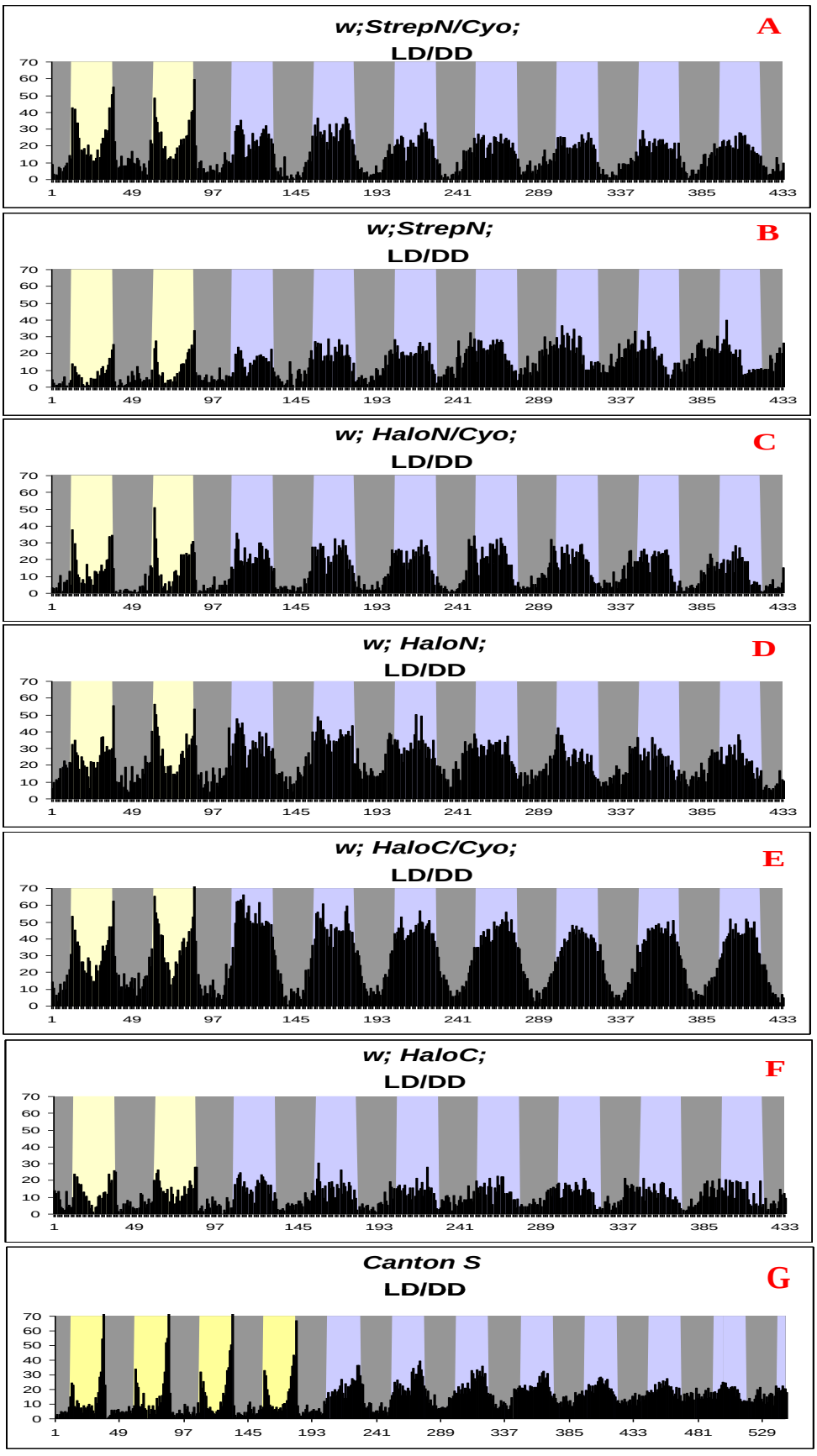

Figure 3.11 - Locomotor activity of tagged constructs in DD. A to F: 2 days LD, 7 days DD. **G:** 4 days LD, 7 days DD. **X-axis:** time in 30 minutes bins. **Y-axis:** mean

level of activity. **Yellow:** day. **Gray:** subjective night. **Blue:** subjective day. All genotypes were rhythmic and are indicated above each histogram.

3.3.4 Rescuing *cyc^{01}* arrhythmicity

It has been shown that *cyc^{01}* recessive mutants are completely arrhythmic in DD when homozygous (Rutila *et al*., 1998). Accordingly, the locomotor activity of flies expressing the tagged transgenes in clock cells was tested in a *cyc^{01}* background to check their ability to rescue *cyc^{01}* arrhythmicity by crossing each UAS line to *tim-Gal4*, which is expressed in all clock neurons (Emery *et al*., 1998).

The flies expressing the Strep N transgene were fully able to rescue *cyc^{01}* phenotype, and showed a wild type period of activity (τ= 24 ± 0.1). Likewise, around 60% of the flies expressing *cyc* tagged with Halo at the N terminus are rhythmic in constant darkness. However, when the Halo tag was fused to the C terminus the rescue level was poor and the flies were largely arrhythmic (see table 3.2 and figure 3.12).

Table 3.2 - Rescuing ability of the constructs in pacemaker cells.

Genotype	N	Period ± SEM (h)	% Rhythmic
w; UAS Strep AG cyc/tim-Gal4; cyc^{01} (STREP N)	16	24 ± 0.1	100
w; UAS Halo AG cyc/tim-Gal4; cyc^{01} (HALO N)	26	24.1 ± 0.3	62
w; UAS cyc AG Halo/tim-Gal4; cyc^{01} (HALO C)	43	-----	18

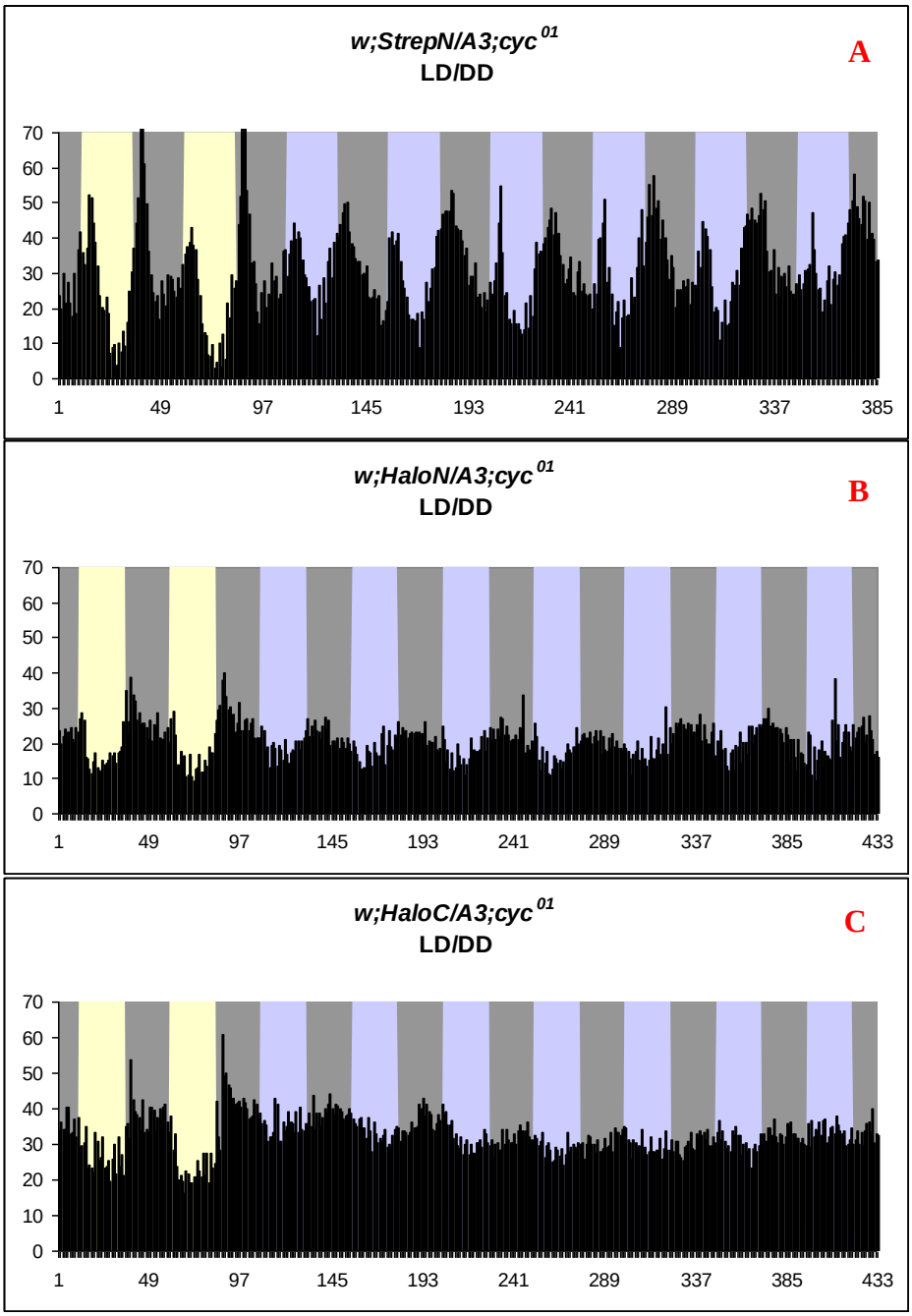

Figure 3.12 - Transgenic flies locomotor activity profiles in a *cyc*^{01} background. Graphs A shows 2 days of LD12:12 followed by 6 days of DD. Graphs B and C show 2 days of LD12:12 followed by 7 days of DD. Flies in graphs A and B are rhythmic in this condition. The X-axis represents the time measured in 30 minutes bins. The Y-axis represents the average level of activity. The yellow columns represent lights on, the grey columns represent lights off and the blue columns represent the subjective day.

3.3.5 Immunodetection of the Tags

Once the presence of the tags in the flies was confirmed by PCR it became necessary to test if they could be detected in Western Blot assays by specific antibodies.

The result of the Western Blot using rabbit polyclonal anti-Halo can be examined in figure 3.13, which illustrates the film after 5 mins of exposure. The antibody was first tested by using it at two different dilutions – 1:500 and 1:1.000 against proteins extracted from heads of wild-type flies (Canton S), flies over-expressing the Halo transgenes (*w; Halo construct/+; actin-Gal4/+*) and flies with the Halo transgenes expression restricted to the clock cells (*w; Halo construct/ tim-Gal4;+*) (figure 3.13). The antibody against Halo was expected to spot bands with approximately 85 kDa, when both constructs were tested. A band a little higher (~ 100 kDa) than 85 kDa (red arrow) could be observed in every lane loaded with proteins from flies expressing the Halo Tag insert, regardless of the antibody concentration. The same band was not observed when proteins from the negative control Canton S were loaded, suggesting that the correct band was identified.

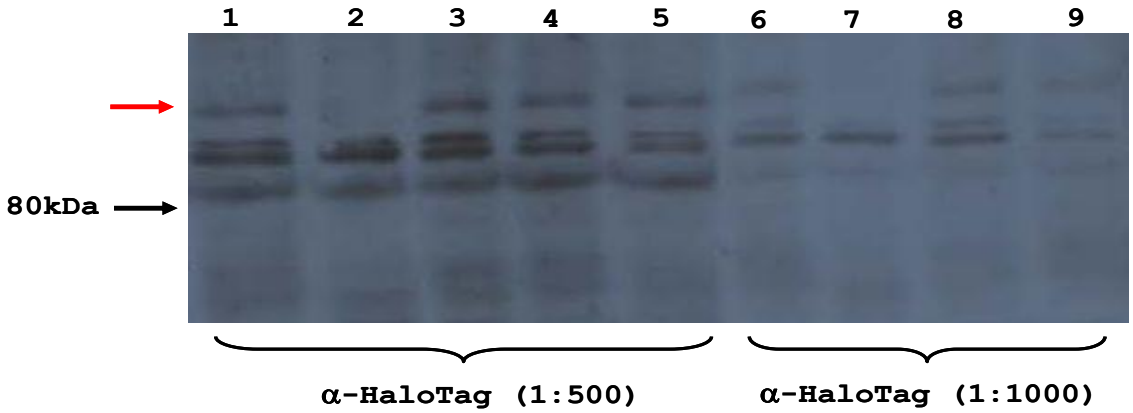

Figure 3.13 - Immunochemical identification of the constructs by mouse rabbit polyclonal anti-Halo in Western Blots. The red arrow points to the Halo Tag bands. The samples loaded in the SDS acrylamide gel are: **1:** *w; C-Halo Tag construct/ tim-*

Gal4; +, **2:** Canton S, **3:** *w; C-Halo Tag construct/ +*; *actin*-Gal4/ +, **4:** *w; N-HaloTag construct/ tim-Gal4; +*, **5:** *w; N-HaloTag construct/ +*; *actin*-Gal4/ +, **6:** *w; C-Halo Tag construct/ tim-Gal4; +*, **7:** Canton S, **8:** *w; C-Halo Tag construct/ +; actin-Gal4/ +*, **9:** *w; N-HaloTag construct/ tim-Gal4; +*. Lanes 1 to 5 were probed with α-Halo (1:500) and lanes 6 to 9 with α-Halo (1:1000).

Western blots were performed on heads of flies to check for expression of the Strep Tag transgene. The first antibody tested was mouse α-Strep Tag II (1:1000) to detect an approximately 50 kDa band (figure 3.14). Among all the detected bands, none has the expected size, not even in the protein extract from the positive control CPTI-001198 (lane 1), which has a protein trap vector containing the Strep Tag inserted (see chapter 4 for details). The closest band (~75kDa) seems to be detected not only in the flies expressing the Strep transgene (lanes 2 and 4) but in every sample incubated with this antibody, including the negative control Canton S (lane 3). The same is observed for the strongest band in the film (~180 kDa).

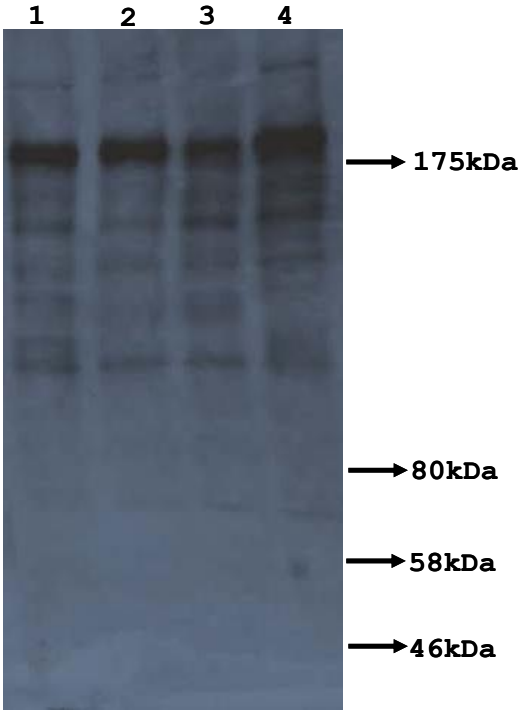

Figure 3.14 - Western Blot to identify the expression of the Strep construct using mouse monoclonal anti-Strep tagII. The samples loaded in the SDS acrylamide gel are: **1:** CPTI-001198, **2:** *w; N-Strep TagII construct/ tim-Gal4; +*, **3:** Canton S, **4:** *w;*

N-Strep TagII construct/ +; actin-Gal4/ +. Samples were probed with mouse α-Strep Tag II (1:1000).

Another attempt was made to identify the Strep construct in Western Blots by probing the proteins with a different antibody (figure 3.15), the anti-Strep TagII Horseradish Peroxidase (HRP) – conjugated (1:4000). Proteins were extracted from five different lines of flies with the Strep Tag construct inserted in different parts of the genome and the expression of the Strep Tag transgene was driven in the pacemaker cells (by *tim-Gal4*), as well as in every cell of the collected heads (by *actin- Gal4*). Only a very high band (~180 kDa) was detected and once again found in every sample including the negative control Canton S, suggesting that it does not represent the Strep Tag construct.

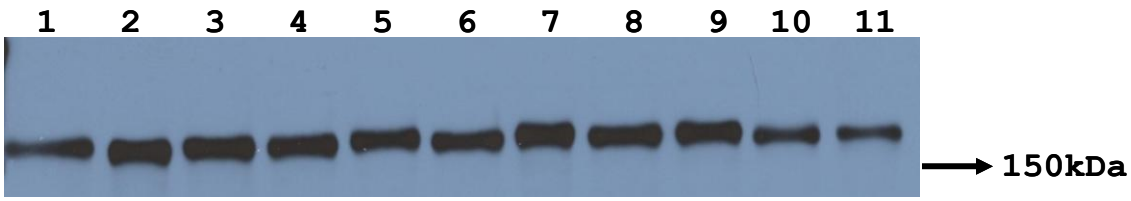

Figure 3.15 - Western Blot to identify the expression of the Strep construct using monoclonal anti-Strep tagII HRP. The samples loaded in the SDS acrylamide gel are: **1:** Canton S, **2:** *w; N-Strep TagII construct1/ tim-Gal4; +*, **3:** *w; N-Strep TagII construct1/ +; actin-Gal4/ +*, **4:** *w; N-Strep TagII construct2/ tim-Gal4; +*, **5:** *w; N-Strep TagII construct2/ +; actin-Gal4/ +*, **6:** *w; N-Strep TagII construct3/ tim-Gal4; +*, **7:** *w; N-Strep TagII construct3/ +; actin-Gal4/ +*,**8:** *w; N-Strep TagII construct4/ tim-Gal4; +*, **9:** *w; N-Strep TagII construct4/ +; actin-Gal4/ +*, **10:** *w; N-Strep TagII construct5/ tim-Gal4; +*, **11:** *w; N-Strep TagII construct5/ +; actin-Gal4/ +*. Samples were probed with α-Strep Tag II HRP (1:4000).

3.3.6 Co-Immunoprecipitation using Halo Tag

Flies containing the Halo Tag constructs were used in Co-Immunoprecipitation (Co-IP) assays in order to identify the proteins that are part of the CYC complex. With the aim of testing the technique, protein extracts collected at ZT 23 from heads of flies expressing the Halo C and Halo N trangenes were immobilised on HaloLink Resin beads. Canton S flies were also used as negative controls. After several washes to remove the proteins not tightly bound to the resin, the specific binding partners were eluted and analysed using SDS- polyacrilamide gel eletrophoresis. The protein extract before immunoprecipitation (input), the supernatant containing contaminants removed from the resin before the first wash (containing the unbound proteins) and the last wash were also loaded onto the gel. Because Halo Tag fusion proteins are covalently bound to the HaloLink resin and cannot be dissociated, antibodies against CYC known partners were used. The guinea-pig α-CLK (1:10000) antibody wasn't able to detect any protein band that was eluted from the HaloLink resin (see lanes 8 and 12 in figure 3.16) and from the washes either. The use of an antibody against PER (rabbit α-PER, 1:15000) also failed to detect a member of the CYC protein complex.

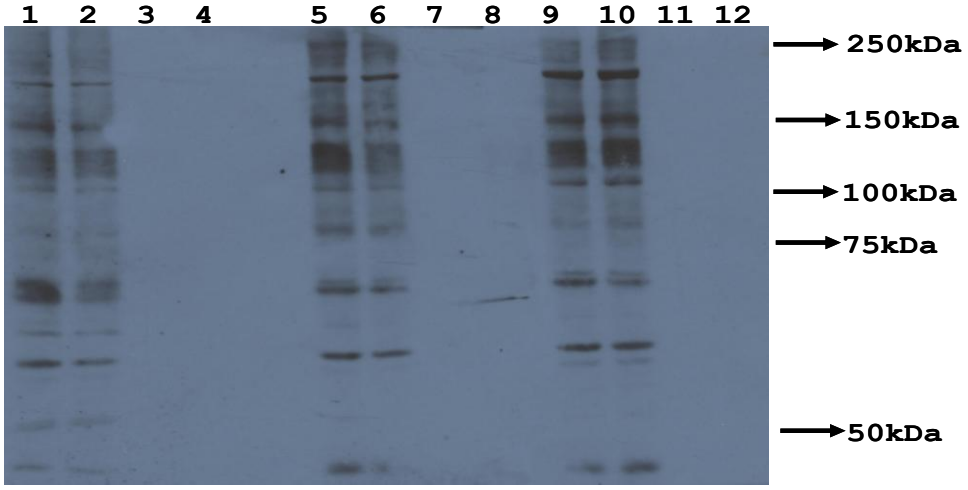

Figure 3.16 - Western Blot to detect the Halo Tag fusion protein bound to HaloLink resin. The samples were probed with guinea-pig α-CLK (1:10000). The

samples loaded in the SDS acrylamide gel are: **1:** Canton S input, **2:** Canton S supernatant, **3:** Canton S wash5, **4:** Canton S IP, **5:** *w; N-HaloTag construct/ tim-Gal4;* + input, **6:** *w; N-HaloTag construct/ tim-Gal4;* + supernatant, **7:** *w; N-HaloTag construct/ tim-Gal4;* + wash5, **8:** *w; N-HaloTag construct/ tim-Gal4;* + IP, **9:** *w; C-HaloTag construct/ tim-Gal4;* + input, **10:** *w; C-HaloTag construct/ tim-Gal4;* + supernatant, **11:** *w; C-HaloTag construct/ tim-Gal4;* + wash5, **12:** *w; C-HaloTag construct/ tim-Gal4;* + IP.

3.4 Discussion

The cloning of the tagged constructs was arduous and lengthy but proved to be successfully prepared by PCR reactions that revealed the presence of the inserts and by sequencing the DNA prior to the injection into the flies (appendix 1). The confirmation of the constructs insertion by PCR had two negative results (figure 3.10), lacking the expected band. It probably occurred due to an ineffective DNA extraction. However, after repeating the procedure the bands were amplified. The successful cloning process generated a number of lines with tagged CYC introduced into different chromosomes that can be useful for further experiments.

The use of the tagged flies in the study of the circadian clock and its molecular components requires that the insertion of the constructs does not disrupt its rhythmic behaviour. Locomotor activity experiments showed that these flies behave rhythmically when placed into constant darkness for several days, regardless of the number of the construct copies that they have (table 3.1). It is also important to check that tagged CYC is normally expressed in these flies and able to act as a key component of the molecular circadian clock. Indeed, flies containing Strep Tag and N Halo Tag inserts in a cyc^{01} background were capable of rescuing the arrhythmicity in DD (table 3.2). Although the line of C Halo Tag flies tested was not capable of recovering the locomotor rhythm in free-running conditions, different lines containing the same construct were not tested due to time constraints. Moreover, the locomotor

behaviour of these flies was not tested with *tim-Gal4* in a wild-type background, which might have disrupted the rhythms.

Another approach used in this work to reveal the expression of tagged CYC was its detection through antibody probing. The band spotted in the Western Blot assay by the Halo Tag antibody (figure 3.13), represents in all probability the introduced construct, even though it ran higher than expected. The prediction of the band size was performed by an online molecular weight calculator (http://au.expasy.org/tools/pi_tool.html) based on the protein's primary structure. For a better prediction, molecular weights can be determined via mass spectrometry. In addition, the lack of the band in Canton S flies, which were used as a negative control, is comforting. The stronger band observed when *actin-Gal4* was used as a driver (samples 3 and 5), as compared to *tim-Gal4* driven expressed proteins (samples 1 and 4), is also supportive since *tim-Gal4* directs the expression only in clock cells opposed to *actin*-Gal4 that drives ubiquitous expression. The immunodetection result indicates that although the flies carrying CYC fused with Halo Tag at its C terminus are not able to rescue cyc^{01} phenotype, the protein seems to be expressed.

Immunochemical reactions using two different antibodies have failed to reveal the expression of CYC tagged by Strep TagII (figures 3.14 and 3.15). Although a ~180 kDa strong band was identified, it cannot be associated with the insert, given that it was also found in the negative control Canton S samples. The reason why the Strep TagII construct was not detected remains unclear. However, the absence of the band in the positive control CPTI-001198 suggests that the antibodies were unproductive. Moreover, the presence of the construct has been shown at the DNA level (figure 3.10), and the expression of Strep tagged CYC was evidenced by the

rescue of locomotor activity (table 3.2), once again indicating that the antibody failed to detect the construct.

Halo Tagged flies were used in CoIP experiment in a struggle to identify the binding partners of CYC. Unfortunately, no expected binding partners (CLK, PER) of the Halo fused CYC was found in the samples eluted from the HaloLink resin after the immunoprecipitation via the Halo Tag. One possible explanation is the inability of the antibodies to detect small amounts of proteins, since some of them could be washed out. Another possibility is that the folding of the protein is somehow hiding the Halo Tag and not allowing it to bind to the resin. Even though the Halo fused proteins were detected by the α-Halo antibody in Western Blots, it is essential to remember that in this case the polypeptides were in a denatured state once they had been treated with strong reducing agents to remove secondary and tertiary structures. New CoIP attempts could be done using different lines containing the C Halo Tag construct, and also trying to use more effective antibodies to detect CYC partners. However, this whole process would be exceedingly time consuming with no guarantee of a successful conclusion. Regrettably, I was forced to abandon this approach to studying protein partners of the CYC complex.

Chapter 4: Clock Mutants Screen - CPTI flies

4.1 Introduction

The CPTI lines have the protein trap vector randomly inserted by a piggyBac transposon-based strategy (figure 4.1). During mRNA production, the introns are spliced out and the exons are joined together before translation. The presence of splice acceptor (SA) and splice donor (SD) sites in the protein trap construct leads to its incorporation into the spliced mRNA product. If the piggyBac element transposes into the intron of a gene in the correct orientation and the correct frame a functional GFP fusion will be created which should be detectable under a fluorescence microscope. The insertion of this construct into the genome can affect the expression and the functionality of the trapped protein.

Figure 4.1 - Representation of the protein trap vector.

Some of the Drosophila canonical genes for the normal functioning of the circadian time-keeping system were identified by forward genetic screens. Mutations in most of these genes cause flies to behave arrhythmically in constant darkness, although morphologically they show no phenotype (Young and Kay, 2001). The circadian behaviour of wild-type flies is also dramatically affected by constant light (LL), resulting in arrhythmic behaviour (Konopka *et al.*, 1989). This response to LL is dependent on the constitutive activation of the photoreceptor CRY which leads to the degradation of the clock protein TIM (Ceriani *et al.*, 1999). In the absence of TIM

flies become arrhythmic as the negative feedback loop is disrupted (Sehgal *et al*., 1994).

Accordingly, a locomotor activity screen under LL conditions using the CPTI lines was performed to identify new components of the light input pathway. In addition the locomotor behaviour of the CPTI lines was also screened in DD to identify any tagged gene that might represent a new core clock gene or a clock controlled output gene. The UAS-GAL4 system was subsequently used to silence any candidate genes (Brand and Perrimon, 1993).

4.2 Methods

The CPTI flies have been generated in Cambridge using a protein trap vector which was randomly inserted throughout the genome into the sequence *TTAA* using the *piggyBac* transposon (http://www.flyprot.org/). As shown in figure 4.1, the vectors are marked by a *mini-white* cassette, contain an artificial *GFP* exon flanked by strong splice-acceptor and splice-donor sequences, and two affinity tags (Calmodulin-binding peptide – CBP and Strep TagII). These flies are being screened by 33 different UK *Drosophila* groups.

4.2.1 Screening

In order to screen the locomotor profile of CPTI lines in free running conditions, both DD and LL, the flies were previously entrained to 12 hour: 12 hour LD cycle at 25ºC for 2 to 3 days. Two hundred lines have been tested in DD and 147 in LL (see appendix 2), revealing interesting phenotypes as such as arrhythmicity in DD, rhythmicity in LL and also altered periods. The trapped genes in these lines were identified in the Flannotator website (http://xena.gen.cam.ac.uk/flannotator /index. php). Finally, 12 lines (table 4.1) were selected for a comprehensive study exploiting

the generation of transgenic flies, using any existing variant in these genes and UAS-RNAi to knock-down these genes. The mutants were obtained from the Bloomington Drosophila Stock Center (http://flystocks.bio.indiana.edu/) and the RNAi lines from "Vienna Drosophila RNAi Center" (http://stockcenter.vdrc.at/ control/main), unless otherwise stated. The RNAi flies were crossed to the driver *tim-Gal4* and had their locomotor behaviour tested as described in section 2.2.2.

Table 4.1 - Lines selected for further investigation.

CPTI Line	Trapped Gene
CPTI-000216	*Lk6*
CPTI-000303	*Got1*
CPTI-000340	CG33158
CPTI-000720	*Ptp69D*
CPTI-000764	*kat80*
CPTI-000850	*pbl*
CPTI-000902	*Glycogenin*
CPTI-100002	*Gs2*
CPTI-100008	*Mi-2*
CPTI-100017	CG31352
CPTI-100034	*14-3-3epsilon*
CPTI-100051	*Rab11*

4.3 Results

4.3.1 CPTI Flies Locomotor Activity Screen

From the screening of 200 different CPTI lines under DD, six candidates were selected, that showed an altered phenotype when compared to wild-type flies. Additionally, 7 out of 147 tested lines behaved differently from wild-type flies when placed in LL and were chosen for further study. The activity records of these atypical

locomotor phenotypes of the 12 CPTI lines selected for supplementary investigation are listed in table 4.2.

Table 4.2 - Selected candidates from CPTI flies locomotor screen.

CPTI Line	Trapped Gene	Locomotor Activity			Light Regime
		% Rhythmic	Mean Period ± SEM	n	
CPTI-000216	*Lk6*	74.19	24.73 ± 0.2	31	Constant Light (LL)
CPTI-000303	*Got1*	90	24.99 ± 0.15	20	
CPTI-000764	*kat80*	66.6	24.45 ± 0.33	21	
CPTI-000850	*pbl*	69.2	25.53 ± 0.4	26	
CPTI-000902	*Glycogenin*	94.7	24.71 ± 0.14	19	
CPTI-100002	*Gs2*	50	25.1 ± 0.2	18	
CPTI-100051	*Rab11*	69	26.28 ± 0.8	9	
CPTI-000340	CG33158	15.4	- - - - -	26	Constant Darkness (DD)
CPTI-000720	*Ptp69D*	20	- - - - -	20	
CPTI-100008	*Mi-2*	69.2	25.07 ± 0.24	26	
CPTI-100017	CG31352	77.4	26.24 ± 0.3	31	
CPTI-100034	*14-3-3ε*	3.7	- - - - -	27	
CPTI-100051	*Rab11*	66.6	26.05 ± 0.3	27	

4.3.1.1 Selected CPTI candidates in LL

The ability of seven CPTI lines to maintain a robust rhythm in LL can be observed in figure 4.2. The spectral analysis and the autocorrelation graph are shown for each selected line in figure 4.3. The flies were entrained to 12-h LD cycles for two to three days and were individually monitored in LL for five to ten days. Additionally, it can be noticed that the behaviour of the control Canton S wild-type control was arrhythmic in LL. These seven trapped genes were select for a detailed locomotor activity analysis exploiting the accessibility of mutants and RNAi lines, since their rhythmicity in LL can indicate an involvement in the light input pathway of the clock.

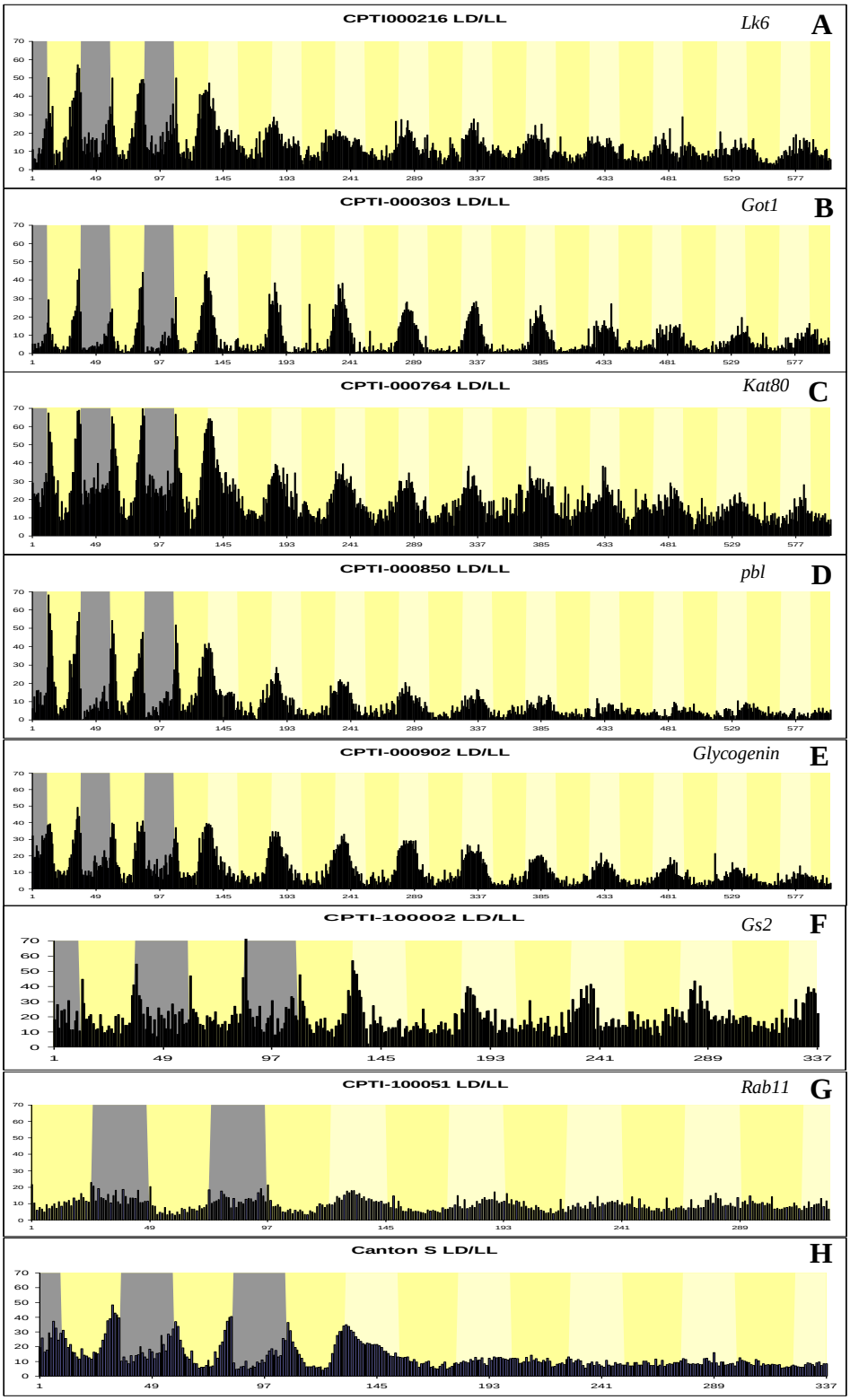

<u>Figure 4.2</u> – Locomotor activity of CPTI lines in LL. A to E: 3 days LD, 10 days LL. **F and H:** 3 days LD, 5 days LL. **G:** 2 days LD, 5 days LL. **X-axis:** time in 30 minutes bins. **Y-axis:** mean level of activity. **Gray:** dark. **Dark yellow:** subjective daylight. **Yellow:** subjective night. **A:** CPTI-000216. **B:** CPTI-000303. **C:** CPTI-000764. **D:** CPTI-000850. **E:** CPTI-000902. **F:** CPTI-100002 **G:** CPTI-100051. **H:** Canton S. All the fly lines were rhythmic, except Canton S (H).

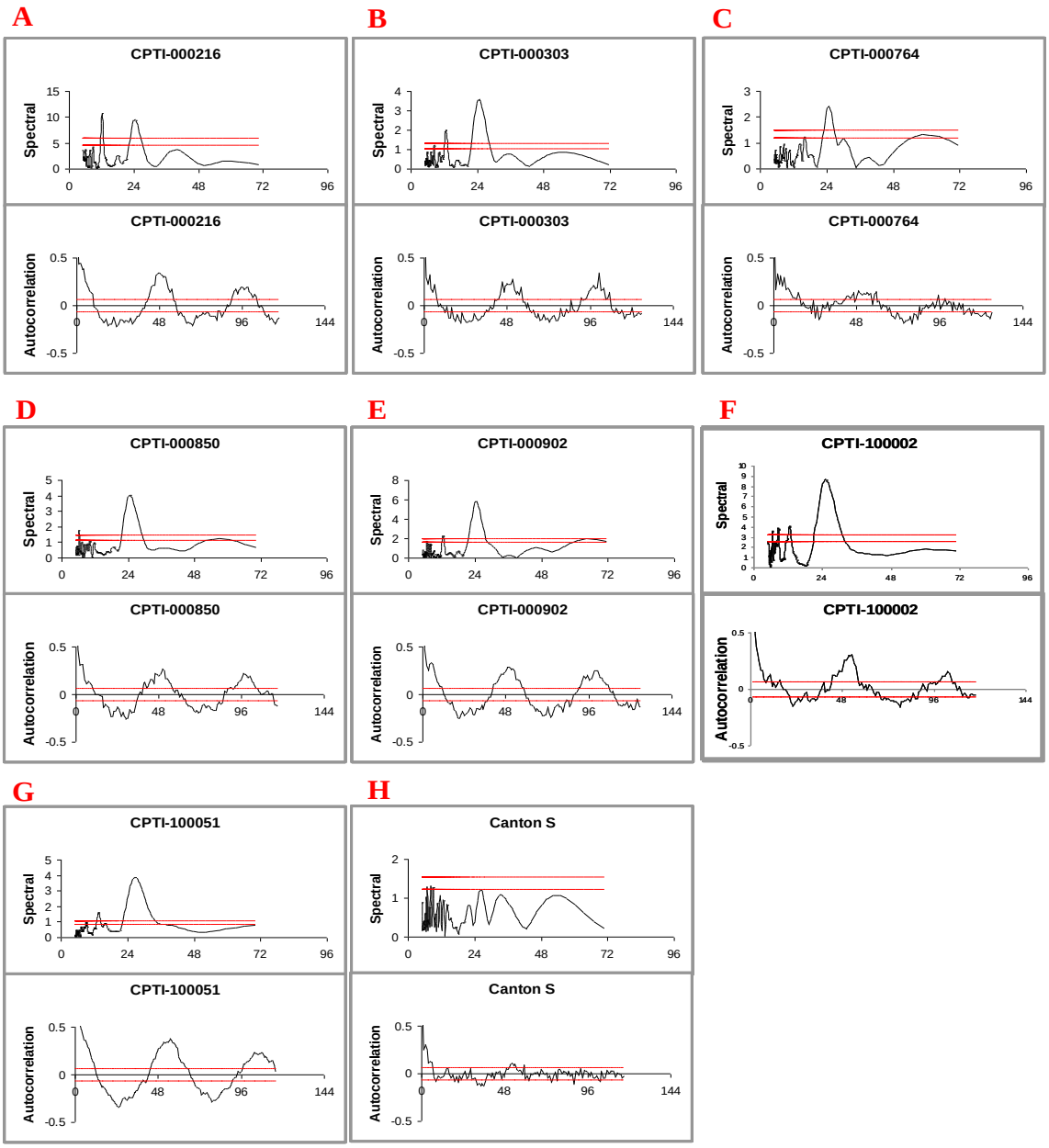

Figure 4.3 - **CPTI lines in LL. Upper panel:** CLEAN spectral plot along with the 95% and 99% Monte Carlo confidence limits. **Lower panel:** Autocorrelogram with the canonical 95% confidence limits. **A:** CPTI-000216. **B:** CPTI-000303. **C:** CPTI-000764. **D:** CPTI-000850. **E:** CPTI-000902. **F:** CPTI-100002 **G:** CPTI-100051. **H:** Canton S.

4.3.1.2 Selected CPTI Candidates in DD

The locomotor activity of CPTI flies analysed in DD revealed 4 arrhythmic CPTI lines (table 4.2). Figure 4.4 shows that during five to seven days of DD these

flies were not able to sustain rhythmic behaviour, contrary to Canton S flies In the same conditions, three different lines displayed long periods (figure 4.5): CPTI-100008 (τ= 25.07 ± 0.24), CPTI-100017 (τ= 26.24 ± 0.3) and CPTI-100051 (26.05 ± 0.3). One-way ANOVA showed that the periods were significantly longer when compared to Canton S: CPTI-100008 ($F_{1,30}$= 23.028, $p< 10^{-4}$), CPTI-100017 ($F_{1,42}$= 43.403, $p< 10^{-5}$) and CPTI-100051 ($F_{1,30}$= 30.079, $p< 10^{-4}$).

These six trapped genes completed the list of mutant flies to be used in the subsequent activity experiments.

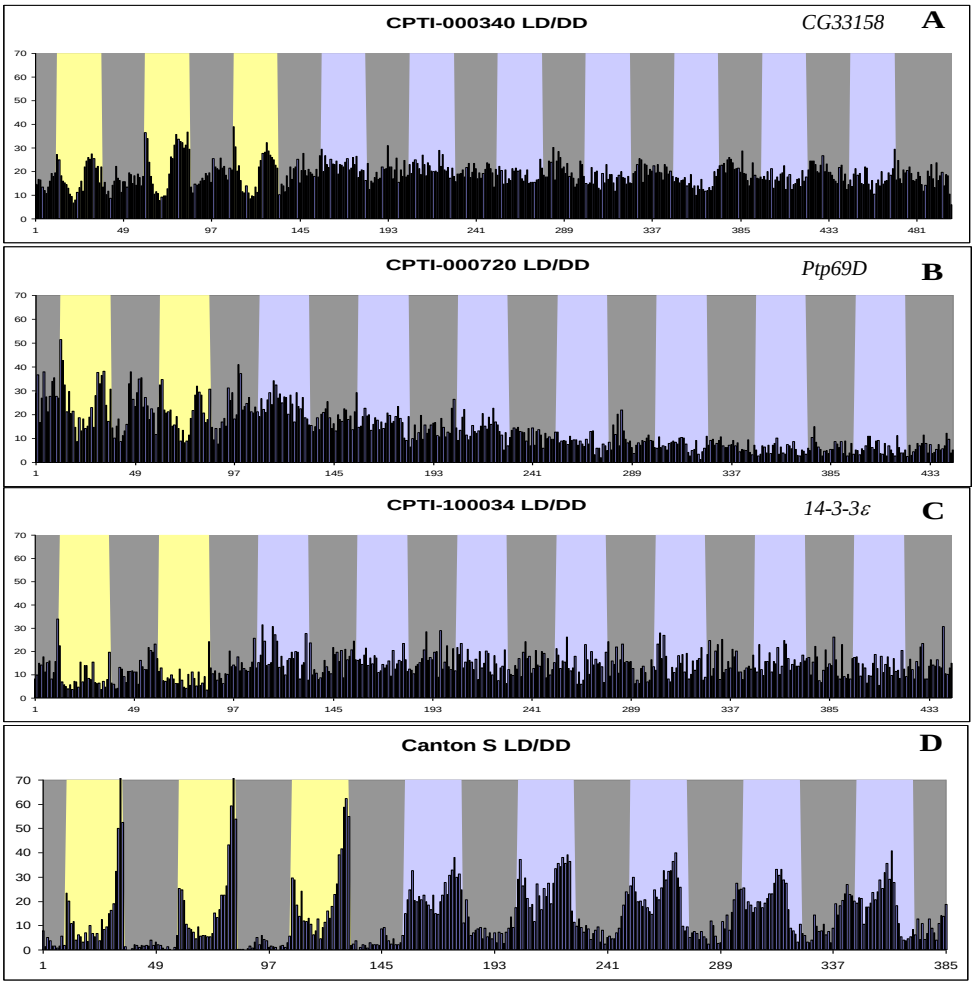

Figure 4.4 – Mean activity of CPTI lines in DD. A: 3 days LD, 7 days DD. **B and C:** 2 days LD, 7 days DD. **D:** 3 days LD, 5 days DD. **X-axis:** time in 30 minutes bins. **Y-axis:** mean level of activity. **Yellow:** day. **Gray:** subjective night. **Blue:** subjective day. **A:** CPTI-000340. **B:** CPTI-000720. **C:** CPTI-100034. **D:** Canton S. All genotypes showed arrhythmicity, except the control Canton S (D).

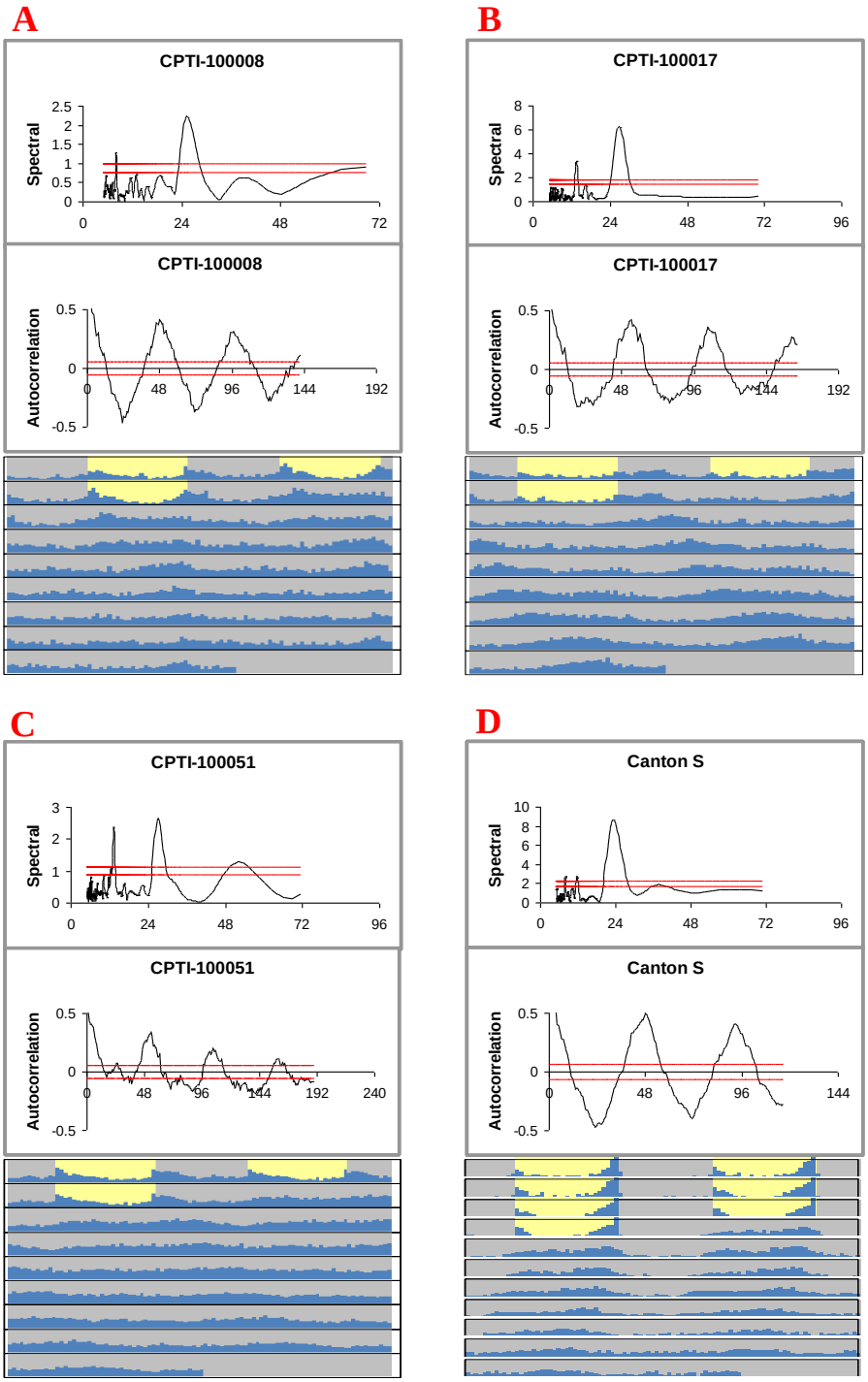

<u>Figure 4.5</u> - CPTI lines showing long period in DD. Upper panel: CLEAN spectral plot along with the 95% and 99% Monte Carlo confidence limits. **Central panel:** Autocorrelogram along with the canonical 95% confidence limits. **Lower panel:** Double-plotted histogram of locomotor activity. **Yellow:** Day. **Gray:** Subjective night. **A:** CPTI-100008, τ= 25.07 h (± 0.24). **B:** CPTI-100017, τ= 26.24 h (± 0.3). **C:** CPTI-100051, τ= 26.05 h (± 0.3). **D:** Canton S, τ= 23.49 h (± 0.2).

4.3.2 RNAi mediated downregulation and mutant analysis of candidate genes

Available UAS-RNAi and mutants of these 12 genes from stock centres were employed in additional studies. All the UAS-RNAi lines were crossed to *tim-Gal4* to downregulate the expression of the target genes in clock cells. To maximise the efficacy of RNAi mediated knockdown in the flies, a *UAS-dicer2* element was co-expressed with some of the RNAi lines (Dietzl *et al*., 2007). *Dicer2* is an important gene for the production of small inhibitory RNAs from double-stranded RNA and the assembly of RNAi silencing complexes in *Drosophila* (Lee *et al*., 2004).

4.3.2.1 *14-3-3ε*- (CPTI-100034 – Arrhythmic in DD)

Although CPTI-100034 (the line in which the gene *14-3-3ε* was trapped) showed arrhythmicity in DD, the same phenotype was not observed when heterozygous mutant and deficiency (in which the gene is deleted) were tested. In both cases, all the flies presented a rhythmic locomotor behaviour with a normal period of activity. The two lines were also tested in LL and showed a normal arrhythmic profile (table 4.3).

The mutant (Bloomington ID 12142) has a *P{lacW}* inserted into an intron of *14-3-3ε* and contains a cDNA minigene of *white* and the *lacZ* reporter gene within the P element (Bier *et al*., 1989).

Table 4.3 - Variants of *14-3-3ε* are rhythmic in DD but not in LL.

Mutant/Deficiency (Bloomington ID)	DD			LL		
	% Rhythmic	Mean period ± SEM	n	% Rhythmic	Mean period ± SEM	n
y^1 *w*;; P{lacW}14-3-3*ε^{j2B10}*/ +* (12142)	100	23.5 ± 0.07	29	33	-----	13
w^{1118}*;; Df(3R)Exel6178/+* (7657)	100	23.38 ± 0.07	16	0	-----	16

4.3.2.2 *CG31352* (CPTI-100017 – Long Period in DD)

CG31352 was studied in more detail as CPTI-100017 has a long period of activity in DD. Conversely, silencing this gene in the clock cells revealed that approximately 87% of the flies displayed a rhythmic profile in LL with a long behavioural period of 27.4 ± 0.7 h (table 4.4 and figure 4.6). The expression of *dicer2* did not increase the proportion of rhythmic flies, nor lengthened the period. As can be seen in table 4.4, the RNAi UAS control (VDRC 49111), *tim-Gal4* control and the mutant (Bloomington ID12941), performed normally in both light regimes. This mutant is characterised by the transposition of the *P{SUPor-P}* element in one *CG31352* intron, which is a modified P element carrying two copies of the suppressor of *Hairy-wing [su(Hw)]* binding regions isolated from *gypsy* transposable element (Roseman *et al*., 1995).

Table 4.4 - Silencing *CG31352* in the pacemaker cells leads to rhythmicity in LL.

Mutants (Bloomington ID)	DD			LL		
	% Rhythmic	Mean period ± SEM	n	% Rhythmic	Mean period ± SEM	n
y^1 w^{67c23};; P{SUPor-P} CG31352^{KG03651} ry^{506} (12941)	93.3	24.19 ± 0.13	14	0	-----	9
RNAi (VDRC ID)	**DD**			**LL**		
	% Rhythmic	**Mean period ± SEM**	**n**	**% Rhythmic**	**Mean period ± SEM**	**n**
w;tim-Gal4/RNAi CG31352;+ (VDRC 49111)	100	24.21 ± 0.13	16	87.5	27.4 ± 0.7	16
w;tim-Gal4 UASdcr2/ RNAi CG31352; (VDRC 49111)	100	24.49 ± 0.12	12	75	26.8 ± 0.18	12
VDRC 49111 (Control)	93.3	23.9 ± 0.09	15	17.9	-----	56
w;tim-Gal4;+ (Control)	71	24.5 ± 0.3	31	4	-----	51
w;tim-Gal4 UASdcr2/+; (Control)	100	24.2 ± 0.06	30	47	----	28

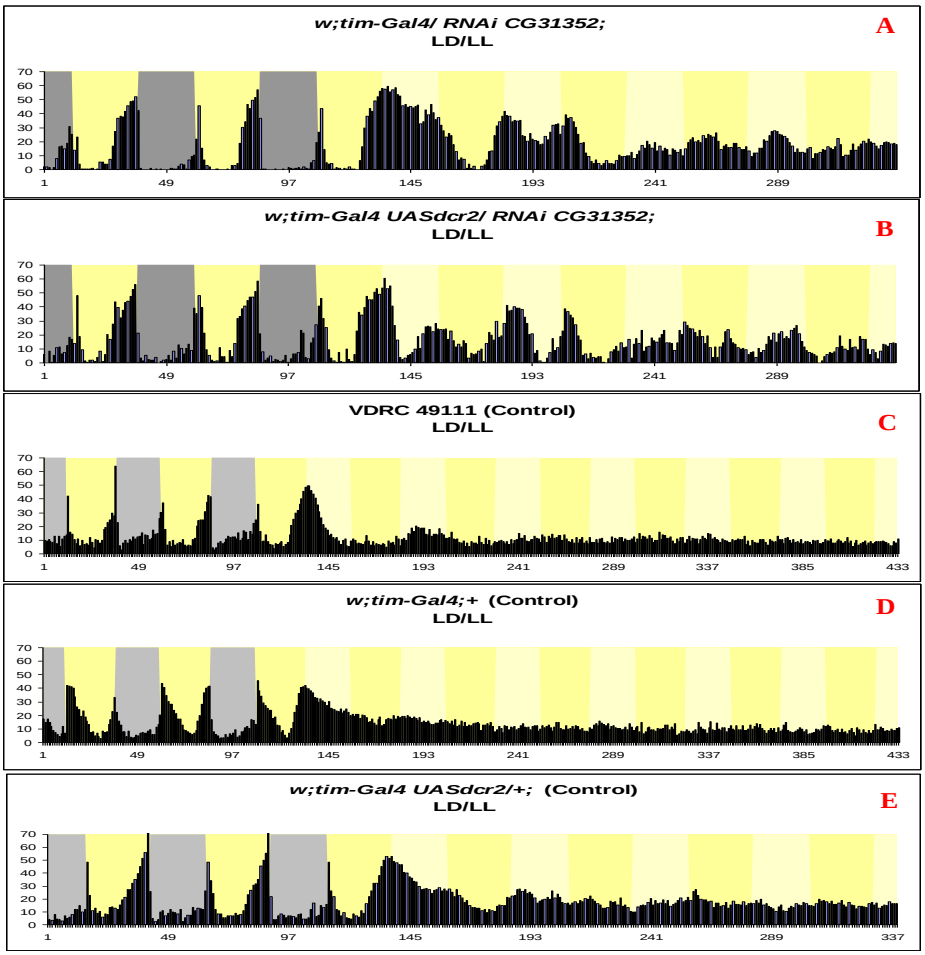

Figure 4.6 – Locomotor activity of silenced *CG31352* in LL. A, B and E: 2 days LD, 5 days LL. **C and D:** 2 days LD, 7 days LL. **X-axis:** time in 30 minutes bins. **Y-axis:** mean level of activity. **Gray:** dark. **Dark yellow:** subjective daylight. **Yellow:** subjective night. Genotypes are indicated above each histogram. Flies down-regulating *CG31352* (graphs A and B) are rhythmic.

4.3.2.3 *Lk6* (CPTI-000216 – Rhythmic in LL)

Two different mutants and two RNAi lines of *Lk6* were studied in DD and LL. The *Lk6* mutants have a P element inserted in the first intron of the gene that has been imprecisely excised from the genome. $Lk6^{1}$ (Bloomington ID 8706) contains a 3kb deletion that removes an alternative 5' exon, and in $Lk6^{2}$ (Bloomington ID 8707) the deletion removes all exons 3' of the P-element insertion site (Arquier *et al*., 2005). None of the lines showed abnormal behaviour in DD or LL (table 4.5).

Table 4.5 - *Lk6* regular behaviour in LL and DD.

Mutants (Bloomington ID)	DD			LL		
	% Rhythmic	Mean period ± SEM	n	% Rhythmic	Mean period ± SEM	n
w^{1118};; $Lk6^{[1]}$/+ (8706)	66.6	23.24 ± 0.24	6	12.5	-----	8
w^{1118};; $Lk6^{[2]}$/+ (8707)	100	23.47 ± 0.07	16	18.8	-----	16
RNAi (VDRC ID)	**DD**			**LL**		
	% Rhythmic	**Mean period ± SEM**	**n**	**% Rhythmic**	**Mean period ± SEM**	**n**
w;tim-Gal4/+;RNAi Lk6/;+ (VDRC 30389)	92.5	24.1 ± 0.07	40	31.8	-----	22
w;tim-Gal4/+;RNAi Lk6/;+ (VDRC 32885)	100	23.9 ± 0.13	15	28.6	-----	14
VDRC 30389 (Control)	75	23.9 ± 0.25	16	-----	-----	---

4.3.2.4 *Rab11* (CPTI-100051 – Rhythmic in LL and Long Period in DD)

CPTI-100051, which has the construct inserted in the *Rab11* gene, was the only line that showed a phenotype in both lighting conditions (table 4.2). Analysis of the mutant and RNAi lines in DD revealed that all the flies were rhythmic and had periods close to 24 h (table 4.6), challenging the 2h lengthened period found for CPTI-100051 flies. Moreover, the mutant (Bloomington ID 21463) that carries the double transposable element *P{wHy}* did not show abnormal behaviour in LL.

Table 4.6 - Normal behaviour of *Rab11* variants in DD and LL.

Mutant (Bloomington ID)	DD			LL		
	% Rhythmic	Mean period ± SEM	n	% Rhythmic	Mean period ± SEM	n
y^1 w^{67c23};;P{wHy} $Rab11^{DG0950}$/+ (21463)	100	23.2 ± 0. 09	16	31	-----	16
RNAi (VDRC ID)	**DD**			**LL**		
	% Rhythmic	**Mean period ± SEM**	**n**	**% Rhythmic**	**Mean period ± SEM**	**n**
w;tim-Gal4/+;RNAi Rab11/;+ (VDRC 22198)	100	24.1 ± 0.08	27	-----	-----	---
VDRC 22198 (Control)	-----	-----	---	20	-----	10

4.3.2.5 *CG33158* (CPTI-000340 – Arrhythmic in DD)

The knockdown of *CG33158* using three different RNAi lines did not disrupt locomotor activity in DD (table 4.7). A similar phenotypic profile was observed with the *Mi{ET1}* transposon (Bloomington ID 24745), and in flies heterozygous for a deficiency (Bloomington ID 7608). The *Mi{ET1}* element has the *Gal4* gene and *GFP* carried by the transposon *Minos*, an element isolated from *Drosophila hydei* (Metaxakis *et al*., 2005). Furthermore, the mutant and two of the down-regulated lines (VDRC 44737 and VDRC 34885) have rhythmic profiles in LL, with long periods of activity (figure 4.7). However, in LL, flies silenced by VDRC 34885 only displayed rhythmicity when *dicer2* was also expressed (table 4.7). Moreover, the control VDRC 44737 was also rhythmic.

Table 4.7 – Disruption of *CG33158* affects behaviour in LL.

Mutant/Deficiency (Bloomington ID)	DD			LL		
	% Rhythmic	Mean ± SEM	n	% Rhythmic	Mean period ± SEM	n
w^{1118};; *Df(3L)Exel6129/+* (7608)	100	24.18 ± 0.07	16	6.7	-----	15
w^{1118};; *Mi{ET1} CG33158*^{MB05135} (24745)	100	24.3 ± 0.07	16	100	28.11 ± 0.4	16
RNAi (VDRC ID)	**DD**			**LL**		
	% Rhythmic	Mean period ± SEM	n	% Rhythmic	Mean period ± SEM	n
w;tim-Gal4/RNAi CG33158;+ (VDRC 44737)	87.5	24.5 ± 0.17	8	100	28.4 ± 1.3	6
w;tim-Gal4/+;RNAi CG33158/;+ (VDRC 34885)	100	24.2 ± 0.11	25	25	-----	16
w;tim-Gal4/+;RNAi CG33158/;+ (VDRC 47738)	100	23.9 ± 0.07	15	35.8	-----	14
w;tim-Gal4 UAS dcr2/+; RNAi CG33158/+ (VDRC 34885)	81.25	24.49 ± 0.11	16	75	28.3 ± 0.47	16
w;tim-Gal4;+ (Control)	71	24.5 ± 0.3	31	4	-----	51
w;tim-Gal4 UASdcr2/+; (Control)	100	24.2 ± 0.06	30	47	----	28
VDRC 34885 (Control)	-----	-----	---	23	-----	17
VDRC 47737 (Control)	-----	-----	---	55	28.8 ± 0.9	11

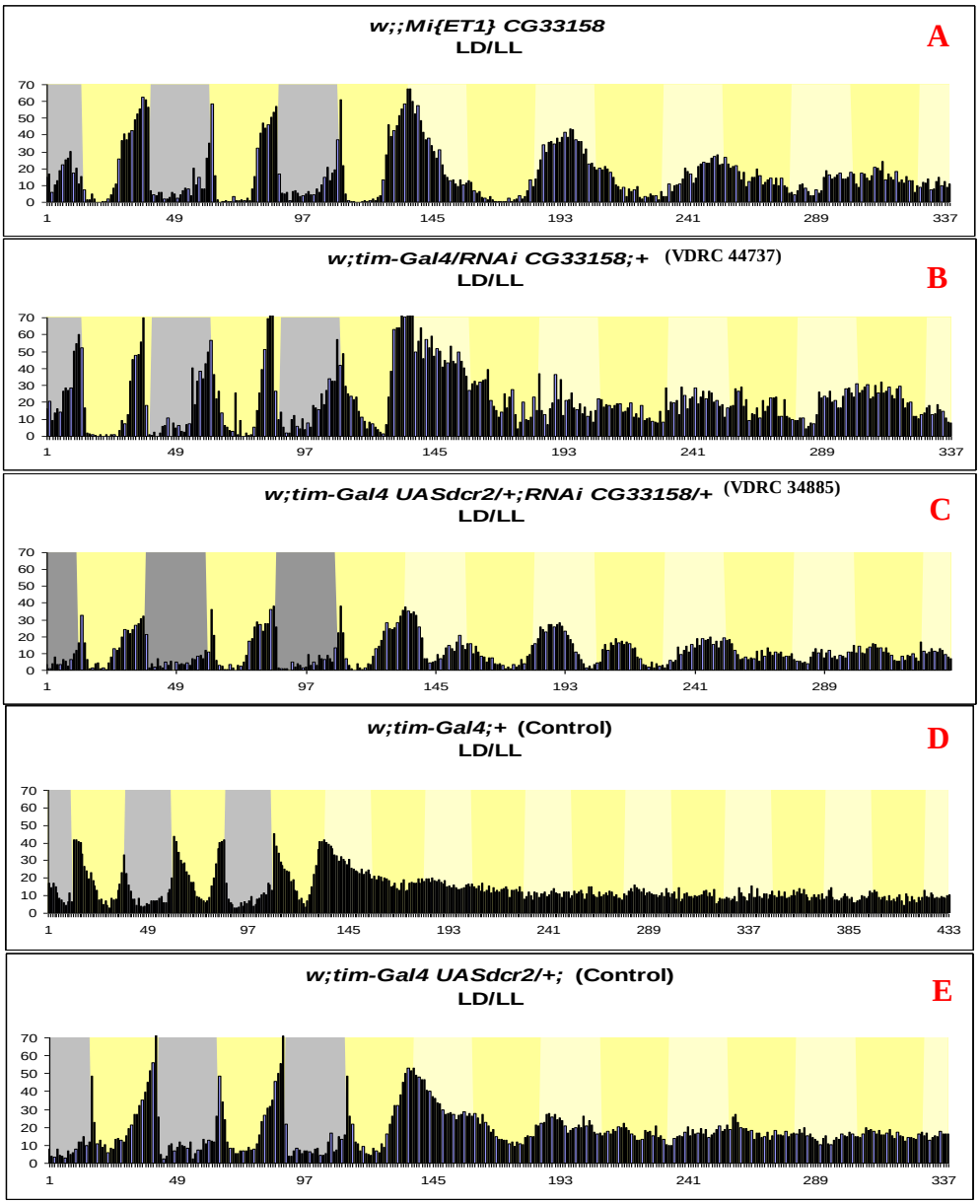

Figure 4.7 –***CG33158* mutants in LL. A, B, C and E:** 2 days LD, 5 days LL. **D:** 2 days LD, 7 days LL. **X-axis:** time in 30 minutes bins. **Y-axis:** mean level of activity. **Gray:** dark. **Dark yellow:** subjective daylight. **Yellow:** subjective night. Genotypes are indicated above each histogram. Flies with disrupted *CG33158* function (A, B and C) are rhythmic. The *tim-Gal4* and *tim-Gal4 UASdcr2* controls are arrhythmic in LL (D and E).

4.3.2.6 *Glycogenin* (CPTI-000902 – Rhythmic in LL)

Down-regulating *Glycogenin* in the clock cells corroborates the previous result from the CPTI line in that flies are rhythmic in LL (table 4.8). However, rhythmic

behaviour was detected in ~56% of the *UAS-RNAi* control flies (VDRC 35452) suggesting that caution should be exercised over any conclusions (figure 4.8). Also, *Glycogenin* RNAi in DD gives a period close to 24 h (table 4.8).

Table 4.8 – Behaviour of flies knocking down *Glycogenin*.

RNAi (VDRC ID)	DD			LL		
	% Rhythmic	Mean period ± SEM	n	% Rhythmic	Mean period ± SEM	n
w;tim-Gal4/RNAi Glycogenin;+ (VDRC 35452)	95.6	24.03 ± 0.13	23	93.7	28.9 ± 0.8	16
VDRC 35452 (Control)	93.75	23.85 ± 0.17	16	56.3	28.8 ± 0.57	55
w;tim-Gal4;+ (Control)	71	24.5 ± 0.3	31	4	-----	51

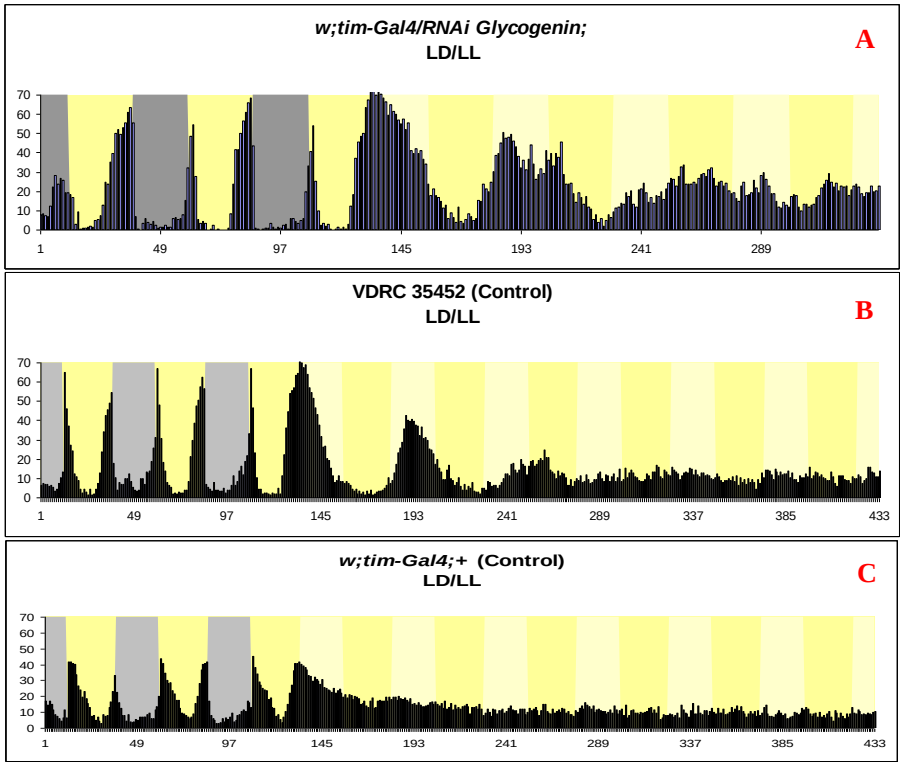

Figure 4.8 - Mean activity of *Glycogenin* RNAi in LL. A: 2 days LD, 5 days LL. **B and C:** 2 days LD, 7 days LL. **X-axis:** time in 30 minutes bins. **Y-axis:** mean level of activity. **Gray:** dark. **Dark yellow:** subjective daylight. **Yellow:** subjective night. Genotypes are indicated above each histogram.

4.3.2.7 *Katanin80* (*kat80*) (CPTI-000764 – Rhythmic in LL)

Two *kat80* mutants (Bloomington ID 12979 and 17187) and one RNA interference line (VDRC 24175) were tested in DD and LL. One of the mutants carries a *P{SUPor-P}* element, described in section 4.3.2.2, and the other has a *P{EP}* element, which contains UAS binding sites and the mini-*white* gene (Rorth *et al*., 1998). In DD, none of these lines showed any obvious abnormalities and they were all robustly rhythmic, with a period length close to that of control flies (table 4.9). On the other hand, down-regulating *kat80* in clock cells with *tim-Gal4* resulted in LL rhythmicity (figure 4.9). However it seems that the rhythmicity was an effect of the background, since the RNAi control (VDRC 24175) was also rhythmic.

Table 4.9 - Down-regulated *kat80* is rhythmic in LL.

Mutants (Bloomington ID)	DD			LL		
	% Rhythmic	Mean period ± SEM	n	% Rhythmic	Mean period ± SEM	n
y^1 *P{SUPor-P}kat80*^{KG02315} *;;* (12979)	86.2	23.58 ± 0.19	29	21.6	-----	26
w^{1118} *P{EP}kat80*^{EP620} (17187)	100	23.52 ± 0.16	15	0	-----	15
RNAi (VDRC ID)	**DD**			**LL**		
	% Rhythmic	Mean period ± SEM	n	% Rhythmic	Mean period ± SEM	n
w;tim-Gal4/RNAi kat80;+ (VDRC 24175)	85.2	24.48 ± 0.11	27	58.3	28.21 ± 0.6	12
VDRC 24175 (Control)	-----	-----	---	55	28.8 ± 1.9	11
w;tim-Gal4;+ (Control)	71	24.5 ± 0.3	31	4	-----	51

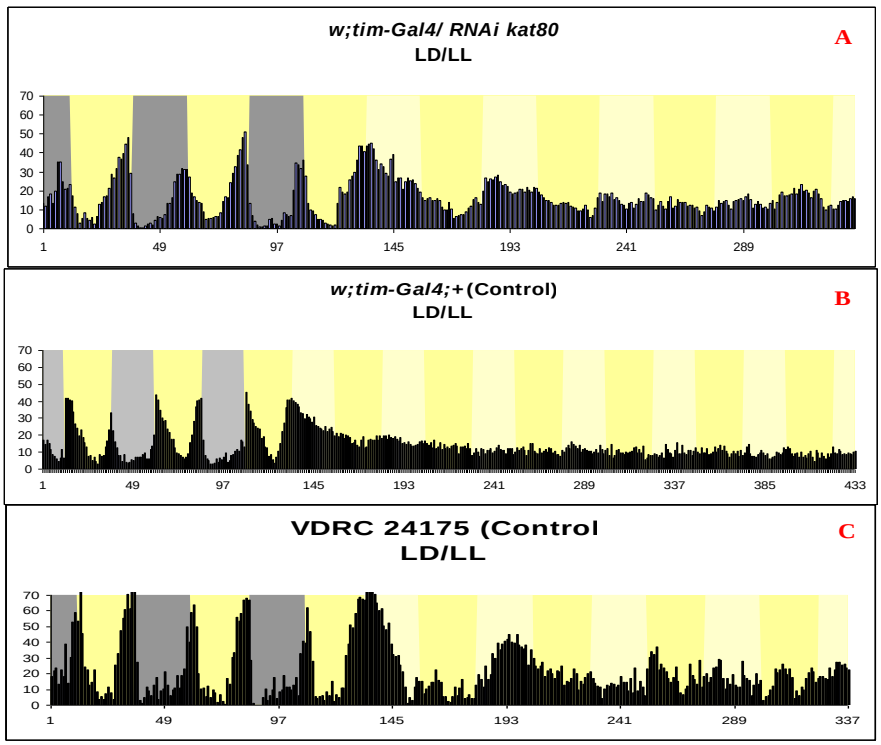

Figure 4.9 – Locomotor activity of knocked down *kat80* flies in LL. A and C: 2 days LD, 5 days LL. **B:** 2 days LD, 7 days LL. **X-axis:** time in 30 minutes bins. **Y-axis:** mean level of activity. **Gray:** dark. **Dark yellow:** subjective daylight. **Yellow:** subjective night. Genotypes are indicated above each histogram.

4.3.2.8 *Mi-2* (CPTI-100008 – Long Period in DD)

In order to check that *Mi-2* misexpression results in a long period of activity, as seen with CPTI-100008 in DD, two mutants, two deficiencies that delete *Mi-2* and one RNA interference line (VDRC10766) were used (table 4.10). Mutants with the *P{EPgy2}* element containing a UAS binding site, mini-*white* gene and an intronless *yellow* gene marker (Bellen *et al.*, 2004) was crossed to *tim-Gal4*. Flies down-regulating *Mi-2* in clock tissues showed long periods. Although the knockdown of *Mi-2* showed significantly long periods (τ= 25.15 ± 0.3) in DD ($F_{1,54}$= 57.466, p=4.68E-06) compared to the UAS control (VDRC10766 control), these flies didn't show a

significantly difference from *tim-Gal4* control ($F_{1,29}$= 0.53666, p= 0.46970). In LL, all mutant and RNAi flies were arrhythmic (table 4.10).

Table 4.10 - Locomotor behaviour of *Mi-2* variants.

Mutants/Deficiencies (Bloomington ID)	DD			LL		
	% Rhythmic	Mean period ± SEM	n	% Rhythmic	Mean period ± SEM	n
y^1 w^{67c23};; P{EPgy2}Mi-$2^{EY13252}$/+ (21089)	93.3	23.63 ± 0.08	16	28.6	-----	14
w; tim-Gal4/+; P{EPgy2}Mi-$2^{EY13252}$/+ (21089)	100	24.2 ± 0.15	16	31.3	-----	16
y^1 w^{67c23};; P{wHy}Mi-$2^{DG14402}$ Su(Tpl)^{DG14402}/+ (20417)	100	23.6 ± 0.06	16	31	-----	16
w^{1118};; Df(3L)BSC1/+ (5086)	92.3	23.7 ± 0.07	26	12	-----	26
w^{1118};; Df(3L)BSC2/+ (5087)	100	23.7 ± 0.07	25	12	-----	25
RNAi (VDRC ID)	**DD**			**LL**		
	% Rhythmic	**Mean period ± SEM**	**n**	**% Rhythmic**	**Mean period ± SEM**	**n**
w;tim-Gal4/+;RNAi Mi-2/+ (VDRC 10766)	100	25.15 ± 0.3	12	47	-----	15
w;tim-Gal4 UAS dicer2/+; RNAi Mi-2/+ (VDRC 10766)	97.4	24.7 ± 0.07	79	-----	-----	---
VDRC10766 (Control)	97.8	23.7 ± 0.06	46	25	-----	5
w;tim-Gal4;+ (Control)	71	24.5 ± 0.3	31	4	-----	51
w;tim-Gal4 UASdcr2/+; (Control)	100	24.2 ± 0.06	30	47	----	28

4.3.2.9 *Pebble* (CPTI-000850 – Rhythmic in LL)

Two ethyl methanesulfonate (EMS) mutants and two RNAi lines were studied. *pbl^3* (Bloomington ID 9358) has a premature stop codon, and represent a loss of function allele, while *pbl^5* (Bloomington ID 2452) represents a missense mutation caused by a nucleotide substitution (Prokopenko *et al.*, 1999). In DD all genotypes

were robustly rhythmic, with a period length close to that of control flies (table 4.11), whereas in LL two lines acted rhythmically (figure 4.10). Half of the tested *pbl*^{3} mutants showed rhythmicity and 78% of RNAi flies have rhythms in LL. However, the same rhythmic phenotype was observed with UAS RNAi control (VDRC 35350) so any conclusions must remain tentative.

Table 4.11 – Rhythmic behaviour in LL of *pbl.*

Mutants (Bloomington ID)	**DD**			**LL**		
	% Rhythmic	**Mean period ± SEM**	**n**	**% Rhythmic**	**Mean period ± SEM**	**n**
w;; pbl*^{3}*/+* (9358)	100	23.56 ± 0.11	16	50	25.5 ± 0.9	15
;;pbl^{5}*/+* (2452)	100	23.67 ± 0.08	16	12.5	-----	16
RNAi (VDRC ID)	**DD**			**LL**		
	% Rhythmic	**Mean period ± SEM**	**n**	**% Rhythmic**	**Mean period ± SEM**	**n**
w;tim-Gal4/RNAi pbl;+ (VDRC 35349)	100	24.2 ± 0.09	25	14.3	-----	7
w;tim-Gal4/RNAi pbl;+ (VDRC 35350)	100	24.18 ± 0.1	28	78.5	26.4 ± 0.3	28
VDRC 35350 (Control)	92.3	23.9 ± 0.14	13	73	26.2 ± 0.5	11
VDRC 35349 (Control)	100	23.8 ± 0.28	6	36	-----	11

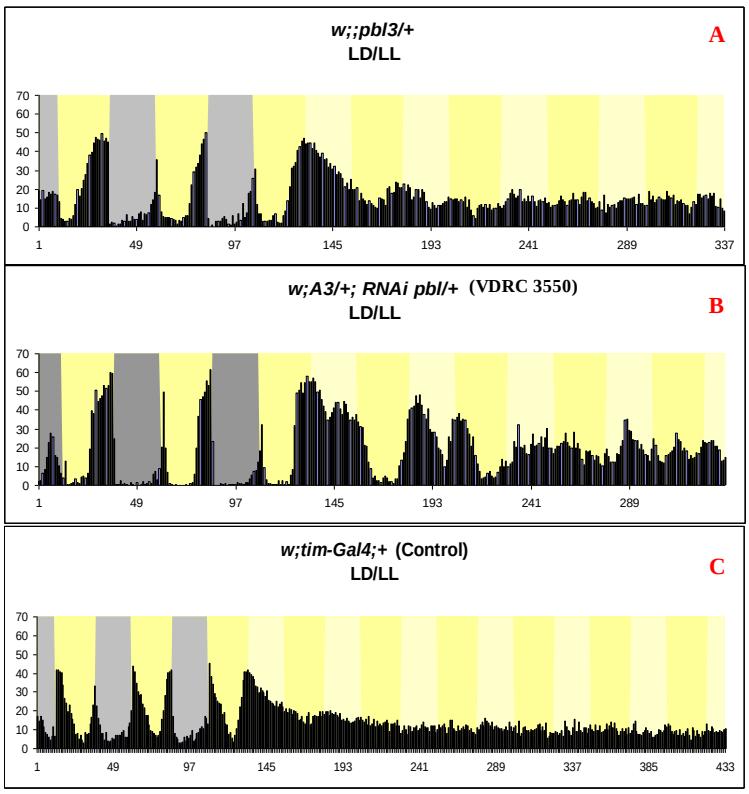

Figure 4.10 – Mean activity of *pbl* variants in LL. A and B: 2 days LD, 5 days LL. **C:** 2 days LD, 7 days LL. **X-axis:** time in 30 minutes bins. **Y-axis:** mean level of activity. **Gray:** dark. **Dark yellow:** subjective daylight. **Yellow:** subjective night. Genotypes are indicated above each histogram. pbl^{3} mutants and flies silencing *pbl* (A) are rhythmic. The *tim-Gal4* control (C) is arrhythmic.

4.3.2.10 *Protein tyrosine phosphatase 69D* (*Ptp69D*) (CPTI-000720 – Arrhythmic in DD

Three loss of function *Ptp69D* mutants were analysed in LL. $Ptp69D^{D1515}$ results in a truncated protein before the catalytic domain. The mutation in $Ptp69D^{D1689}$ is also predicted to result in a shortened protein caused by an amino acid replacement to a stop codon (W54STOP). The mutation in $Ptp69D^{H24}$ replaces an invariant Gly residue (G1105R) flanking the active site of the first phosphatase domain (Newsome *et al.*, 2000). The three mutants did not show abnormal behaviour in DD nor LL. The same profile was observed in homozygous flies that carried a deletion of *Ptp69D* (Bloomington ID 5090). Among five RNAi lines, two (VDRC 4789 and VDRC

40631) showed rhythmicity in LL (figure 4.11). In fact, the rhythm in VDRC 4789 RNAi flies was also confirmed when *dicer2* was expressed (table 4.12), however the period did not seem to be lengthened in these flies.

Table 4.12 – Knocking down *Ptp69D* causes rhythmicity in LL.

Mutants/Deficiency (Bloomington ID)	DD			LL		
	% Rhythmic	Mean period ± SEM	n	% Rhythmic	Mean period ± SEM	n
w;;Ptp69D^{D1515}/+ (*)	100	23.9 ± 0.14	16	0	-----	16
w;;Ptp69D^{D1689}/+ (*)	100	23.4 ± 0.07	16	0	-----	15
w;;Ptp69D^{H24}/+ (*)	93.7	23.9 ± 0.07	16	6.3	-----	16
w*;; Df(3L)8ex25 (5090)	93.75	23.21 ± 0.19	16	25	-----	16
RNAi (VDRC ID)	**DD**			**LL**		
	% Rhythmic	**Mean period ± SEM**	**n**	**% Rhythmic**	**Mean period ± SEM**	**n**
w;tim-Gal4/+; RNAiPtp69D/;+ (VDRC 4789)	100	23.8 ± 0.09	20	60	27 ± 0.6	15
w;tim-Gal4/+; RNAiPtp69D/;+ (VDRC 27090)	100	24.17 ± 0.12	16	37.5	-----	16
w;tim-Gal4/+; RNAiPtp69D/;+ (VDRC 27091)	100	24.3 ± 0.12	15	13.4	-----	15
w;tim-Gal4/RNAiPtp69D;+ (VDRC 40631)	100	24.5 ± 0.12	15	66.6	26.2 ± 0.55	15
w;tim-Gal4/RNAiPtp69D;+ (VDRC 942)	100	24.2 ± 0.14	16	37.5	-----	16
w;tim-Gal4 UAS dcr2/+; RNAi Ptp69D/+ (VDRC 4789)	93.75	23.85 ± 0.2	16	62.5	26.6 ± 0.5	16
VDRC 27090 (Control)	93.3	23.9 ± 0.18	15	27	-----	11
VDRC 942 (Control)	-----	-----	---	29	-----	7
VDRC 4789 (Control)	-----	-----	---	25	-----	5

(*)These fly lines were kindly provided by Takashi Suzuki at Max Planck Institute of Neurobiology.

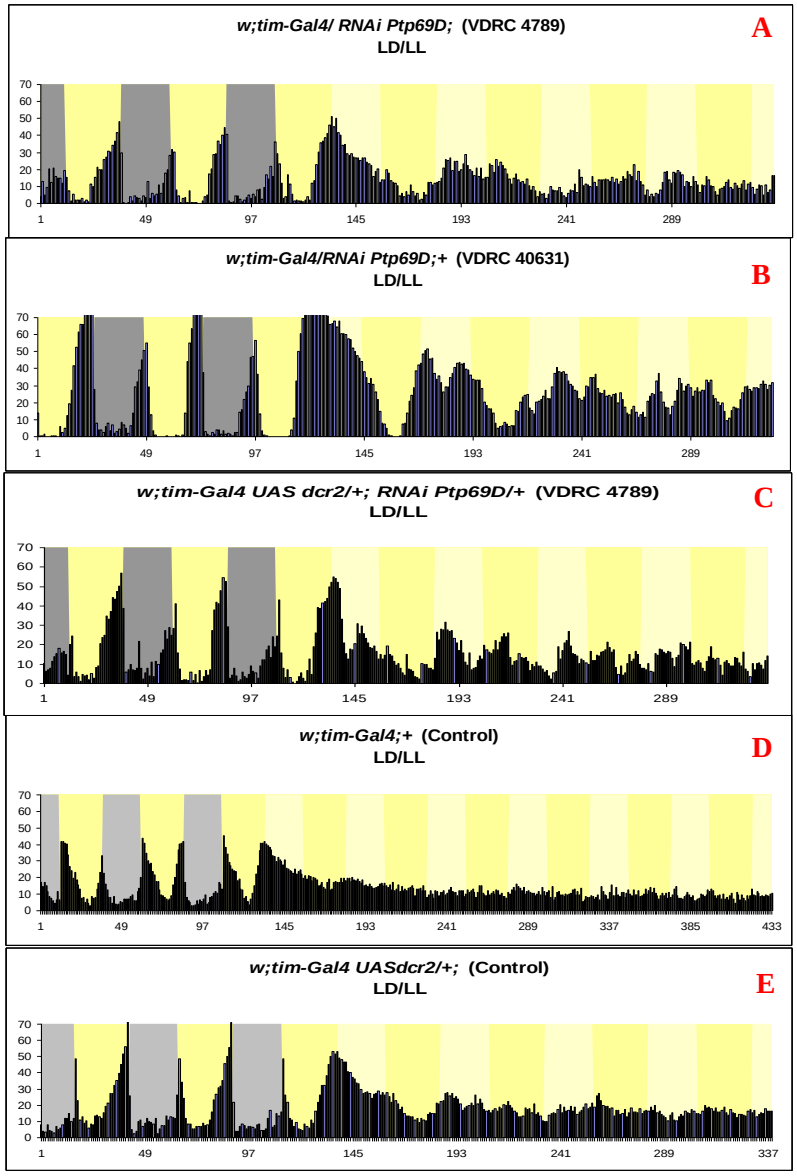

Figure 4.11 – Locomotor activity of knocked down *Ptp69D* flies in LL. A, B, C and E: 2 days LD, 5 days LL. **D:** 2 days LD, 7 days LL. **X-axis:** time in 30 minutes bins. **Y-axis:** mean level of activity. **Gray:** dark. **Dark yellow:** subjective daylight. **Yellow:** subjective night. Genotypes are indicated above each histogram. Flies silencing *Ptp69D* (A, B and C) are rhythmic. The *tim-Gal4* and *tim-Gal4 dcr2* controls (D and E, respectively) are arrhythmic.

4.3.2.11 *Glutamine synthetase 2* (*Gs2*) (CPTI-100002 – Rhythmic in LL)

A *Gs2* mutant carrying a *P{GT1}* element does not show altered behaviour in DD, but disrupting this gene seems to result in robust rhythmicity in LL with long

periods (table 4.13). *GT1* has the *Gal4* sequence from *Saccharomyces cerevisiae* without its promoter and can be used as gene trap; it also carries the mini-white gene (Lukacsovich *et al.*, 2001). The knockdown of *Gs2* in *tim* cells revealed that most flies where rhythmic in LL. Moreover, the rhythm persisted when *dicer2* was co-expressed and was not observed in the UAS (VDRC 32929), *tim-Gal4* nor *tim-Gal4 UAS dcr2* controls (figure 4.12).

Table 4.13 - *Gs2* locomotor rhythms.

Mutant (Bloomington ID)	**DD**			**LL**		
	% Rhythmic	**Mean period ± SEM**	**n**	**% Rhythmic**	**Mean period ± SEM**	**n**
w^{1118} *P{GT1}Gs2*^{BG01223} *;;* (12563)	100	24.06 ± 0.15	32	80	28.6 ± 0.55	25
RNAi (VDRC ID)	**DD**			**LL**		
	% Rhythmic	**Mean period ± SEM**	**n**	**% Rhythmic**	**Mean period ± SEM**	**n**
w;tim-Gal4/+;RNAiGs2/;+ (VDRC 32929)	100	24.33 ± 0.19	16	81.25	25.4 ± 0.5	16
w;tim-Gal4 UAS dicer2/+; RNAi Gs2/+ (VDRC 32929)	100	24.8 ± 0.12	32	80.6	26.04 ± 0.27	31
VDRC 32929 (Control)	85.7	24.16 ± 0.25	14	15	------	53
w;tim-Gal4;+ (Control)	71	24.5 ± 0.3	31	4	-----	51
w;tim-Gal4 UASdcr2/+; (Control)	100	24.2 ± 0.06	30	47	----	28

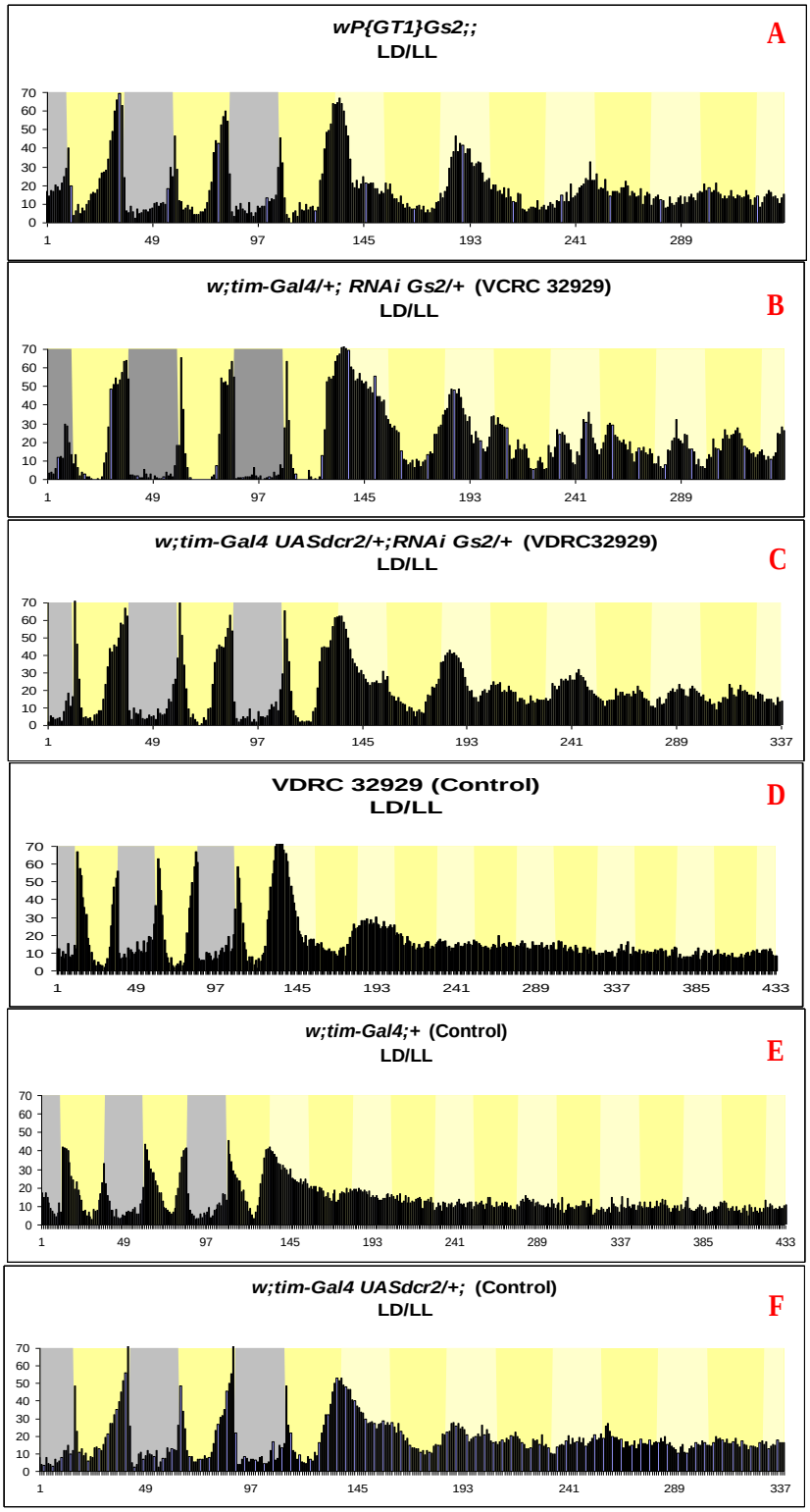

<u>Figure 4.12</u> - Locomotor activity of *Gs2* mutant and RNAi. A, B, C and F: 2 days LD, 5 days LL. **D and E:** 2 days LD, 7 days LL. **X-axis:** time in 30 minutes bins. **Y-axis:** mean level of activity. **Gray:** dark. **Dark yellow:** subjective daylight. **Yellow:** subjective night. Genotypes are indicated above each histogram.

4.3.2.12 *Glutamate oxaloacetate transaminase 1* (*Got1*) (CPTI-000303 – Rhythmic in LL)

Two *Got1* mutants and three RNAi lines were studied. Under DD, the mutant carrying a *P{GT1}* element (described in section 4.3.2.11) did not show unusual locomotor phenotypes (table 4.14). In addition, the mutant containing the *P{wHy}* element (described previously in section 4.3.2.4) failed to show rhythmic locomotor behaviour (figure 4.13). In contrast, the knockdown of *Got1* in clock cells revealed a rhythmic and robust locomotor activity with normal period close to 24 h (table 4.14).

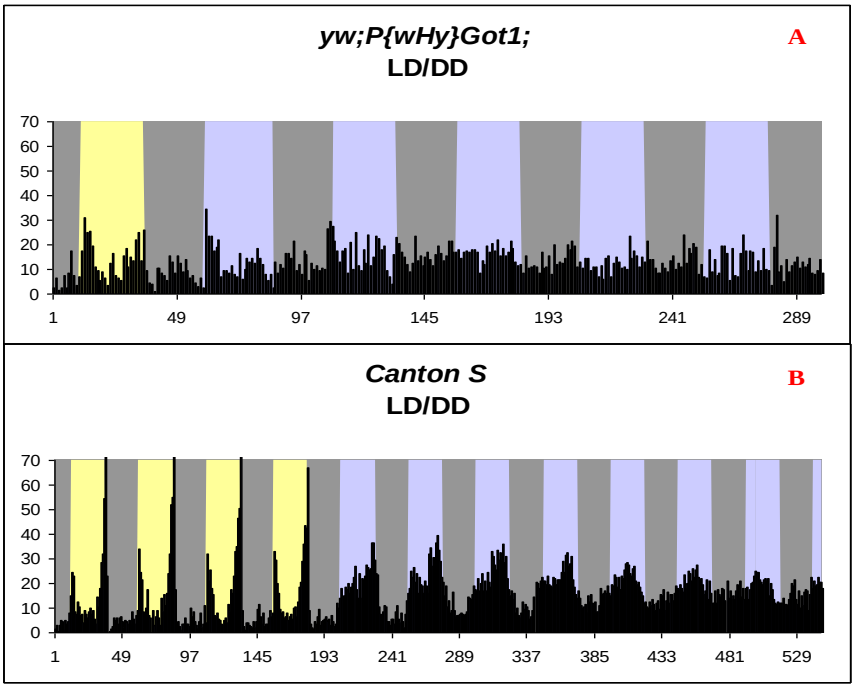

Figure 4.13 – Mean activity of *Got1* mutant in DD. A: 1 day LD, 5 days DD. **B:** 4 days LD, 7 days DD. **X-axis:** time in 30 minutes bins. **Y-axis:** mean level of activity. **Yellow:** day. **Gray:** subjective night. **Blue:** subjective day. Genotypes are indicated on top of each histogram. Got1 mutant is arrhythmic, while the control Canton S shows rhythmicity.

The mutant with *P{GT1}* element (Bloomington ID 12601) and two RNAi lines (VDRC 108247 and 8430-2) showed rhythmicity in LL (figure 4.14).

Furthermore, a slight increase on the percentage of rhythmic flies was noticed when *dicer2* was co-expressed with VDRC 108247 in LL and the RNAi controls were arrhythmic (table 4.14).

Table 4.14 – Locomotor behaviour of *Got1* variants

Mutants (Bloomington ID)	**DD**			**LL**		
	% Rhythmic	**Mean period ± SEM**	**n**	**% Rhythmic**	**Mean period ± SEM**	**n**
w^{1118}; P{GT1}Got1^{BG01081} ; (12601)	96.7	23.3 ± 0.14	31	84.6	29.8 ± 0.8	22
y^{1} w^{67c23}; P{wHy} Got1^{DG14503};+ (20423)	36	-----	14	0	-----	13
RNAi (VDRC ID)	**DD**			**LL**		
	% Rhythmic	**Mean period ± SEM**	**n**	**% Rhythmic**	**Mean period ± SEM**	**n**
w; tim-Gal4/ RNAi Got1;+ (VDRC108247)	-----	-----	---	88.8	27.6 ± 0.7	18
w;tim-Gal4 UASdcr2/ RNAi Got1;+ (VDRC 108247)	-----	-----	---	89.6	26.9 ± 0.5	29
w; tim-Gal4/+; RNAi Got1/+ (8340R-2)	-----	-----	---	62.5	26.5 ± 0.8	8
w;tim-Gal4 UASdcr2/+; RNAi Got1/+ (8430R-2)	-----	-----	---	41	-----	22
w; tim-Gal4/ RNAi Got1;+ (8340R-1)	96.7	24.3 ± 0.09	31	26	-----	27
w;tim-Gal4 UASdcr2/ RNAi Got1;+ (8430R-1)	-----	-----	---	43	-----	22
VDRC108247 (Control)	-----	-----	---	33.4	-----	9
8430R-1 (Control)	-----	-----	---	9.1	-----	11
8430R-2 (Control)	-----	-----	---	8	-----	13

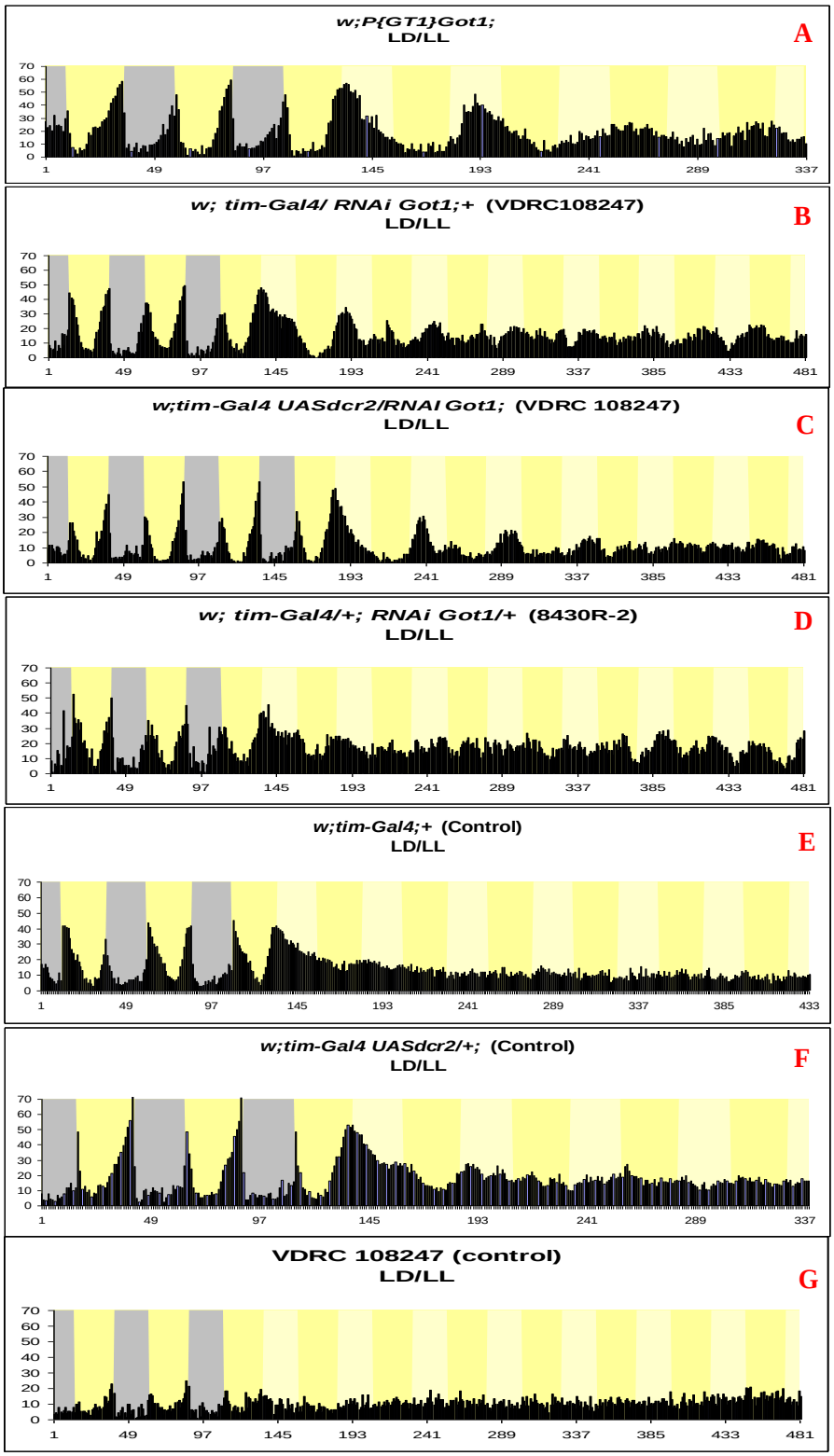

Figure 4.14 - Locomotor activity of *Got1* mutant and RNAi. A, and F: 2 days LD, 5 days LL. **B, D, E and G:** 2 days LD, 7 days LL. **C:** 3 days LD, 7 days LL. **X-axis:** time in 30 minutes bins. **Y-axis:** mean level of activity. **Gray:** dark. **Dark yellow:** subjective daylight. **Yellow:** subjective night. Genotypes are indicated above each histogram.

4.4 Discussion

In *Drosophila*, transposon mediated mutagenesis efforts have been based largely on using P elements. This approach is limited, however, because the insertion of P elements is far from random, integrating preferentially into certain hotspots, such as the 5' ends of genes (Kelley *et al*., 1987). In contrast, the *piggyBac* transposon from the lepidopteran *Trichoplusia ni*, inserts nearly randomly throughout the genome into the sequence TTAA (Horn *et al*., 2003). More importantly, it has been shown in two large *piggyBac* screens that 18% of inserts fall in introns within protein coding regions (Hacker *et al*., 2003; Thibault *et al*., 2004). For this reason, the protein trap vector inserted into the CPTI lines used in this chapter has been constructed using *piggyBac*.

Using the *piggyBac* transposon, the frequency of inserts that disrupt protein folding to produce non-functional proteins is unexpectedly low. Most introns fall between protein domains, and insertions in these regions are less likely to disrupt the protein's activity. Therefore, the best way to create mutations on the trapped genes would be mediated by imprecise transposon excision through P element ends placed inside the *piggyBac* ends. However, the locomotor activity experiments performed with the CPTI lines revealed that indeed some of these are showing differences in behaviour, although the constructs were not excised from the introns. If the presence of the insert was not interfering in the gene's activity, one would expect to have the same pattern of locomotor behaviour for all CPTI lines. All CPTI flies would behave like wild-type flies being rhythmic in DD with activity periods of around 24 hours, and arrhythmic in LL.

Among the lines that were rhythmic in the CPTI screen under LL, *Rab11* and *lk6* did not show rhythmicity when mutants and RNA interference were used. It has

been shown that *Drosophila Rab11* is involved in several biological processes, including compound eye photoreceptor development and synaptic transmission (Khodosh *et al*., 2006). The development of the *Drosophila* adult compound eye begins at the third-instar larval stage, when precursor cells differentiate into R-cells (photoreceptors) in the eye-imaginal disc. It has been proposed that *Rab11* function in a vesicular transport pathway is required for positioning R-cells in the developing eye. Indeed, knocking down *Rab11* in the eye caused an R-cell mis-location phenotype (Houalla *et al*., 2010). Moreover, the small GTPase *Rab11* implicated in membrane traffic is required for transporting two membrane proteins to the photosensory organelle called the rhabdomere (Satoh *et al*., 2005). Consequently, a role for *Rab11* in the light input could be explained by the fact that photoreceptors in the compound eye are critical for the light entrainment of clock neurons (Helfrich-Forster, 2004). Although the tested *Rab11* mutant was arrhythmic in LL, this does not necessarily preclude an involvement of this gene in light entrainment, since the P element was not inserted into the coding sequence and might not be affecting the functioning of the gene.

The *Drosophila* kinase *lk6* controls cell growth through the phosphorylation of the eukaryotic initiation factor 4E (eIF4E). The loss of *lk6* compromises eIF4E phosphorylation, consequently affecting development (Arquier *et al*., 2005). In my study, the *lk6* CPTI line was rhythmic in LL. Nonetheless, the use of RNA interference and loss-of-function alleles did not support my previous data, and these mutants were completely arrhythmic in LL. It has been shown by high-density oligonucleotide-based arrays that *lk6* oscillates in fly bodies (Ceriani *et al*., 2002). Furthermore, RNAse protection and Northern Blot assays revealed that *lk6* mRNA cycles in heads in phase with *cry* mRNA (Dubruille *et al*., 2009). A LL genetic screen

of EP lines (Dubruille *et al*., 2009), carrying randomly inserted P elements containing UAS binding sites, identified *lk6* as a potential regulator of CRY-dependent light responses, as the EP line that tagged *lk6* showed rhythms in ~50% of the flies. However, additional studies showed that *lk6* RNA interference (VDRC 32885) applied in clock cells, and the mutants $lk6^{1}$ and $lk6^{2}$, were totally arrhythmic in LL (Dubruille *et al*., 2009), confirming my own results and suggesting that follow up experiments with this gene would not be worthy.

Although CPTI-000764 was rhythmic in LL, the *kat80* mutant containing the *P{EP}* element was arrhythmic. This result corroborated the screen of EP lines by Dubruille and colleagues (Dubruille *et al*., 2009). Additionally, the *P{SUPor-P}kat80* mutant and the RNAi did not show rhythmicity in LL. No clear evidence associated *kat80* to the circadian clock. *kat80* was previously implicated in cellular division. Microtubules disassembly at centrosomes is involved in the mitotic spindle of a dividing cell. *Katanin* is a microtubule-severing protein which consists of a 60 kDa ATPase and an 80 kDa accessory protein. The p60 subunit possesses enzymatic activity and the p80 subunit targets the enzyme to the centrosome (Hartman *et al*., 1998).

CPTI-000902 (tagged *Glycogenin*) and CPTI-000850 (tagged *pbl*) were rhythmic in LL. Down-regulating *Glycogenin*, a gene involved in mesoderm development, and *pbl* in *tim* cells resulted in rhythmicity in LL. Unfortunately, the UAS RNAi controls of both genes were also rhythmic in LL. This result discouraged us to pursue *Glycogenin*'s role in the clock machinery. The same did not happened to *pebble*, which encodes a GTP-exchange factor that activates Rho 1 GTPase (an essential regulator of cytokinesis) (Prokopenko *et al*., 1999). It has been demonstrated that overexpressing *pbl* in the *Drosophila* eye by driving the EP line expression with

eyeless-Gal4 reduces the size of the adult eye (Tseng and Hariharan, 2002). This connection between *pbl* and the compound eye, which is a crucial component of the light input pathway of the clock, could help to explain the rhythmic phenotype found in LL. Although the RNA interference did not support rhythmicity under this condition, the mutant pbl^{3} carrying one copy of a loss-of-function allele was rhythmic. In addition, the arrhythmicity found in the hypomorphic mutant pbl^{5} could be explained by the fact that these flies carry one wild-type allele. A possible role of *pbl* in the circadian system remains unclear.

Two long period candidates in DD from the CPTI screen, *Mi-2* and *CG31352*, did not exhibit the same phenotype when down-regulated by *tim-Gal4* or mutated. Although knocking down *Mi-2* in clock neurons resulted in long period (τ= 25.15 ± 0.3), this finding was invalidated by an ANOVA test that showed no significant difference when compared to the *tim-Gal4* control ($F_{1,29}$= 0.53666, p= 0.46970). Not even the co-expression of dicer2 was capable of generating long periods, making it difficult to correlate this gene with the circadian clock. *Mi-2*, a member of the Snf2 superfamily of ATPases, is involved in chromatin remodelling to facilitate DNA binding by creating a more dynamic chromatin structure (Brehm *et al*., 2000).

Unexpectedly, down-regulating *CG31352* resulted in rhythmicity under LL conditions instead of long period in DD, which was found for the CPTI line (CPTI-100017). The function of this gene remains unclear, although it has been suggested that it may be involved in cytoskeletal organization (Flybase). The possible connection between *CG31352* and the circadian clock remains obscure.

A possible explanation for the fact that these two long period CPTI lines did not have the phenotype confirmed by other transgenic flies would be the presence of the per^{SLIH} mutation. The per^{SLIH} mutant has an amino acid substitution, serine to

tyrosine at residue 45, and exhibits a long period of 27 h in DD (Hamblen *et al*., 1998). In fact, the CPTI background appears to be polymorphic for per^{SLIH} (Ralf Stanewsky, personal communication, August 2010), however the long period lines, CPTI-100008 and CPTI-100017, were not genotyped for *per* allele.

Neither the mutants nor the RNA interference study corroborated that *14-3-3ε*, *GG33158* and *Ptp69D* are arrhythmic in DD as suggested by the initial CPTI screen. The mutant and deficiency for *14-3-3ε* did not alter the locomotor behaviour of the flies in both light regimes, excluding any involvement with the circadian clock. However, the *14-3-3ε* mutant used is a transgenic transposon (Bier *et al*., 1989) that was inserted outside the coding sequence, and hence may not necessarily be affecting the gene's activity. Moreover, both the mutation and deficiency are heterozygous. There is experimental evidence that *14-3-3ε* is involved in several biological processes such as the regulation of mitosis and DNA damage checkpoint (Su *et al*., 2001), but at present any role in the circadian cycle is tentative.

CG33158 has been predicted to be involved in translational elongation based on sequence similarities (Flybase). The *Minos* element insertional mutation out of the *CG33158* coding sequence may not be affecting the gene function and flies behave normally in DD. However, down-regulating *CG33158* in clock tissues using 3 different RNAi lines did not affect the locomotor activity of the flies in DD. This eliminates a possible connection between *CG33158* and the core of the circadian clock. On the other hand, there is a possibility that this gene could function in the light input pathway since flies were rhythmic in LL when mutated or silenced by *tim-Gal4* in the presence of *dicer2*.

Another gene that might be important for clock entrainment is *Ptp69D*, since down-regulating it with two RNAi lines caused rhythmicity in LL. Supporting this

idea, it is known that *Drosophila* compound eye contains eight uniquely identifiable photoreceptor neurons R1 to R8, and their axons are easily visualised. *Ptp69* was implicated in the decision of R1-R6 axons to stop at the lamina, and is necessary for proper R7 axon targeting through the lamina into the medulla. In addition, *Ptp69D* function in the eye is necessary, but not sufficient, to target R-cell axons to a particular layer of the brain (Tayler and Garrity, 2003).

The CPTI line that tagged *Gs2* was rhythmic in LL (CPTI-10002). The same altered phenotype was observed in LL conditions for the *Gs2* mutant: ~ 80% of tested flies were rhythmic with a long period of activity (~28 hours). The knockdown of this gene in clock neurons generated the same rhythmic effect when *dicer2* was co-expressed. This implicates *Glutamine synthetase 2* (*Gs2*) in the light input of the circadian clock, most probably in TIM degradation. This gene is involved in neurotransmitter receptor metabolic processes. Glutamate participates in synaptogenesis in two different ways: vesicular glutamate release mediates fast synaptic transmission as well as non-vesicular glutamate release (Featherstone *et al*., 2002). One of the enzymes that regulate the size of glutamate neurotransmitter pools is *Glutamine synthetase*, which catalyzes the conversion of glutamate to glutamine and is particularly abundant within *Drosophila* embryonic nervous system (Featherstone *et al.*, 2002)

The experiments using the *Got1* mutant and RNA interference agreed with the initial screen, in that rhythms were observed in constant light. *Glutamate oxaloacetate transaminase 1* (*Got1*) is involved in glutamate production and is another enzyme that regulates the size of glutamate neurotransmitter pools (Featherstone *et al*., 2002).

It is important to highlight that the significant number of genes found in this work that seem to be implicated into the light entrainment of the clock could have

been due to a mutation in the *jetlag* gene. It has been shown that flies containing the jet^{c} mutation are rhythmic when constantly exposed to light, specifically in a *ls-tim* background (Peschel *et al*., 2006). Therefore it is important to check for the jet^{c} mutations in these candidates prior to proceeding to detailed studies. The two genes involved in glutamate metabolism, *Got1* and *Gs2*, were thus selected for further studies because of their possible connection with clock light input, and the next chapter of this work is dedicated to these genes, including a more detailed discussion about them.

Chapter 5: Glutamate and the Circadian Clock

5.1 Introduction

The behavioural screening of the CPTI lines and further mutant analyses (chapter 4) implicated two genes that regulate glutamate metabolism in the light input pathway to the clock: *Glutamate oxaloacetate transaminase 1* (*Got1*) and *Glutamine synthetase 2* (*Gs2*). Flies carrying mutations of *Gs2* and *Got1* and lines in which RNA interference was expressed in clock neurons, showed a robust rhythm when exposed to LL.

Glutamate is an abundant neurotransmitter known to act on fast glutamatergic transmission mediated by ligand-gated ion channel ionotropic glutamate receptors (iGLURs), and on slower G-protein coupled pathways signalled by metabotropic glutamate receptors (mGluRs) (Anwyl, 1999; Dingledine *et al*., 1999). In *Drosophila*, DmGluRA is the only functional metabotropic glutamate receptor encoded by the genome (Bogdanik *et al*., 2004). Glutamate neurotransmission has been extensively studied at the *Drosophila* neuromuscular junction, where both types of receptors have been identified (Bogdanik *et al*., 2004; Marrus *et al*., 2004; Qin *et al*., 2005). Recently, glutamate and its metabotropic receptor have been shown to be involved in signalling within the clock circuits of the *Drosophila* brain, and modulating rhythmic behaviour patterns (Hamasaka *et al*., 2007).

As represented in figure 5.1, *Glutamate oxaloacetate transaminase* (*Got*), *Glutamine synthetase* (*Gs*) and *Glutamate decarboxylase* (*Gad*) are enzymes that regulate the size of glutamate neurotransmitter pools. *Got* is involved in glutamate synthesis during the transamination of aspartate. *Gs* catalyzes the switch of glutamate to glutamine, whereas Gad participates in the production of GABA (an inhibitory

neurotransmitter) (Featherstone *et al.*, 2002). Glutamine participates in the recycling of glutamate to neurons. The presynaptically released extracellular glutamate is taken up by glia, converted to glutamine by glutamine synthetase, and transported back to neurons for reuse (Freeman and Doherty, 2006).

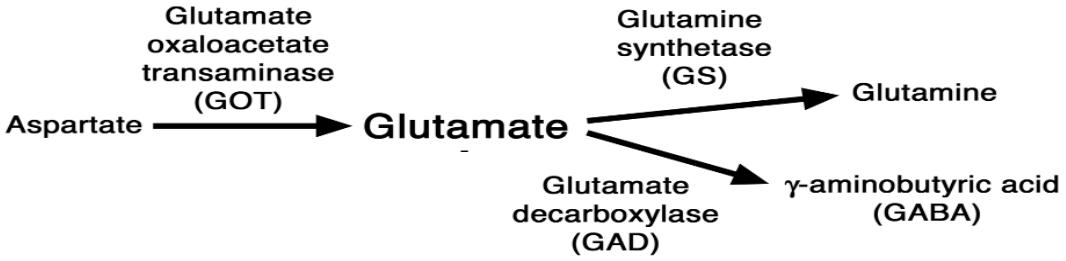

Figure 5.1 – Enzymatic processes involved in glutamate metabolism. Figure modified from (Featherstone *et al.*, 2002).

The aim of this chapter was to verify whether the glutamate signalling is an important modulator of behavioural light-entrainment, and which subset of neurons might be involved.

5.2 Results

5.2.1 Checking the background

5.2.1.1 *P{GT1} elements*

A large proportion (~80%) of both *Gs2* and *Got1* mutants carrying the *P{GT1}* element showed robust rhythms in LL (chapter 4). It is conceivable that this could indicate that the behavioural phenotype was a manifestation of the genetic background. To probe this possibility further, the locomotor activity of flies with the *P{GT1}* transposed into three different non- clock genes was tested in LL.

In the first mutant analysed, the P-element was inserted into the gene *Translocase of outer membrane7* (*Tom7*), which is related to protein targeting to the

mitochondrion (Hwa *et al.*, 2004). Around 78% of *w;P{GT1}Tom7;* mutants were arrhythmic in LL (table 5.1 and figure 5.2). Another tested *P{GT1}* mutant has two genes interrupted, *Alcohol dehydrogenase* (*Adh*) that is part of the alcohol catabolic process (Khaustova *et al.*, 1992) and *Adh-related* (*Adhr*), which has been predicted to be involved in oxidation (bioinformatically - Flybase). Table 5.1 shows that 80% of *w;P{GT1}AdhAdhr;* mutants were not able to sustain rhythmicity under LL. Finally, the last mutant checked, *wP{GT1}prtp. Pretaporter* (*prtp*), is an insertion in a gene that participates in phagocytosis of apoptotic cells (Kuraishi *et al.*, 2009). The great percentage of these mutants (~84%) showed arrhythmicity when exposed to LL (table 5.1 and figure 5.2).

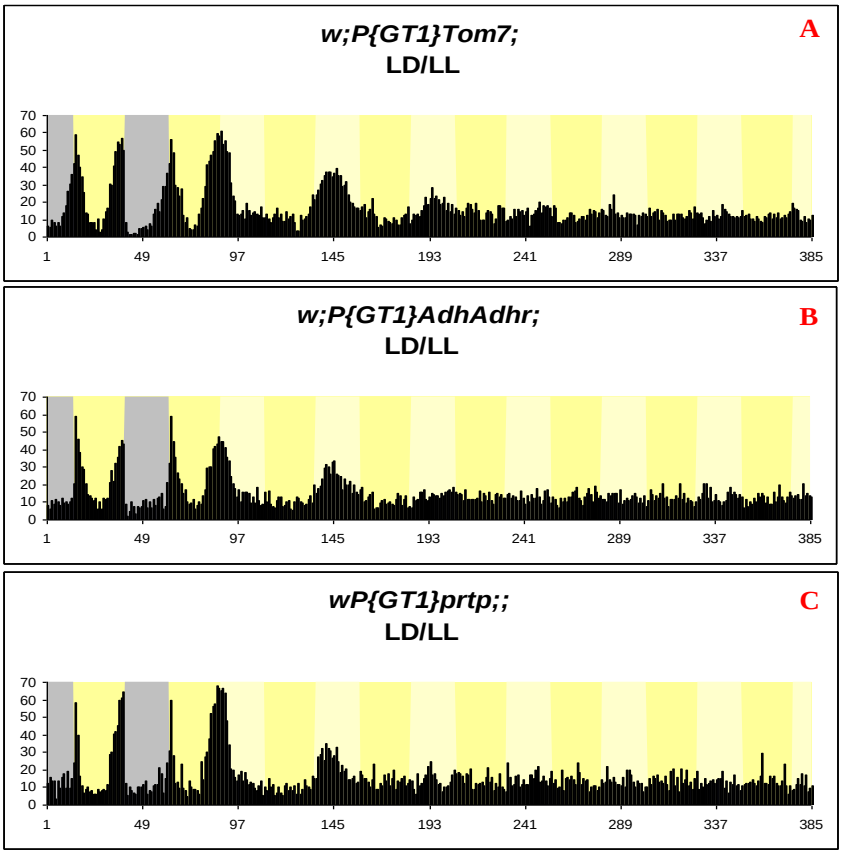

Figure 5.2 – Locomotor activity profile of *P{GT1}* mutants in LL. A: *w;P{GT1}Tom7*. **B:** *w;P{GT1}Adh Adh*. **C:** *wP{GT1}prtp*. The flies were entrained for 2 days in LD and then exposed to 7 days of LL. **X-axis:** time in 30 minutes bins. **Y-axis:** mean level of activity. **Gray:** dark. **Dark yellow:** subjective daylight. **Yellow:** subjective night. All genotypes showed arrhythmicity.

Table 5.1 - *P{GT1}* mutants are arrhythmic in LL.

Mutants (Bloomington ID)	LL		
	% Rhythmic	Mean Period ± SEM	n
w^{1118}; $P\{GT1\}Tom7^{BG02496}$; (12698)	21.9	-----	32
w^{1118}; $P\{GT1\}Adh^{BG01049}$ $Adhr^{BG01049}$; (12535)	20	-----	30
$w^{1118}P\{GT1\}prtp^{BG00450}$;; (12488)	16.2	-----	31

The observation t that three different mutants with the same background behaved like wild-type flies in LL suggested that the rhythmicity found for *Gs2* and *Got1* is a result of the mutation within these genes.

5.2.1.2 Randomising the background

Another way to check if the rhythm found for *Gs2* and *Got1* mutants in LL was a simply manifestation of the background, was to cross these mutants with flies in a different background (w^{1118}). Females of homozygous *Got1* mutants were crossed to male w^{1118}, generating heterozygous progeny. The heterozygous siblings were then crossed among themselves, resulting in a progeny of flies carrying one copy of the mutant allele with light orange eye colour, two copies of the mutation with dark orange eye colour or no copies with white eyes (figure 5.3). Males from the three F2 genotypes had their locomotor activity tested in LL.

After changing the background, around 60% of homozygous *Got1* mutants behaved rhythmically in LL, whereas 44% of the heterozygous showed rhythmicity and only 26% of the flies lacking the mutant allele were rhythmic (table 5.2 and figure 5.4). This result supports the idea that the background is not responsible for the rhythms previously found in *w;P{GT1}Got1;* mutants, since a large proportion of

homozygous mutants still show rhythms after randomising the background. Moreover, the fact that flies carrying only the wild-type alleles generally showed arrhythmicity provides further support for the role of *Got1* in the LL phenotype.

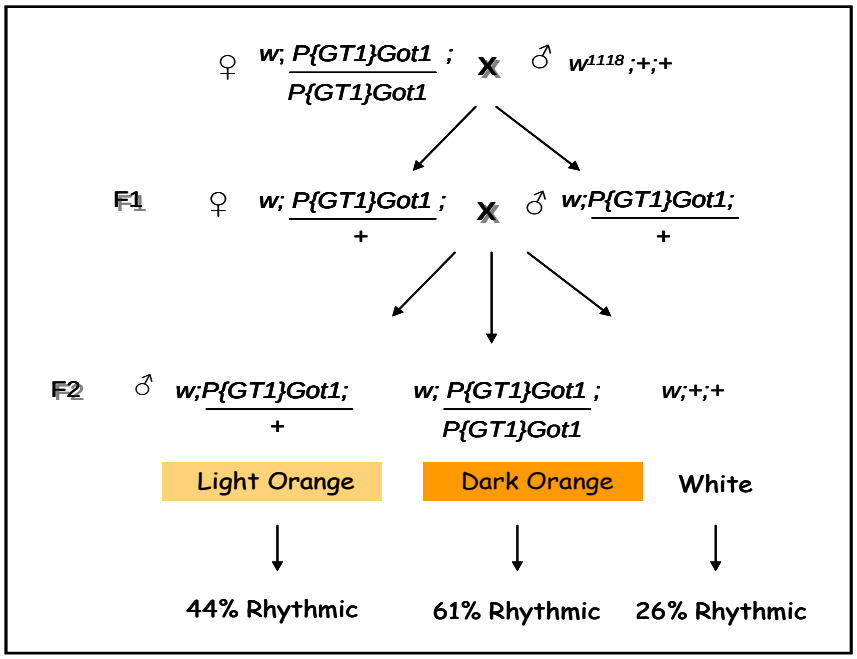

Figure 5.3 - Mating scheme to randomise *Got1* mutant background. *Got1* mutants were crossed to w^{1118} and the F1 siblings were crossed among themselves to produce the F2. *Got1* mutant allele is on the second chromosome. Light Orange, dark orange and white correspond to the eye colour of F2 flies and their locomotor behaviour in LL is also represented in percentage of rhythmic flies.

Table 5.2 – *Got1* mutants after randomisation of the background.

Mutants with randomised background	LL		
	% Rhythmic	Mean Period ± SEM	n
w; P{GT1}Got1; (homozygous)	61	29 ± 0.9	32
w; P{GT1}Got1; (heterozygous)	44	28 ± 1.6	31
w^{1118};; (wild-type)	26	-----	31

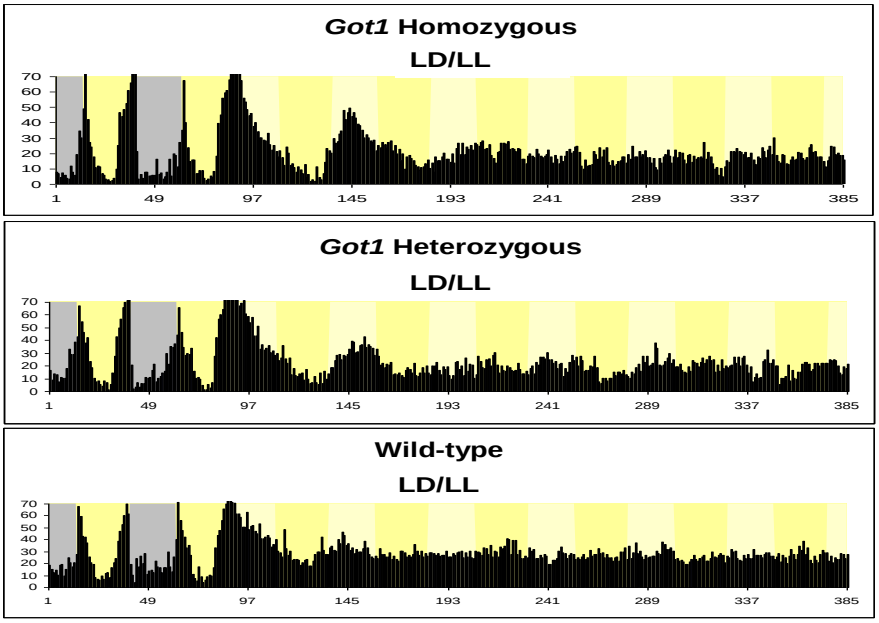

Figure 5.4 - Mean activity of *Got1* mutants after genetic background change. Flies were entrained for 2 days in LD and then exposed to 7 days of LL. **X-axis:** time in 30 minutes bins. **Y-axis:** mean level of activity. **Gray:** Dark. **Dark yellow:** subjective daylight. **Yellow:** subjective night.

The same mating scheme was used with *Gs2* mutants for a better understanding about the mutation and background effects (figure 5.5). However, in this case the F2 progeny generated from the cross between the F1 siblings was represented only by two male genotypes: flies containing one *Gs2* mutant allele and files with a wild-type allele instead because *Gs2* is sex-linked.

The result of the background modification was a high percentage of rhythmic flies (63%) carrying the mutation and only a small number of flies lacking the insertion of the P-element maintaining rhythms in LL (table 5.3 and figure 5.6). Once again, the results suggested an association between the mutation and the rhythms in LL.

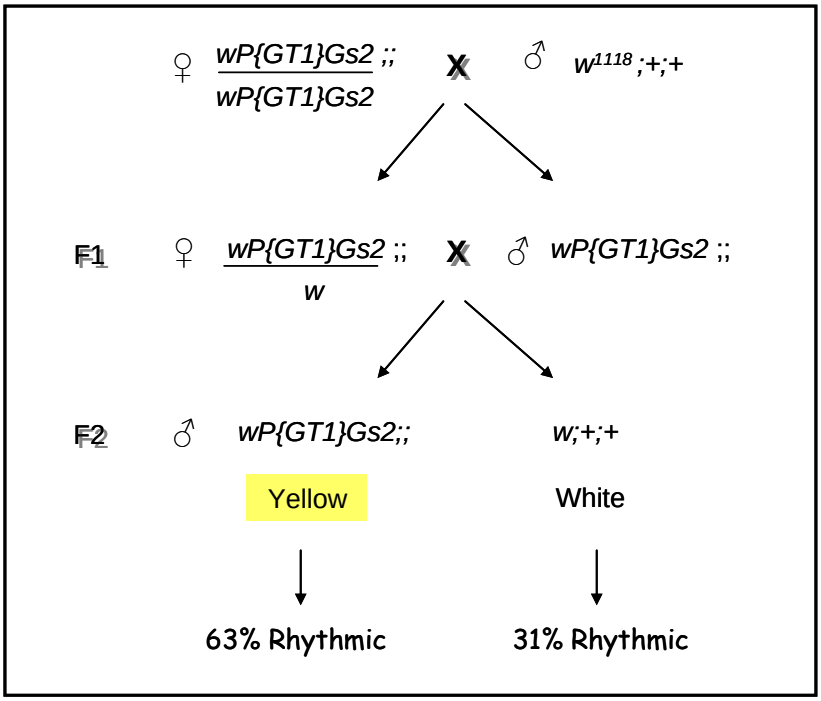

Figure 5.5 – Crosses scheme used to change *Gs2* mutant background. In the first cross, *Gs2* mutants were mated with w^{1118} and the progeny is shown in F1. Afterwards, F1 siblings were crossed among themselves generating the F2 progeny. Yellow represent the eye colour of flies carrying one copy of the mutant allele, whereas white eye coloured flies only have the wild-type allele. The locomotor behaviour of F2 flies in LL is represented in percentage of rhythmic flies.

Table 5.3 – *Gs2* mutants after randomisation of the background.

Mutants with randomised background	LL		
	% Rhythmic	Mean Period ± SEM	n
wP{GT1}Gs2;; (hemizygous)	63	29.4 ± 0.8	31
w^{1118}*;;* (wild-type)	31	-----	29

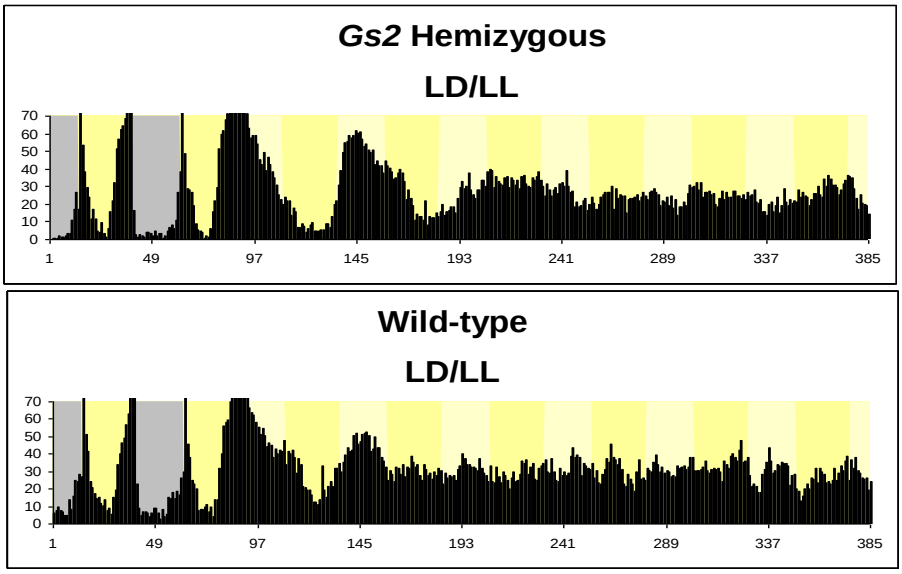

Figure 5.6 - Locomotor activity of *Gs2* mutants with randomised background. Flies were entrained for 2 days in LD and then exposed to 7 days of LL. The number of *Gs2* mutant alleles is described on top of each graph. **X-axis:** time in 30 minutes bins. **Y-axis:** mean level of activity. **Gray:** Dark. **Dark yellow:** subjective daylight. **Yellow:** subjective night.

Although after modifying the background, *Got1* and *Gs2* mutants were still able to maintain a rhythmic profile in LL, a reduction in the percentage of rhythmic flies was observed. Previously, around 85% of *w;P{GT1}Got1* and 80% of *wP{GT1}Gs2* were rhythmic in LL, whereas after altering the background, about 20% less flies from both genotypes showed rhythmicity. Moreover, because the periods of the flies were very variable, it is difficult to visualise in the graphs the rhythm after the third day in LL. Fore this reason, a spectral graph and an autocorrelogram corresponding to the rhythmic genotypes are shown in figure 5.7.

The w^{1118} flies used to mate with the mutants were genotyped as *s-tim* flies (see next section for explanation). It has been shown on previous work that flies in *ls-tim* background are less responsive to light than *s-tim* (Sandrelli *et al*., 2007). Since *Got1* and *Gs2* mutants seem to be acting in the light-entrainment process and crossing

them to *s-tim* flies reduced the percentage of rhythmicity, it was important to check if the rhythmic phenotype depends on the underlying TIM isoform.

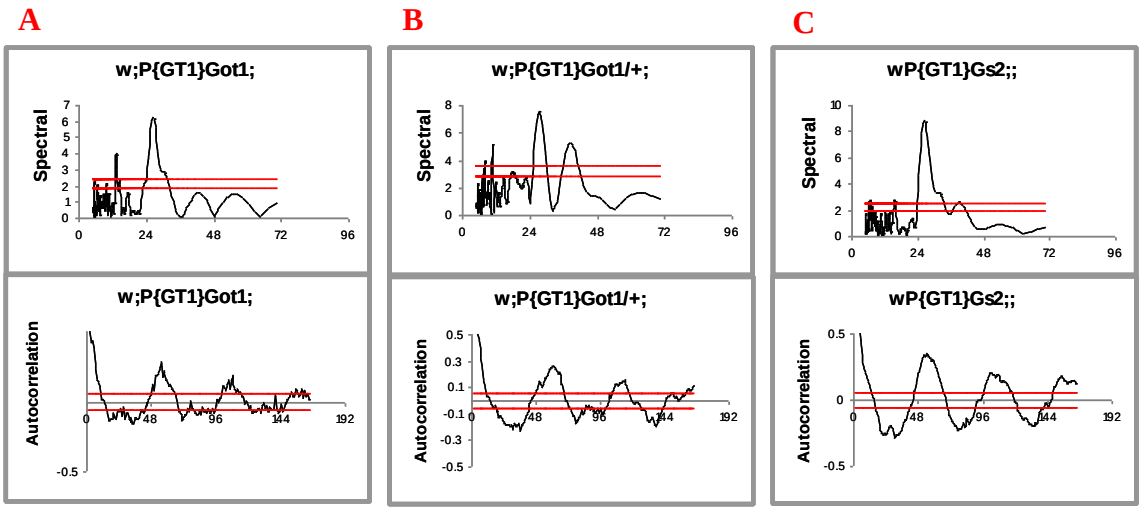

Figure 5.7 – Mutants with randomised background in LL. Upper panel: CLEAN spectral plot along with the 95% and 99% Monte Carlo confidence limits. **Lower panel:** Autocorrelogram with the canonical 95% confidence limits. **A:** *w;P{GT1}Got1;*. **B:** *w;P{GT1}Got1/+;*. **C:** *wP{GT1}Gs2;;*.

5.2.1.3 Defining *timeless* alleles

The parental flies from the crosses described in the previous section (5.2.1.1) were used in PCR reactions to determine their *tim* haplotypes. In figures 5.8, 5.9 and 5.10 the lower band is a control for PCR efficiency, whereas the higher band represents *ls-tim* and *s-tim* (indicated in the figures). Ten flies of each parental line were genotyped for their *tim* alleles.

Flies *wP{GT1)Gs2* (figure 5.8, samples 1 to 10) and *w;P{GT1}Got1* (figure 5.9, samples 1 to 10) are in *ls-tim* background, while w^{1118} flies have only the *s-tim* allele (figure 5.10, samples 1 to 10). The *s-tim* control (sample s) and *ls-tim* control (sample ls) amplified only the expected band and the negative control lacking DNA (samples H_20) did not amplify any band.

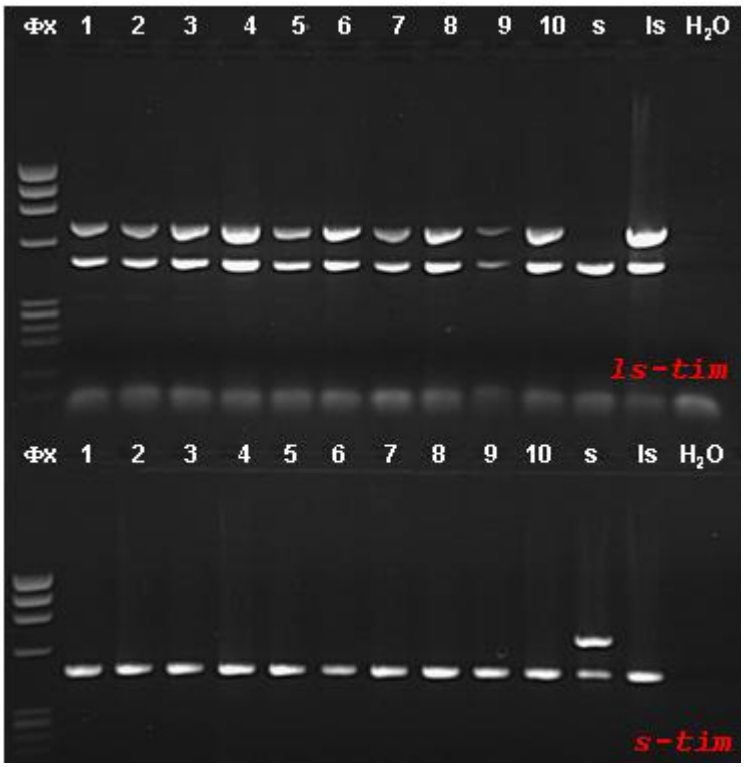

Figure 5.8 - *tim* genotyping of *Gs2* mutants. The PCR products were resolved on a 1.5% agarose gel. **Top Panel:** Reactions using *ls-tim* primers. **Lower Panel:** Reactions using *s-tim* primers. The numbers above each lane represent each fly tested. **ϕX:** ϕX Hae III. **1 to 10:** *wP{GT1)Gs2*. **s:** *s-tim* positive control. **ls:** *ls-tim* positive control. **H_2O:** water control (no DNA).

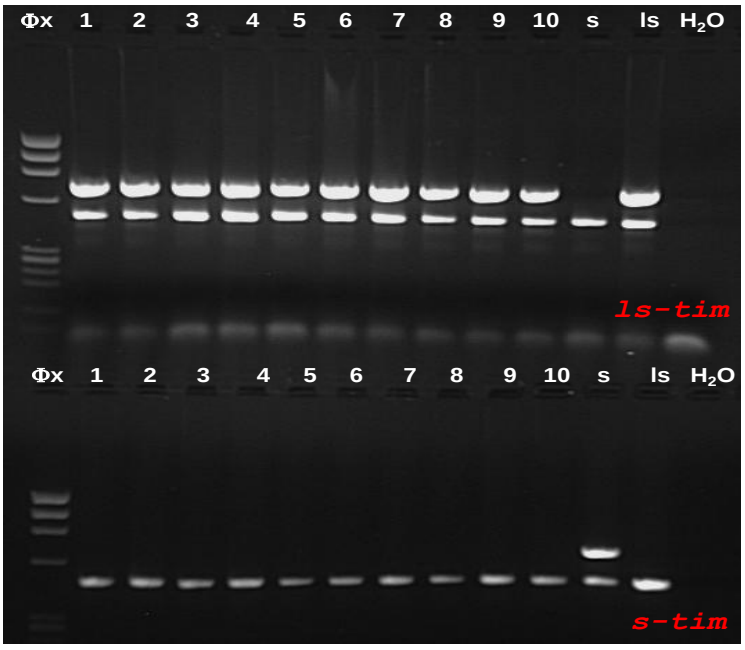

Figure 5.9 - *tim* genotyping of *Got1* mutants. The PCR products were resolved on a 1.5% agarose gel. **Top Panel:** Reactions using *ls-tim* primers. **Lower Panel:** Reactions using *s-tim* primers. The numbers above each lane represent each fly tested.

ϕX: ϕX Hae III. **1 to 10:** *w;P{GT1}Got1*. **s:** *s-tim* positive control. **ls:** *ls-tim* positive control. **H_2O:** water control (no DNA).

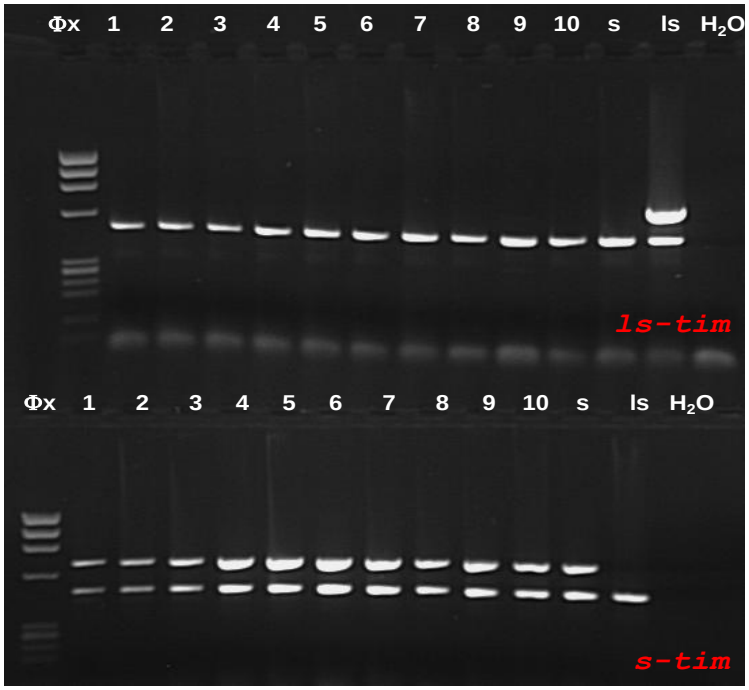

Figure 5.10 - *tim* genotyping of w^{1118} mutants. The PCR products were resolved on a 1.5% agarose gel. **Top Panel:** Reactions using *ls-tim* primers. **Lower Panel:** Reactions using *s-tim* primers. The numbers above each lane represent each fly tested. **ϕX:** ϕX Hae III. **1 to 10:** w^{1118}. **s:** *s-tim* positive control. **ls:** *ls-tim* positive control. **H_2O:** water control (no DNA).

The decrease in the levels of LL rhythmicity after crossing *ls-tim* homozygous *Gs2* and *Got1* mutants to *s-tim* homozygous w^{1118} flies (figure 5.3 and 5.5) suggested a possible interaction between *tim* and the glutamate genes. To address this question, the mutants with modified background from the F2 progeny (figure 5.3 and 5.5) carrying either two copies of *P{GT1}Got1* or 1 copy of *P{GT1}Gs2* were also genotyped for their *tim* allele. The correlation between the *tim* haplotype and the locomotor behaviour is shown in table 5.2.

The locomotor activity experiment under LL revealed that among the nine *ls-tim* homozygotes *wP{GT1}Gs2* flies, all of them showed rhythmicity. Moreover, when *wP{GT1}Gs2* mutants were heterozygous *ls-tim/s-tim*, ten out of sixteen flies

were rhythmic and six were arrhythmic. Interestingly, all *Gs2* mutants in the *s-tim* background were LL arrhythmic (table 5.4).

Similarly, the great majority of *Got1* mutants in the *ls-tim* background are rhythmic in LL, whereas seven out of the seventeen *ls-tim/s-tim* flies are rhythmic and ten showed arrhythmicity. Unfortunately, none of the genotyped flies were homozygous for *s-tim* (table 5.4).

Table 5.4 - Correlation between *tim* allele and locomotor behaviour in LL.

wP{GT1}Gs2;;			
***timeless* alleles**	**Total n**	**n of Rhythmic Flies**	**n of Arrhythmic Flies**
ls-tim/ls-tim	9	9	0
ls-tim/s-tim	16	10	6
s-tim/s-tim	5	0	5
w; P{GT1}Got1/ P{GT1}Got1;			
***timeless* alleles**	**Total n**	**n of Rhythmic Flies**	**n of Arrhythmic Flies**
ls-tim/ls-tim	14	12	2
ls-tim/s-tim	17	7	10
s-tim/s-tim	0	0	0

These data suggest that *wP{GT1}Gs2* and *w;P{GT1}Got1* are interacting with *timeless* to modulate the light response of these flies, and the less photosensitive *tim* allele (*ls-tim*) is essential for a rhythmic phenotype.

Based on this, it became necessary to verify whether the three mutants utilised to check the *P{GT1}* background in section 5.2.1.1 (*w;P{GT1}Tom7*, *w;P{GT1}AdhAdhr* and *wP{GT1}prtp*) behaved arrhythmically as a consequence of the TIM isoform expressed. Their *tim* genotyping by PCR revealed that all three mutants are *ls-tim* homozygous (figure 5.11), confirming that the *P{GT1}* background is not responsible for LL rhythmicity.

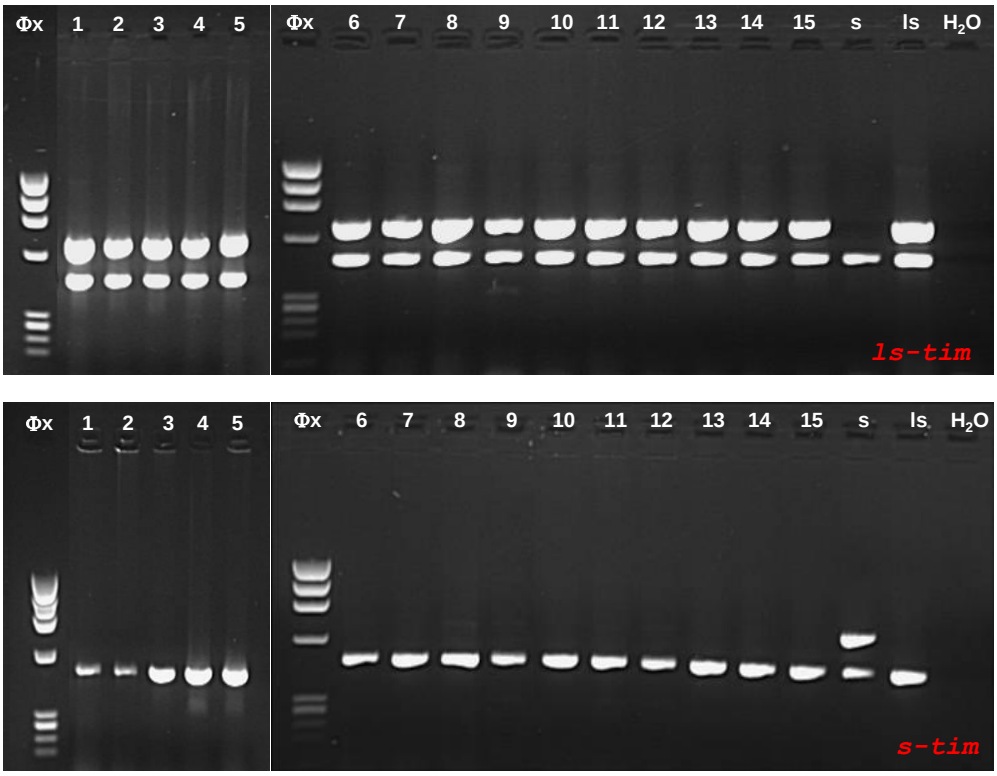

Figure 5.11 –Genotyping *tim* alleles of *P{GT1}* mutants by PCR. The PCR products were resolved on a 1.5% agarose gel. The lower band is a control of PCR efficacy. **Top Panel:** Reactions using *ls-tim* primers. **Lower Panel:** Reactions using *s-tim* primers. The numbers above each lane represent each fly tested. **ϕX:** ϕX Hae III. **1 to 5:** *w;P{GT1}AdhAdhr*. **6 to 10:** *w;P{GT1}Tom7*. **11 to 15:** *wP{GT1}prtp*. **s:** *s-tim* positive control. **ls:** *ls-tim* positive control. **H_2O:** water control (no DNA).

5.2.1.4 Looking for mutations in *jetlag*

The behaviour of *Gs2* and *Got1* mutants resembled that of *Veela* flies, which carry the *jetlag* genetic variant jet^c and behave abnormally rhythmically in LL only in the simultaneous presence of the less light-sensitive form of *tim* (Peschel *et al*., 2006). Thus it became important to check whether *Gs2* and *Got1* mutants' rhythmic behaviour was a result of the presence of jet^c. I also checked for the jet^r polymorphism, a rare *jetlag* mutation that also leads to rhythmic behaviour in LL (Koh *et al*., 2006). Both variants involve an amino acid substitution: a phenylalanine-to-isoleucine (F209I) and a serine-to-leucine (S220L), respectively in jet^c and jet^r

(Koh *et al*., 2006). To check for *jet* mutations, firstly a fragment of the gene comprising both amino acid substitution sites was amplified by PCR and sequenced.

As shown in figure 5.12, ten flies from each genotype were examined. Gel A illustrates the amplified *jet* band from the *Gs2* mutant while gel B represents the *Got1* mutant. w^{1118} flies were also checked, since they were used to randomise *Gs2* and *Got1* mutants' background (detailed in 5.2.1.2), and are represented in gel C. Every tested fly had the expected band of 282 bp amplified and the negative controls lacking DNA did not detect any band (figure 5.12).

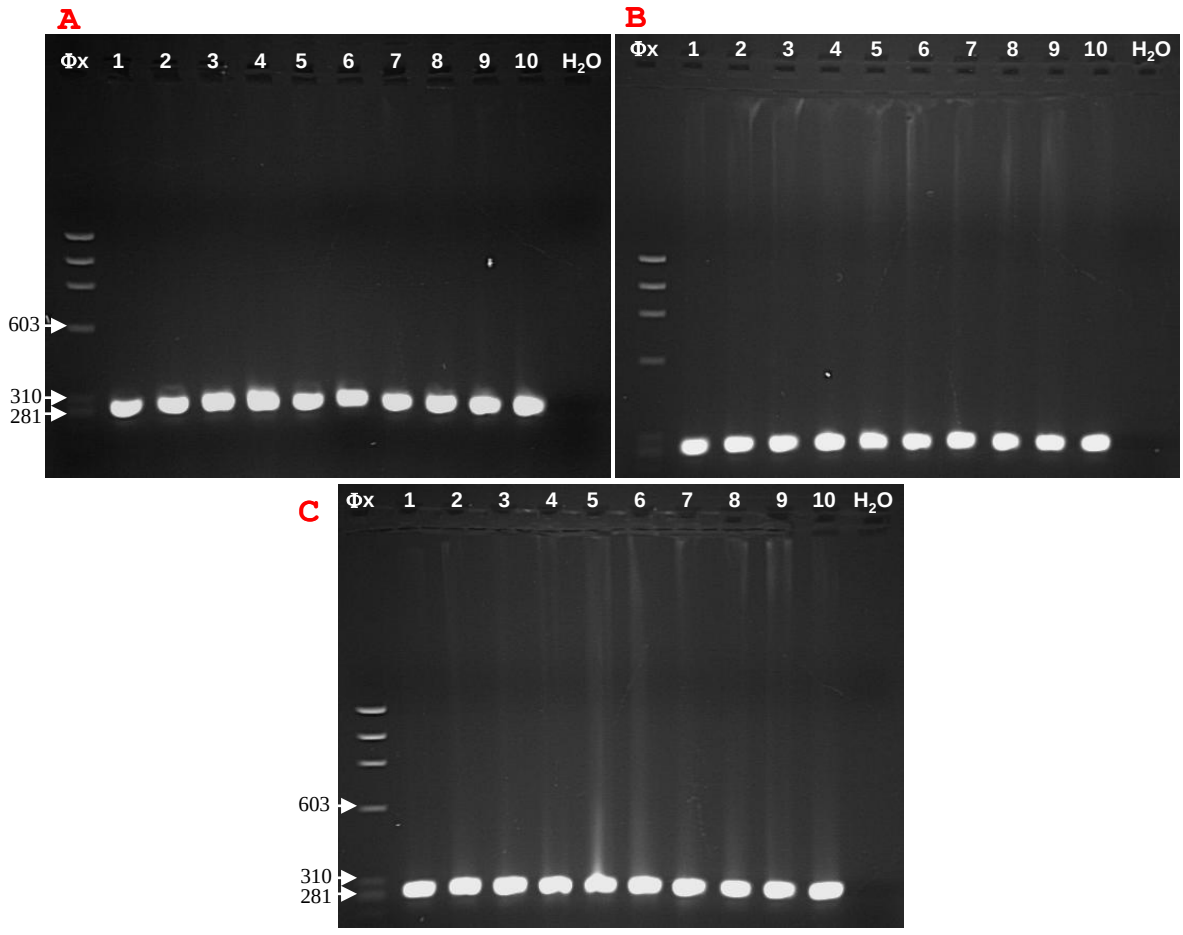

Figure 5.12 - Amplification of *jetlag* sequence by PCR. The PCR products were resolved on a 1.5% agarose gel. The band corresponds to a fragment of *jetlag* sequence comprising jet^{c} mutation site. The numbers above each lane represent each fly tested. **A:** *wP{GT1}Gs2*. **B:** *w;P{GT1}Got1;* **C:** w^{1118}. **ϕX:** ϕX Hae III. **H_20:** water control (no DNA).

Sequencing the amplified DNA fragments revealed that none of the examined flies carries the described mutations in *jetlag*. A perfect sequence match can be seen in the alignment between *jetlag* from wild-type flies and from the investigated flies (figure 5.13, A). The DNA region of the jet^c polymorphism is highlighted in red, whereas the site for the jet^r polymorphism is highlighted in green. A chromatogram from one of the non-mutated tested flies is also illustrated in figure 5.13, panel B. The red arrow indicates the specific nucleotide position where a point mutation can cause the amino acid substitution found in jet^c flies, while the black arrow points to the jet^r polymorphic site.

The idea that *P{GT1}Gs2* and *P{GT1}Got1* mutations are responsible for the abnormal rhythmic behaviour in LL was reinforced by the lack of both *jetlag* mutations in these flies.

A

```
jetlag      TGGAGAGCGCTGCTTGATTATCTTCTTCAGGAAACTTAACAAGCTCACCGTCCTGTCGCTGGCAAATACGCCCAGTGTCA
Gs2-1       TGGAGAGCGCTGCTTGATTATCTTCTTCAGGAAACTTAACAAGCTCACCGTCCTGTCGCTGGCAAATACGCCCAGTGTCA
Gs2-2       TGGAGAGCGCTGCTTGATTATCTTCTTCAGGAAACTTAACAAGCTCACCGTCCTGTCGCTGGCAAATACGCCCAGTGTCA
Gs2-3       TGGAGAGCGCTGCTTGATTATCTTCTTCAGGAAACTTAACAAGCTCACCGTCCTGTCGCTGGCAAATACGCCCAGTGTCA
Gs2-4       TGGAGAGCGCTGCTTGATTATCTTCTTCAGGAAACTTAACAAGCTCACCGTCCTGTCGCTGGCAAATACGCCCAGTGTCA
Gs2-5       TGGAGAGCGCTGCTTGATTATCTTCTTCAGGAAACTTAACAAGCTCACCGTCCTGTCGCTGGCAAATACGCCCAGTGTCA
Gs2-6       TGGAGAGCGCTGCTTGATTATCTTCTTCAGGAAACTTAACAAGCTCACCGTCCTGTCGCTGGCAAATACGCCCAGTGTCA
Gs2-7       TGGAGAGCGCTGCTTGATTATCTTCTTCAGGAAACTTAACAAGCTCACCGTCCTGTCGCTGGCAAATACGCCCAGTGTCA
Gs2-8       TGGAGAGCGCTGCTTGATTATCTTCTTCAGGAAACTTAACAAGCTCACCGTCCTGTCGCTGGCAAATACGCCCAGTGTCA
Gs2-9       TGGAGAGCGCTGCTTGATTATCTTCTTCAGGAAACTTAACAAGCTCACCGTCCTGTCGCTGGCAAATACGCCCAGTGTCA
Gs2-10      TGGAGAGCGCTGCTTGATTATCTTCTTCAGGAAACTTAACAAGCTCACCGTCCTGTCGCTGGCAAATACGCCCAGTGTCA

jetlag      TGGAGAGCGCTGCTTGATTATCTTCTTCAGGAAACTTAACAAGCTCACCGTCCTGTCGCTGGCAAATACGCCCAGTGTCA
Got1-1      TGGAGAGCGCTGCTTGATTATCTTCTTCAGGAAACTTAACAAGCTCACCGTCCTGTCGCTGGCAAATACGCCCAGTGTCA
Got1-2      TGGAGAGCGCTGCTTGATTATCTTCTTCAGGAAACTTAACAAGCTCACCGTCCTGTCGCTGGCAAATACGCCCAGTGTCA
Got1-3      TGGAGAGCGCTGCTTGATTATCTTCTTCAGGAAACTTAACAAGCTCACCGTCCTGTCGCTGGCAAATACGCCCAGTGTCA
Got1-4      TGGAGAGCGCTGCTTGATTATCTTCTTCAGGAAACTTAACAAGCTCACCGTCCTGTCGCTGGCAAATACGCCCAGTGTCA
Got1-5      TGGAGAGCGCTGCTTGATTATCTTCTTCAGGAAACTTAACAAGCTCACCGTCCTGTCGCTGGCAAATACGCCCAGTGTCA
Got1-6      TGGAGAGCGCTGCTTGATTATCTTCTTCAGGAAACTTAACAAGCTCACCGTCCTGTCGCTGGCAAATACGCCCAGTGTCA
Got1-7      TGGAGAGCGCTGCTTGATTATCTTCTTCAGGAAACTTAACAAGCTCACCGTCCTGTCGCTGGCAAATACGCCCAGTGTCA
Got1-8      TGGAGAGCGCTGCTTGATTATCTTCTTCAGGAAACTTAACAAGCTCACCGTCCTGTCGCTGGCAAATACGCCCAGTGTCA
Got1-9      TGGAGAGCGCTGCTTGATTATCTTCTTCAGGAAACTTAACAAGCTCACCGTCCTGTCGCTGGCAAATACGCCCAGTGTCA
Got1-10     TGGAGAGCGCTGCTTGATTATCTTCTTCAGGAAACTTAACAAGCTCACCGTCCTGTCGCTGGCAAATACGCCCAGTGTCA

jetlag      TGGAGAGCGCTGCTTGATTATCTTCTTCAGGAAACTTAACAAGCTCACCGTCCTGTCGCTGGCAAATACGCCCAGTGTCA
W1118-1     TGGAGAGCGCTGCTTGATTATCTTCTTCAGGAAACTTAACAAGCTCACCGTCCTGTCGCTGGCAAATACGCCCAGTGTCA
W1118-2     TGGAGAGCGCTGCTTGATTATCTTCTTCAGGAAACTTAACAAGCTCACCGTCCTGTCGCTGGCAAATACGCCCAGTGTCA
W1118-3     TGGAGAGCGCTGCTTGATTATCTTCTTCAGGAAACTTAACAAGCTCACCGTCCTGTCGCTGGCAAATACGCCCAGTGTCA
W1118-4     TGGAGAGCGCTGCTTGATTATCTTCTTCAGGAAACTTAACAAGCTCACCGTCCTGTCGCTGGCAAATACGCCCAGTGTCA
W1118-5     TGGAGAGCGCTGCTTGATTATCTTCTTCAGGAAACTTAACAAGCTCACCGTCCTGTCGCTGGCAAATACGCCCAGTGTCA
W1118-6     TGGAGAGCGCTGCTTGATTATCTTCTTCAGGAAACTTAACAAGCTCACCGTCCTGTCGCTGGCAAATACGCCCAGTGTCA
W1118-7     TGGAGAGCGCTGCTTGATTATCTTCTTCAGGAAACTTAACAAGCTCACCGTCCTGTCGCTGGCAAATACGCCCAGTGTCA
W1118-8     TGGAGAGCGCTGCTTGATTATCTTCTTCAGGAAACTTAACAAGCTCACCGTCCTGTCGCTGGCAAATACGCCCAGTGTCA
W1118-9     TGGAGAGCGCTGCTTGATTATCTTCTTCAGGAAACTTAACAAGCTCACCGTCCTGTCGCTGGCAAATACGCCCAGTGTCA
W1118-10    TGGAGAGCGCTGCTTGATTATCTTCTTCAGGAAACTTAACAAGCTCACCGTCCTGTCGCTGGCAAATACGCCCAGTGTCA
```

B

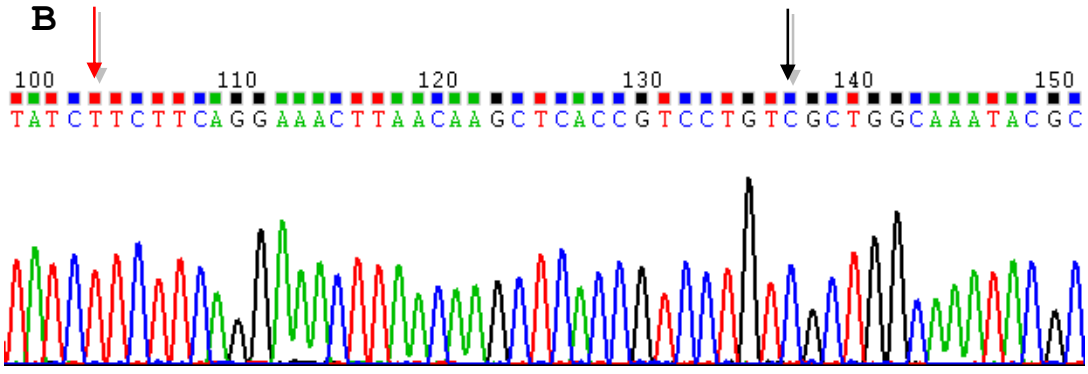

Figure 5.13 – Looking for *jetlag* mutations. A: Alignment of *wP{GT1}Gs2*, *w;P{GT1}Got1;* and w^{1118} *jet* sequence. **B:** Representative chromatogram of wild-type jetlag. **Red arrow:** jet^{c} mutation site. **Black arrow:** jet^{r} mutation site.

5.2.1.5 Checking if other *Gs2* and *Got1* variants are *Veela* strains.

Besides *wP{GT1}Gs2* and *w;P{GT1}Got1*, other mutants and RNAi lines for G*s2* and *Got1* were also genotyped for *tim*. Table 5.5 shows the *tim* alleles found for each fly line as well as their locomotor behaviour in LL (previously shown in chapter 4). These flies were also sequenced to check for *jetlag* mutations and the results are also represented in table 5.5. As shown in table 5.5, all the rhythmic fly lines in LL carry at least one copy of the *ls-tim* allele, indicating once again its association with the *Gs2* and *Got1* phenotypes. Again, mutations in *jetlag* were not found in any fly line.

PCR reactions revealed that *tim-Gal4* flies are homozygous *s-tim* and that the *Gs2* RNAi line (VDRC 32929) is *ls-tim/s-tim* heterozygous (figure 5.14). Consequently, crossing these two lines to knock down of *Gs2* in the clock neurons should result in flies with two different *tim* genotypes (*s-tim* homozygous and *ls-tim/s-tim* heterozygous) (table 5.5). These flies were not genotyped by PCR because the *tim* background of their parental lines was well-known. However, since a high percentage of them are rhythmic in LL, it is likely that the majority of the flies tested in locomotor behaviour experiments carry one *ls-tim* allele.

Similarly, the *tim* alleles of flies downregulating *Got1* in clock neurons were inferred from their parental lines, as they are not kept as a stock. Two RNAi lines, 8430R-1 and 8430R-2, are *s-tim* homozygous while the third RNAi line (VDRC108247) amplified only the *ls-tim* band in PCR reactions (figure 5.14). Crossing 8430R-1 and 8430R-2 *s-tim* RNAi lines to *tim-Gal4* (*s-tim*) generated homozygous *s-tim* arrhythmic flies (table 5.5). On the other hand, flies knocking down *Got1* via the RNAi line VDRC 108247 (*ls-tim*) are obligatory *ls-tim/s-tim*

heterozygotes and showed rhythmicity in LL (table 5.5). Finally, the completely LL arrhythmic *Got1* mutant, *yw; P{wHy} Got1*, carries only the *s-tim* allele (figure 5.14).

Table 5.5 – Identification of *tim* and *jetlag* alleles.

***Gs2* tested variants**	**% Rhythmic in LL**	***tim* allele**	***jet*^{C}/ *jet*^{R}**
w;tim-Gal4/+;RNAiGs2/+ (VDRC 32929)	81.25	*s-tim* *ls-tim/s-tim*	No
VDRC 32929 (Control)	15	*ls-tim/s-tim*	No
w;tim-Gal4;+ (Control)	4	*s-tim*	No
***Got1* tested variants**			
y^{1} *w*^{67c23}*; P{wHy} Got1*^{DG14503}*;+* (20423)	0	*s-tim*	No
w; tim-Gal4/RNAi Got1; (VDRC108247)	72.2	*ls-tim/s-tim*	No
w; tim-Gal4/+; RNAi Got1/+ (8340R-2)	37.5	*s-tim*	No
w; tim-Gal4/ RNAi Got1;+ (8340R-1)	26	*s-tim*	No
VDRC108247 (Control)	33.4	*ls-tim*	No
8430R-1 (Control)	9.1	*s-tim*	No
8430R-2 (Control)	8	*s-tim*	No

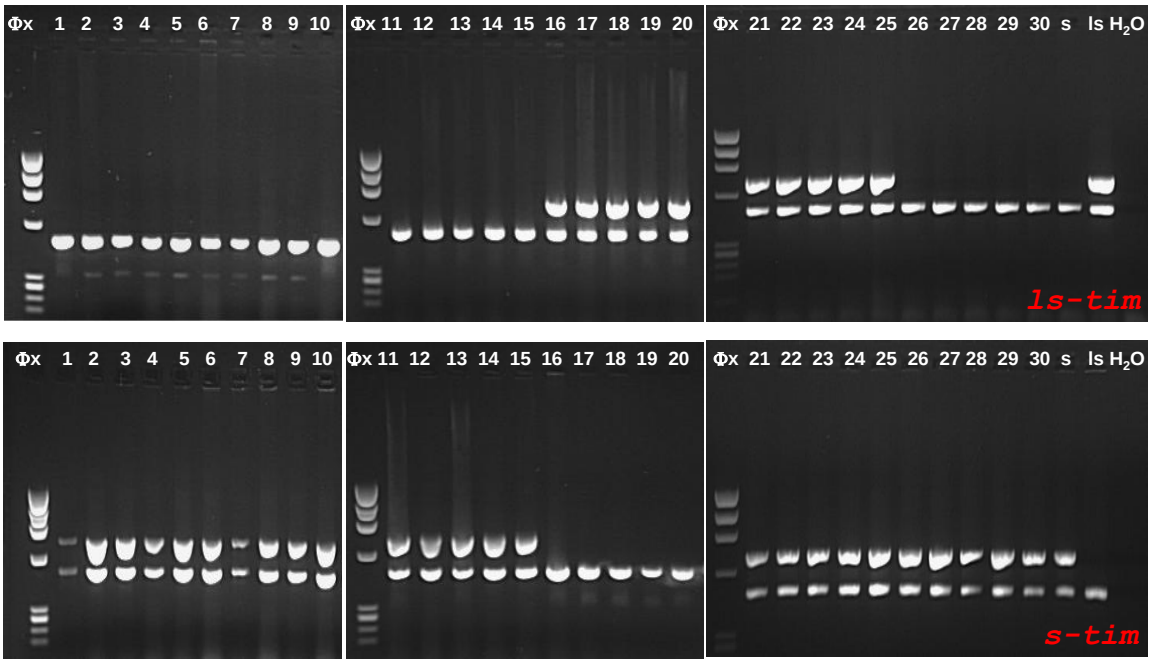

Figure 5.14 - Genotyping *tim* allele by PCR. The PCR products were resolved on a 1.5% agarose gel. The lower band is a control of PCR efficacy. **Top Panel:** Reactions using *ls-tim* primers. **Lower Panel:** Reactions using *s-tim* primers. The numbers above each lane represent each fly tested. **ϕX:** ϕX Hae III. **1 to 5:** 8430R-1 control. **6**

to 10: 8430R-2 control. **11 to 15:** *w;tim-Gal4;*.**16 to 20:** VDRC 108247 control. **21 to 25:** VDRC 32929 control. **26 to 30:** *yw; P{wHy} Got1;*. **s:** *s-tim* positive control. **ls:** *ls-tim* positive control. **H_2O:** water control (no DNA).

5.2.1.6 Checking *tim* correlation with *Gs2* and *Got1*.

In order to verify whether the LL phenotypes of *wP{GT1}Gs2* and *w;P{GT1}Got1* mutants are associated with *ls-tim*, they were both placed on the *s-tim* background. *Gs2* and *Got1* mutants (both *ls-tim*) were crossed to w^{1118} (*s-tim*) and the progeny mated among themselves. The *s-tim* flies genotyped by PCR were selected to make a stock (figure 5.16) and after a few generations double-checked by PCR.

Under LL, only 21.8% of *wP{GT1}Gs2;;* (*s-tim*) flies were rhythmic (figure 5.15), whereas 20% of *w;P{GT1}Got1;* (*s-tim*) mutants showed rhythmicity. These data suggests that only when *Gs2* and *Got1* mutants are linked to the *ls-tim* allele, which encodes the less-light-sensitive form of *tim*, will abnormal rhythmicity in LL be observed at high levels.

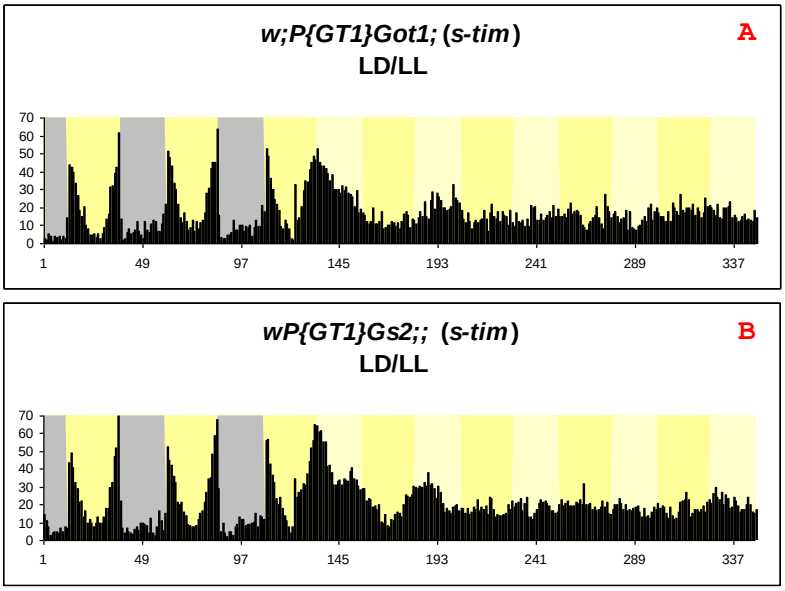

Figure 5.15 - Mean activity of *Got1* and *Gs2* mutants in *s-tim* background. Flies were entrained for 3 days in LD and then exposed to 5 days of LL. **A:** *w;P{GT1}Got1;* in *s-tim* background. **B:** *wP{GT1}Gs2;* in *s-tim* background **X-axis:** time in 30 minutes bins. **Y-axis:** mean level of activity. **Gray:** Dark. **Dark yellow:** Subjective daylight. **Yellow:** Subjective night.

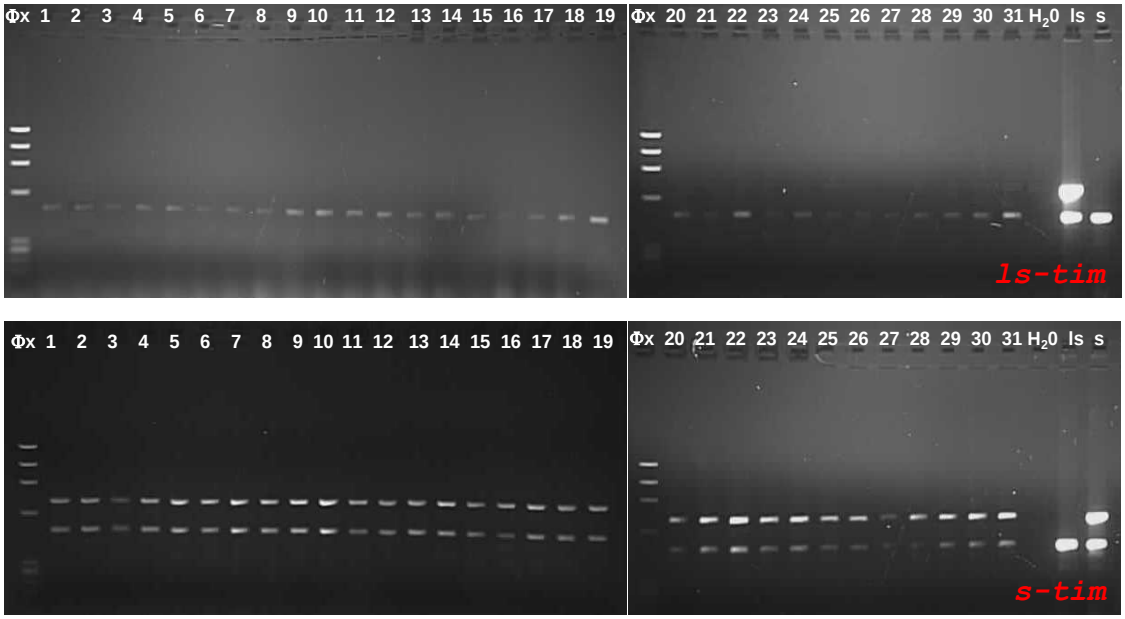

Figure 5.16 - Genotyping *tim* to create *s-tim* stocks. The PCR products were resolved on a 1.5% agarose gel. The lower band is a control of PCR efficacy. **Top Panel:** Reactions using *ls-tim* primers. **Lower Panel:** Reactions using *s-tim* primers. The numbers above each lane represent each fly tested. **ϕX:** ϕX Hae III. **1 to 15:** *wP{GT1}Gs2;*. **16 to 31:** *w;P{GT1}Got1;*. **s:** *s-tim* positive control. **ls:** *ls-tim* positive control. **H_2O:** water control (no DNA).

5.2.2 TIM stability in LL

In order to study whether the light-induced degradation of TIM is affected in *Got1* and *Gs2* mutants, I analysed TIM abundance in LL from two independent Western blots. Flies were entrained for 3 days in LD12:12 and heads were collected in the first day of LL, at four different time points (CTs 1,7,13 and 19). In order to correct for loading errors, the membranes were probed for constitutively expressed Tubulin, which was used to normalise the intensity of TIM bands. Also, tim^{01} was used as a negative control and Canton S flies collected at ZT21 as a positive control. As expected, TIM abundance in head protein extracts was increased in *Got1* and *Gs2* mutants when compared to Canton S flies (figure 5.17).

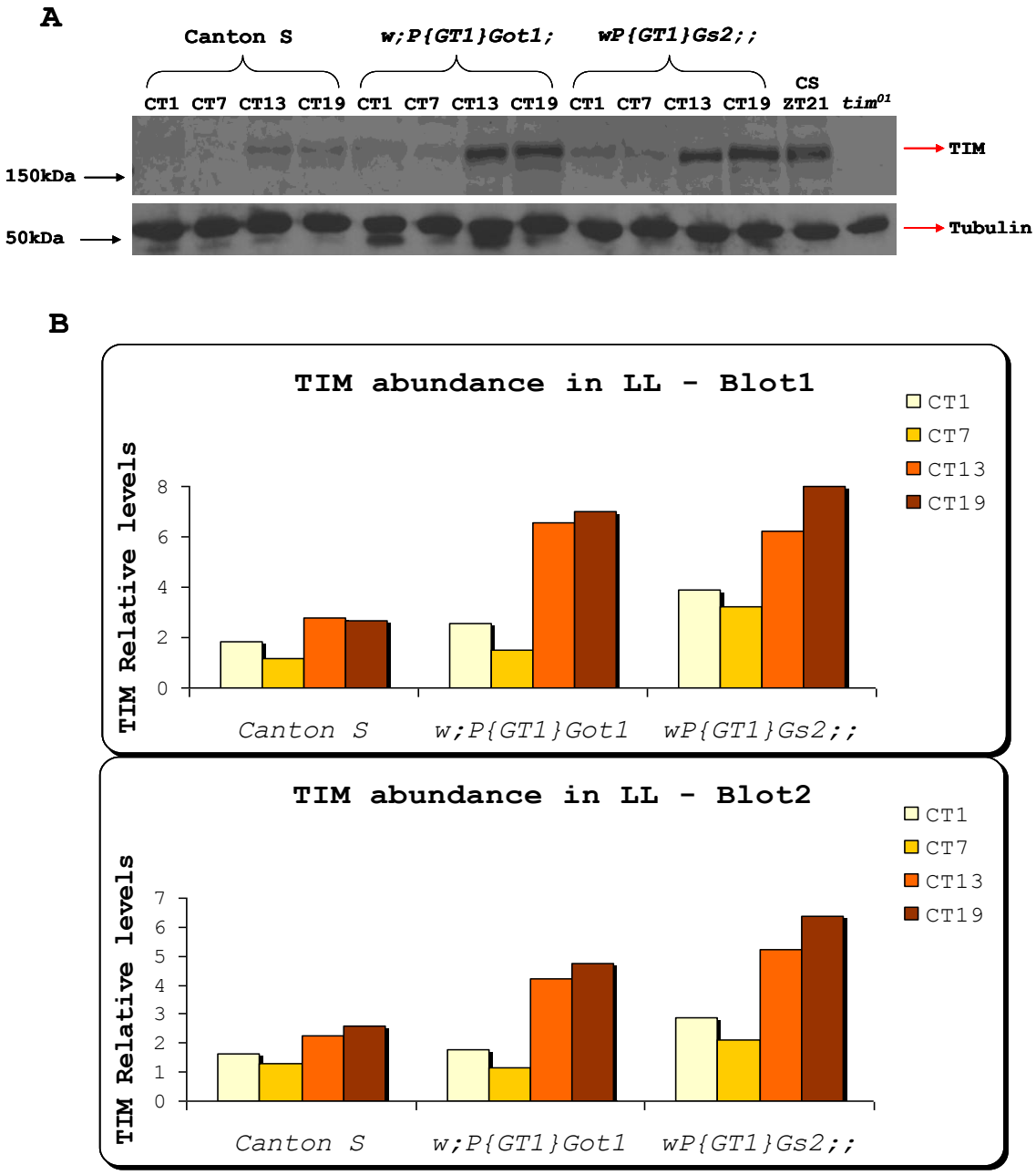

Figure 5.17 - Western Blots reveal TIM stabilisation in *Got1* and *Gs2* mutants. A: Western Blot of head extracts from *w;P{GT1}Got1*, *wP{GT1}Gs2;* and Canton S flies collected in LL. Canton S collected in LD cycles and tim^{01} were used as positive and negative controls, respectively. Genotypes and time points of collection (CT) are indicated above the blot. **B:** Quantification of TIM bands from two Western Blot replicates

5.2.3 Light induced phase shifts in *Got1* and *Gs2* mutants

The *Got1* and *Gs2* mutants' locomotor phase response to 10 min light pulses, delivered at ZT15 and ZT21, were also examined. *w;P{GT1}AdhAdhr* flies were used as control since they are in the same background as the mutants and have normal arrhythmic responses to light in LL.

Figure 5.18 shows the mean phase shift of two independent experiments three days after the light pulse. ANOVA revealed that when the light pulse is administrated at ZT 21 (figure 5.18 A), *Got1* mutants have a significantly smaller phase advance than the control ($F_{1,79}$ =8.22, $p<0.005$) and also when compared to *Gs2* mutants ($F_{1,116}$=31.62, $p<10^{-6}$). On the contrary, *Gs2* mutants are similarly affected as the control by the light pulse, showing an advance of about 1.5h ($F_{1,81}$=1.54, p=0.22).

Similarly for delays, statistical analyses revealed that *Got1* mutants are less phase shifted comparatively to the control ($F_{1,72}$=9.09, p=0.0035) and to *Gs2* mutants ($F_{1,122}$=13.52, $p<10^{-3}$). Additionally, *Gs2* mutants consistently showed a delay similar to the control flies ($F_{1,70}$=1.25, p=0.27) (figure 5.18 B). The *Gs2* results are somewhat unexpected given that TIM is more stable in LL, and would be expected to produce a smaller phase shift under light pulsing conditions.

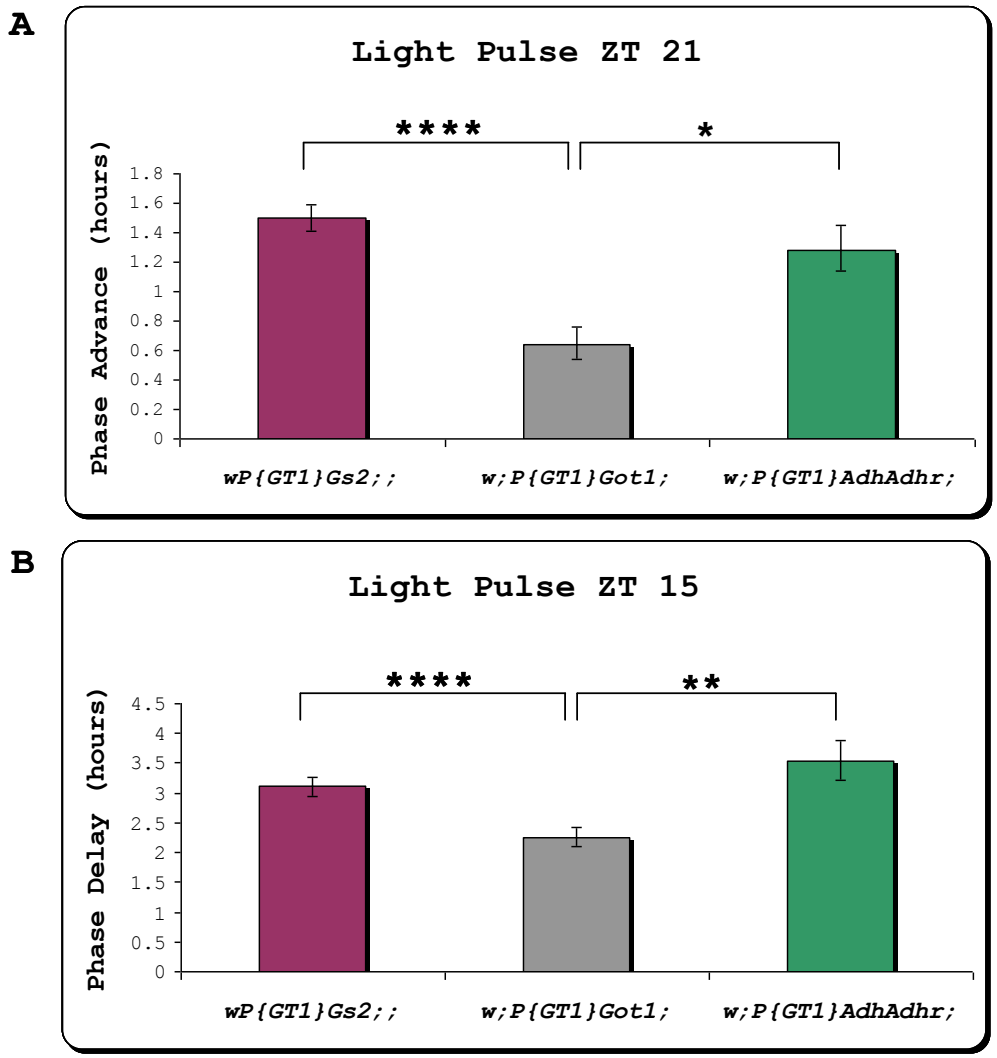

Figure 5.18 - Phase response to light pulses of *Got1* and *Gs2* mutants. Phase responses in hours (±SEM) to 10 min light pulses. The data shown is the mean phase shift of two independent experiments three days after the light pulse. **A:** Light pulse delivered at ZT21, giving phase advances. **B:** Light pulse delivered at ZT15, giving phase delays. The genotypes are indicated bellow the graphs. * $p<0.05$, **$p<0.01$, ***$p<0.001$ and ****$p<0.0001$.

5.2.4 Directing *Got1* and *Gs2* expression to specific neurons subsets

Since *Got1* and *Gs2* mutants behave rhythmically in LL, it was interesting to define which subset of the clock neurons would drive this behaviour or whether all neurons would be affected equally by these genetic variants. To answer this question, *Got1* and *Gs2* were knocked down by RNA interference in different clusters of

neurons. The use of RNAi for targeted knockdown of gene expression to address cell specific gene function was used in conjunction with the *Gal4*/*Gal80* system. *Gal80* inhibits *Gal4*-mediated transcriptional activation when binding to its carboxy-terminal (Duffy, 2002).

The knockdown of *Got1* and *Gs2* in peptidergic neurons, including the l-LNvs, but excluding all other known clock neurons, with the *c929-Gal4* driver {{139 Taghert,P.H. 2001; 32 Grima,B. 2004}} resulted in arrhythmicity in LL (table 5.6 and figure 5.19). Similarly, the great majority of these flies were arrhythmic under constant light when the *mai179-Gal4* driver was used (table 5.6). The *mai179-Gal4* driver manipulated the levels of *Got1* and *Gs2* primarily in the s-LNvs, but also in three CRY+ LNds and possibly in one of the two DN1as (Grima *et al.*, 2004).

In *Drosophila*, the *cry-Gal80* driver suppresses *Gal4* activity in a broad subset of neurons. Consequently, when the pan-clock-cell *tim-Gal4* driver is combined with *cry-Gal80*, the expression is restricted to the DN1p, DN2 and DN3 (Stoleru *et al.*, 2004). Downregulating *Got1* in the DNs resulted in 62.5% of rhythmic flies in LL, whereas for *Gs2*, rhythmicity was observed in 53% of the flies (table 5.6 and figure 5.19).

Because *pdf-Gal80* suppresses *Gal4* activation in the LNvs, combining *tim-Gal4* driver with the *pdf-Gal80* repressor restricted *Got1* and *Gs2* knockdown to the LNds and DNs. In this case, 73% of down regulated *Got1* flies were rhythmic in LL and knocking down *Gs2* in these neurons resulted in more than 90% of rhythmic flies (table 5.6 and figure 5.19).

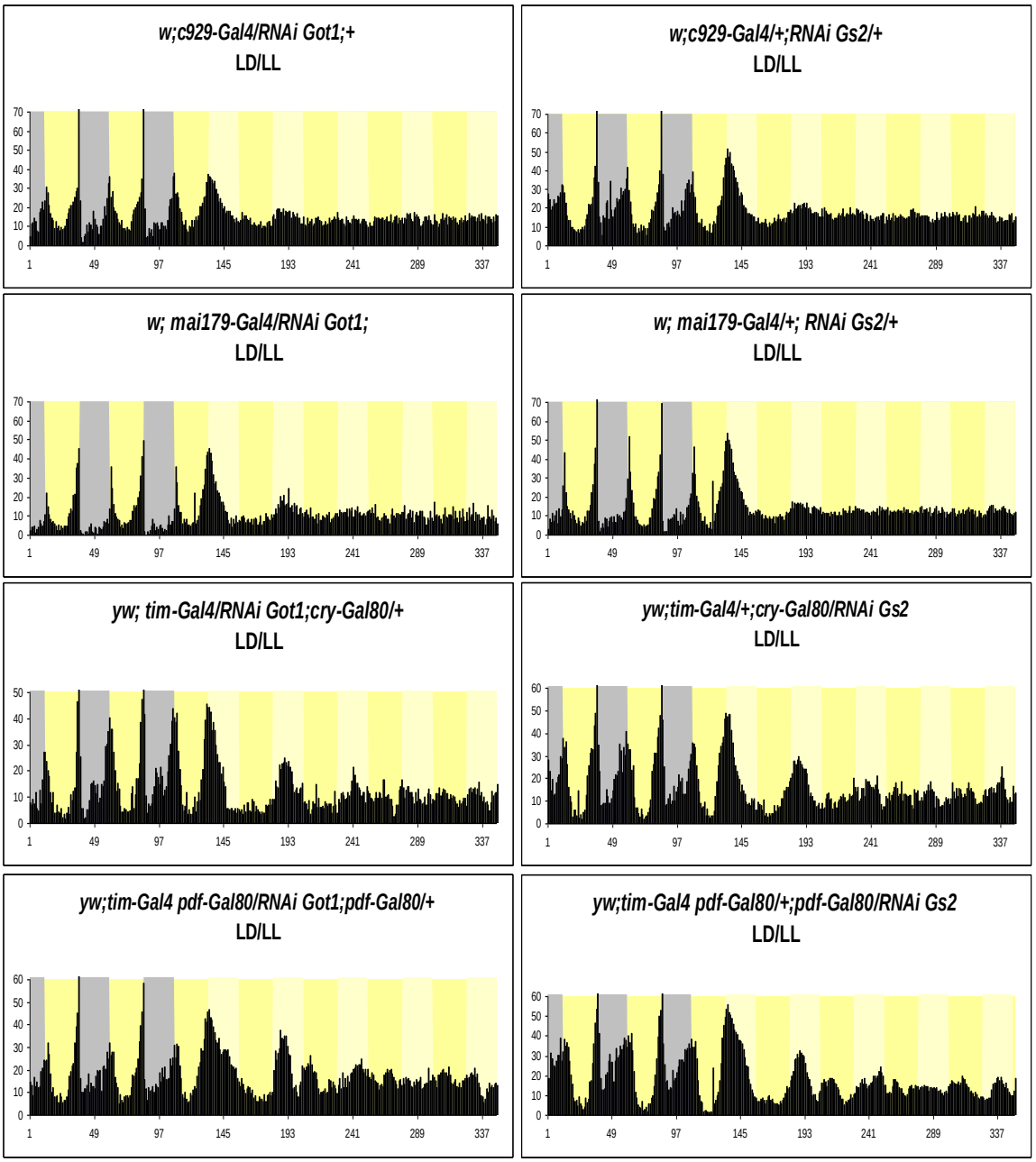

Figure 5.19 - Locomotor activity of flies downregulating *Got1* and *Gs2* in different cells. Flies were entrained for 3 days in LD and then exposed to 5 days of LL. **Left:** Graphs representing the manipulation of *Got1* expression in different neurons. **Right:** Graphs representing the manipulation of *Gs2* expression in different neurons. **X-axis:** time in 30 minutes bins. **Y-axis:** mean level of activity. **Gray:** Dark. **Dark yellow:** Subjective daylight. **Yellow:** Subjective night. Genotypes are indicated on top of each graph.

Table 5.6 – RNAi knockdown of *Gs2* and *Got1* in different clock neuronal subsets.

Genotype	LL		
	% Rhythmic	Mean Period ± SEM	n
w; c929-Gal4/RNAi Got1; (VDRC 108247)	12.5	-----	32
w; c929-Gal4/+;RNAi Gs2/+ (VDRC 32929)	18.7	-----	32
w; mai179-Gal4/RNAiGot1; (VDRC 108247)	30	-----	30
w; mai179-Gal4/+;RNAi Gs2/+ (VDRC 32929)	18.8	-----	32
yw;tim-Gal4/RNAi Got1;cry-Gal80/+ (VDRC 108247)	62.5	25.5 ± 0.6	20
yw;tim-Gal4/+;cry-Gal80/RNAi Gs2 (VDRC 32929)	53	25.9 ± 0.5	32
yw;tim-Gal4 pdf-Gal80/RNAi Got1;pdf-Gal80/+ (VDRC 108247)	73.3	25.8 ± 0.6	30
yw;tim-Gal4 pdf-Gal80/+;pdf-Gal80/RNAi Gs2 (VDRC 32929)	96	26 ± 0.4	30
Controls	**LL**		
	% Rhythmic	**Mean Period ± SEM**	**n**
w; c929-Gal4/+;	0	-----	31
yw;tim-Gal4/+;cry-Gal80/+	28	-----	32
yw;tim-Gal4 pdf-Gal80/+;pdf-Gal80/+	41	-----	32
w; mai179-Gal4/+;	15.7	----	19

The transgenic flies carrying the drivers used to silence *Got1* and *Gs2* were also tested in LL as controls and none of them behaved rhythmically (table 5.6). Moreover, it was previously shown in chapter 4 that the RNAi lines for *Gs2* (VDRC 32929) and *Got1* (VDRC 108247) are also arrhythmic in LL.

Figure 5.20 shows a representative scheme of the locomotor behaviour in LL of files downregulating *Got1* and *Gs2* in different groups of cells. It can be noticed that the LNvs do not seem to be involved in the rhythmic phenotype observed, since downregulating both genes in this group of cells generated arrhythmicity. On the

contrary, the DNs by themselves or along with LNds seem to be sufficient to maintain locomotor rhythms in LL.

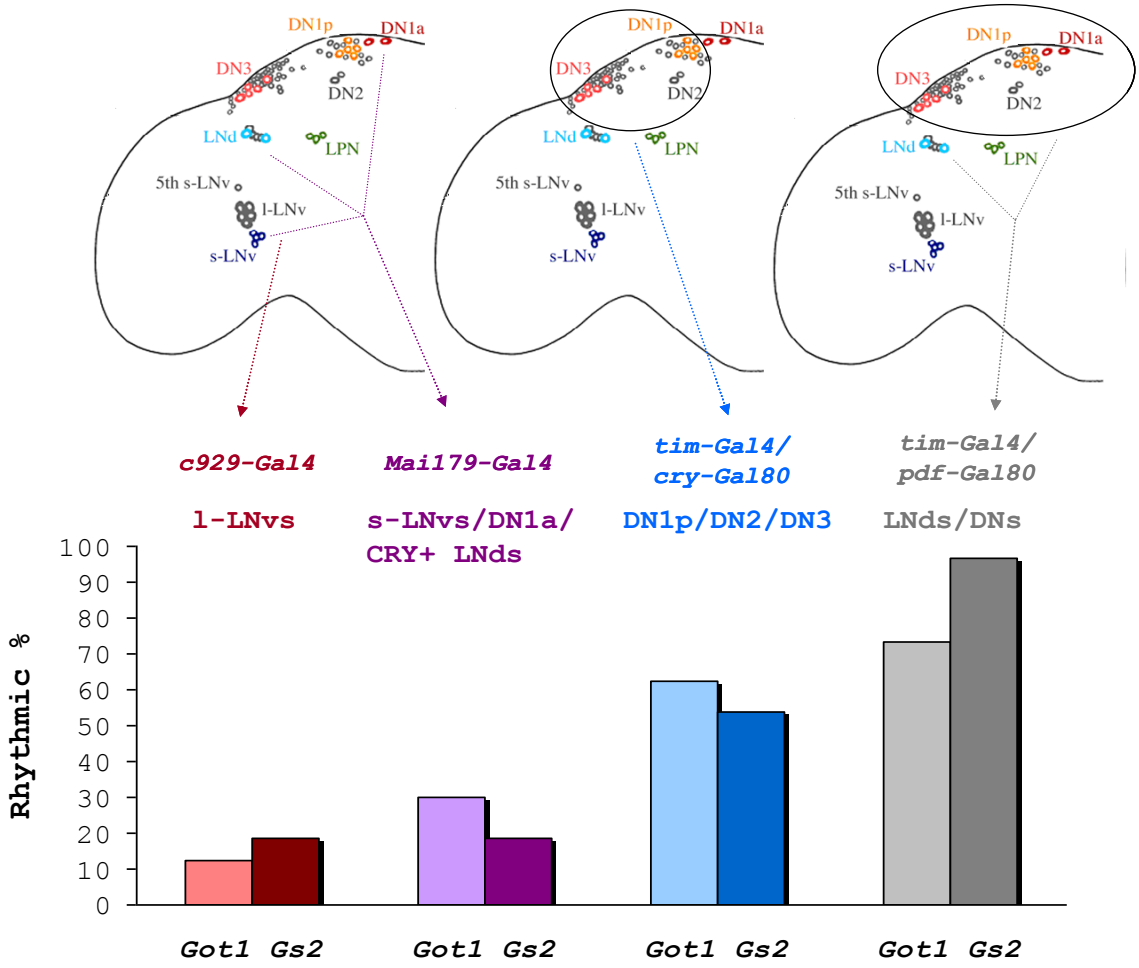

Figure 5.20 –Clock neuron clusters involved in *Got1* and *Gs2* rhythmicity. The graph shows the percentage of rhythmic flies in each group of neurons. The drivers used in combination with the RNAi lines are indicated on the top of the graph, along with the cells in which the manipulation occurred. The figure of the brain was taken from (Shafer *et al.*, 2006).

5.2.5 Manipulating the metabotropic receptor of glutamate and the metabolism pathway.

RNA interference was used in order to check whether blocking glutamate reception in clock neurons, via its metabotropic receptor DmGluRA, affects the

circadian clock. Among the three RNAi lines used, two of them (VDRC 1793 and VDRC 1794) targeted the same region of the *DmGluRA* gene, while the third one (VDRC 103736) targeted a different portion of the gene.

In DD, no effect on the locomotor behaviour was observed when *DmGluRA* was knocked down with *tim-Gal4* (table 5.7). As shown in figure 5.21, the flies were rhythmic in DD with normal 24-h periods. On the other hand, under LL these flies behaved abnormally rhythmically, while their RNAi controls were arrhythmic (figure 5.22).

Glutamate serves as the precursor for the synthesis of the inhibitory GABA neurotransmitter and this reaction is catalyzed by glutamate decarboxylase (GAD). The down regulation of *Gad* in clock cells was driven by *tim-Gal4* and the locomotor behaviour of the flies was observed in DD and LL. When placed in DD the flies showed robust 24-h rhythms (figure 5.21), and in LL, locomotor rhythms were also observed (figure 5.23). Once again, the RNAi control was arrhythmic in LL.

Table 5.7 – Knockdown of *DmGluRA* and *Gad* in clock cells.

Genotype	DD			LL		
	% Rhythmic	Mean Period ± SEM	n	% Rhythmic	Mean Period ± SEM	n
w;tim-Gal4/+;RNAi DmGluRA/+ (VDRC 1793)	100	24.1± 0.14	28	52	23.5 ± 0.5	31
w;tim-Gal4/+;RNAi DmGluRA/+ (VDRC 1794)	100	23.8 ± 0.09	31	65.6	23.9 ± 0.5	32
w;tim-Gal4/RNAi DmGluRA; (VDRC 103736)	100	23.7 ± 0.06	32	64.5	24.8 ± 0.5	31
w;tim-Gal4/+;RNAi Gad1/+ (VDRC 32344)	100	23.7 ± 0.09	31	56.3	24 ± 0.55	32
VDRC 1793 (Control)	96.7	23.9 ± 0.1	30	26.7	-----	30
VDRC 1794 (Control)	100	23.8 ± 0.07	32	25	-----	32
VDRC 103736 (Control)	93.8	23.4 ± 0.06	32	15.6	-----	32
VDRC 32344 (Control)	96.5	23.7 ± 0.1	29	31.3	-----	30
w; tim-Gal4; (Control)	71	24.5 ± 0.3	31	4	-----	51

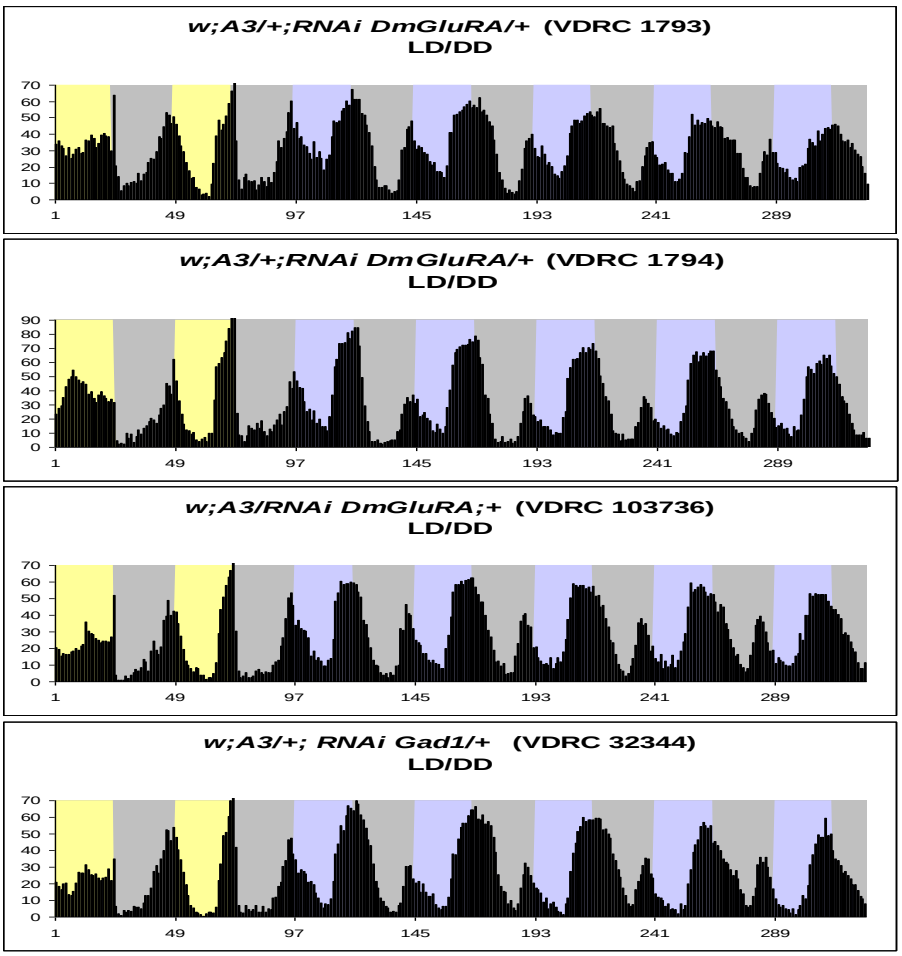

Figure 5.21 - Locomotor activity of *DmGluRA* and *Gad* RNAi in DD. Flies were entrained for 2 days in LD and placed in DD for 5 days. **X-axis:** time in 30 minutes bins. **Y-axis:** mean level of activity. **Yellow:** day. **Gray:** subjective night. **Blue:** subjective day. Genotypes are indicated on top of each histogram. All genotypes were rhythmic and are indicated above each graph.

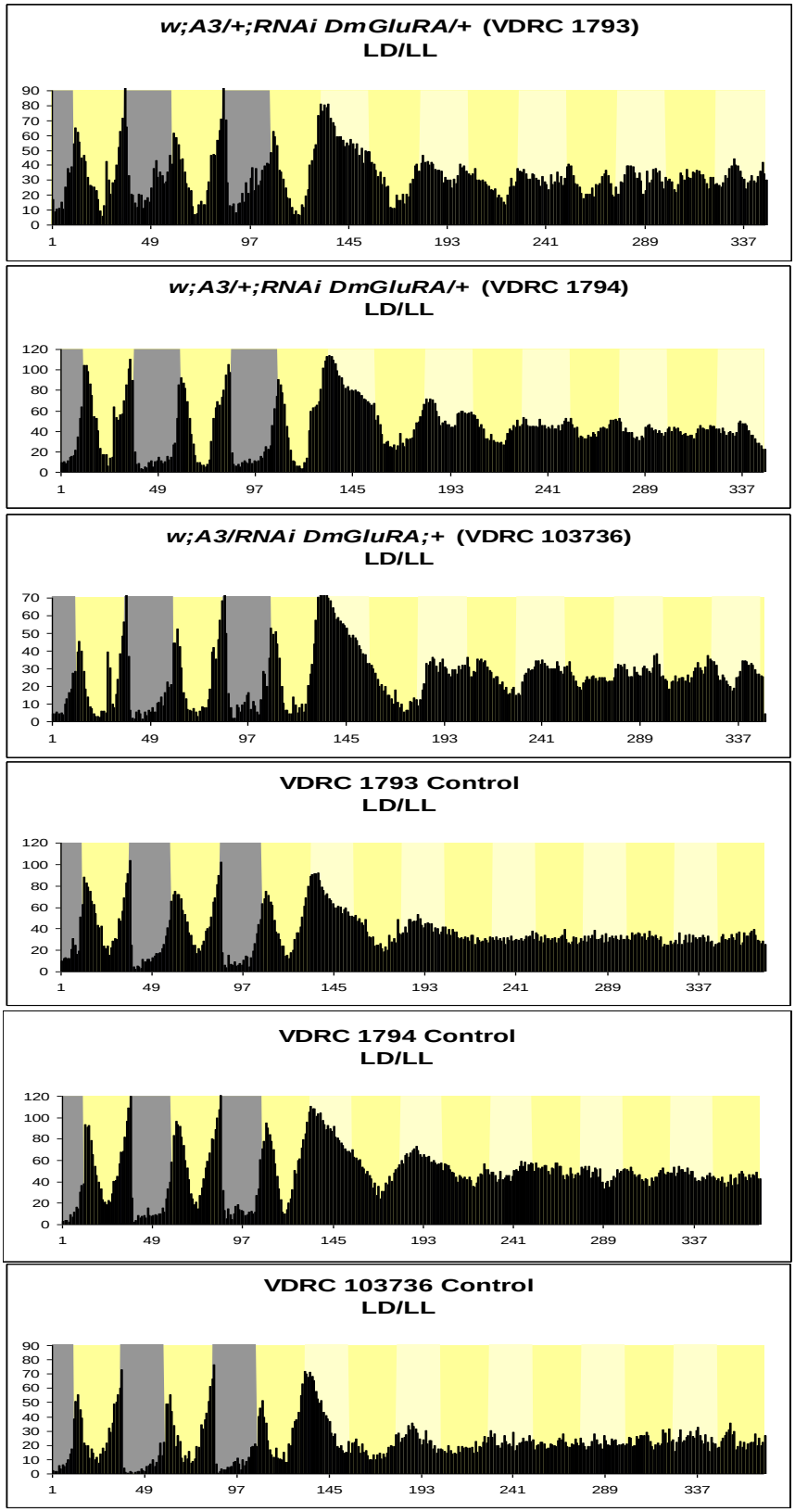

Figure 5.22 - Mean activity of *DmGluRA* RNAi in LL. Flies were entrained for 3 days in LD and then exposed to 5 days of LL. **X-axis:** time in 30 minutes bins. **Y-axis:** mean level of activity. **Gray:** Dark. **Dark yellow:** Subjective daylight. **Yellow:** Subjective night. Genotypes are indicated above each graph.

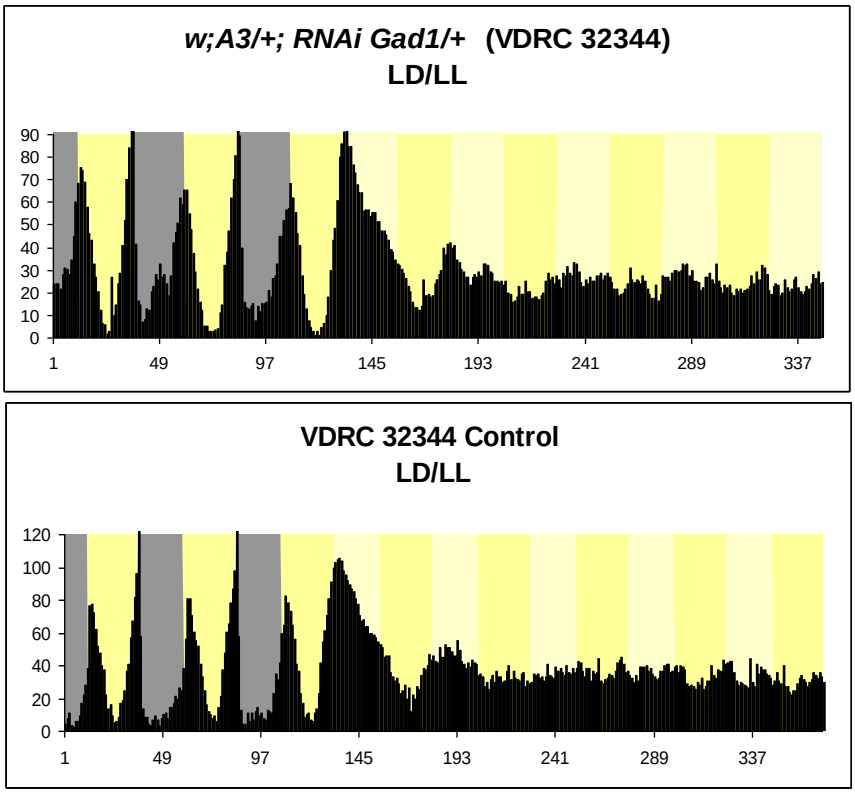

Figure 5.23 – Activity profile of *Gad* RNAi in LL. Flies were entrained for 3 days in LD and then exposed to 5 days of LL. **X-axis:** time in 30 minutes bins. **Y-axis:** mean level of activity. **Gray:** Dark. **Dark yellow:** Subjective daylight. **Yellow:** Subjective night. Genotypes are indicated above graphs.

The RNAi lines of *DmGluRA* and *Gad* were genotyped by PCR for *tim* and *jetlag* alleles. As shown in figure 5.24, all the *DmGluRA* RNAi lines are *ls-tim* homozygous and the three possible *tim* genotypes were found among *Gad* RNAi flies (*ls-tim* homozygous, *s-tim* homozygous and *ls-tim*/*s-tim* heterozygous). These RNAi lines were then crossed to *s-tim* homozygous *w;tim-Gal4;* and none of them carry jet^c or jet^r mutations (table 5.7).

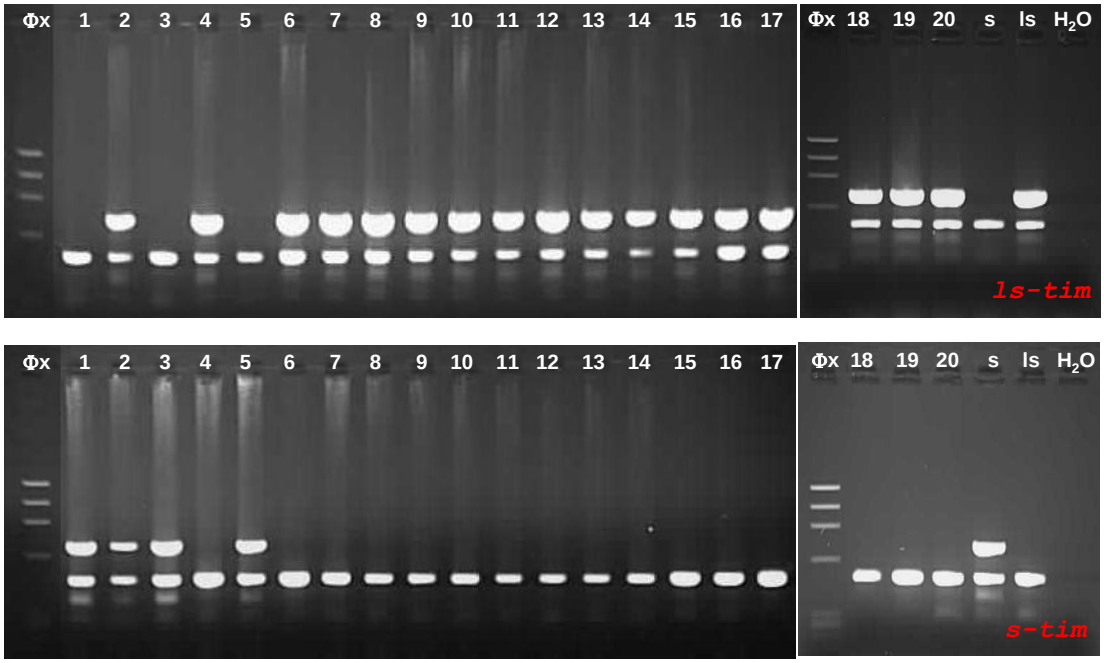

Figure 5.24 - Determining *tim* alleles of *DmGluRA* and *Gad* RNAi by PCR. The PCR products were resolved on a 1.5% agarose gel. The lower band is a control of PCR efficacy. **Top Panel:** Reactions using *ls-tim* primers. **Lower Panel:** Reactions using *s-tim* primers. The numbers above each lane represent each fly tested. **ϕX:** ϕX Hae III. **1 to 5:** VDRC 32344. **6 to 10:** VDRC 103736. **11 to 15:** VDRC 1793. **16 to 20:** VDRC 1794. **s:** *s-tim* positive control. **ls**: *ls-tim* positive control. **H_2O:** water control (no DNA).

Table 5.8 - Genotyping *DmGluRA* and *Gad* RNAi for *tim* and *jetlag* alleles

***DmGluRA* RNAi**	***tim* allele**	***jet*^{C}/ *jet*^{R}**
VDRC 1793 (Control)	*ls-tim*	No
VDRC 1794 (Control)	*ls-tim*	No
VDRC 1794 (Control)	*ls-tim*	No
w;tim-Gal4;+ (Control)	*s-tim*	No
***Gad1* RNAi**		
VDRC 32344 (Control)	*ls-tim* *s-tim* *ls-tim/s-tim*	No

5.3 Discussion

The neuropeptide pigment dispersing factor (PDF) is the only neurotransmitter that has been functionally identified in *Drosophila* clock neurons, more specifically in the LNvs (Helfrich-Forster, 1995; Renn *et al.*, 1999). Since little is known about the synaptic connections and neurotransmitters in the circadian circuitry, the identification of new neurotransmitters in clock neurons is the key to understanding the circuits of the *Drosophila* circadian system.

In *Drosophila*, the neurotransmission by glutamate is mediated by ionotropic receptors that form cation channels (Anwyl, 1999; Dingledine *et al.*, 1999) and metabotropic G-protein coupled receptor (Bogdanik *et al.*, 2004). Previous work has implicated glutamate and its metabotropic receptor, DmGluRA, in the *Drosophila* clock circuitry (Hamasaka *et al.*, 2007). Transgenic flies with altered expression of DmGluRA in the LNvs showed altered locomotor activity under LD and DD. In free running conditions, a lengthening in the period of activity could be observed, whereas in LD cycles a strong increase in the activity after lights-off was noticed (Hamasaka *et al.*, 2007).

The locomotor behaviour studies on flies with altered expression levels of *Gs2* and *Got1*, both involved in the glutamate metabolism pathway, implicated these genes in the circadian clock light entrainment. The use of transgenic mutants and RNAi to knockdown these genes in clock neurons, led to rhythmicity in LL. The effect of the mutants' background on locomotor behaviour was verified and the robust rhythms in LL were attributed to modifications on *Gs2* and *Got1* expression. Transgenic flies carrying the *P{GT1}* element inserted in non-clock genes, were arrhythmic in LL (table 5.1 and figure 5.2), excluding rhythmicity as a consequence of the background.

Another way of showing that *P{GT1}Got1* and *P{GT1}Gs2* were causing rhythmicity in LL was the randomization of the mutants' background (figures 5.3 and 5.5). Homozygous flies for *P{GT1}Got1* and *P{GT1}Gs2* mutant alleles were crossed to w^{1118} flies, and in the F2, flies carrying *P{GT1}Got1* (figure 5.4) and *P{GT1}Gs2* (figure 5.6) were rhythmic in LL, while flies carrying only the wild-type allele were arrhythmic. Additionally, crossing *ls-tim* homozygous *Gs2* and *Got1* mutants to *s-tim* homozygous w^{1118} flies (figure 5.3 and 5.5) resulted in 20% less rhythmic flies. Indeed, a correlation between *tim* alleles and LL behavioural rhythmicity was observed. Almost all *ls-tim* homozygous *P{GT1}Got1* and *P{GT1}Gs2* mutants were rhythmic in LL, whereas all *P{GT1}Gs2 s-tim* homozygous were arrhythmic. No *P{GT1}Got1* in an *s-tim* background was isolated (table 5.4).

To test the hypothesis that *Gs2* and *Got1* mutants depend on the *ls-tim* background to modulate the locomotor rhythnms in LL, an *s-tim* stock of *wP{GT1}Gs2;;* and *w;P{GT1}Got1;* mutants (both originally *ls-tim*) were created (figure 5.16). In fact, *s-tim P{GT1}Got1* and *P{GT1}Gs2* mutants behaved like wild-type flies and became arrhythmic in LL (figure 5.15), suggesting that these mutants genetically interact with *tim* possibly functioning in the same circadian light synchronization pathway. Moreover, the less-light-sensitive TIM isoform encoded by *ls-tim* seems to be necessary and sufficient to attenuate the light input into the circadian clock of *P{GT1}Got1* and *P{GT1}Gs2* flies.

The *Drosophila* strain *Veela* behaves abnormally rhythmically in LL as a consequence of the simultaneous presence of the *ls-tim* haplotype and the jet^{c} mutation characterised by an amino acid substitution (Peschel *et al*., 2006). Since *Got1* and *Gs2* genetic variants resembled *Veela* rhythmic behaviour in LL, they were genotyped for *jetlag* alleles. None of the tested flies carried *jetlag* mutation (table

5.5), reinforcing that *Gs2* and *Got1* are implicated in rhythmic behaviour under LL conditions.

To check molecularly whether *Got1* and *Gs2* variants impair light input to the clock, Western Blots for TIM were performed with *Got1* and *Gs2* mutant heads collected in LL. Confirming this theory, light induced degradation of TIM was affected in these mutants (figure 5.17). TIM levels were much higher in the mutants than in Canton S control flies, especially during subjective night, indicating that rhythms with robust amplitude in TIM cycling might exist even in LL. That provides a good molecular correlate to the rhythms observed at the behavioural level.

DmGluRA is the only functional metabotropic receptor encoded by the *Drosophila* genome (Bogdanik *et al*., 2004). Therefore, downregulating or mutating this single gene provides the unique opportunity to study the entire metabotropic receptor dependent processes in *Drosophila*. The knockdown of DmGluRA in clock cells using three RNAi lines caused rhythmicity in LL and flies showed normal 24 h rhythms in DD. This data suggests that glutamate and its metabotropic receptor influences the light input pathway of the circadian clock, but not the functioning of the core clock.

The distribution of GABA, the major inhibitory neurotransmitter produced in *Drosophila* neurons, has been previously mapped to different areas of the brain (Kuppers *et al*., 2003). Recently, it has been shown by GABA antiserum and flies expressing GFP driven by *Gad1* promoter that s-LNvs receive GABAergic inputs and utilises GABA as a slow inhibitory neurotransmitter (Hamasaka *et al*., 2005). *Glutamate decarboxylase* (*Gad*) is responsible for catalyzing the production of GABA and also for regulating the size of glutamate neurotransmitter pools (Featherstone *et al*., 2002). Our results revealed that downregulating *Gad1* in *Drosophila* clock

neurons generated rhythmicity in LL and normal behaviour in DD, supporting the idea that GABA is part of the light input pathway to the master clock neurons (the s-LNvs).

In this work, the levels of enzymes required for glutamate metabolism in *Drosophila* (*Got1* and *Gs2*) were genetically manipulated in specific subsets of clock neurons, using RNA interference in combination with the system *Gal4*/*Gal80*. The knockdown of both genes in the DNs, via *tim-Gal4/cry-Gal80* driver, led to rhythmic behaviour in LL. In addition, directing the downregulation to the DNs and LNds through *tim-Gal4*/*pdf-Gal80* also resulted in rhythmicity. On the contrary, modifying the levels of *Got1* and *Gs2* in the l-LNvs by *c929-Gal4* and in the s-LNvs and CRY+ LNds with *mai179-Gal4* did not affect locomotor behaviour and flies were arrhythmic in LL. These results suggest that the glutamate metabolism in the DNs is important for entraining the clock. Supporting this theory, it has been previously shown that the *Drosophila* dorsal neurons, DN1s and DN3s, are glutamatergic, since these cells were immunolabeled for vesicular glutamate transporter (DvGluT) (Hamasaka *et al*., 2007). Additionally, antiserum against DmGluRA labelled the LNvs dendrites, indicating that the glutamate signal from the DNs modulates the behaviour pattern on the LNvs (Hamasaka *et al*., 2007). Indeed, axons from DN3s seem to communicate with the LNvs (Veleri *et al*., 2003), whereas axons from DN1s seem to contact the s-LNvs (Helfrich-Forster *et al*., 2001; Helfrich-Forster *et al*., 2002; Veleri *et al*., 2003).

Our results with *Got1* and *Gs2* mutants clearly indicate that glutamate signalling is an important modulator of behavioural light-entrainment. That probably involves the DNs, considering the fact that selective manipulation of these cells was sufficient to drive rhythmicity in LL. However, the way light information is processed in these neurons and transmitted to others to regulate the behavioural phase-shifts is

still obscure. Based on our data, one could speculate on a model where neurotransmitter mediated signalling is driving this response (figure 5.25). As previously mentioned, *Got1* and *Gs2* mutants exhibited different phenotypes, the first with smaller and the latter with normal phase-shifts. In *Got1* mutants, the levels of both glutamate and GABA would be reduced, while in *Gs2* mutants, the biochemical pathway could be shunted towards an excess of GABA and maybe also reduced levels of glutamate, since there would be less glutamine re-uptake from glial cells (Freeman and Doherty, 2006). Therefore, it is possible that overall neurotransmitter levels or the balance of GABA/glutamate in the termini of some clock neurons are driving the phase shift. Given the often inhibitory nature of GABA in the nervous system, one could idealize that, in *Gs2* mutants, GABAergic processes should be more active on the inhibitory neurons regulating the phase-shift, and compensate for any defects in the reuptake of glutamine, which results in a wild-type response. In *Got1* mutants, GABAergic signalling is downregulated and, as a consequence, phase shifts are inhibited.

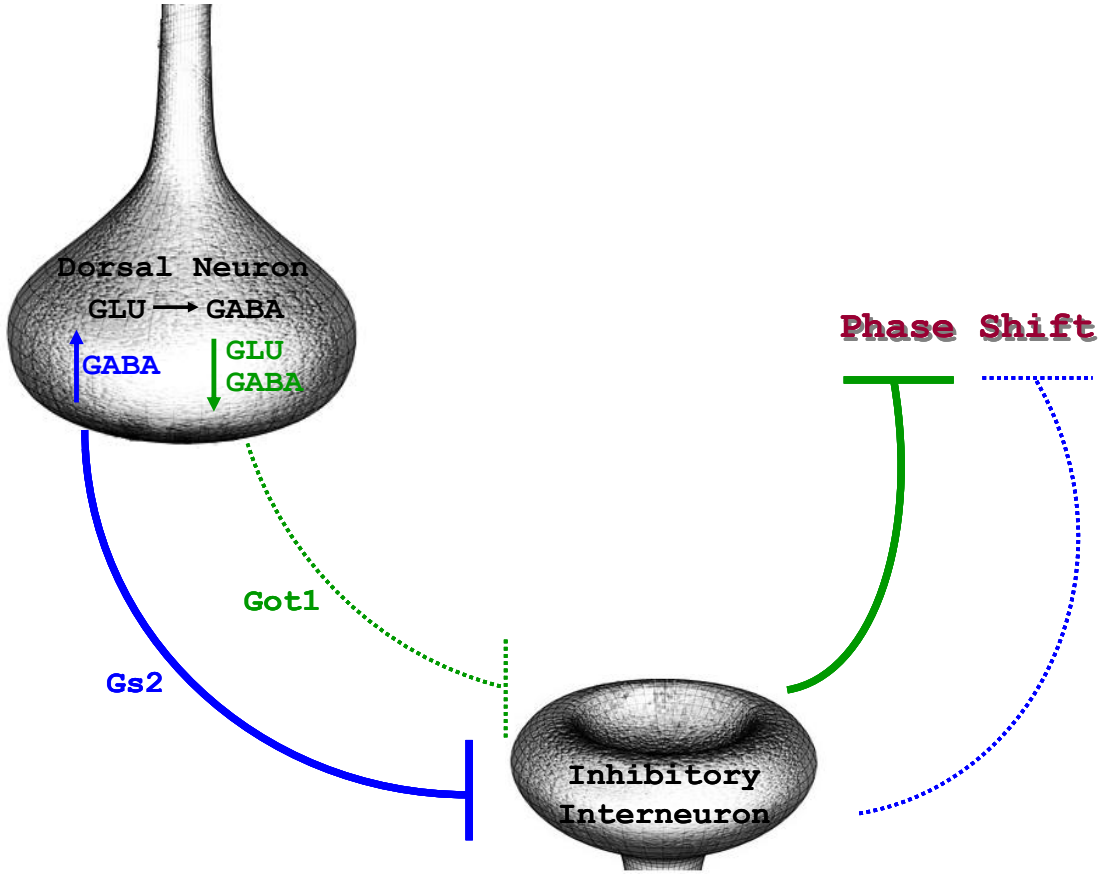

Figure 5.25 - Model of phase shift modulation. Green: Low levels of glutamate and GABA in *Got1* mutants cause a reduced phase shift. **Blue:** The excess of GABA represses the action of neurons that inhibit the phase shift.

Although it is known that the light entrainment of the clock is mediated by visual photoreceptor inputs from the compound eyes, extraocular photoreceptors and via cryptochrome (*cry*) expressed in the lateral brain neurons (Helfrich-Forster *et al.*, 2001; Helfrich-Forster *et al.*, 2002; Stanewsky *et al.*, 1998), not much is known about how entrainment signals are transmitted in the clock neuronal network. In this work, we suggested that glutamate and GABA are essential components of the *Drosophila* circadian clock light entrainment, probably through the signalling from DNs to the LNvs.

Chapter 6: Identification of *Drosophila* homologues of mammalian genes

6.1 Introduction

Neurons produce neurotransmitters that are transported along their neurites to the synapses. The release of neurotransmitters from the presynaptic nerve terminals is based on an elaborate sequence of events. The synaptic vesicles filled with neurotransmitters dock at release sites and go through a maturation process (priming) to participate in exocytosis. The chemical synapses initiate when an action potential invades the terminal of the presynaptic neuron, causing the opening of voltage-gated calcium channels in the presynaptic membrane. The rise of presynaptic Ca^{+2} concentration allows synaptic vesicles to fuse with presynaptic membrane and secrete the neurotransmitters into the synaptic cleft. The neurotransmitters bind to receptor molecules in the postsynaptic membrane and the vesicular membranes are retrieved by endocytosis from the plasma membrane to be recycled and make new synaptic vesicles (Sudhof, 1995).

Several of the important proteins for neurotransmitter release are also involved in other types of membrane fusion events common to all cells. During priming, the vesicular membrane proteins known as v-SNAREs, and the target membrane proteins known as t-SNAREs, can form a SNARE (soluble *N*-ethylmaleimide sensitive factor attachment receptor – SNAP receptor) complex that promotes the fusion of the two membranes. A soluble ATPase, known as the *N*-ethylmaleimide-sensitive fusion protein (NSF), regulates the assembly of the SNAREs by coupling SNARE complex disassembly to ATP hydrolysis (Jahn and Sudhof, 1999; Klenchin and Martin, 2000; Lin and Scheller, 2000). The soluble NSF attachment protein (SNAP) promotes SNARE complex disassembly along with NSF. It has been shown that the recruitment

of NSF to SNARE complexes is via SNAP after binding to the complex (Clary and Rothman, 1990). The *Drosophila* genome contains two distinct NSF genes, *dNsf1* and *dNsf2*.

Synapsins are one of the best-studied groups of synaptic genes. Synapsins are abundant synaptic vesicle-associated phosphoproteins, which bind to synaptic vesicles, to actin, and to ATP, and show structural similarity to ATP-utilizing enzymes (Esser *et al*., 1998; Greengard *et al*., 1993; Hilfiker *et al*., 1999; Hosaka and Sudhof, 1998). *Synapsins* have been proposed to fine-regulate neurotransmitter release by phosphorylation-dependent control of synaptic vesicle motility.

The *Drosophila* gene *leonardo* appears to be involved in exocytosis and encodes a conserved member of the *14-3-3* protein family, the ζ isoform. This gene is involved in learning and seems to have a role in secretory vesicle dynamics, specifically by regulating the size of releasable pools of transmitter vesicles at presynaptic fusion sites (Broadie *et al*., 1997).

In a recent proteomic study of cycling murine SCN proteins by our group, proteins extracted at different circadian time points were analysed by two-dimensional gel eletrophoresis (2D-DIGE) combined with mass spectrometry, revealing a number of proteins under strong circadian control (Deery *et al*., 2009). Among these proteins, four cycling synaptic proteins were identified, N-ethylmaleimide sensitive fusion protein (NSF), the binding protein for NSF (SNAP-β), synapsin 2 and 14-3-3ζ.

6.2 Results

6.2.1 Locomotor Activity

6.2.1.1 *Synapsin*: the *Drosophila* homologous of *synapsin2*

Seven S*ynapsin* mutants were analysed in behavioural experiments under LL and DD (table 6.1). The mutants containing a *Mi{ET1}* element are rhythmic in DD (figure 6.2) and do not behave differently from wild-type flies in LL (figure 6.3). Moreover, *yw;;Mi{ET1}Syn* (Bloomington ID 22772) showed a slightly long period of activity (τ=24.6 ± 0.15) (figure 6.1), that is significantly different from w^{1118} flies when compared by ANOVA ($F_{1,24}$ =6.56, p= 0.017).

Two mutant lines containing the transgenic transposon piggyBac were tested. These mutants remained behaviourally rhythmic in DD and showed a normal arrhythmic behavioural response to LL (table 6.1). The piggyBac transposon carrying the RB element, which contains an FRT site and the mini-*white* marker, was inserted into a *Syn* intron (Thibault *et al*., 2004). Moreover, in *w;;PBac{WH}Syn* mutants the transposition of the WH element carrying the FRT site, the mini-*white* marker and UAS sequence, occurred within the *Syn* 5'UTR sequence (Thibault *et al*., 2004).

Two null mutants, *Syn97* and *Syn79*, and the hypomorphic mutant *Syn168* generated by transposon jump-out mutagenesis had their locomotor activity studied in DD and LL (table 6.1). However, neither reducing nor eliminating *Syn* expression resulted in altered locomotor behaviour (figure 6.2 and figure 6.3). Both null mutant lines are viable, fertile and show no obvious anatomical defects in the synaptic neuropil of the adult brain (Godenschwege *et al*., 2004). The *Syn97* mutant has a deletion of 1397 bp including the putative promotor and the first known exon, whose absence is believed to abolish detectable SYN signals in Western Blots or immunohistochemistry. In the *Syn79* strain ~10 kb have been deleted and SYN cannot

be detected in Western Blots, while *Syn168* has a deletion of only 10 bp before the first exon and is responsible for a reduction in the protein expression (Godenschwege *et al*., 2004).

In accordance with the previous results, heterozygous flies for the deficiency that completely deletes the *Syn* gene by FLP recombinase (*Df(3R)Exel6156/+*, Bloomington ID 7635) exhibited circadian locomotor activity rhythms in DD and were arrhythmic in LL (table 6.1). However, a short period of $\tau = 23.08 \pm 0.12$ was observed for *w;;Df(3R)Exel6156/+* (figure 6.1), and this period is significantly different from w^{1118} flies ANOVA ($F_{1,25} = 25.34$, $p = 0.00003$).

Since flies containing *Df(3R)Exel6156* are not homozygous viable and carry one wild-type allele, a number of combinations with different *Syn* mutations were tested (table 6.1). Once again the flies had a normal arrhythmic behavioural response in LL (figure 6.3). In DD, only *yw;;Mi{ET1}Syn/Df(3R)Exel6156* showed an abnormal phenotype, in that the percentage of flies exhibiting circadian rhythm in locomotor activity was 44%.

Table 6.1 - *Syn* mutants and deficiency used in locomotor activity experiments.

***Syn* Mutants/ Deficiency (Bloomington ID)**	**DD**			**LL**		
	% Rhythmic	**Mean Period ± SEM**	**n**	**% Rhythmic**	**Mean Period ± SEM**	**n**
$y^1 w^{67c23;}$; *Mi{ET1}Syn*^{MB00351} (22772)	100	24.6 ± 0.15	16	43	----	16
$y^1 w^{67c23;}$; *Mi{ET1} Syn*^{MB01857} *Timp*^{MB01857} (23762)	80	23.6 ± 0.17	15	23	-----	13
w^{1118};; *PBac{RB}Syn*^{e00238} (17829)	67	24.1 ± 0.16	15	0	-----	15
w^{1118}; ;*PBac{WH}Syn*^{f04401} (18767)	56	23.8 ± 0.17	27	0	-----	13
;;Syn97 *	72	24 ± 0.1	59	31	-----	26
;;Syn79 *	80	24.1 ± 0.3	12	0	-----	4
;;Syn168 *	100	23.6 ± 0.16	14	13	-----	15
w^{1118};; *Df(3R)Exel6156, P{XP-U}Exel6156/+* (7635)	100	23.08 ± 0.12	15	8	-----	12
yw;; Mi{ET1}Syn/ Df(3R)Exel6156	44	-----	16	6	----	16
yw;; Mi{ET1}SynTimp/ Df(3R)Exel6156	82	23.7 ± 0.14	17	7	----	15
w;; PBac{WH}Syn / Df(3R)Exel6156	88	23.5 ± 0.1	16	23	----	15
;;Syn97/Df(3R)Exel6156	88	23.5 ± 0.09	16	25	-----	16

(*) These fly lines were kindly provided by Erich Buchner at University of Wuerzburg, Germany (Godenschwege *et al*., 2004).

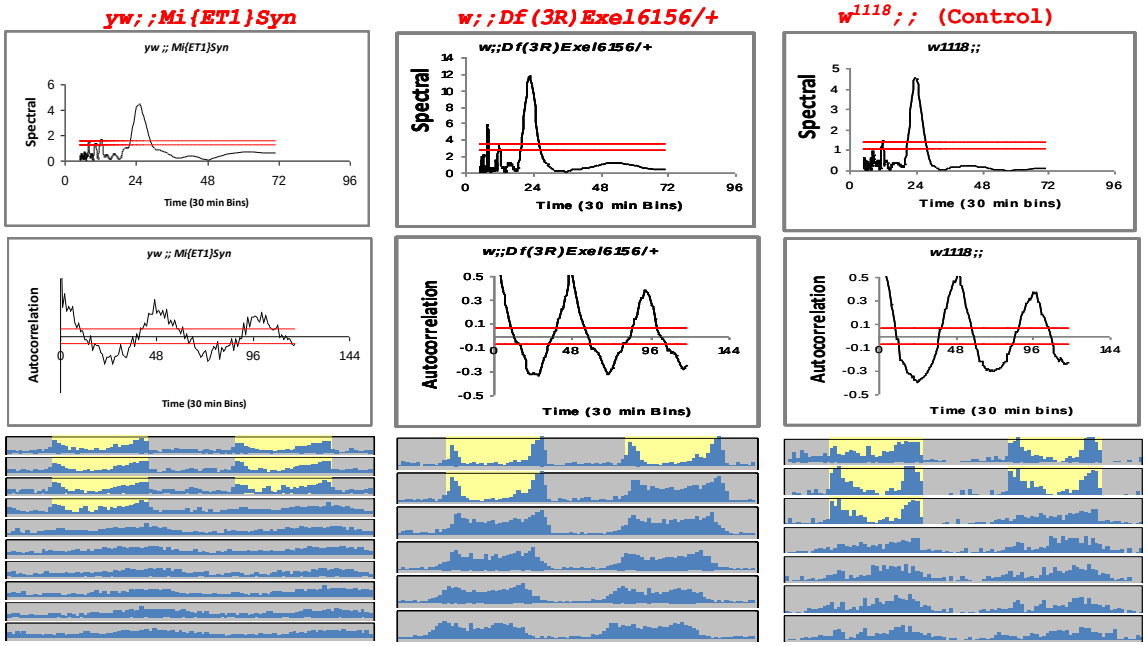

Figure 6.1 – Circadian rhythms in *yw;;Mi{ET1}Syn* and *w;;Df(3R)Exel6156/+* in DD. *yw;;Mi{ET1}Syn* τ= 24.6 h (± 0.15), *w;;Df(3R)Exel6156/+* τ= 23.08 (± 0.12) and

w^{1118} (control) τ= 24.1 (±0.17). **Upper panel:** CLEAN spectral plot along with the 95% and 99% Monte Carlo confidence limits. **Central panel:** Autocorrelogram along with the canonical 95% confidence limits. **Lower panel:** Double-plotted histogram of locomotor activity. **Yellow:** Day. **Gray:** Subjective night. Genotypes are indicated above the spectral plots.

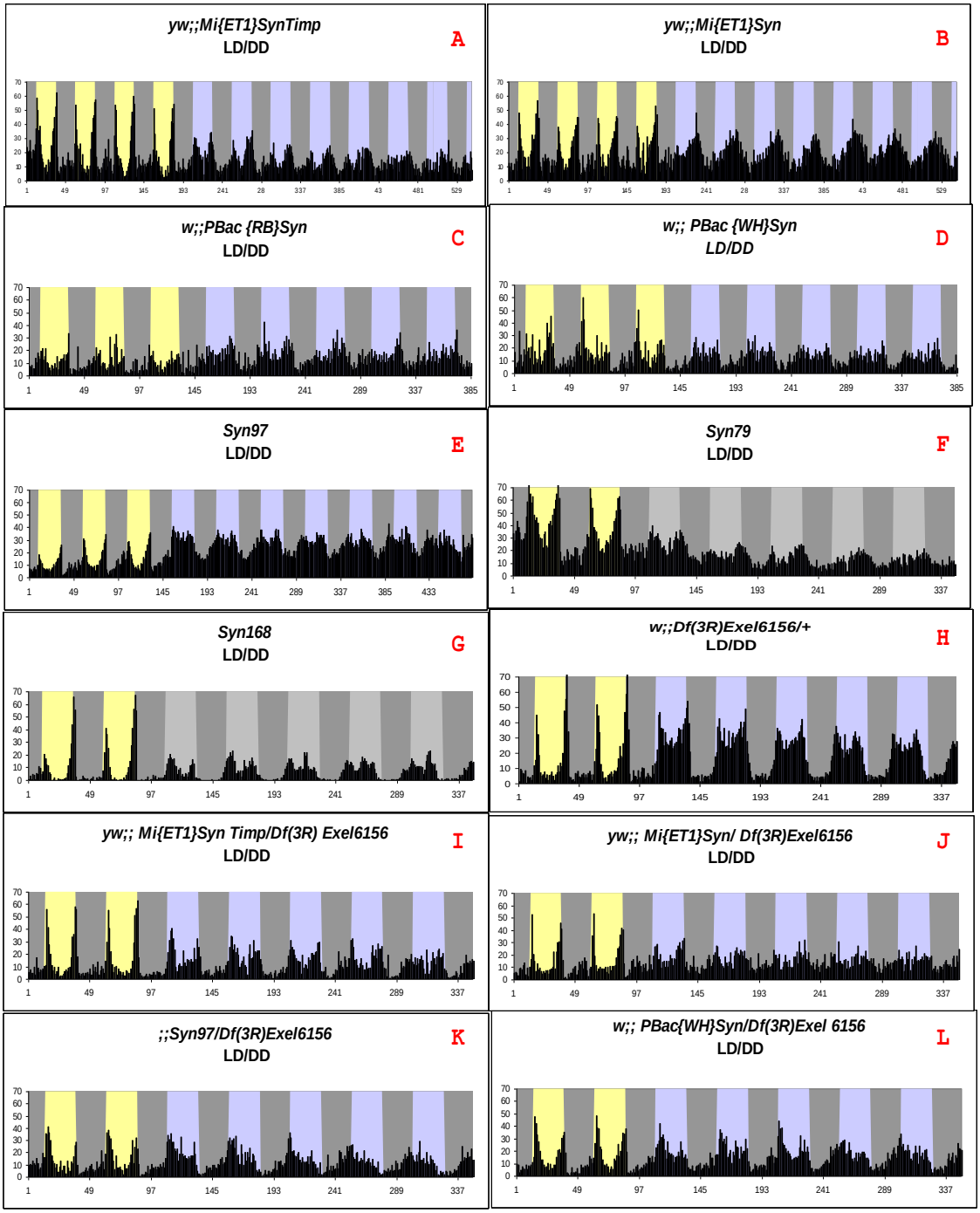

Figure 6.2 - *Syn* mutants and deficiency locomotor activity profile in DD. A and B: 4 days LD, 7 days DD. **C and D:** 3 days LD, 5 days DD. **E:** 3 days LD, 7 days DD. **F to L:** 2 days LD, 5 days DD. **X-axis:** time in 30 minutes bins. **Y-axis:** mean level of activity. **Yellow:** day. **Gray:** subjective night. **Blue:** subjective day. Genotypes are indicated on top of each histogram. All genotypes showed rhythmicity.

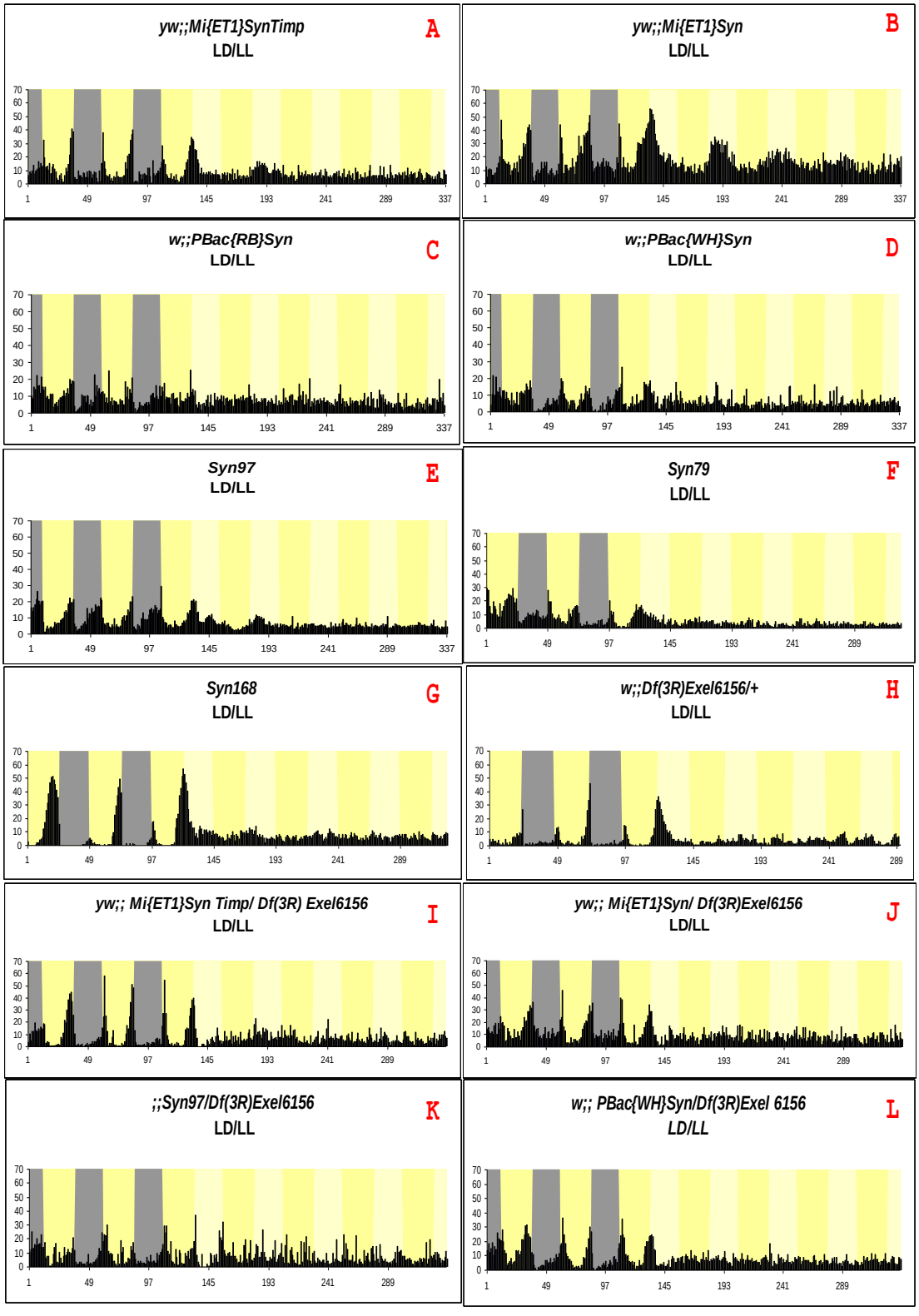

Figure 6.3 - ***Syn* mutants and deficiency locomotor activity profile in LL. A to E, I to L:** 3 days LD, 5 days LL. **F and G:** 2 days LD, 5 days LL. **H:** 2 days LD, 4 days LL. **X-axis:** time in 30 minutes bins. **Y-axis:** mean level of activity. **Gray:** dark. **Dark yellow:** subjective daylight. **Yellow:** subjective night. Genotypes are indicated above each histogram. All genotypes were arrhythmic.

In order to knock down *Syn* in clock cells, two different RNA interference lines (VDRC 46480 and VDRC 46482) were crossed to *tim-Gal4* flies and had their locomotor behaviour studied in DD and LL (table 6.2). In LL, all tested fly lines were arrhythmic (figure 6.5). In addition, the flies showed robust rhythmicity in DD (figure 6.4) and the average period of activity was close to 24 h (table 6.2). The co-expression of *dicer2* with VDRC 46482 lengthened the period by 0.4 h, therefore these flies have a significantly longer period from the control *w;tim-Gal4 UASdcr2/+;* ($F_{1,58}$=6.41, p=0.014). This corroborates the result observed with *yw;;Mi{ET1}Syn* mutants that also have a long period of activity under DD conditions.

Table 6.2 - Downregulating *Syn* in clock cells.

***Syn* RNAi (VDRC ID)**	**DD**			**LL**		
	% Rhythmic	**Mean Period ± SEM**	**n**	**% Rhythmic**	**Mean Period ± SEM**	**n**
w; tim-Gal4/RNAi Syn; (VDRC 46480)	100	24.3 ± 0.07	32	-----	-----	---
w; tim-Gal4 UAS dcr2/ RNAi Syn; (VDRC 46480)	75	24 ± 0.14	20	28	-----	18
w; tim-Gal4/RNAi Syn; (VDRC 46482)	100	24.2 ± 0.2	12	20	-----	10
w; tim-Gal4 UAS dcr2/ RNAi Syn; (VDRC 46482)	100	24.6 ± 0.12	32	-----	-----	---
VDRC 46480 Control	80	24 ± 0.3	15	0	-----	15
w;tim-Gal4;+ (Control)	71	24.5 ± 0.3	31	4	-----	51
w;tim-Gal4 UASdcr2/+; (Control)	100	24.2 ± 0.06	30	47	----	28

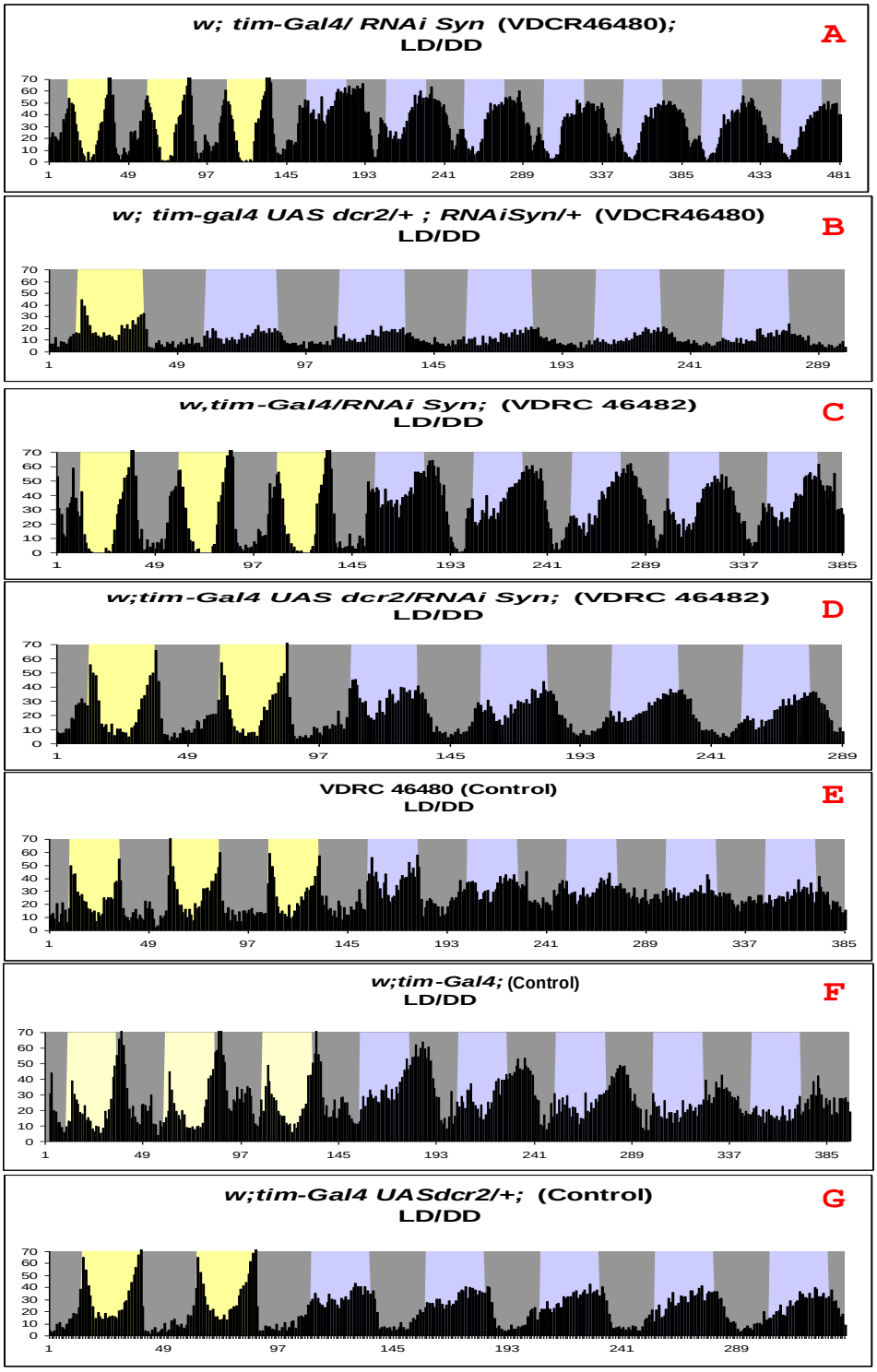

Figure 6.4 – Mean activity of *Syn* RNAi lines in DD. A: 3 days LD, 7 days DD. **B:** 1 day LD, 5 days DD. **C, E and F:** 3 days LD, 5 days DD. **D and G:** 2 days LD, 5 days DD. **X-axis:** time in 30 minutes bins. **Y-axis:** mean level of activity. **Yellow:** day. **Gray:** subjective night. **Blue:** subjective day. All genotypes showed rhythmicity.

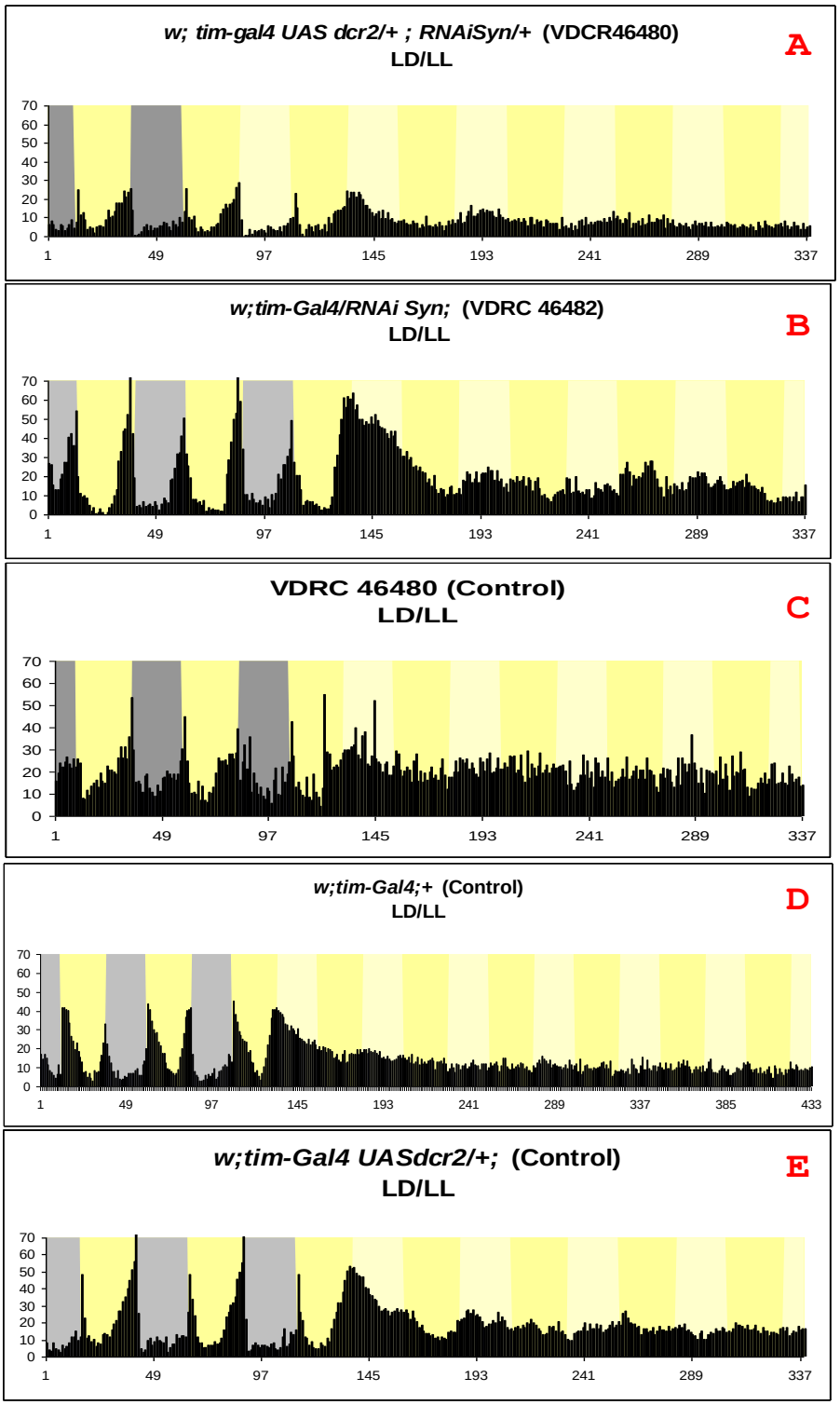

Figure 6.5 - Activity profile of *Syn* RNAi lines in LL. A: 1 day LD, 6 days LL. **B, C and E:** 2 days LD, 5 days LL. **D:** 2 days LD, 7 days LL. **X-axis:** time in 30 minutes bins. **Y-axis:** mean level of activity. **Gray:** dark. **Dark yellow:** subjective daylight. **Yellow:** subjective night. All genotypes showed arrhythmicity.

6.2.1.2 *Nsf2*: The *Drosophila* homologous of *Nsf*

One RNAi line, one deficiency and four ethyl methanesulfonate (EMS) mutated *Nsf2* lines had their locomotor behaviour investigated in DD and LL (table 6.3). The mutation $Nsf2^{A6}$ is characterised by the replacement of the Alanine residue in position 597 to a valine, while $Nsf2^{A15}$ consists of a deletion of the sequence encoding the amino acid residues 555 to 641, resulting in a frameshift (Mahoney *et al*., 2006). Both mutations are homozygous lethal. Initially, these two mutants were tested in the presence of a balancer. Although no effect was noticed when w^{1118}; $Nsf2^{A15}$/*TM6B* were exposed to LL (figure 6.8), a notable lengthening in the behaviour period was observed in constant darkness (figure 6.7). In the latter case, the period of activity of these flies was strikingly long (τ= 27.17 h ± 0.16) and significantly different from w^{1118} flies ($F_{1,44}$= 103.7, $p<<10^{-10}$) (figure 6.6). In addition, w^{1118}; $Nsf2^{A6}$/*TM3* also showed an interesting phenotype in DD, since 73% of the flies were arrhythmic (figure 6.7). Subsequently, the mutant alleles $Nsf2^{A15}$ and $Nsf2^{A6}$ were analysed in combination with a wild-type allele (table 6.3) to eliminate the balancer and surprisingly, both mutants were rhythmic. However, the period of *w;* $Nsf2^{A6}$/ + flies was significantly shorter (τ= 23.2 h ± 0.06) relative to w^{1118} ($F_{1,56}$= 41.4, $p<10^{-7}$) (figure 6.6).

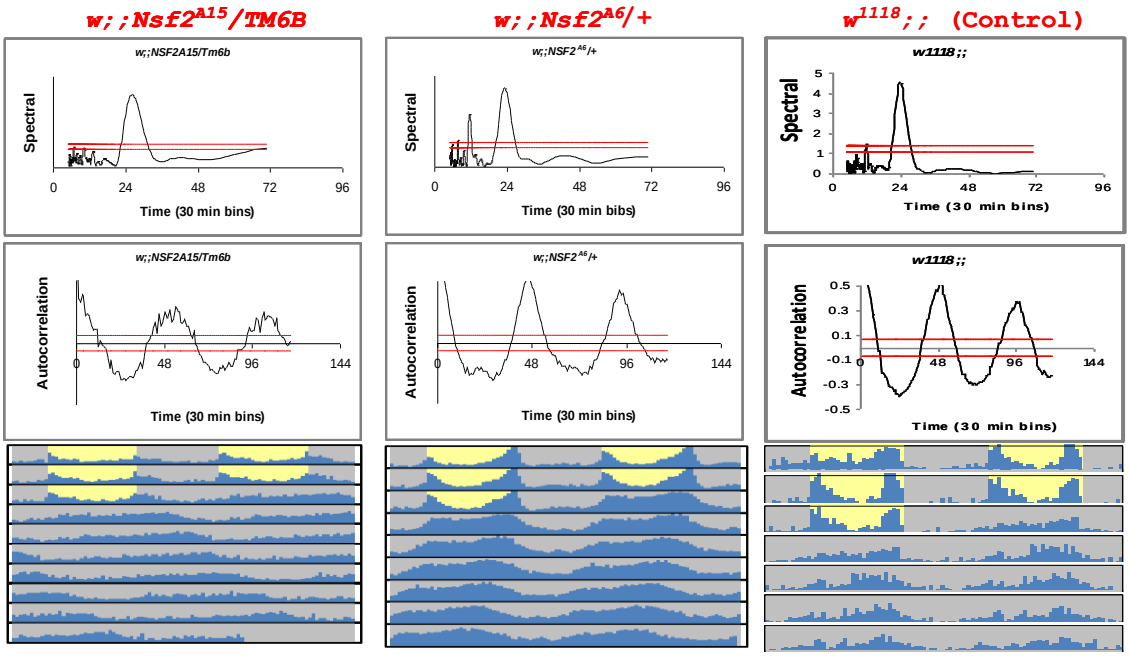

Figure 6.6 - *Nsf2^{A15}/TM6B* and *Nsf2^{A6}/+* mutants in DD. *w;;Nsf2^{A15}/TM6B* τ= 27.2 (±0.17), *w;;Nsf2^{A6}/+* τ= 23.2 (±0.06) and *w^{1118};;* (control) τ= 24.1 (±0.17). **Upper panel:** CLEAN spectral plot along with the 95% and 99% Monte Carlo confidence limits. **Central panel:** Autocorrelogram with the canonical 95% confidence limits. **Lower panel:** Double-plotted histogram of locomotor activity. **Yellow:** Day. **Gray:** Subjective night. Genotypes are indicated on top of the spectral plots

Two severe EMS mutated alleles were observed in behavioural tests: the loss-of-function *dNsf2^{15}* and the hypomorphic *dNsf2^{21}* (Golby *et al.*, 2001). The allele *dNsf2^{15}* is characterised by an amino acid replacement causing a premature stop codon in the *Nsf2* coding sequence (CDS), while *dNsf2^{21}* does not have a mutation in the CDS suggesting that the mutation had affected the gene transcription or splicing (Golby *et al.*, 2001). Both mutants exhibited robust rhythms in DD and lacked rhythms under LL (table 6.3).

Flies with *Df(3R)urd* deletion that covers *Nsf2* did not differ from wild-type flies when their locomotor activity was measured in DD and LL (table 6.3). Because these flies carried a wild-type allele, one attempt was made to put *dNsf2^{15}* and *dNsf2^{21}* as hemizygotes with the *Df(3R)urd* chromosome. Unfortunately, the flies did not reach the adult phase.

The down regulation of the *Nsf2* gene in clock neurons by crossing the RNAi line to *tim-Gal4* flies did not alter the locomotor behaviour of these flies, which remained rhythmic in DD (figure 6.7)

Table 6.3 - *Nsf2* mutants and RNAi lines used in locomotor activity experiments.

***Nsf2* Mutants/ Deficiency (Bloomington ID)**	**DD**			**LL**		
	% Rhythmic	**Mean Period ± SEM**	**n**	**% Rhythmic**	**Mean Period ± SEM**	**n**
w^{1118}; $Nsf2^{A15}$/*TM6B* (8282)	76	27.2 ± 0.17	45	27	-----	26
w^{1118}; $Nsf2^{A15}$/ + (8282)	90	23.9 ± 0.05	21	-----	-----	---
w^{1118}; $Nsf2^{A6}$/*TM3* (8281)	37	-----	46	11	-----	36
w^{1118}; $Nsf2^{A6}$/ + (8281)	96	23.2 ± 0.06	48	19	-----	16
;;$dNsf2^{21}$/*TM3**	93.8	23.8 ± 0.1	16	37	-----	16
;;$dNsf2^{15}$/*TM3**	100	24 ± 0.18	16	37	----	8
;;$dNsf2^{15}$/+	100	23.5 ± 0.04	14	28	----	14
;;*DF(3R)urd*/+ (3639)	100	23.8 ± 0.06	16	19	-----	16
***Nsf2* RNAi (VDRC ID)**	**DD**			**LL**		
	% Rhythmic	**Mean Period ± SEM**	**n**	**% Rhythmic**	**Mean Period ± SEM**	**n**
w; tim-Gal4/RNAi Nsf2; (VDRC 7743)	82	24 ± 0.2	22	-----	-----	---

(*) These fly lines were kindly provided by Leo Pallanck at University of Washington, USA (Golby *et al*., 2001).

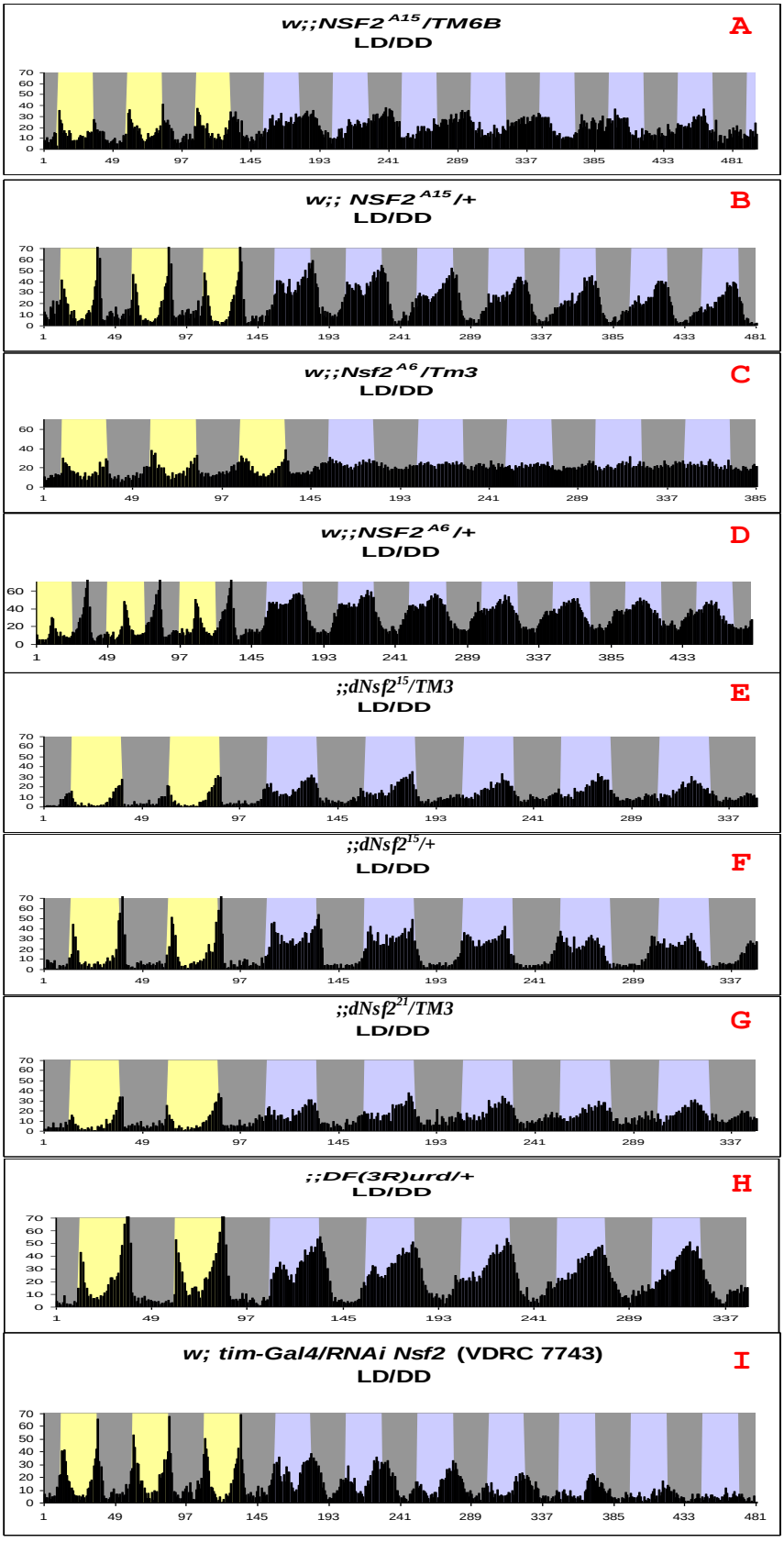

Figure 6.7 - Mean activity of *Nsf2* variants in DD. A, B, D and I: 3 days LD, 7 days DD. **C, E to H:** 3 days LD, 5 days DD. **X-axis:** time in 30 minutes bins. **Y-axis:** mean level of activity. **Yellow:** day. **Gray:** subjective night. **Blue:** subjective day. **C:** *w;;Nsf2^{A6}/TM3* flies are arrhythmic. All other genotypes showed rhythmicity.

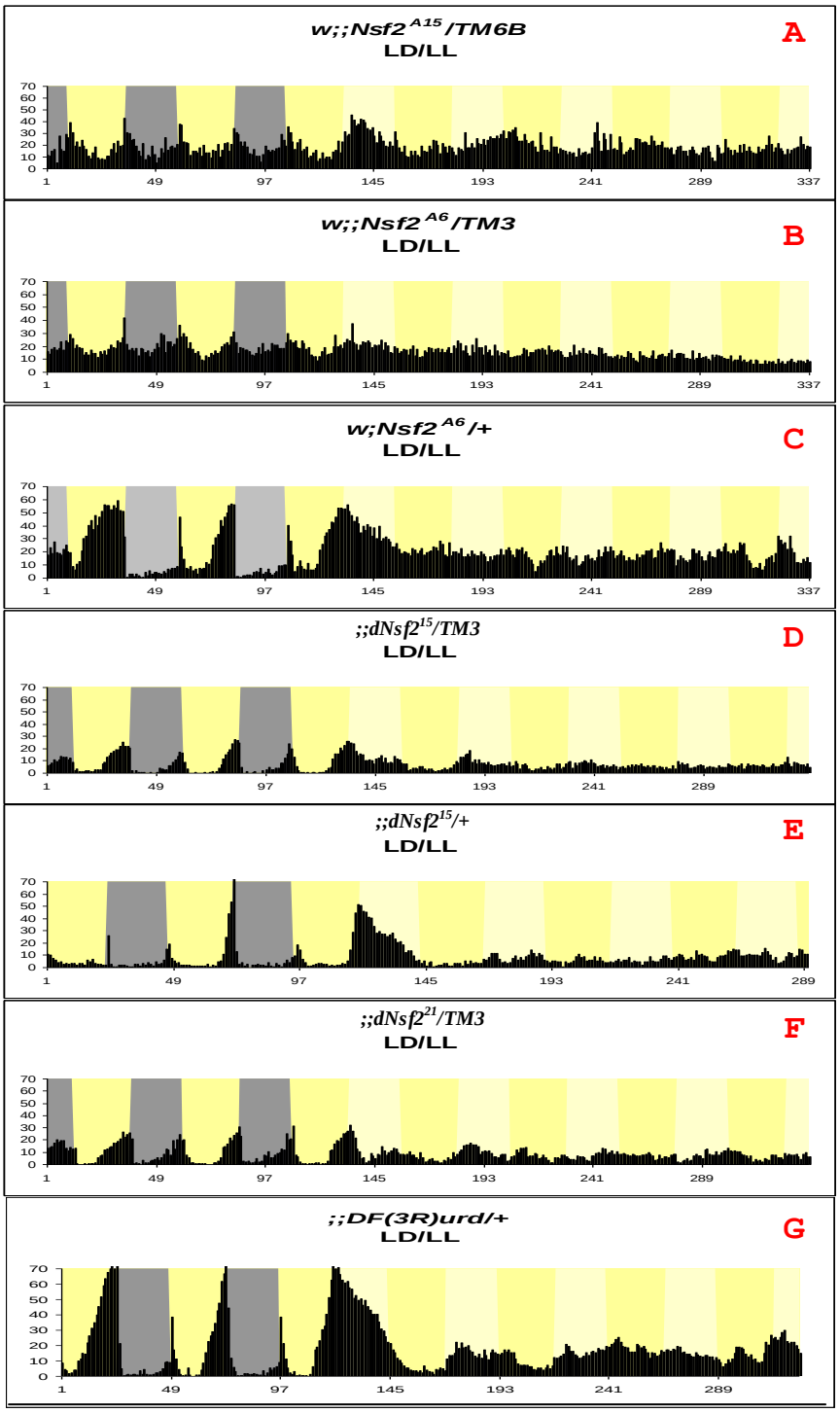

Figure 6.8 - ***Nsf2* variants locomotor activity profile in LL. A to D and F:** 3 days LD, 5 days LL. **E:** 2 days LD, 4 days LL. **G:** 2 days LD, 5 days LL. **X-axis:** time in 30 minutes bins. **Y-axis:** mean level of activity. **Gray:** dark. **Dark yellow:** subjective daylight. **Yellow:** subjective night. All genotypes showed arrhythmicity.

6.2.1.3 *Nsf1* (*comatose*): Another *Drosophila* homologue of *Nsf*

The *Nsf1* mutant, *comt*^{6}*;;* (Bloomington ID 26708) is characterised by the replacement of the amino acid proline to serine at the residue 398. The mutation is within the D1 domain, which contains a high-affinity ATP-binding site (Littleton *et al*., 2001). A rhythmic profile is observed when the mutant is placed in DD (figure 6.9) and the period of these flies is close to 24 h (table 6.4).

Downregulating *Nsf1* in clock cells by crossing the RNAi to *tim-Gal4* or restricting the knock down to the LNvs by crossing it to *pdf-Gal4*, also resulted in rhythmicity in DD (figure 6.9).

Table 6.4 - *Nsf1* mutants and RNAi used in locomotor activity experiments.

***Nsf1* Mutant/ RNAi (Bloomington ID)**	**DD**		
	% Rhythmic	**Mean Period ± SEM**	**n**
comt^{6}*;;* (26708)	66.7	23.8 ± 0.3	12
w; tim-Gal4/RNAi Nsf1; (VDRC 105552)	100	23.9 ± 0.06	26
w; pdf-Gal4/RNAi Nsf1; (VDRC 105552)	100	23.8 ± 0.05	26
VDRC 105552 (Control)	79	24.2 ± 0.2	14
w;tim-Gal4; (Control)	71	24.5 ± 0.3	31
yw;pdf-Gal4; (Control)	65	24.4 ± 0.17	50

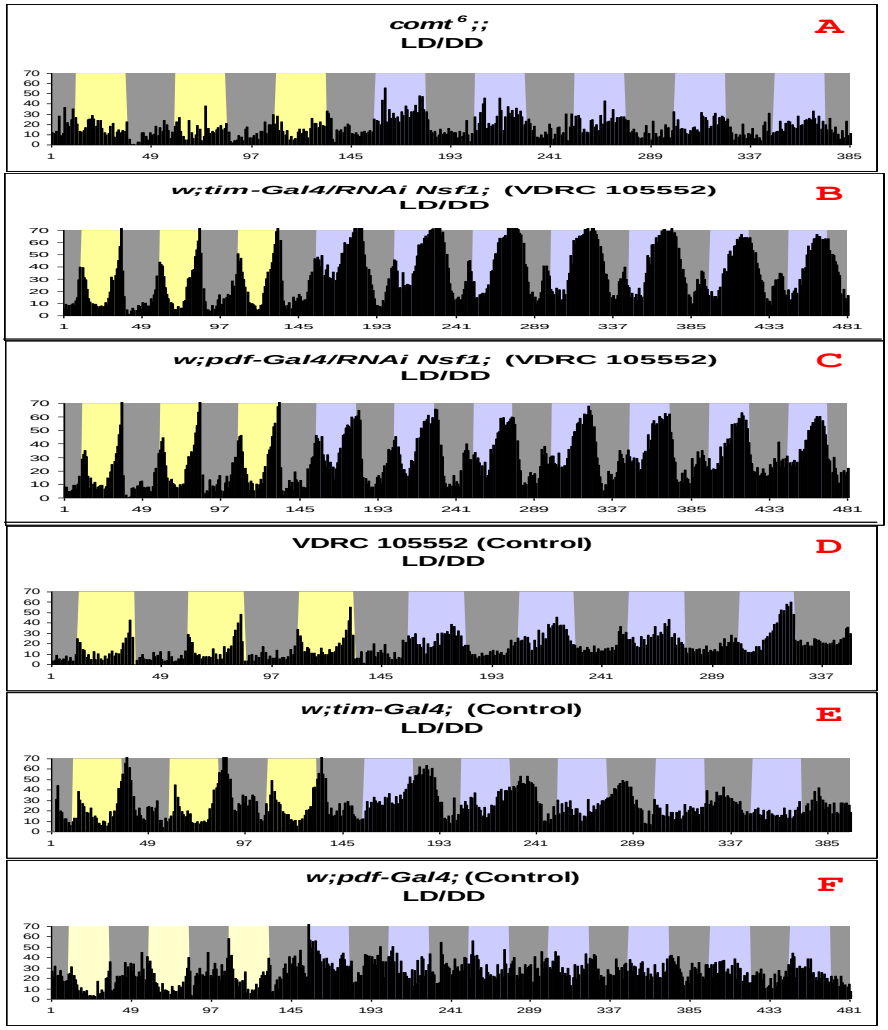

Figure 6.9 – Locomotor activity of *Nsf1* mutant and RNAi. A and E: 3 days LD, 5 days DD. **B, C and F:** 3 days LD, 7 days DD. **D:** 3 days LD, 4 days DD. **X-axis:** time in 30 minutes bins. **Y-axis:** mean level of activity. **Yellow:** day. **Gray:** subjective night. **Blue:** subjective day. The mutant *comt*^{6}*;;* (A) and flies downregulating *Nsf1* (B and C) are rhythmic.

6.2.1.4 *leonardo* (*14-3-3ζ*): The *Drosophila* homologue of *14-3-3ζ*

Two 14-3-3ζ mutants were used in locomotor activity experiments. Both mutants, *14-3-3ζ*$^{2.3}$*;ry*^{506} (Bloominton ID 9573) and *w*^{1118}*; 14-3-3ζ*^{12BL}/+ (Bloomington ID 9572), are characterised by the imprecise excision of the *14-3-3ζ*^{P1375} insertion by the Δ 2-3 element (Skoulakis and Davis, 1996), which has high transposase activity (Robertson *et al*., 1988). Additionally, *14-3-3ζ*^{12BL} represents a

loss-of-function mutation, since no detectable levels of Leonardo protein are found in Western Blot analysis (Broadie *et al.*, 1997).

Although both mutants are rhythmic in DD (figure 6.11) and showed arrhythmicity in LL (figure 6.12), their period were affected in opposite directions (table 6.5). A significantly short period was observed in w^{1118}; *14-3-3*ζ^{12BL}/+ (τ=23 ± 0.06) in DD when compared to w^{1118} flies ($F_{1,\ 40}$=62.5, $p<10^{-8}$). On the contrary, a slightly long period for *14-3-3*$\zeta^{2.3}$;ry^{506} mutants was revealed (τ=24.5 ± 0.15) when compared to Canton S flies ($F_{1,\ 39}$=19.5, $p<10^{-4}$) (figure 6.10). The mutants were compared to control flies with different genotypes since only 14-3-3ζ^{12BL} is in a w^{1118} background.

The *leonardo* gene was knocked down in clock cells by *tim-Gal4*, using two different RNA interference lines (VDRC 48724 and 48725), as well as in the presence of *dicer2*. These flies were arrhythmic in LL (figure 6.12), but unexpectedly, both lines showed a long period only in the absence of *dicer2* (table 6.5). However, this period lengthening seems to be an effect of the *tim-Gal4* background, as suggested by the comparison of *w;tim-Gal4;* to *w;tim-Gal4/RNAi 14-3-3*ζ*;* (VDRC 48724) ($F_{1,32}$=0.3, p=ns) and to *w;tim-Gal4/+;RNAi 14-3-3*ζ/+ (VDRC 42725) ($F_{1,32}$=0.2, p=ns).

Table 6.5 - *14-3-3ζ* locomotor profile.

***14-3-3ζ* Mutants (Bloomington ID)**	**DD**			**LL**		
	% Rhythmic	**Mean Period ± SEM**	**n**	**% Rhythmic**	**Mean Period ± SEM**	**n**
w^{1118}; *14-3-3*ζ^{12BL}/+ (9572)	94	23 ± 0.06	30	43	----	30
; *14-3-3*$\zeta^{2.3}$; ry^{506} (9573)	87	24.5 ± 0.15	30	31	----	29
***14-3-3ζ* RNAi (VDRC ID)**	**DD**			**LL**		
	% Rhythmic	**Mean Period ± SEM**	**n**	**% Rhythmic**	**Mean Period ± SEM**	**n**
w tim-Gal4/+;RNAi 14-3-3ζ/ + (VDRC 48725)	100	24.6 ± 0.13	15	23	----	13
w tim-Gal4/RNAi 14-3-3ζ ; (VDRC 48724)	100	24.5 ± 0.14	15	33	----	6
w tim-Gal4 UAS dcr2/+;RNAi 14-3-3ζ/ + (VDRC 48725)	97	23.8 ± 0.09	30	46	-----	30
w tim-Gal4 UAS dcr2/RNAi 14-3-3ζ ; (VDRC 48724)	100	24.3 ± 0.1	31	-----	----	---

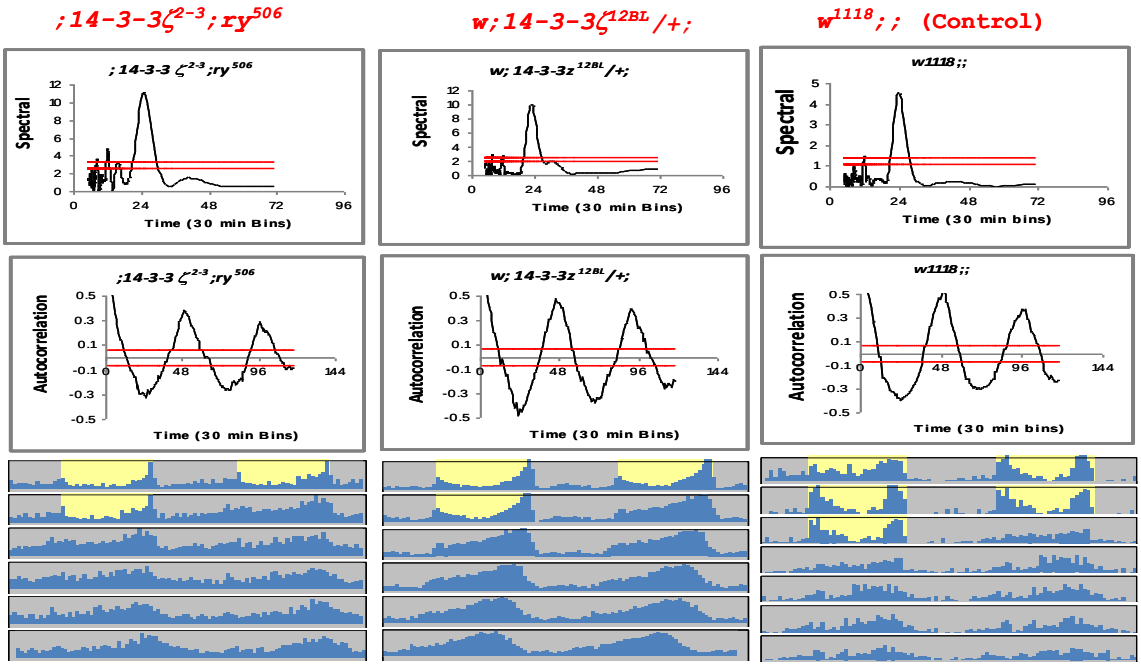

Figure 6.10 – *14-3-3*$\zeta^{2.3}$ and *14-3-3*ζ^{12BL} have altered period of activity in DD. *14-3-3*$\zeta^{2.3}$ τ= 24.5 (±0.15), *14-3-3*ζ^{12BL} τ= 23 (±0.06) and w^{1118};; (control) τ= 24.1 (±0.17). **Upper panel:** CLEAN spectral plot along with the 95% and 99% Monte Carlo confidence limits. **Central panel:** Autocorrelogram along with the canonical 95% confidence limits. **Lower panel:** Double-plotted histogram of locomotor activity mean. **Yellow:** Day. **Gray:** Subjective night. Genotypes are indicated above the spectral plots.

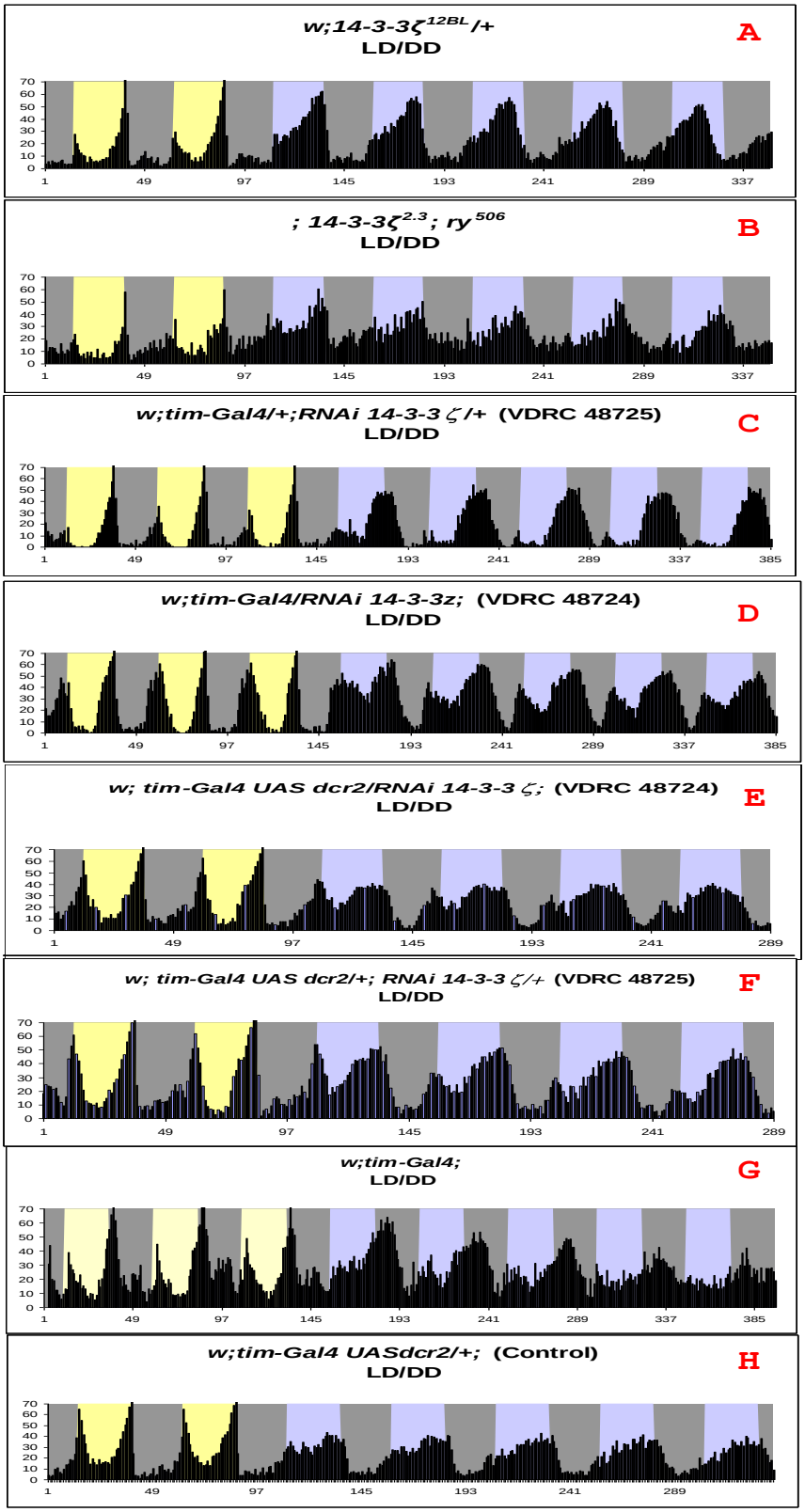

Figure 6.11 – Mean activity of *leonardo* mutants and RNAi in DD. A, B and H: 2 days LD, 5 days DD. **C, D and G:** 3 days LD, 5 days DD. **E and F:** 2 days LD, 4 days DD. **X-axis:** time in 30 minutes bins. **Y-axis:** mean level of activity. **Yellow:** day. **Gray:** subjective night. **Blue:** subjective day. All different shown genotypes are rhythmic.

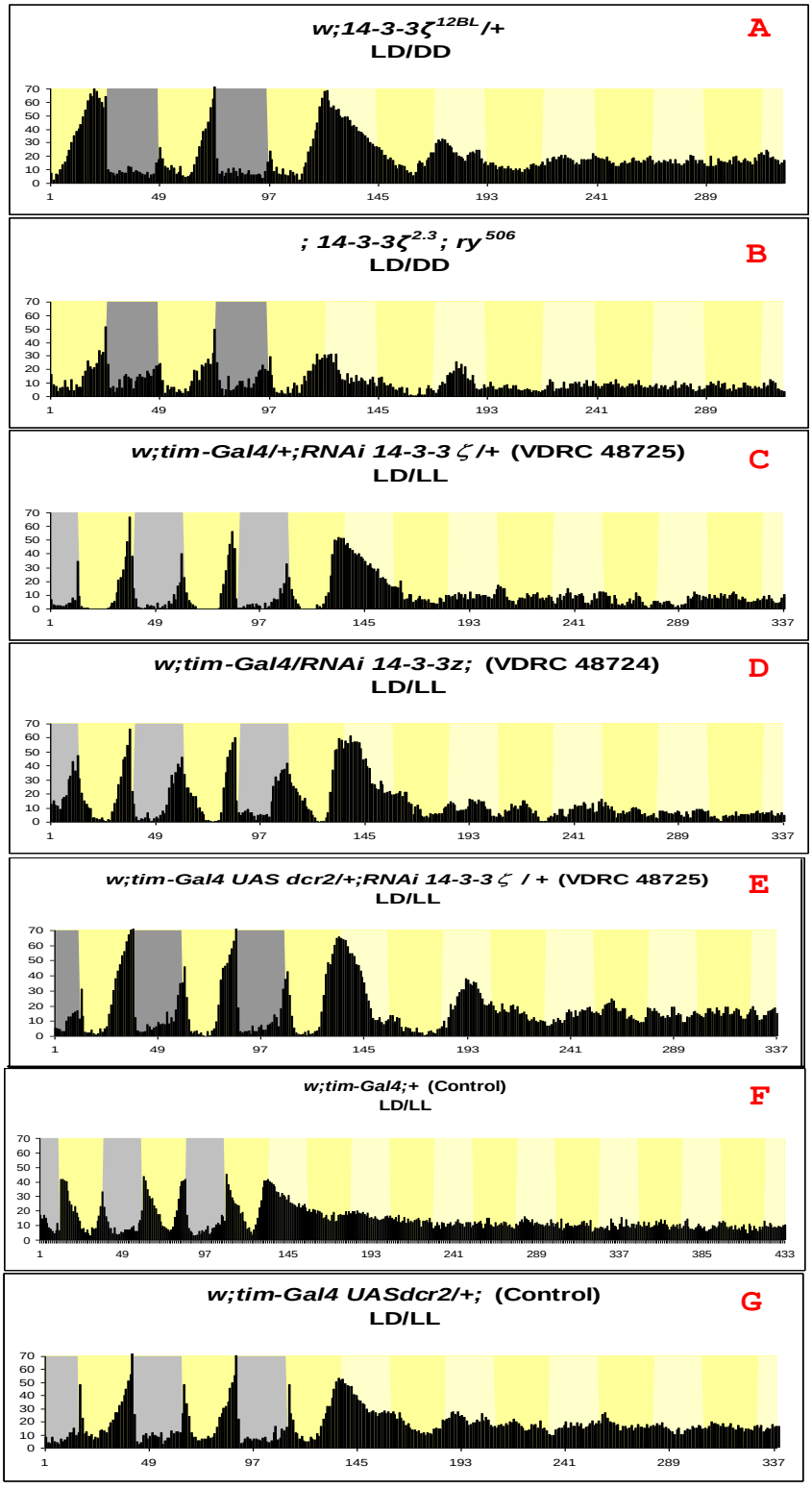

Figure 6.12 – ***14-3-3ζ* variants locomotor activity profile in LL. A and B:** 2 days LD, 5 days LL. **C, D, E and G:** 3 days LD, 5 days LL. **F:** 3 days LD, 7 days LL. **X-axis:** time in 30 minutes bins. **Y-axis:** mean level of activity. **Gray:** dark. **Dark yellow:** subjective daylight. **Yellow:** subjective night. All genotypes showed arrhythmicity.

6.2.1.5 *Snap:* The *Drosophila* homologous of *Snap* β

Three different *Snap* mutants and another two *Snap* deficiencies were used in locomotor activity experiments (table 6.6). The $Snap^{G8}$ hypomorphic mutation was caused by EMS mutagen and is characterised by the substitution of a guanine to an adenine in the first intron. It has been shown that in fact, there is a reduction of approximately 70% of the protein levels in this mutant (Babcock *et al*., 2004). The EMS induced mutation present in $Snap^{M4}$ (Bloomington ID 5465) is characterised by an amino acid replacement (A59T) (Babcock *et al*., 2004). *Df(3L)rdgC-co2* uncovers the cytological interval 77A-D completely deleting the *Snap* gene and *Df(3L)Exel6136* deletes the segment 77B2-77C6, also including the *Snap* gene. Mutants carrying the *P{EPgy2}* element containing a UAS binding site, mini-*white* gene and an intronless *yellow* gene marker (Bellen *et al*., 2004) had the transposon inserted in the 5'UTR region.

All the tested mutants and deficiencies proved to have robust rhythms in DD (figure 6.14) and *yw;; P{EPgy2} Snap/+* behaved arrhythmically in LL (figure 6.16).

The mutant $Snap^{G8}$ and both deficiencies were tested over the balancer, and also over a wild type allele. In fact, the deficiency *Df(3L)Exel6136/TM6B* and the mutant $Snap^{G8}$ (over TM6C or over +) showed a short period of activity (figure 6.13). Statistical analysis revealed that when compared to Canton S flies, $Snap^{G8}$/+ ($F_{1,28}$= 4.22, p= 0.049) and $Snap^{G8}$*/TM6C* ($F_{1,25}$= 7.98, p= 0.009) have significantly shorter period, and *w;;Df(3L)Exel6136/TM6B* period is significantly shorter than w^{1118} ($F_{1,18}$= 14.6, p= 0.001).

Table 6.6 - Locomotor activity of *Snap* mutants and deficiencies.

***Snap* Mutants/ Deficiency (Bloomington ID)**	**DD**			**LL**		
	% Rhythmic	**Mean Period ± SEM**	**n**	**% Rhythmic**	**Mean Period ± SEM**	**n**
;;Snap^{G8}/TM6C (5467)	80	22.6 ± 0.2	15	-----	----	---
;;Snap^{G8}/ + (5467)	100	23.02 ± 0.13	16	-----	----	---
;;Snap^{M4}/TM6C (5465)	75	23.7 ± 0.14	16	-----	----	---
Df(3L)rdgC-co2/ + (2052)	100	24 ± 0.09	16	-----	----	---
Df(3L)rdgC-co2/ TM6C (2052)	81	23.9 ± 0.15	16	-----	----	---
w^{1118}; Df(3L)Exel6136, P{XP-U} Exel 6136/TM6B (7615)	57	23.2 ± 0.14	14	-----	----	---
w^{1118}; Df(3L)Exel6136, P{XP-U} Exel 6136/ + (7615)	100	23.8 ± 0.1	16	-----	----	---
y^{1} w^{67c23};; P{EPgy2} Snap^{EY06922}/+ (16770)	100	23.8 ± 0.06	15	13	----	15

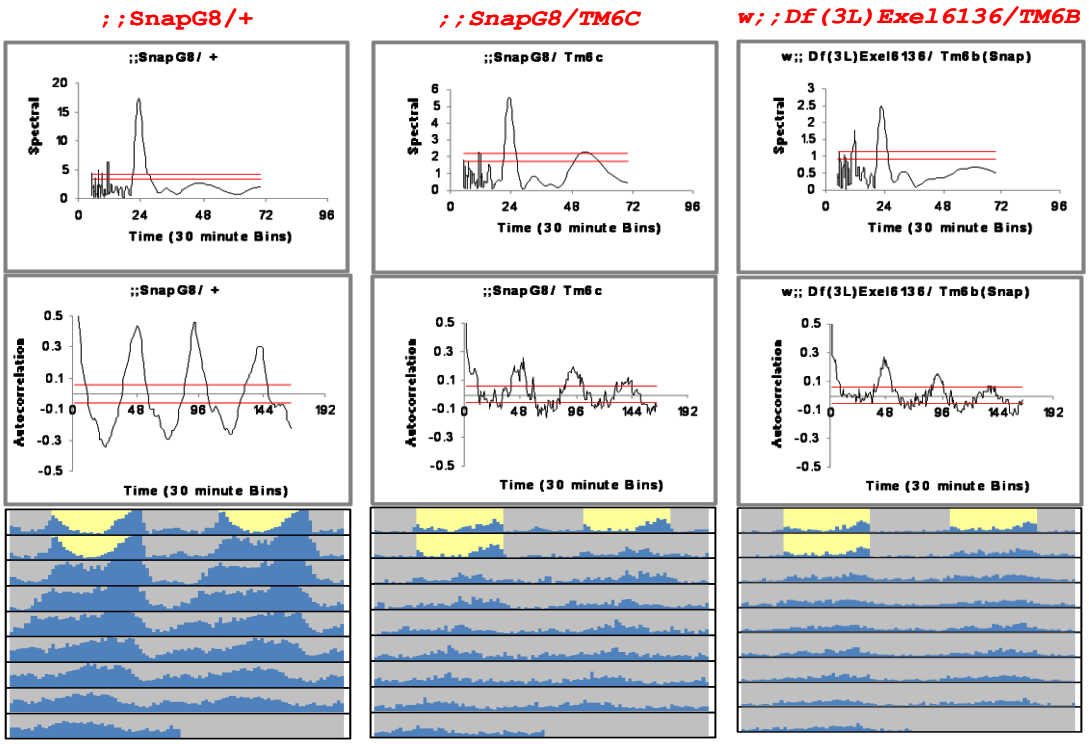

Figure 6.13 - *Snap^{G8}* mutant and *Df(3L)Exel6136/TM6B* have short period in DD. *;;Snap^{G8}*/+ τ= 23.02 (±0.13), *;;Snap^{G8}/TM6C* τ= 22.6 (±0.2) and w;;*Df(3L)Exel6136/ TM6B* τ= 23.2 (±0.14). **Upper panel:** CLEAN spectral plot along with the 95% and 99% Monte Carlo confidence limits. **Central panel:** Autocorrelogram along with the canonical 95% confidence limits. **Lower panel:** Double-plotted actogram of

locomotor activity mean. **Yellow:** Day. **Gray:** Subjective night. Genotypes are indicated on top of the spectral plots.

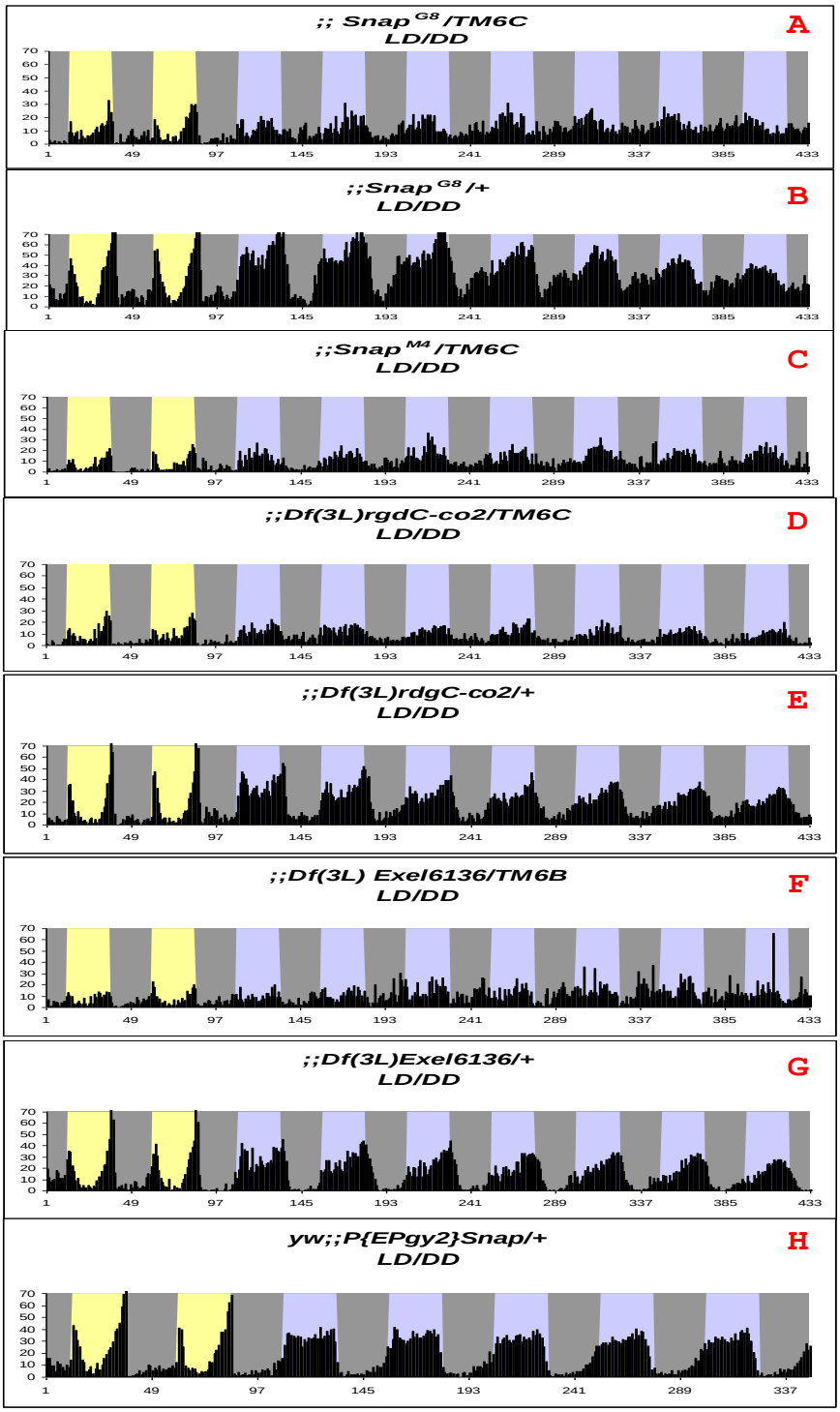

Figure 6.14 - *Snap* mutants and deficiencies locomotor activity profile in DD. A, to G: 2 days LD, 7 days DD. **H:** 2 days LD, 5 days DD. **X-axis:** time in 30 minutes bins. **Y-axis:** mean level of activity. **Yellow:** day. **Gray:** subjective night. **Blue:** subjective day. All different shown genotypes are rhythmic.

In order to down regulate *Snap* in the clock cells, two RNA interference lines were crossed to *tim-Gal4*, but unfortunately, only few flies reached the adult stage and they lived for a few days only.

An attempt to drive the knockdown to the LNvs using *pdf-Gal4* was successfully achieved (table 6.7) and the flies showed rhythmic behaviour in DD (figure 6.15) and were arrhythmic in LL (figure 6.16). Moreover, when the RNAi line VDRC 101341 was used, the flies showed a short period of activity (τ=22.8 h ± 0.06) that is significantly different from the controls VDRC 101341 ($F_{1,130}$= 47.9, $p<10^{-9}$) and *yw;pdf-Gal4;+* ($F_{1,139}$= 120.3, $p<<10^{-10}$) (figure 6.17).

Table 6.7 - Downregulating *Snap* in the LNvs.

***Snap* RNAi (VDRC ID)**	**DD**			**LL**		
	% Rhythmic	**Mean Period ± SEM**	**n**	**% Rhythmic**	**Mean Period ± SEM**	**n**
w;pdf-Gal4/RNAi Snap; (VDRC 101341)	72	22.8 ± 0.06	151	12	-----	24
w;pdf-Gal4/+;RNAi Snap/+ (VDRC 22379)	91	23.8 ± 0.09	32	41	-----	29
VDRC 101341 (Control)	92	23.9 ± 0.19	25	-----	-----	---
VDRC 22379/+ (Control)	95	23.7 ± 0.05	21	-----	-----	---
yw;pdf-Gal4;+ (Control)	65	24.5 ± 0.17	50	-----	-----	---

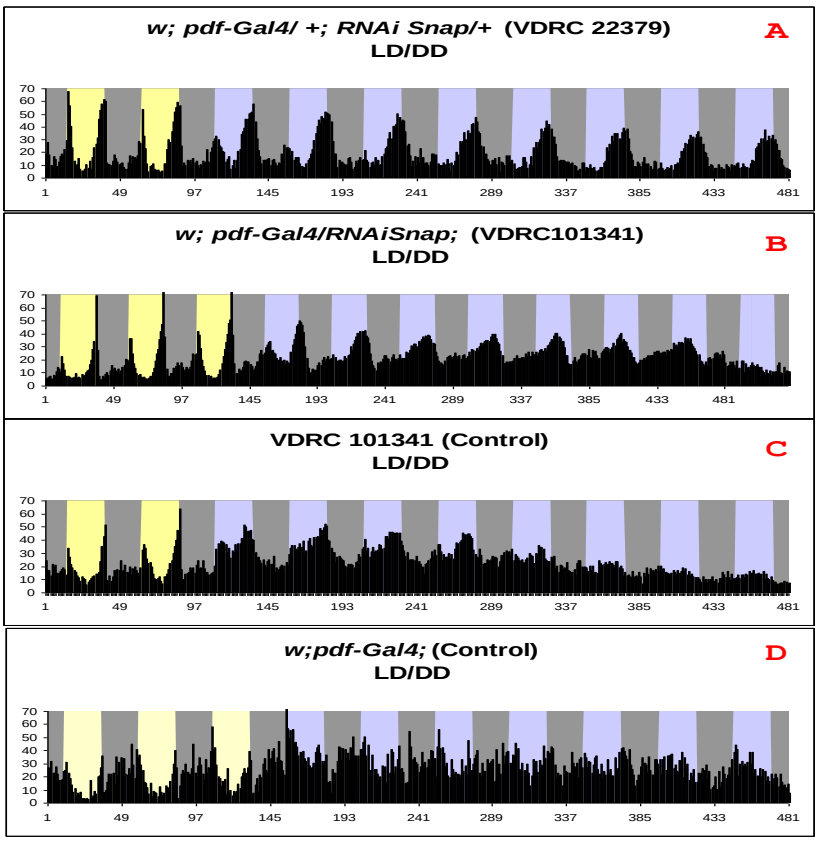

Figure 6.15 – Locomotor activity of *Snap* RNAi in DD. A and C: 2 days LD, 8 days DD. **B:** 3 days LD, 8 days DD. **D:** 3 days LD, 7 days DD. **X-axis:** time in 30 minutes bins. **Y-axis:** mean level of activity. **Yellow:** day. **Gray:** subjective night. **Blue:** subjective day. All different shown genotypes are rhythmic.

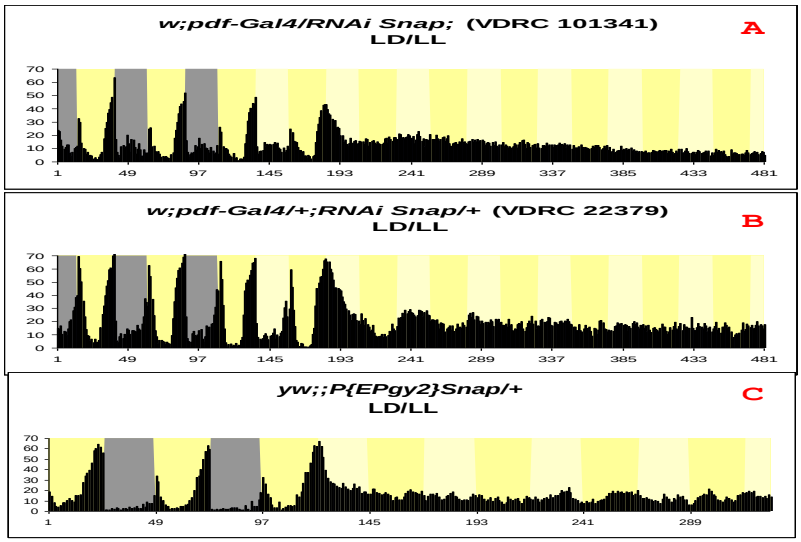

Figure 6.16 – *Snap* variants locomotor activity profile in LL. A and B: 2 days LD, 7 days LL. **C:** 2 days LD, 5 days LL. **X-axis:** time in 30 minutes bins. **Y-axis:** mean level of activity. **Gray:** dark. **Dark yellow:** subjective daylight. **Yellow:** subjective night. All genotypes showed arrhythmicity.

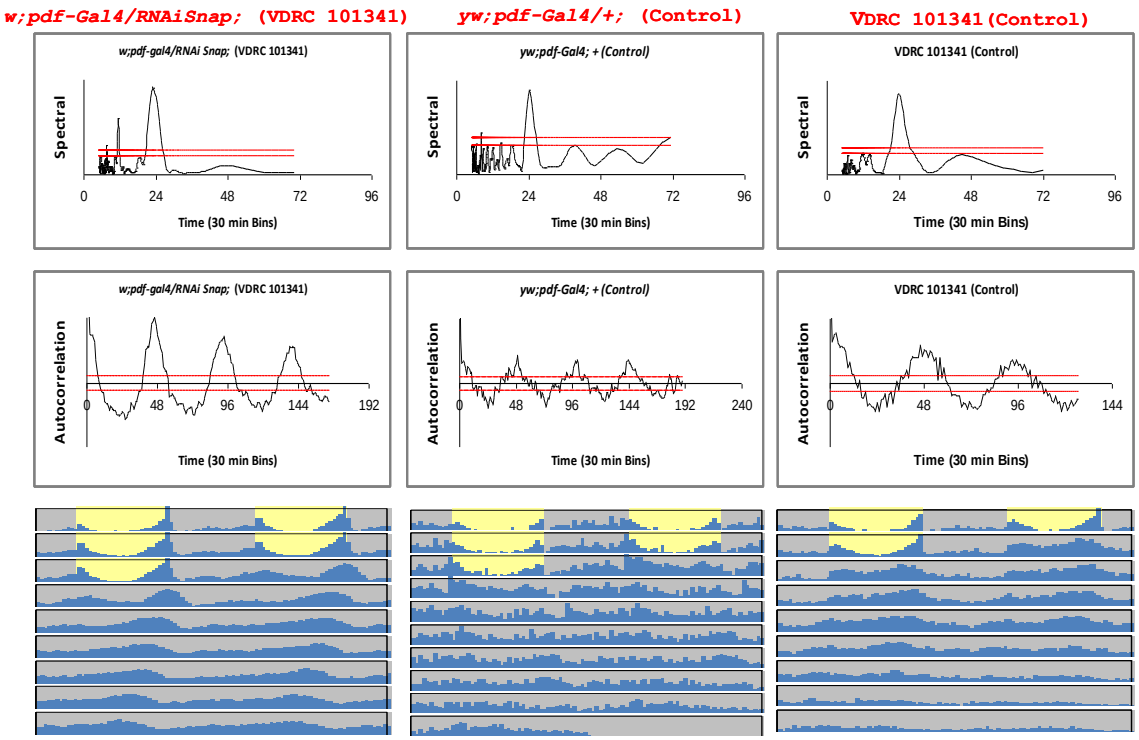

Figure 6.17 – Knocking down *Snap* in the LNvs causes short period in DD. *w;pdf-Gal4, RNAi Snap (VDRC 101341)* τ= 22.8 (± 0.06), *yw;pdf-Gal4;* (Control) τ= 24.5 (± 0.17) and VDRC 101341 (Control) τ= 23.9 (± 0.19). **Upper panel:** CLEAN spectral plot along with the 95% and 99% Monte Carlo confidence limits. **Central panel:** Autocorrelogram along with the canonical 95% confidence limits. **Lower panel:** Double-plotted actogram of locomotor activity mean. **Yellow:** Day. **Gray:** Subjective night. Genotypes are indicated on top of the spectral plots.

6.2.1.6 Double Mutants

Double mutants for synaptic genes were analysed in order to check if the effect of single mutations would be amplified in the presence of another mutation in a different gene. The double mutants showed rhythmicity in DD (figure 6.18) and were arrhythmic in LL (figure 6.19).

The co-presence of the alleles $Nsf2^{A6}$ and $Snap^{G8}$ (as transheterozygotes) resulted in a short circadian period (table 6.8). However, this effect was only observed when the flies were not in the w^{1118} background (τ=22.8 h ± 0.04). The presence of the *white* mutation increased the period to a normal 24 h (table 6.8). Moreover, flies

;Snap^{G8}/Nsf2^{A6} (transheterozygotes) showed a significantly shorter period when compared to *w;;Nsf2^{A6}*/+ ($F_{1,101}$=18.9, $p<10^{-4}$) but the same was not observed when compared to *Snap^{G8}*/+ ($F_{1,71}$=2.4, p=0.1.23).

Putting *Df(3R)Exel6156*, which deletes the gene *synapsin*, *in trans* with *Snap^{G8}* resulted in a period close to 24 h (τ=23.6 h ± 0.1) and longer than the one observed in flies containing only the deficiency (τ=23.08 h ± 0.12) or the *SnapG8* mutant allele (τ=23.02 h ± 0.13). The same kind of result was observed when *Df(3R)Exel6156* was tested along with *Nsf2^{A6}*. The double mutant period was τ=23.4 ± 0.04, whereas flies containing only *Df(3R)Exel6156* or *Nsf2^{A6}* had a shorter period of τ=23.08 ± 0.12 and τ=23.2± 0.06, respectively.

Table 6.8 - Double mutants' locomotor activity.

Double Mutants	DD			LL		
	% Rhythmic	Mean Period ± SEM	n	% Rhythmic	Mean Period ± SEM	n
w;;Snap^{G8}/ Nsf2^{A6}	91.1	24 ± 0.3	45	-----	----	---
;;Snap^{G8}/ Nsf2^{A6}	98.3	22.8 ± 0.04	58	-----	----	---
;;Snap^{G8}/ Df(3R)Exel6156 (Syn)	100	23.6 ± 0.1	15	6.7	----	15
w;; Nsf2^{A6}/ Df(3R)Exel6156 (Syn)	87.5	23.4 ± 0.04	8	0	----	8

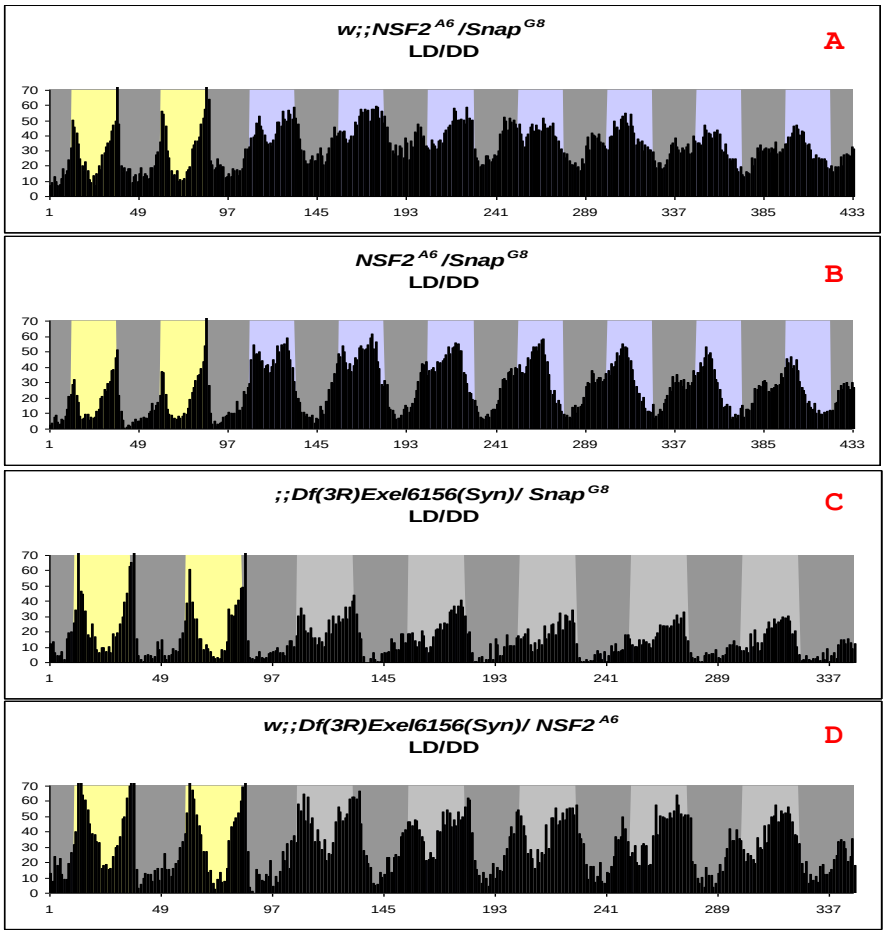

Figure 6.18 - Mean activity of double mutants in DD. A and B: 2 days LD, 7 days DD. **C and D:** 2 days LD, 5 days DD. **X-axis:** time in 30 minutes bins. **Y-axis:** mean level of activity. **Yellow:** day. **Gray:** subjective night. **Blue:** subjective day. The different genotypes are rhythmic.

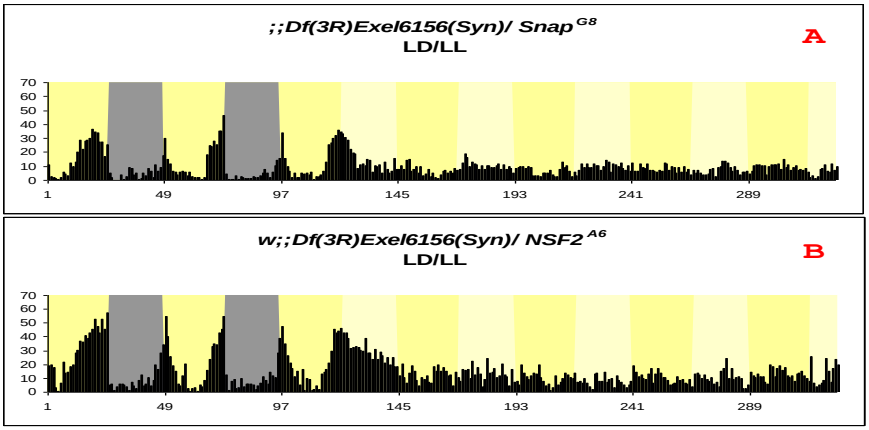

Figure 6.19 - Locomotor activity of double mutants in LL. A and B: 2 days LD, 5 days LL. **X-axis:** time in 30 minutes bins. **Y-axis:** mean level of activity. **Gray:** dark. **Dark yellow:** subjective daylight. **Yellow:** subjective night. Both genotypes are arrhythmic.

6.2.2 Immunocytochemistry (ICC)

The locomotor behaviour study revealed that the mutant $Snap^{G8}$ has a short period of activity, independently of the presence of a balancer, and the same phenotype was observed when the *Snap* deletion *Df(3L)Exel6136/TM6B* was analysed (see details in section 6.2.1.5). Moreover, when *Snap* was silenced in the LNvs, the period was even shorter (τ=22.8 h ± 0.06) and significantly different from the appropriate controls.

In order to check the molecular oscillations that underlie the behavioural rhythms in the absence of environmental cues, specifically the effect of eliminating *Snap* in the PDF-expressing cells, a whole-mount immunocytochemistry assay (ICC) was conducted.

For the ICC, the RNAi *Snap* flies (VDRC 101341) were knocked down by *pdf-Gal4* and *dicer2*. Although the locomotor activity of these flies had not been tested before the ICC, one would expect that the presence of *dicer2* would amplify the knocking down effect and a shorter period would be detected. Surprisingly, the behavioural period of these flies in DD was longer (τ=23.4 h ± 0.05) than in the absence of *dicer2* (τ=22.8 h ± 0.06). The unexpected lengthening of the period seems to be caused by the background, since the control *UAS-dcr2; pdf-Gal4* also showed a long period of activity in DD (τ=24.5 h ± 0.11).

Flies *UAS-dcr2; pdf-Gal4/RNAi Snap;* and the control *UAS-dcr2; pdf-Gal4* were entrained to a 12 hr LD cycle for 3 days and then kept under DD at constant temperature (25°C). After three days in DD, the flies were collected and the brains were dissected at two circadian times, CT16 and CT22 (where CT0 corresponds to the time of lights on during the LD cycle). Flies were collected at the third day of DD in order to allow an earlier accumulation of nuclear TIM in the flies down regulating

Snap compared to the control, since after 3 days their clocks should be running with a 3 h difference.

The brains were double-stained for PDF and TIM. The antisera raised against PDF can only identify the LNvs (Renn *et al*., 1999) and its signal is restricted to the cytoplasm, allowing the identification of the nuclei in the optical sections.

The large-LNvs and the cell compartments were quantified for TIM staining using ImageJ 1.42 for both time-points and the expression profile is reported in figure 6.20. In accordance with the behavioural results, a strong signal of nuclear TIM was detected at CT16 (figure 6.20 A and C) and CT22 (figure 6.20 B and D) in flies knocking down *Snap*. On contrary, in the control flies TIM signal was stronger in the cytoplasm. These results indicate that knocking down *Snap* in the LNvs leads to the earlier entrance of TIM into the nucleus, corroborating with the short period found in activity experiments.

The down regulated *Snap* flies showed a higher TIM accumulation not only in the nucleus but also in the cytoplasm and in the whole neuron, at both circadian times. ANOVA analysis followed by Post Hoc test (Tukey HSD test) showed that at CT16, significant differences in nuclear ($p=0.002$), cytoplasmic ($p=0.03$) and total ($p=0.02$) TIM levels were detected when compared to the control (figure 6.20 C). As shown in figure 6.20 D, the same statistical tests also revealed significant differences between the two genotypes when comparing TIM signals measured at CT22: nuclear TIM ($p<10^{-3}$), cytoplasmic TIM ($p=0.03$) and total TIM ($p=0.02$).

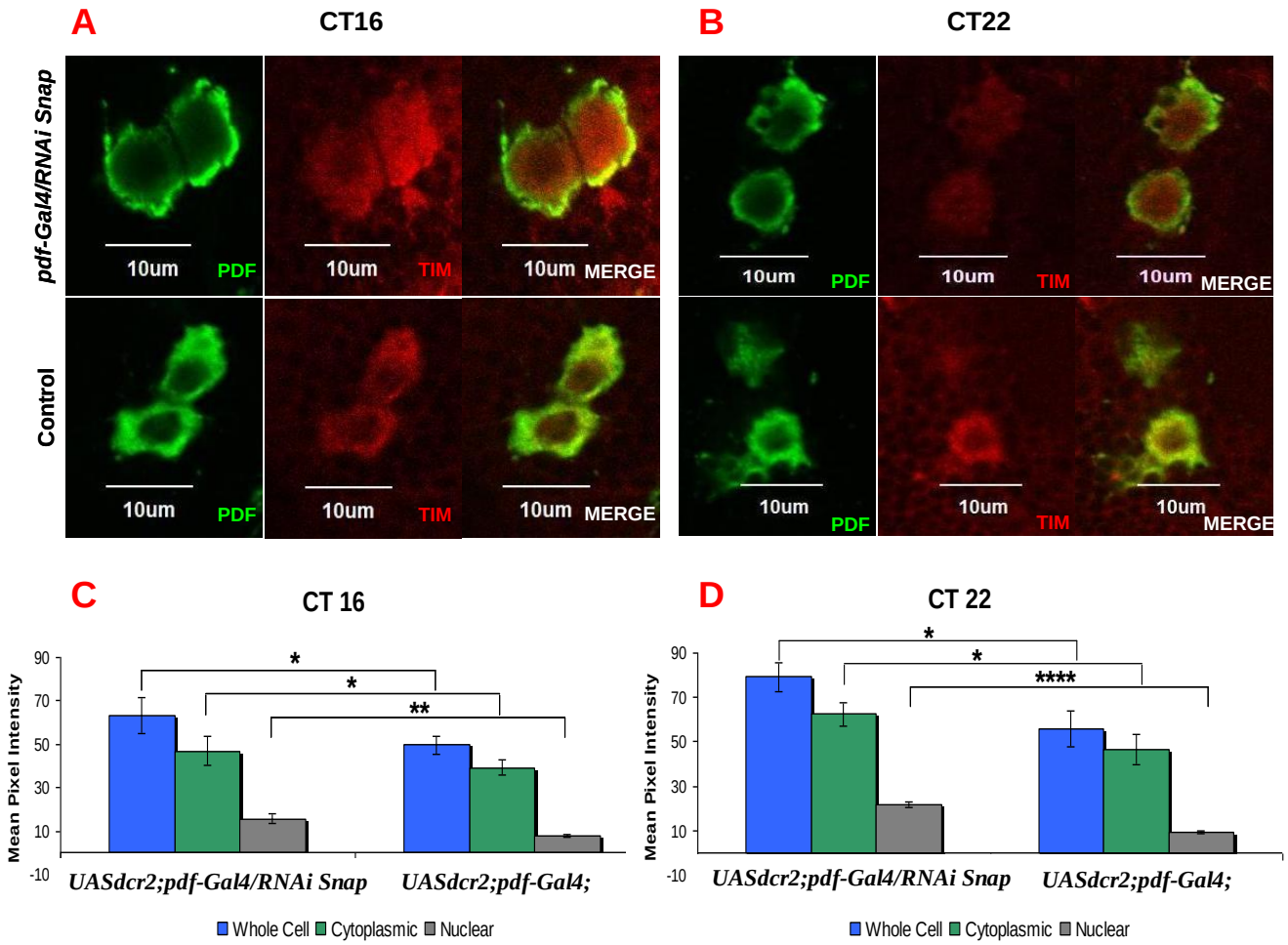

Figure 6.20 - TIM expression in the large LNvs at CTs 16 and 22. A and B: Optical sections of l-LNvs stained for PDF and TIM. CTs are indicated above each set of optical sections and genotypes are indicated on the left. Control: *UASdcr2;pdf-Gal4;+* and pdf-Gal4/RNAiSnap: *UASdcr2;pdf-Gal4/RNAiSnap;+* (VDRC 101341). **C and D:** Quantification of cytoplasmic, nuclear and whole cell TIM staining in the l-LNvs as a function of CT. For each genotype, the quantification is based on images of six to nine brains per time point and two to eight l-LNvs were imaged from both brain hemispheres. * $p<0.05$, ** $p<0.01$, *** $p<0.001$ and **** $p<0.0001$.

6.3 Discussion

Synaptic transmission, is a fundamental mechanism of intracellular communication, that has been conserved in evolution between vertebrates and invertebrates (Klagges *et al.*, 1996), thus synaptic protein should have conserved functions between mammals and flies. Indeed, *Drosophila* appears to be an excellent

model organism for studying the function of the synapse (Keshishian *et al*., 1996; Parfitt *et al*., 1995) and the insights gained from studies in fruit flies are generally applicable to vertebrates.

The study of the circadian proteome of the SCN highlighted synaptic vesicle cycling as a novel point of clock cell regulation in mammals. Vesicle exocytosis and endocytosis were blocked by the toxins botulinum or dynasore, respectively, in cultures of SCN, compromising its circadian gene expression (Deery *et al*., 2009).

shibire is the *Drosophila* homolog of *dynamin*, which is a GTPase responsible for endocytosis in eukaryotic cells, principally involved in the scission of newly formed vesicles. Recently, it has been shown that the expression of the dominant negative allele $shibire^{ts1}$ (shi^{ts1}) in pacemaker neurons results in remarkably long periods. This effect is enhanced when shi^{ts1} is co-expressed with other components of the endocytic pathways. These data suggests that endocytosis has an important function in circadian timing (Kilman *et al*., 2009).

Based on these observations, I conducted a study on the role of five *Drosophila* genes (*Syn*, *Nsf2*, *Nsf1*, *Leonardo* and *Snap*) that are homologous to synaptic proteins that had been determined by proteomic analysis to cycle in the mouse SCN (Deery *et al*., 2009). The strategy used to correlate these synaptic proteins with the circadian clock was examining the locomotor activity of mutants and down regulation of these genes in clock neurons.

Locomotor behavioural analysis of seven different *Syn* mutants did not give strong evidence of an association between this gene and the circadian system. The *Syn* mutant lines *w;;PBac{RB}Syn* (Bloomington ID 17829) and *w; ;PBac{WH}Syn* (Bloomington ID 18767) are rhythmic with normal periods of activity in DD. These mutants have the *PiggyBac* element transposed outside the *Syn* coding sequence

regions (CDS) so it may be that gene expression is not necessarily being affected in the mutants.

The coding sequence of *yw;Mi{ET1}Syn* (Bloomington ID 22772) and *yw;Mi{ET1}SynTimp* (Bloomington ID 23762) was not interrupted by the insertion of the *Minos* element, however only *yw;Mi{ET1}SynTimp* behaved normally in DD. The mutant *yw;Mi{ET1}Syn* showed a slightly long period of activity (τ=24.6 h ± 0.15). In addition, an opposite effect was noticed in flies carrying only one copy of *Syn* as a result of a deletion. Flies *w;;Df(3R)Exel6156/+* (Bloomington ID 7635) displayed a short period of τ=23.08 h ± 0.12 when tested in DD.

Three *synapsin* genes are found in the mammalian genome and multiple isoforms are generated (Kao *et al*., 1998; Sudhof *et al*., 1989). In *Drosophila*, the *Syn* gene presumably represents the only *synapsin* homologue and this single gene codes for several isoforms (Klagges *et al*., 1996). However, the role of the different isoforms generated by alternative splicing is still unknown.

The presence of multiple isoforms of a protein can cloud the interpretations of mutant phenotypes. Mutations in the *Syn* gene may not necessarily affect all isoforms, therefore some of the mutants analysed in this work could have unaltered isoforms maintaining the gene function. In addition, is possible that only some isoforms could be involved in the circadian clock. To address this question, *Syn* null mutant flies lacking all *Drosophila synapsin* isoforms were tested, thus eliminating the possibility of complementation.

Syn97 and *Syn79* null mutants cannot synthesise functional *synapsin* abolishing detectable signals in Western Blots (Godenschwege *et al*., 2004). Locomotor activity tests revealed that *Syn97* and *Syn79* are rhythmic in DD and their periods of activity are close to 24 hours, suggesting a lack of involvement in the

circadian clock. A similar result was found in flies with reduced expression of *synapsin*, the hypomorphic mutant *Syn168*.

The results from behavioural experiments with flies down regulating *Syn* in clock cells were not very promising. Two *Syn* RNAi lines (VDRC 46480 and VDRC 46482) were crossed to *tim-Gal4* flies and showed 24-h rhythmicity in DD. The co-expression of *dicer2* and VDRC 46482 resulted in a slight lengthening of the period (τ= 24.6 h ± 0.12), not seen when VDRC 46480 was used. Although both RNAi lines are targeting the same region of *Syn* gene, the insertion point of the transgene could affect the down regulating strength through regulatory elements present in the insertion region.

Molecular analysis in *Drosophila* has revealed two closely related NSF genes, *dNsf-1* and *dNsf-2* (Boulianne and Trimble, 1995; Ordway *et al*., 1994). The NSF2 protein shares 84.5% of sequence identity with dNSF1, but they map to different chromosomes (Boulianne and Trimble, 1995). Behavioural tests showed that the mutant *w;;Nsf2^{A15}/TM6B* (Bloomington ID 8282) has a significantly long period of activity (τ= 27.17 h ±0.16) in DD , however when the balancer is removed a normal locomotor behaviour is detected. This result suggests that the period lengthening is an effect caused by the balancer, and not by the mutation. In fact, the cytological map location of the *Nsf2* is 87F15 and there is a breakpoint in the *TM6B* balancer nearby in 87B4 that could be affecting the gene.

An interesting result was obtained from the activity experiment in DD using *w;;Nsf2^{A6}/TM3* (Bloomington ID 8281), showing that more than 60% of the flies were arrhythmic when balanced. However in the absence of the balancer these flies were rhythmic and had short period of activity (τ=23.2 h± 0.06). The loss-of-function *dNsf2^{15}* and the hypomorphic *dNsf2^{21}* mutants were also rhythmic in DD and had

around 24-h periods. However, these mutations are homozygous lethal and the tested flies carried only one copy of the mutant allele. The attempt to put $dNsf2^{15}$ and $dNsf2^{21}$ in trans with *Df(3R)urd* (Bloomington ID 3639), which deletes the region enclosing *Nsf2* and also behaved rhythmically in DD as heterozygote, was unsuccessful. This fact indicates that *Nsf2* is required during developmental stages. Finally, silencing *Nsf2* in clock cells failed to associate this gene with the circadian clock, since flies showed robust 24-h rhythms in DD. Since the locomotor behaviour of the *Nsf2* variants did not imply its participation in the circadian mechanism I did not pursue this line of work further.

Downregulating *Nsf1* in clock cells by *tim-Gal4,* or specifically in the LNvs by *pdf-Gal4* was not able to disrupt the locomotor rhythm of these flies in DD. *comt6* mutants also showed robust rhythmicity under DD.

Although no substantial behavioural effect was found for both *Drosophila Nsf* homologues, a redundancy of function could mean that one gene is complementing the function of the other. Previous work has shown that *Nsf1* and *Nsf2* have different spatial and temporal expression. Tissue-specific rescue experiments suggested an essential role for NSF1 in the nervous system, whereas NSF2 is required in the mesoderm. Despite this fact, ectopic expression studies showed that NSF1 and NSF2 proteins have the ability to substitute for one another, indicating that they have overlapping functional properties (Golby *et al*., 2001).

Another synaptic gene analysed in this work was *leonardo* (14-3-3ζ). Two *leonardo* mutants, $14\text{-}3\text{-}3\zeta^{2.3}$(Bloomington ID 9573) and the loss-of-function $14\text{-}3\text{-}3\zeta^{\Delta 12BL}$ (Bloomington ID 9572) showed opposite effects when tested under DD. The mutant $14\text{-}3\text{-}3\zeta^{2.3}$ has a slightly long period (τ=24.5 h ± 0.15), whereas $14\text{-}3\text{-}3\zeta^{\Delta 12BL}$ showed short period of activity (τ=23 ± 0.06). Conversely, knocking down this gene

in the clock neurons does not confirm an effect in the period. In fact, a long period was found when the RNAi lines (VDRC 48724 and VDRC 48725) were tested. However statistical analysis revealed that the lengthening in the period was caused by the background. Consequently, no clear association between *leonardo* and the circadian clock was found.

The most promising locomotor behaviour among the synaptic genes was found for *Snap* variants. The $Snap^{G8}$ hypomorphic mutation has short period in DD, when balanced by *TM6C* (τ= 22.6 h ± 0.2) or not (τ= 23.02 h ± 0.13), although carrying only one mutant allele copy. The same phenotype (τ= 23.2 h ± 0.14) was observed for *w;;Df(3L)Exel6136/TM6B*, in which one copy of *Snap* has been deleted.

Manipulating *Snap* with the use of RNA interference in the clock neurons led to lethality, showing that this gene is required for flies' viability. Attempts were made with two RNAi lines targeting *Snap* in different regions of the gene (VDRC 101341 and VDRC 22379). Restricting the action of the RNAi lines to pdf-cells (LNvs) allowed the flies survival. Interestingly, the *Snap* knockdown through RNAi line VDRC 101341 resulted in a strikingly short period of activity (τ= 22.8 h ± 0.06), agreeing with the phenotype found for $Snap^{G8}$ and *Df(3L)Exel6136/TM6B*.

In accordance with the behavioural results, it has been shown that knocking down *Snap* in the LNvs induced an earlier accumulation of TIM when compared to the control flies. This event was observed not only at the nuclear level, but also at the cytoplasmic (figure 6.20). Flies used in the immunocytochemistry experiment (*UASdcr2;pdf-Gal4/RNAi Snap;*) did not show a period as short as flies that do not express *dicer2*. However, the clock of these flies runs faster than the control and after 3 days in free-running conditions the ICC results were consistent with the phase difference of 3 hours observed.

Previous work has suggested that a reduction in Snap activity result in diminished neurotransmitter release and accumulation of a neural SNARE complex (Babcock *et al*., 2004). Although speculative, there are two hypotheses to explain the way *Snap* could modulate the circadian rhythms. The first would be by impairing the communication of pacemaker neurons. That is true for the classical mutant pdf^{01}, which presents arrhythmic profiles in free-running conditions due to neuronal desynchronization. In this case, the pace of core clock proteins is not affected within each cell (Peng *et al*., 2003). *Snap* could be regulating PDF release in the termini of LNs and disrupting its function would cause a phenotype similar to pdf^{01} flies. Moreover, *Snap* mutants and RNAi have short free-running period resembling the few rhythmic pdf^{01} individuals (Renn *et al*., 1999).

The alternative hypothesis involves the feedback of *Snap* on the expression or stability of core clock components. Since the evidence presented here points to the observation that down-regulation of *Snap* promotes a faster accumulation of TIM and subsequent nuclear entry, it seems that the second possibility might be favoured.

Supporting this idea, synaptic vesicle cycling has been previously implicated in modulating the core clock in mammals and flies. Treating cultures of SCN with drugs that block exocytosis and endocytosis has compromised SCN circadian pacemaking. The amplitude of *mPer1* and mPER2 cycling was significantly reduced and the period of oscillation was lengthened by approximately 1hr (Deery *et al*., 2009).

In *Drosophila*, disrupting endocytosis expressing the mutant allele $shibire^{ts1}$ (shi^{ts1}) in pacemaker neurons results in strikingly long periods and reduces CLOCK levels. In addition, the co-expression of other components of the endocytic pathway enhance this effect (Kilman *et al*., 2009). Moreover, two other transcripts involved in

endocytosis, *syndapin* and *beta-adaptin*, cycle in *Drosophila* head (Claridge-Chang *et al*., 2001). All these facts are indicatives that vesicle cycling might define a further feedback loop in the clockwork.

Chapter 7: Discussion

Although we have a basic knowledge of the *Drosophila* molecular clock circuits and how the molecular oscillations take place, it is still necessary to identify the nature of the protein complexes that subserve circadian pacemakers. Additionally, questions regarding the connections between the oscillator and the overt rhythms and the entrainment of the clock remain unanswered.

In this work, transgenic flies were used in three different approaches in order to identify new clock components. In the first, flies in which the circadian factor CYC is tagged by the Strep tagII or Halo tag were created to be used in co-immunoprecipitation (coIP) experiments. The second strategy was based on the locomotor behaviour screen of tagged flies and the last employed a comparative approach with the mammalian circadian SCN proteome. Mutants and RNA interference were used to disrupt and knockdown the clock candidate genes.

The laborious cloning of the StrepII and Halo tagged constructs described in chapter 3, was successfully achieved as shown by PCR reactions, which confirmed the presence of the constructs previously sequenced to check for possible errors. Also, it was shown that the transgenic flies could be useful in studies involving the circadian system, since the presence of the construct in the genome did not disrupt circadian rhythms as measured by locomotor behaviour experiments in DD. It was previously shown that homozygous cyc^{01} flies show arrhythmic locomotor activity pattern in DD (Rutila *et al.*, 1998). Supporting the idea that tagged CYC protein is functional, flies carrying StrepII and Halo transgenes in cyc^{01} background were able to rescue the rhythmicity in DD. Moreover, immunodetection using Halo tag antiserum was another indication that tagged CYC was normally expressed.

Unfortunately, Halo tagged CYC failed to pull down its binding partners. One possible explanation for this is that the recombinant protein conformation might be hiding the tag and not allowing it to bind the resin. Another possibility is that the antibody is not able to detect such small amount of proteins.

Another tag-based system which explores the high affinity between biotin and (strept)avidin has proven very efficient for allowing single-step capture of lower abundance protein complexes, such as those containing transcription factors (de Boer *et al*., 2003). The technique involves the use of short peptide tags that are efficiently biotinylated *in vivo* by the bacterial BirA biotin ligase. Subsequently, the tagged proteins can be purified by affinity chromatography and identified by mass spectrometry. This approach, which was recently successfully applied to diverse cell line factors (de Boer *et al*., 2003), could also be used in flies to detect protein complexes interacting with CYC. In fact, a research group has generated transgenic flies in which core clock components, such as CLK and CYC, were tagged with the activatable peptide BLRP by ends out homologous recombination (Antonio Meireles, personal communication). Using the *UAS/Gal4* system, the biotinylation of this tag, by BirA, could be directed to pacemaker cells. Therefore this strategy represents another opportunity to screen for new clock proteins.

A number of clock genes have been identified from locomotor activity screens of mutant flies. The isolation and analysis of these mutants with altered circadian rhythms have led to a better understanding of the circadian rhythms at the molecular level. The first clock gene, *period*, identified in *Drosophila* has three mutant alleles that show aberrant locomotor activity in free-running conditions (Konopka and Benzer, 1971). Some other genes essential for the normal functioning of circadian time-keeping system were also identified by forward genetic screens (Young and Kay,

2001). In *Drosophila*, mutations have also identified components of the light input pathway, such as cry^b flies which behave rhythmically in LL (Emery *et al*., 2000).

Mutations in flies can be produced by transposable elements when inserted in the vicinity of a gene. When transposed, these elements can directly disrupt the reading frame of the gene, or more commonly, alter its transcription or splicing. The CPTI lines used in chapter 4 had a protein trap vector inserted by the *piggyBac* transposon. In order to check for new components of the circadian clock, a screen through locomotor activity experiments, the most common behavioural assay in flies to measure circadian rhythms, was performed in DD and LL. This approach was efficient, since twelve candidate lines showed altered locomotor behaviour, and were selected for further studies.

The follow up experiments using mutants and RNAi lines for the chosen CPTI candidates excluded an association between some of them (*lk6*, *kat80*, *glycogenin*, *Mi-2* and *14-3-3ε*) and the circadian clock. The involvement of other genes, like *Rab11*, *pbl*, *CG31352*, *CG33158* and *Ptp69D*, with the circadian system was still obscure. However, other candidates were worthy of investigation in more details. The most interesting genes were *Gs2* and *Got1* (both involved in the neurotransmitter glutamate metabolism pathway), since their mutants and RNAi lines showed consistent robust rhythmicity in LL. Moreover, previous works had connected glutamate and GABA, another neurotransmitter which is synthesised from glutamate, to *Drosophila* circadian circuitry (Hamasaka *et al*., 2005; Hamasaka *et al*., 2007).

In chapter 5, dissecting the effect of *Got1* and *Gs2* mutants' background was valuable not only to confirm the participation of these genes in the light entrainment to the clock, but also to reveal their genetic interaction with *tim*. Our results showed that *Got1* and *Gs2* mutants need to be in the simultaneous presence of the *ls-tim*

haplotype to show rhythmic behaviour in LL, indicating that these genes and *tim* function in the same circadian light synchronization pathway. This result resembles that with the *Veela* strain, in which the jet^c mutation only causes LL rhythmicity in conjunction with *ls-tim*, the less light sensitive *tim* allele (Peschel *et al*., 2006). Although the jet^c allele was not found among the mutants and RNAi lines used in this work, its frequent and random occurrence in laboratory strains highlight the importance of being cautious when studying light input pathways to the circadian clock.

Molecular evidence of the interaction between *Gs2* and *Got1* mutants with TIM was provided in a Western Blot assay (figure 5.16) for TIM cycling and stability. These mutants showed high levels of TIM when heads were collected in LL, especially during the subjective night, even though the control Canton S lacked TIM oscillations.

Gs2 and *Got1* seem to be affecting the clock entrainment by sending signals through synapses between clock neurons. As evidence for this hypothesis, downregulating the glutamate metabotropic receptor (DmGluRA) in clock neurons resulted in rhythmic behaviour in LL (figure 5.21). Indeed, it has been demonstrated that DmGluRA is expressed in the LNvs, which receive projections from the DNs (Helfrich-Forster *et al*., 2001; Helfrich-Forster *et al*., 2002; Veleri *et al*., 2003), considered to be clock glutamatergic neurons (Hamasaka *et al*., 2007). Manipulating the levels of expression of *Gs2* and *Got1* in specific subsets of clock neurons, support the view that glutamate metabolism in the DNs is important for entraining the clock. In this experiment, directing the knockdown of both genes to the DNs was sufficient to maintain robust rhythms in LL (figure 5.19). Based on these facts, it would be of great interest to knock down DmGluRA in the LNvs, using the *pdf-Gal4* driver, to

confirm that this group of neurons is receiving the glutamatergic signals from the DNs.

Although speculative, it seems that GABA follows the pattern of glutamate signalling and is also part of the light input pathway, since the s-LNvs receive GABAergic inputs and utilise GABA as a slow inhibitory neurotransmitter (Hamasaka *et al*., 2005). Accordingly, in this work we showed that downregulating *Gad1* (the enzyme that catalyses GABA synthesis) in clock neurons also resulted in rhythmic behaviour in LL (figure 5.22).

Although our results indicated that glutamate and GABA signalling are essential modulators of behavioural light entrainment, probably via DN projections, the way in which they regulate the phase-shifts is not completely understood. In this work we found that administration of light pulses, either at the beginning or at the end of the night, caused different effects in *Got1* and *Gs2* mutants. The former showed reduced phase shifts when compared to control flies in the same background, whereas the latter showed normal phase shifts (figure 5.17). *Got1* and *Gs2* have different functions in the glutamate metabolism pathway. *Got1* participates in glutamate synthesis during the transamination of aspartate, while *Gs2* catalyzes the switch of glutamate to glutamine (Featherstone *et al*., 2002). Moreover, glutamate is also used to synthesise GABA with the help of *Gad1* (Featherstone *et al*., 2002). In that way, our speculative model suggests a neurochemical regulation of phase shift based on the balance of GABA/glutamate in some clock neurons. *Got1* mutants have reduced levels of glutamate and consequently of GABA. On the contrary, *Gs2* mutants decrease the synthesis of glutamine and its re-uptake from glial cells, leading to perhaps an excess of GABA. The difference in the GABA/glutamate equilibrium might be responsible for the different reactions to the light pulses, generating

divergent post synaptic events, as for example differences in cytosolic Ca^{+2} concentration. Indeed, glutamate was previously linked to phase shifts in mammals. The circadian rhythms in mammals are generated by the suprachiasmatic nucleus of the hypothalamus (SCN), which can be photically entrained via the direct retinohypothalamic tract (RTH) (Moore, 1983). Glutamate is the primary neurotransmitter utilised by RTH (Ebling, 1996) and when administrated to the hamsters SCN, a phase shift of the circadian activity rhythm is observed (Meijer *et al*., 1988). The same effect was noticed in rats when *in vitro* experiments showed that the application of glutamate to the SCN during late subjective night produced phase advances (Shirakawa and Moore, 1994). Moreover, the elevation of cytosolic Ca^{+2} levels in SCN is thought to be a key step toward the light-induced resetting of the circadian clock in mammals (Ding *et al*., 1998).

Previous work has shown vesicle cycling as an important mechanism in maintaining circadian clock genes expression (Deery *et al*., 2009). Organotypic SCN slices were treated with either a drug that inhibits endocytosis (dynasore) or an inhibitor of exocytosis (Botox A). The expression of the clock gene *Per1* and clock protein PER2 were compromised and reduced amplitudes were observed. Moreover, the administration of Botox A also lengthened the period of oscillation (Deery *et al*., 2009). In flies, impaired endocytosis also disrupts the pacemaker. This was shown through the expression of the mutant allele *shibire*^{ts1} (the homologue of mammalian *dynamin*) in pacemaker neurons, which generated strikingly long periods and reduced CLOCK levels (Kilman *et al*., 2009).

In chapter 6, the possible connection between five synaptic genes (*syn*, *Nsf2*, *Nsf1*, *14-3-3ζ* and *Snap*) and the circadian clock were verified by locomotor activity assays. These genes were chosen for study because the circadian proteome of the SCN

in mammals identified their homologues as cyclic proteins (Deery *et al*., 2009). However, the locomotor behavioural tests did not implicate these genes with the circadian clock machinery. *Nsf1* and *14-3-3ζ* genes did not provide any evidence of their participation in the circadian clock system. Interestingly, behavioural and molecular assays indicated that *Snap*, a gene involved in SNARE complex disassembly (an essential step in vesicle recycling) (Clary and Rothman, 1990), might be modulating the expression or stability of core clock components. Downregulating *Snap* in the LNvs with *pdf-Gal4* and mutating this gene resulted in short period of activity (figure 6.18). Moreover, faster TIM accumulation and nuclear entry promoted by *Snap* knock down was observed in ICC experiments (figure 6.27). The way *Snap* is modulating the circadian clock is still obscure, however this result provides further support to the view that vesicle cycling might define a further conserved feedback loop in the clockwork (Deery *et al*., 2009).

Appendix 1

In chapter 3, prior to sending the constructs to be injected into embryos, they were checked by sequencing. A final consensus sequence and its map were made for the three constructs (figures 1, 2 and 3).

Figure 1 shows the translation of the 725 amino acids consensus sequence of the C-terminus Halo Tag. As expected, the construct starts with a start codon (Methionine) followed by *cyc* sequence (highlighted in gray) without the stop codon. Subsequently, a 13 amino acid AG linker is marked in pink. Finally, the 296 amino acid Halo Tag sequence is represented in green, ending with a stop codon.

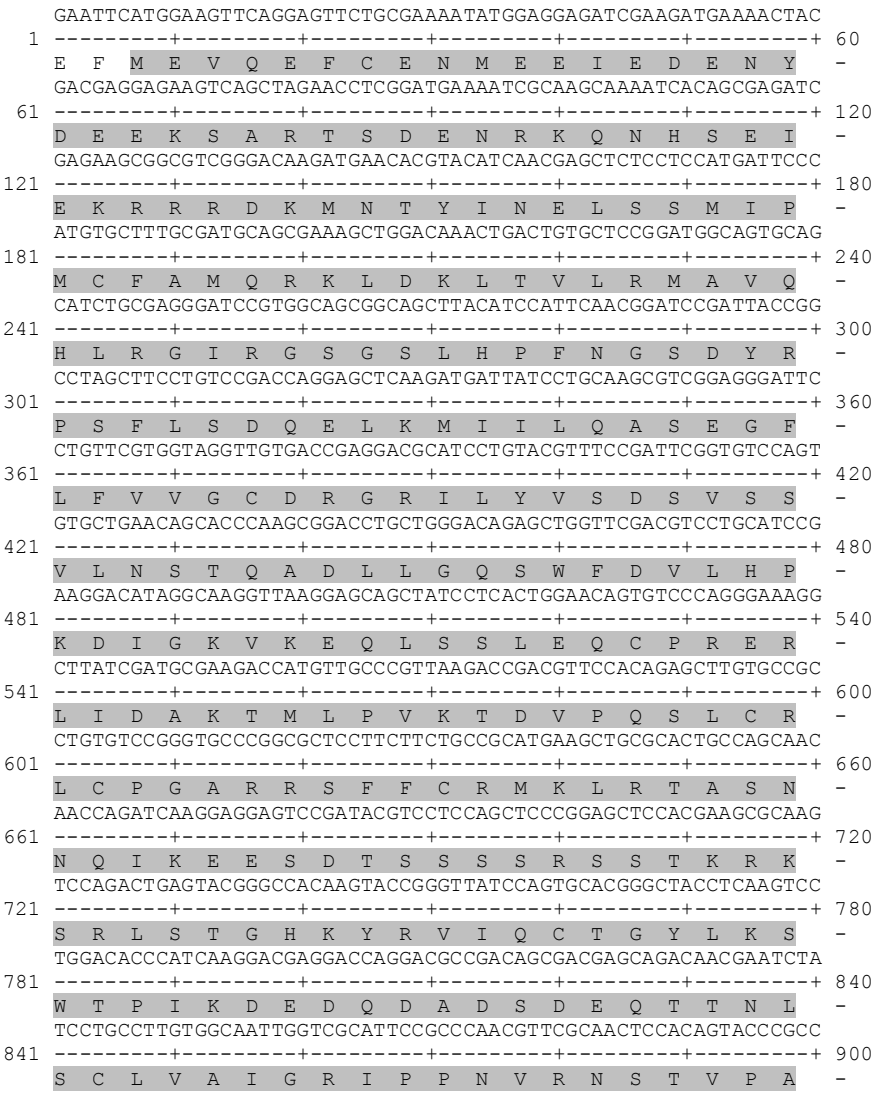

Figure 1 – C-terminus Halo Tag map sequence.

The map of the N-terminus Halo Tag showed that the 725 aa construct was correct and in frame (figure 2). The sequence starts with the first Methionine of the Halo Tag, which is highlighted in green. The 14 aa AG linker emphasized in pink is separating the Halo Tag from *cyc*. The latter is shown in gray and the presence of a unique stop codon can be noticed at its very end.

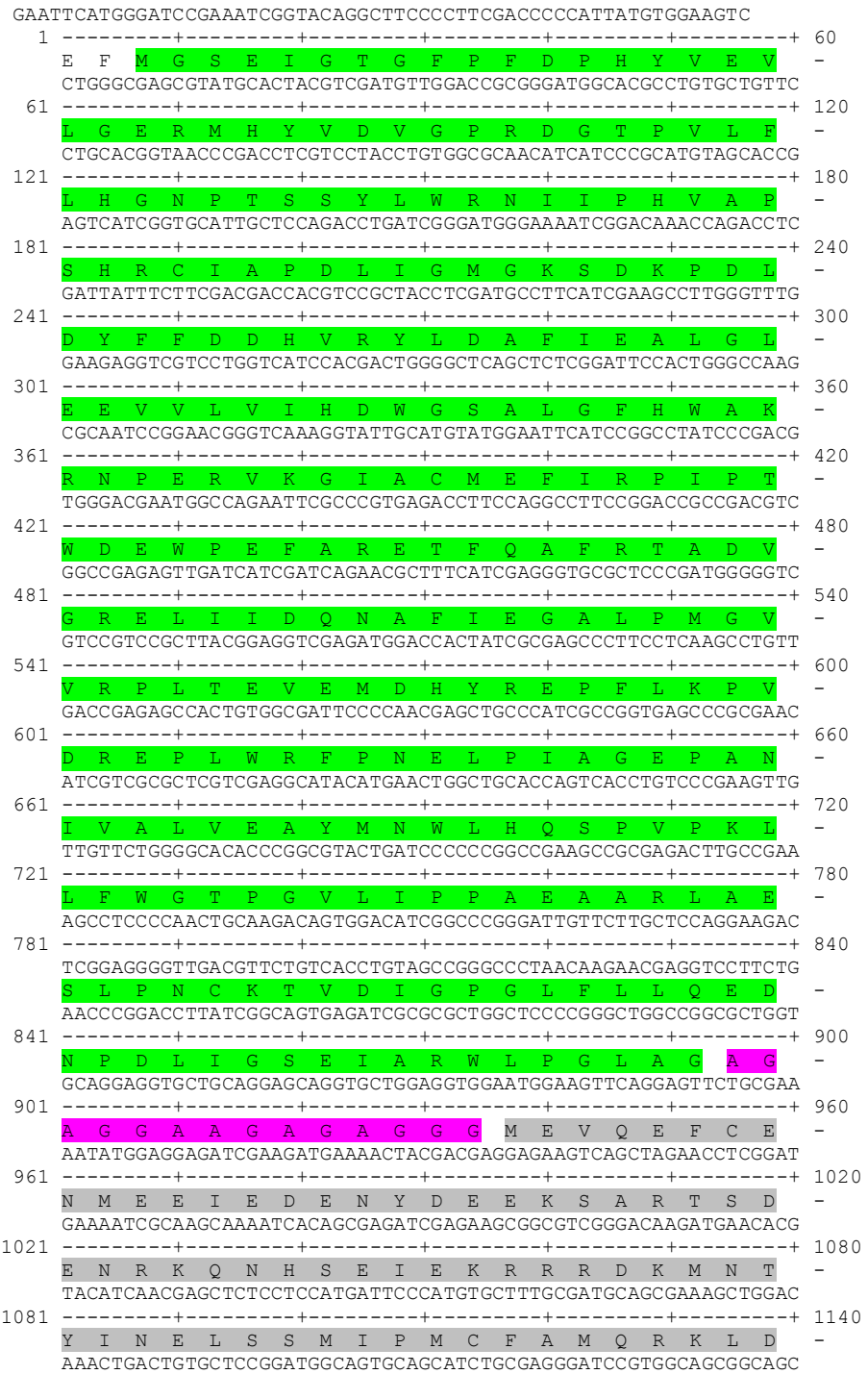

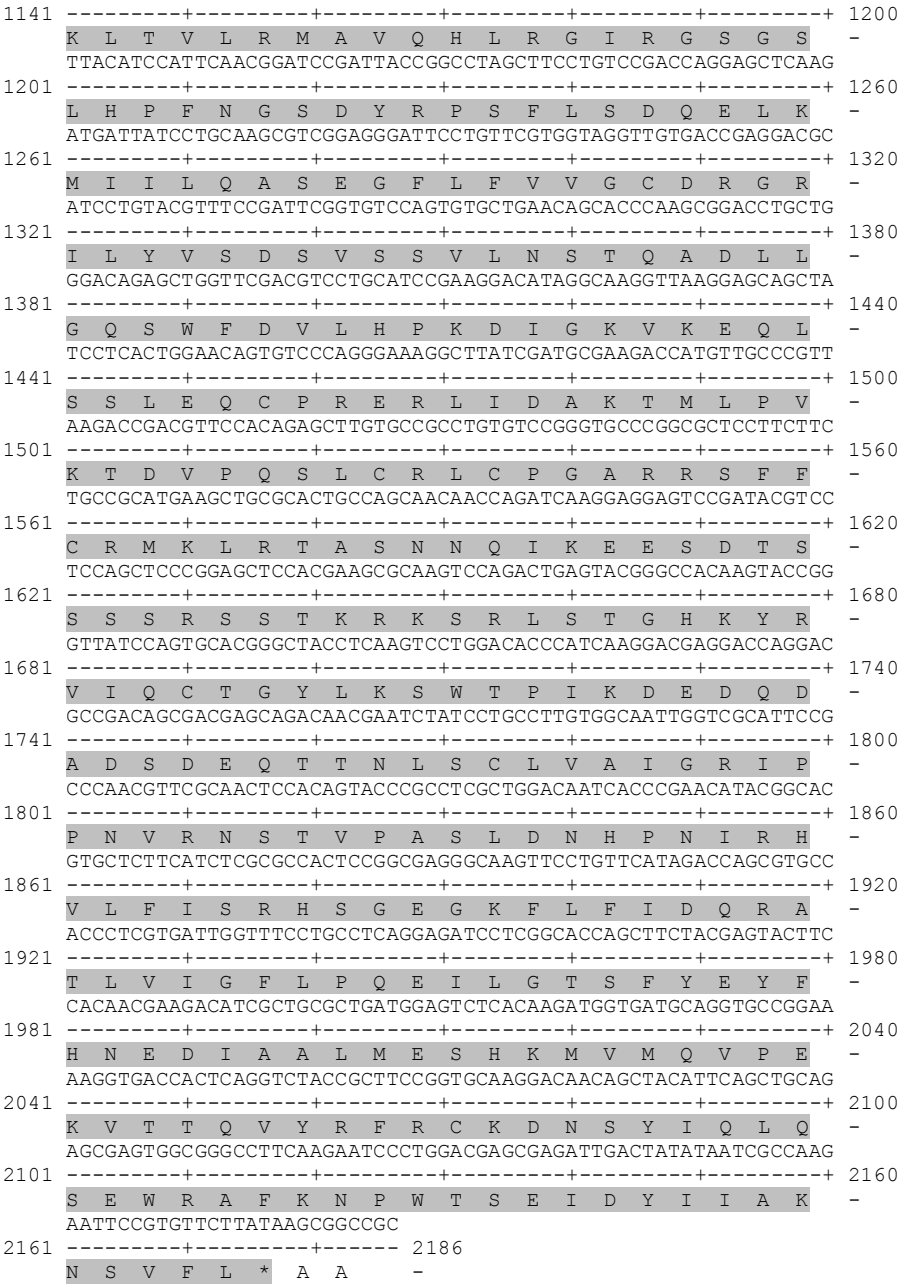

Figure 2 – N-terminus Halo Tag map sequence.

The map of the 437 aa N-terminus Strep TagII insert starts with the short 8 aa sequence of Strep TagII, represented in yellow. The following part of the sequence, corresponds to a 14 aa AG linker (showed in pink) carried on by *cyc* sequence, which appears in gray and continues in frame until the final stop codon (figure 3).

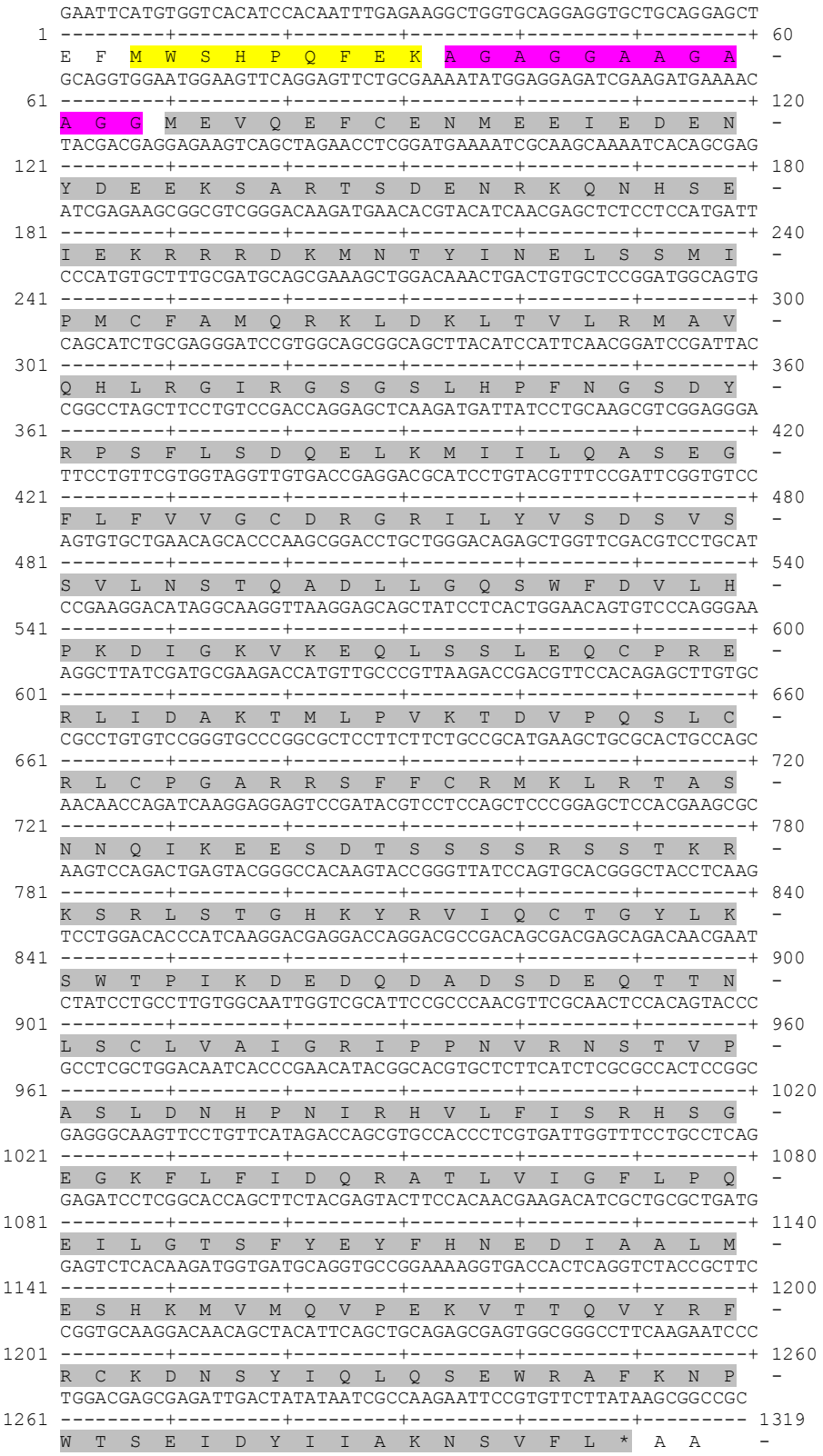

Figure 3 - N-terminus Strep TagII map sequence.

Appendix 2

The CPTI lines used in the locomotor activity screen under DD and LL conditions are listed in the table bellow.

CPTI lines analysed in DD	CPTI lines analysed in LL
CPTI-000016	CPTI-000016
CPTI-000020	CPTI-000020
CPTI-000023	CPTI-000023
CPTI-000031	CPTI-000031
CPTI-000033	CPTI-000033
CPTI-000038	CPTI-000038
CPTI-000049	CPTI-000049
CPTI-000056	CPTI-000056
CPTI-000076	CPTI-000076
CPTI-000077	CPTI-000077
CPTI-000091	CPTI-000091
CPTI-000106	CPTI-000107
CPTI-000107	CPTI-000113
CPTI-000113	CPTI-000155
CPTI-000155	CPTI-000165
CPTI-000165	CPTI-000168
CPTI-000168	CPTI-000194
CPTI-000194	CPTI-000196
CPTI-000196	CPTI-000205
CPTI-000205	CPTI-000207
CPTI-000207	CPTI-000216
CPTI-000216	CPTI-000232
CPTI-000218	CPTI-000245
CPTI-000232	CPTI-000252
CPTI-000245	CPTI-000274
CPTI-000252	CPTI-000286
CPTI-000274	CPTI-000299
CPTI-000286	CPTI-000303
CPTI-000299	CPTI-000328
CPTI-000303	CPTI-000332

CPTI-000318	CPTI-000335
CPTI-000326	CPTI-000337
CPTI-000328	CPTI-000340
CPTI-000332	CPTI-000342
CPTI-000335	CPTI-000365
CPTI-000337	CPTI-000379
CPTI-000340	CPTI-000408
CPTI-000342	CPTI-000426
CPTI-000349	CPTI-000442
CPTI-000365	CPTI-000448
CPTI-000371	CPTI-000454
CPTI-000379	CPTI-000471
CPTI-000408	CPTI-000493
CPTI-000426	CPTI-000560
CPTI-000433	CPTI-000616
CPTI-000442	CPTI-000633
CPTI-000448	CPTI-000655
CPTI-000454	CPTI-000658
CPTI-000471	CPTI-000688
CPTI-000493	CPTI-000720
CPTI-000560	CPTI-000736
CPTI-000616	CPTI-000737
CPTI-000633	CPTI-000738
CPTI-000655	CPTI-000760
CPTI-000658	CPTI-000763
CPTI-000688	CPTI-000764
CPTI-000720	CPTI-000794
CPTI-000736	CPTI-000798
CPTI-000737	CPTI-000850
CPTI-000738	CPTI-000854
CPTI-000739	CPTI-000876
CPTI-000743	CPTI-000883
CPTI-000760	CPTI-000902
CPTI-000763	CPTI-000905
CPTI-000764	CPTI-000915
CPTI-000794	CPTI-000924
CPTI-000798	CPTI-000925

CPTI-000833	CPTI-000992
CPTI-000850	CPTI-001015
CPTI-000854	CPTI-001018
CPTI-000876	CPTI-001025
CPTI-000883	CPTI-001029
CPTI-000886	CPTI-001036
CPTI-000902	CPTI-001039
CPTI-000905	CPTI-001053
CPTI-000915	CPTI-001063
CPTI-000924	CPTI-001064
CPTI-000925	CPTI-001113
CPTI-000992	CPTI-001117
CPTI-001015	CPTI-001119
CPTI-001018	CPTI-100000
CPTI-001025	CPTI-100002
CPTI-001029	CPTI-100003
CPTI-001036	CPTI-100004
CPTI-001039	CPTI-100005
CPTI-001053	CPTI-100008
CPTI-001063	CPTI-100013
CPTI-001064	CPTI-100017
CPTI-001113	CPTI-100022
CPTI-001117	CPTI-100026
CPTI-001119	CPTI-100027
CPTI-001137	CPTI-100033
CPTI-100000	CPTI-100034
CPTI-100002	CPTI-100036
CPTI-100003	CPTI-100039
CPTI-100004	CPTI-100041
CPTI-100005	CPTI-100044
CPTI-100008	CPTI-100048
CPTI-100013	CPTI-100050
CPTI-100017	CPTI-100051
CPTI-100022	CPTI-100059
CPTI-100026	CPTI-100062
CPTI-100027	CPTI-100063
CPTI-100033	CPTI-100065

CPTI-100034	CPTI-000668
CPTI-100035	CPTI-000762
CPTI-100036	CPTI-001360
CPTI-100039	CPTI-000774
CPTI-100041	CPTI-001234
CPTI-100044	CPTI-001046
CPTI-100048	CPTI-001214
CPTI-100050	CPTI-001291
CPTI-100051	CPTI-000161
CPTI-100059	CPTI-002315
CPTI-100062	CPTI-002487
CPTI-100063	CPTI-001728
CPTI-100065	CPTI-001902
CPTI-000668	CPTI-000944
CPTI-000762	CPTI-001977
CPTI-001360	CPTI-002103
CPTI-000774	CPTI-000263
CPTI-001234	CPTI-001279
CPTI-001046	CPTI-000727
CPTI-001214	CPTI-001506
CPTI-001291	CPTI-001303
CPTI-000161	CPTI-001997
CPTI-002315	CPTI-000977
CPTI-002487	CPTI-001740
CPTI-001728	CPTI-001450
CPTI-001902	CPTI-100038
CPTI-000944	CPTI-001589
CPTI-001977	CPTI-001341
CPTI-002103	CPTI-001879
CPTI-000263	CPTI-001170
CPTI-001279	CPTI-001695
CPTI-000727	CPTI-000349
CPTI-001506	CPTI-001516
CPTI-001303	CPTI-001990
CPTI-001997	CPTI-000703
CPTI-000977	CPTI-001771
CPTI-001740	CPTI-001718

CPTI-001450	CPTI-002085
CPTI-100038	CPTI-001991
CPTI-001589	CPTI-002049
CPTI-001341	CPTI-001796
CPTI-001879	CPTI-002927
CPTI-001170	CPTI-003146
CPTI-001695	
CPTI-000349	
CPTI-000762	
CPTI-001328	
CPTI-001769	
CPTI-001488	
CPTI-001654	
CPTI-000279	
CPTI-001714	
CPTI-000344	
CPTI-001056	
CPTI-000884	
CPTI-001277	
CPTI-001427	
CPTI-001775	
CPTI-001692	
CPTI-001282	
CPTI-001259	
CPTI-001081	
CPTI-001409	
CPTI-000546	
CPTI-001412	
CPTI-000256	
CPTI-001111	
CPTI-000130	
CPTI-000147	
CPTI-000190	
CPTI-000200	
CPTI-001332	
CPTI-001044	
CPTI-001273	

CPTI-001308	
CPTI-001516	
CPTI-001990	
CPTI-000703	
CPTI-001771	
CPTI-001718	
CPTI-002085	
CPTI-001991	
CPTI-002049	
CPTI-001796	
CPTI-002927	
CPTI-003146	
CPTI-003526	
CPTI-003522	
CPTI-003513	
CPTI-003504	
CPTI-003505	
CPTI-003532	
CPTI-003588	
CPTI-003445	
CPTI-003501	
CPTI-003490	

Bibliography

Akhtar, R.A., Reddy, A.B., Maywood, E.S., Clayton, J.D., King, V.M., Smith, A.G., Gant, T.W., Hastings, M.H., and Kyriacou, C.P. (2002). Circadian cycling of the mouse liver transcriptome, as revealed by cDNA microarray, is driven by the suprachiasmatic nucleus. Curr. Biol. *12,* 540-550.

Akten, B., Jauch, E., Genova, G.K., Kim, E.Y., Edery, I., Raabe, T., and Jackson, F.R. (2003). A role for CK2 in the Drosophila circadian oscillator. Nat. Neurosci. *6,* 251-257.

Allada, R., White, N.E., So, W.V., Hall, J.C., and Rosbash, M. (1998). A mutant Drosophila homolog of mammalian Clock disrupts circadian rhythms and transcription of period and timeless. Cell *93,* 791-804.

Allemand, R., and David, J.R. (1984). Genetic analysis of the circadian oviposition rhythm in Drosophila melanogaster: effects of drift in laboratory strains. Behav. Genet. *14,* 31-43.

Anwyl, R. (1999). Metabotropic glutamate receptors: electrophysiological properties and role in plasticity. Brain Res. Brain Res. Rev. *29,* 83-120.

Arquier, N., Bourouis, M., Colombani, J., and Leopold, P. (2005). Drosophila Lk6 kinase controls phosphorylation of eukaryotic translation initiation factor 4E and promotes normal growth and development. Curr. Biol. *15,* 19-23.

Ashmore, L.J., Sathyanarayanan, S., Silvestre, D.W., Emerson, M.M., Schotland, P., and Sehgal, A. (2003). Novel insights into the regulation of the timeless protein. J. Neurosci. *23,* 7810-7819.

Babcock, M., Macleod, G.T., Leither, J., and Pallanck, L. (2004). Genetic analysis of soluble N-ethylmaleimide-sensitive factor attachment protein function in Drosophila reveals positive and negative secretory roles. J. Neurosci. *24,* 3964-3973.

Bargiello, T.A., Jackson, F.R., and Young, M.W. (1984). Restoration of circadian behavioural rhythms by gene transfer in Drosophila. Nature *312,* 752-754.

Baylies, M.K., Bargiello, T.A., Jackson, F.R., and Young, M.W. (1987). Changes in abundance or structure of the per gene product can alter periodicity of the Drosophila clock. Nature *326,* 390-392.

Bellen, H.J., Levis, R.W., Liao, G., He, Y., Carlson, J.W., Tsang, G., Evans-Holm, M., Hiesinger, P.R., Schulze, K.L., Rubin, G.M., Hoskins, R.A., and Spradling, A.C. (2004). The BDGP gene disruption project: single transposon insertions associated with 40% of Drosophila genes. Genetics *167,* 761-781.

Bier, E., Vaessin, H., Shepherd, S., Lee, K., McCall, K., Barbel, S., Ackerman, L., Carretto, R., Uemura, T., and Grell, E. (1989). Searching for pattern and mutation in the Drosophila genome with a P-lacZ vector. Genes Dev. *3,* 1273-1287.

Blau, J., and Young, M.W. (1999). Cycling vrille expression is required for a functional Drosophila clock. Cell *99,* 661-671.

Bogdanik, L., Mohrmann, R., Ramaekers, A., Bockaert, J., Grau, Y., Broadie, K., and Parmentier, M.L. (2004). The Drosophila metabotropic glutamate receptor DmGluRA regulates activity-dependent synaptic facilitation and fine synaptic morphology. J. Neurosci. *24,* 9105-9116.

Boulianne, G.L., and Trimble, W.S. (1995). Identification of a second homolog of N-ethylmaleimide-sensitive fusion protein that is expressed in the nervous system and secretory tissues of Drosophila. Proc. Natl. Acad. Sci. U. S. A. *92,* 7095-7099.

Brand, A.H., and Perrimon, N. (1993). Targeted gene expression as a means of altering cell fates and generating dominant phenotypes. Development *118,* 401-415.

Brehm, A., Langst, G., Kehle, J., Clapier, C.R., Imhof, A., Eberharter, A., Muller, J., and Becker, P.B. (2000). dMi-2 and ISWI chromatin remodelling factors have distinct nucleosome binding and mobilization properties. EMBO J. *19,* 4332-4341.

Broadie, K., Rushton, E., Skoulakis, E.M., and Davis, R.L. (1997). Leonardo, a Drosophila 14-3-3 protein involved in learning, regulates presynaptic function. Neuron *19,* 391-402.

Ceriani, M.F., Darlington, T.K., Staknis, D., Mas, P., Petti, A.A., Weitz, C.J., and Kay, S.A. (1999). Light-dependent sequestration of TIMELESS by CRYPTOCHROME. Science *285,* 553-556.

Ceriani, M.F., Hogenesch, J.B., Yanovsky, M., Panda, S., Straume, M., and Kay, S.A. (2002). Genome-wide expression analysis in Drosophila reveals genes controlling circadian behavior. J. Neurosci. *22,* 9305-9319.

Chang, D.C., and Reppert, S.M. (2003). A novel C-terminal domain of drosophila PERIOD inhibits dCLOCK:CYCLE-mediated transcription. Curr. Biol. *13,* 758-762.

Cheng, Y., and Hardin, P.E. (1998). Drosophila photoreceptors contain an autonomous circadian oscillator that can function without period mRNA cycling. J. Neurosci. *18,* 741-750.

Claridge-Chang, A., Wijnen, H., Naef, F., Boothroyd, C., Rajewsky, N., and Young, M.W. (2001). Circadian regulation of gene expression systems in the Drosophila head. Neuron *32,* 657-671.

Clary, D.O., and Rothman, J.E. (1990). Purification of three related peripheral membrane proteins needed for vesicular transport. J. Biol. Chem. *265,* 10109-10117.

Collins, B.H., Rosato, E., and Kyriacou, C.P. (2004). Seasonal behavior in Drosophila melanogaster requires the photoreceptors, the circadian clock, and phospholipase C. Proc. Natl. Acad. Sci. U. S. A. *101,* 1945-1950.

Colot, H.V., Hall, J.C., and Rosbash, M. (1988). Interspecific comparison of the period gene of Drosophila reveals large blocks of non-conserved coding DNA. EMBO J. *7,* 3929-3937.

Curtin, K.D., Huang, Z.J., and Rosbash, M. (1995). Temporally regulated nuclear entry of the Drosophila period protein contributes to the circadian clock. Neuron *14,* 365-372.

Cyran, S.A., Buchsbaum, A.M., Reddy, K.L., Lin, M.C., Glossop, N.R., Hardin, P.E., Young, M.W., Storti, R.V., and Blau, J. (2003). vrille, Pdp1, and dClock form a second feedback loop in the Drosophila circadian clock. Cell *112,* 329-341.

Darlington, T.K., Wager-Smith, K., Ceriani, M.F., Staknis, D., Gekakis, N., Steeves, T.D., Weitz, C.J., Takahashi, J.S., and Kay, S.A. (1998). Closing the circadian loop: CLOCK-induced transcription of its own inhibitors per and tim. Science *280,* 1599-1603.

de Boer, E., Rodriguez, P., Bonte, E., Krijgsveld, J., Katsantoni, E., Heck, A., Grosveld, F., and Strouboulis, J. (2003). Efficient biotinylation and single-step purification of tagged transcription factors in mammalian cells and transgenic mice. Proc. Natl. Acad. Sci. U. S. A. *100,* 7480-7485.

Deery, M.J., Maywood, E.S., Chesham, J.E., Sladek, M., Karp, N.A., Green, E.W., Charles, P.D., Reddy, A.B., Kyriacou, C.P., Lilley, K.S., and Hastings, M.H. (2009). Proteomic analysis reveals the role of synaptic vesicle cycling in sustaining the suprachiasmatic circadian clock. Curr. Biol. *19,* 2031-2036.

Dietzl, G., Chen, D., Schnorrer, F., Su, K.C., Barinova, Y., Fellner, M., Gasser, B., Kinsey, K., Oppel, S., Scheiblauer, S., *et al.* (2007). A genome-wide transgenic RNAi library for conditional gene inactivation in Drosophila. Nature *448,* 151-156.

Ding, J.M., Buchanan, G.F., Tischkau, S.A., Chen, D., Kuriashkina, L., Faiman, L.E., Alster, J.M., McPherson, P.S., Campbell, K.P., and Gillette, M.U. (1998). A neuronal ryanodine receptor mediates light-induced phase delays of the circadian clock. Nature *394,* 381-384.

Dingledine, R., Borges, K., Bowie, D., and Traynelis, S.F. (1999). The glutamate receptor ion channels. Pharmacol. Rev. *51,* 7-61.

Dubruille, R., Murad, A., Rosbash, M., and Emery, P. (2009). A constant light-genetic screen identifies KISMET as a regulator of circadian photoresponses. PLoS Genet. *5,* e1000787.

Duffy, J.B. (2002). GAL4 system in Drosophila: a fly geneticist's Swiss army knife. Genesis *34,* 1-15.

Dunlap, J.C. (1999). Molecular bases for circadian clocks. Cell *96*, 271-290.

Ebling, F.J. (1996). The role of glutamate in the photic regulation of the suprachiasmatic nucleus. Prog. Neurobiol. *50*, 109-132.

Emery, P., So, W.V., Kaneko, M., Hall, J.C., and Rosbash, M. (1998). CRY, a Drosophila clock and light-regulated cryptochrome, is a major contributor to circadian rhythm resetting and photosensitivity. Cell *95*, 669-679.

Emery, P., Stanewsky, R., Hall, J.C., and Rosbash, M. (2000a). A unique circadian-rhythm photoreceptor. Nature *404*, 456-457.

Emery, P., Stanewsky, R., Helfrich-Forster, C., Emery-Le, M., Hall, J.C., and Rosbash, M. (2000b). Drosophila CRY is a deep brain circadian photoreceptor. Neuron *26*, 493-504.

Esser, L., Wang, C.R., Hosaka, M., Smagula, C.S., Sudhof, T.C., and Deisenhofer, J. (1998). Synapsin I is structurally similar to ATP-utilizing enzymes. EMBO J. *17*, 977-984.

Featherstone, D.E., Rushton, E., and Broadie, K. (2002). Developmental regulation of glutamate receptor field size by nonvesicular glutamate release. Nat. Neurosci. *5*, 141-146.

Freeman, M.R., and Doherty, J. (2006). Glial cell biology in Drosophila and vertebrates. Trends Neurosci. *29*, 82-90.

Gekakis, N., Saez, L., Delahaye-Brown, A.M., Myers, M.P., Sehgal, A., Young, M.W., and Weitz, C.J. (1995). Isolation of timeless by PER protein interaction: defective interaction between timeless protein and long-period mutant PERL. Science *270*, 811-815.

Giebultowicz, J.M., Stanewsky, R., Hall, J.C., and Hege, D.M. (2000). Transplanted Drosophila excretory tubules maintain circadian clock cycling out of phase with the host. Curr. Biol. *10*, 107-110.

Glaser, F.T., and Stanewsky, R. (2005). Temperature synchronization of the Drosophila circadian clock. Curr. Biol. *15*, 1352-1363.

Glossop, N.R., and Hardin, P.E. (2002). Central and peripheral circadian oscillator mechanisms in flies and mammals. J. Cell. Sci. *115*, 3369-3377.

Glossop, N.R., Lyons, L.C., and Hardin, P.E. (1999). Interlocked feedback loops within the Drosophila circadian oscillator. Science *286*, 766-768.

Godenschwege, T.A., Reisch, D., Diegelmann, S., Eberle, K., Funk, N., Heisenberg, M., Hoppe, V., Hoppe, J., Klagges, B.R., Martin, J.R., *et al.* (2004). Flies lacking all synapsins are unexpectedly healthy but are impaired in complex behaviour. Eur. J. Neurosci. *20*, 611-622.

Golby, J.A., Tolar, L.A., and Pallanck, L. (2001). Partitioning of N-ethylmaleimide-sensitive fusion (NSF) protein function in Drosophila melanogaster: dNSF1 is required in the nervous system, and dNSF2 is required in mesoderm. Genetics *158,* 265-278.

Greengard, P., Valtorta, F., Czernik, A.J., and Benfenati, F. (1993). Synaptic vesicle phosphoproteins and regulation of synaptic function. Science *259,* 780-785.

Grima, B., Chelot, E., Xia, R., and Rouyer, F. (2004). Morning and evening peaks of activity rely on different clock neurons of the Drosophila brain. Nature *431,* 869-873.

Grima, B., Lamouroux, A., Chelot, E., Papin, C., Limbourg-Bouchon, B., and Rouyer, F. (2002). The F-box protein slimb controls the levels of clock proteins period and timeless. Nature *420,* 178-182.

Hacker, U., Nystedt, S., Barmchi, M.P., Horn, C., and Wimmer, E.A. (2003). piggyBac-based insertional mutagenesis in the presence of stably integrated P elements in Drosophila. Proc. Natl. Acad. Sci. U. S. A. *100,* 7720-7725.

Hall, J.C. (2003). Genetics and molecular biology of rhythms in Drosophila and other insects. Adv. Genet. *48,* 1-280.

Hamasaka, Y., Rieger, D., Parmentier, M.L., Grau, Y., Helfrich-Forster, C., and Nassel, D.R. (2007). Glutamate and its metabotropic receptor in Drosophila clock neuron circuits. J. Comp. Neurol. *505,* 32-45.

Hamasaka, Y., Wegener, C., and Nassel, D.R. (2005). GABA modulates Drosophila circadian clock neurons via GABAB receptors and decreases in calcium. J. Neurobiol. *65,* 225-240.

Hamblen, M.J., White, N.E., Emery, P.T., Kaiser, K., and Hall, J.C. (1998). Molecular and behavioral analysis of four period mutants in Drosophila melanogaster encompassing extreme short, novel long, and unorthodox arrhythmic types. Genetics *149,* 165-178.

Hardie, R.C. (2001). Phototransduction in Drosophila melanogaster. J. Exp. Biol. *204,* 3403-3409.

Hardie, R.C., and Raghu, P. (2001). Visual transduction in Drosophila. Nature *413,* 186-193.

Hardin, P.E. (2005). The circadian timekeeping system of Drosophila. Curr. Biol. *15,* R714-22.

Hardin, P.E. (1994). Analysis of period mRNA cycling in Drosophila head and body tissues indicates that body oscillators behave differently from head oscillators. Mol. Cell. Biol. *14,* 7211-7218.

Hardin, P.E., Hall, J.C., and Rosbash, M. (1990). Feedback of the Drosophila period gene product on circadian cycling of its messenger RNA levels. Nature *343,* 536-540.

Harmar, A.J., Marston, H.M., Shen, S., Spratt, C., West, K.M., Sheward, W.J., Morrison, C.F., Dorin, J.R., Piggins, H.D., Reubi, J.C., *et al.* (2002). The VPAC(2) receptor is essential for circadian function in the mouse suprachiasmatic nuclei. Cell *109*, 497-508.

Hartman, J.J., Mahr, J., McNally, K., Okawa, K., Iwamatsu, A., Thomas, S., Cheesman, S., Heuser, J., Vale, R.D., and McNally, F.J. (1998). Katanin, a microtubule-severing protein, is a novel AAA ATPase that targets to the centrosome using a WD40-containing subunit. Cell *93*, 277-287.

Hege, D.M., Stanewsky, R., Hall, J.C., and Giebultowicz, J.M. (1997). Rhythmic expression of a PER-reporter in the Malpighian tubules of decapitated Drosophila: evidence for a brain-independent circadian clock. J. Biol. Rhythms *12*, 300-308.

Helfrich-Forster, C. (2005). Techniques that revealed the network of the circadian clock of Drosophila. Methods Enzymol. *393*, 439-451.

Helfrich-Forster, C. (2004). The circadian clock in the brain: a structural and functional comparison between mammals and insects. J. Comp. Physiol. A. Neuroethol Sens. Neural Behav. Physiol. *190*, 601-613.

Helfrich-Forster, C. (2003). The neuroarchitecture of the circadian clock in the brain of Drosophila melanogaster. Microsc. Res. Tech. *62*, 94-102.

Helfrich-Forster, C. (1995). The period clock gene is expressed in central nervous system neurons which also produce a neuropeptide that reveals the projections of circadian pacemaker cells within the brain of Drosophila melanogaster. Proc. Natl. Acad. Sci. U. S. A. *92*, 612-616.

Helfrich-Forster, C., Edwards, T., Yasuyama, K., Wisotzki, B., Schneuwly, S., Stanewsky, R., Meinertzhagen, I.A., and Hofbauer, A. (2002). The extraretinal eyelet of Drosophila: development, ultrastructure, and putative circadian function. J. Neurosci. *22*, 9255-9266.

Helfrich-Forster, C., Tauber, M., Park, J.H., Muhlig-Versen, M., Schneuwly, S., and Hofbauer, A. (2000). Ectopic expression of the neuropeptide pigment-dispersing factor alters behavioral rhythms in Drosophila melanogaster. J. Neurosci. *20*, 3339-3353.

Helfrich-Forster, C., Winter, C., Hofbauer, A., Hall, J.C., and Stanewsky, R. (2001). The circadian clock of fruit flies is blind after elimination of all known photoreceptors. Neuron *30*, 249-261.

Helfrich-Forster, C., Yoshii, T., Wulbeck, C., Grieshaber, E., Rieger, D., Bachleitner, W., Cusamano, P., and Rouyer, F. (2007). The lateral and dorsal neurons of Drosophila melanogaster: new insights about their morphology and function. Cold Spring Harb. Symp. Quant. Biol. *72*, 517-525.

Hilfiker, S., Pieribone, V.A., Czernik, A.J., Kao, H.T., Augustine, G.J., and Greengard, P. (1999). Synapsins as regulators of neurotransmitter release. Philos. Trans. R. Soc. Lond. B. Biol. Sci. *354*, 269-279.

Horn, C., Offen, N., Nystedt, S., Hacker, U., and Wimmer, E.A. (2003). piggyBac-based insertional mutagenesis and enhancer detection as a tool for functional insect genomics. Genetics *163*, 647-661.

Hosaka, M., and Sudhof, T.C. (1998). Synapsins I and II are ATP-binding proteins with differential Ca2+ regulation. J. Biol. Chem. *273*, 1425-1429.

Houalla, T., Shi, L., van Meyel, D.J., and Rao, Y. (2010). Rab-mediated vesicular transport is required for neuronal positioning in the developing Drosophila visual system. Mol. Brain *3*, 19.

Houl, J.H., Yu, W., Dudek, S.M., and Hardin, P.E. (2006). Drosophila CLOCK is constitutively expressed in circadian oscillator and non-oscillator cells. J. Biol. Rhythms *21*, 93-103.

Huang, Y., Genova, G., Roberts, M., and Jackson, F.R. (2007). The LARK RNA-binding protein selectively regulates the circadian eclosion rhythm by controlling E74 protein expression. PLoS One *2*, e1107.

Huang, Z.J., Edery, I., and Rosbash, M. (1993). PAS is a dimerization domain common to Drosophila period and several transcription factors. Nature *364*, 259-262.

Hunter-Ensor, M., Ousley, A., and Sehgal, A. (1996). Regulation of the Drosophila protein timeless suggests a mechanism for resetting the circadian clock by light. Cell *84*, 677-685.

Hwa, J.J., Zhu, A.J., Hiller, M.A., Kon, C.Y., Fuller, M.T., and Santel, A. (2004). Germ-line specific variants of components of the mitochondrial outer membrane import machinery in Drosophila. FEBS Lett. *572*, 141-146.

Hyun, S., Lee, Y., Hong, S.T., Bang, S., Paik, D., Kang, J., Shin, J., Lee, J., Jeon, K., Hwang, S., Bae, E., and Kim, J. (2005). Drosophila GPCR Han is a receptor for the circadian clock neuropeptide PDF. Neuron *48*, 267-278.

Ishikawa, T., Matsumoto, A., Kato, T.,Jr, Togashi, S., Ryo, H., Ikenaga, M., Todo, T., Ueda, R., and Tanimura, T. (1999). DCRY is a Drosophila photoreceptor protein implicated in light entrainment of circadian rhythm. Genes Cells *4*, 57-65.

Ito, C., Goto, S.G., Shiga, S., Tomioka, K., and Numata, H. (2008). Peripheral circadian clock for the cuticle deposition rhythm in Drosophila melanogaster. Proc. Natl. Acad. Sci. U. S. A. *105*, 8446-8451.

Jahn, R., and Sudhof, T.C. (1999). Membrane fusion and exocytosis. Annu. Rev. Biochem. *68*, 863-911.

Kadener, S., Stoleru, D., McDonald, M., Nawathean, P., and Rosbash, M. (2007). Clockwork Orange is a transcriptional repressor and a new Drosophila circadian pacemaker component. Genes Dev. *21,* 1675-1686.

Kao, H.T., Porton, B., Czernik, A.J., Feng, J., Yiu, G., Haring, M., Benfenati, F., and Greengard, P. (1998). A third member of the synapsin gene family. Proc. Natl. Acad. Sci. U. S. A. *95,* 4667-4672.

Keegan, K.P., Pradhan, S., Wang, J.P., and Allada, R. (2007). Meta-analysis of Drosophila circadian microarray studies identifies a novel set of rhythmically expressed genes. PLoS Comput. Biol. *3,* e208.

Kelley, M.R., Kidd, S., Berg, R.L., and Young, M.W. (1987). Restriction of P-element insertions at the Notch locus of Drosophila melanogaster. Mol. Cell. Biol. *7,* 1545-1548.

Keshishian, H., Broadie, K., Chiba, A., and Bate, M. (1996). The drosophila neuromuscular junction: a model system for studying synaptic development and function. Annu. Rev. Neurosci. *19,* 545-575.

Khaustova, N.D., Totskii, V.M., and Strel'tsova, N.A. (1992). Gene-enzyme system of alcohol dehydrogenase and adaptation of Drosophila to increased temperature. Genetika *28,* 73-80.

Khodosh, R., Augsburger, A., Schwarz, T.L., and Garrity, P.A. (2006). Bchs, a BEACH domain protein, antagonizes Rab11 in synapse morphogenesis and other developmental events. Development *133,* 4655-4665.

Kilman, V.L., Zhang, L., Meissner, R.A., Burg, E., and Allada, R. (2009). Perturbing dynamin reveals potent effects on the Drosophila circadian clock. PLoS One *4,* e5235.

Kim, E.Y., and Edery, I. (2006). Balance between DBT/CKIepsilon kinase and protein phosphatase activities regulate phosphorylation and stability of Drosophila CLOCK protein. Proc. Natl. Acad. Sci. U. S. A. *103,* 6178-6183.

Klagges, B.R., Heimbeck, G., Godenschwege, T.A., Hofbauer, A., Pflugfelder, G.O., Reifegerste, R., Reisch, D., Schaupp, M., Buchner, S., and Buchner, E. (1996). Invertebrate synapsins: a single gene codes for several isoforms in Drosophila. J. Neurosci. *16,* 3154-3165.

Klenchin, V.A., and Martin, T.F. (2000). Priming in exocytosis: attaining fusion-competence after vesicle docking. Biochimie *82,* 399-407.

Kloss, B., Price, J.L., Saez, L., Blau, J., Rothenfluh, A., Wesley, C.S., and Young, M.W. (1998). The Drosophila clock gene double-time encodes a protein closely related to human casein kinase Iepsilon. Cell *94,* 97-107.

Ko, H.W., Jiang, J., and Edery, I. (2002). Role for Slimb in the degradation of Drosophila Period protein phosphorylated by Doubletime. Nature *420,* 673-678.

Koh, K., Zheng, X., and Sehgal, A. (2006). JETLAG resets the Drosophila circadian clock by promoting light-induced degradation of TIMELESS. Science *312,* 1809-1812.

Konopka, R.J., and Benzer, S. (1971). Clock mutants of Drosophila melanogaster. Proc. Natl. Acad. Sci. U. S. A. *68,* 2112-2116.

Konopka, R.J., Pittendrigh, C., and Orr, D. (1989). Reciprocal behaviour associated with altered homeostasis and photosensitivity of Drosophila clock mutants. J. Neurogenet. *6,* 1-10.

Krishnan, B., Dryer, S.E., and Hardin, P.E. (1999). Circadian rhythms in olfactory responses of Drosophila melanogaster. Nature *400,* 375-378.

Kula, E., Levitan, E.S., Pyza, E., and Rosbash, M. (2006). PDF cycling in the dorsal protocerebrum of the Drosophila brain is not necessary for circadian clock function. J. Biol. Rhythms *21,* 104-117.

Kuppers, B., Sanchez-Soriano, N., Letzkus, J., Technau, G.M., and Prokop, A. (2003). In developing Drosophila neurones the production of gamma-amino butyric acid is tightly regulated downstream of glutamate decarboxylase translation and can be influenced by calcium. J. Neurochem. *84,* 939-951.

Kuraishi, T., Nakagawa, Y., Nagaosa, K., Hashimoto, Y., Ishimoto, T., Moki, T., Fujita, Y., Nakayama, H., Dohmae, N., Shiratsuchi, A., *et al.* (2009). Pretaporter, a Drosophila protein serving as a ligand for Draper in the phagocytosis of apoptotic cells. EMBO J. *28,* 3868-3878.

Kyriacou, C.P., and Rosato, E. (2000). Squaring up the E-box. J. Biol. Rhythms *15,* 483-490.

Lear, B.C., Merrill, C.E., Lin, J.M., Schroeder, A., Zhang, L., and Allada, R. (2005). A G protein-coupled receptor, groom-of-PDF, is required for PDF neuron action in circadian behavior. Neuron *48,* 221-227.

Lee, C., Bae, K., and Edery, I. (1999). PER and TIM inhibit the DNA binding activity of a Drosophila CLOCK-CYC/dBMAL1 heterodimer without disrupting formation of the heterodimer: a basis for circadian transcription. Mol. Cell. Biol. *19,* 5316-5325.

Lee, C., Parikh, V., Itsukaichi, T., Bae, K., and Edery, I. (1996). Resetting the Drosophila clock by photic regulation of PER and a PER-TIM complex. Science *271,* 1740-1744.

Lee, Y.S., Nakahara, K., Pham, J.W., Kim, K., He, Z., Sontheimer, E.J., and Carthew, R.W. (2004). Distinct roles for Drosophila Dicer-1 and Dicer-2 in the siRNA/miRNA silencing pathways. Cell *117,* 69-81.

Lim, C., Chung, B.Y., Pitman, J.L., McGill, J.J., Pradhan, S., Lee, J., Keegan, K.P., Choe, J., and Allada, R. (2007). Clockwork orange encodes a transcriptional repressor important for circadian-clock amplitude in Drosophila. Curr. Biol. *17,* 1082-1089.

Lin, F.J., Song, W., Meyer-Bernstein, E., Naidoo, N., and Sehgal, A. (2001). Photic signaling by cryptochrome in the Drosophila circadian system. Mol. Cell. Biol. *21*, 7287-7294.

Lin, J.M., Kilman, V.L., Keegan, K., Paddock, B., Emery-Le, M., Rosbash, M., and Allada, R. (2002). A role for casein kinase 2alpha in the Drosophila circadian clock. Nature *420*, 816-820.

Lin, R.C., and Scheller, R.H. (2000). Mechanisms of synaptic vesicle exocytosis. Annu. Rev. Cell Dev. Biol. *16*, 19-49.

Lin, S.C., Lin, M.H., Horvath, P., Reddy, K.L., and Storti, R.V. (1997). PDP1, a novel Drosophila PAR domain bZIP transcription factor expressed in developing mesoderm, endoderm and ectoderm, is a transcriptional regulator of somatic muscle genes. Development *124*, 4685-4696.

Lin, Y., Han, M., Shimada, B., Wang, L., Gibler, T.M., Amarakone, A., Awad, T.A., Stormo, G.D., Van Gelder, R.N., and Taghert, P.H. (2002). Influence of the period-dependent circadian clock on diurnal, circadian, and aperiodic gene expression in Drosophila melanogaster. Proc. Natl. Acad. Sci. U. S. A. *99*, 9562-9567.

Lin, Y., Stormo, G.D., and Taghert, P.H. (2004). The neuropeptide pigment-dispersing factor coordinates pacemaker interactions in the Drosophila circadian system. J. Neurosci. *24*, 7951-7957.

Littleton, J.T., Barnard, R.J., Titus, S.A., Slind, J., Chapman, E.R., and Ganetzky, B. (2001). SNARE-complex disassembly by NSF follows synaptic-vesicle fusion. Proc. Natl. Acad. Sci. U. S. A. *98*, 12233-12238.

Los, G.V., Encell, L.P., McDougall, M.G., Hartzell, D.D., Karassina, N., Zimprich, C., Wood, M.G., Learish, R., Ohana, R.F., Urh, M., Simpson, D., Mendez, J., Zimmerman, K., Otto, P., Vidugiris, G., Zhu, J., Darzins, A., Klaubert, D.H., Bulleit, R.F., and Wood, K.V. (2008). HaloTag: a novel protein labeling technology for cell imaging and protein analysis. ACS Chem Biol. *20*, 373-82.

Lowrey, P.L., Shimomura, K., Antoch, M.P., Yamazaki, S., Zemenides, P.D., Ralph, M.R., Menaker, M., and Takahashi, J.S. (2000). Positional syntenic cloning and functional characterization of the mammalian circadian mutation tau. Science *288*, 483-492.

Lukacsovich, T., Asztalos, Z., Awano, W., Baba, K., Kondo, S., Niwa, S., and Yamamoto, D. (2001). Dual-tagging gene trap of novel genes in Drosophila melanogaster. Genetics *157*, 727-742.

Mahoney, M.B., Parks, A.L., Ruddy, D.A., Tiong, S.Y., Esengil, H., Phan, A.C., Philandrinos, P., Winter, C.G., Chatterjee, R., Huppert, K., *et al.* (2006). Presenilin-based genetic screens in Drosophila melanogaster identify novel notch pathway modifiers. Genetics *172*, 2309-2324.

Majercak, J., Chen, W.F., and Edery, I. (2004). Splicing of the period gene 3'-terminal intron is regulated by light, circadian clock factors, and phospholipase C. Mol. Cell. Biol. *24*, 3359-3372.

Majercak, J., Sidote, D., Hardin, P.E., and Edery, I. (1999). How a circadian clock adapts to seasonal decreases in temperature and day length. Neuron *24*, 219-230.

Marrus, S.B., Portman, S.L., Allen, M.J., Moffat, K.G., and DiAntonio, A. (2004). Differential localization of glutamate receptor subunits at the Drosophila neuromuscular junction. J. Neurosci. *24*, 1406-1415.

Martinek, S., Inonog, S., Manoukian, A.S., and Young, M.W. (2001). A role for the segment polarity gene shaggy/GSK-3 in the Drosophila circadian clock. Cell *105*, 769-779.

Matsumoto, A., Matsumoto, N., Harui, Y., Sakamoto, M., and Tomioka, K. (1998). Light and temperature cooperate to regulate the circadian locomotor rhythm of wild type and period mutants of Drosophila melanogaster. J. Insect Physiol. *44*, 587-596.

Matsumoto, A., Ukai-Tadenuma, M., Yamada, R.G., Houl, J., Uno, K.D., Kasukawa, T., Dauwalder, B., Itoh, T.Q., Takahashi, K., Ueda, R., *et al.* (2007). A functional genomics strategy reveals clockwork orange as a transcriptional regulator in the Drosophila circadian clock. Genes Dev. *21*, 1687-1700.

McDonald, M.J., and Rosbash, M. (2001). Microarray analysis and organization of circadian gene expression in Drosophila. Cell *107*, 567-578.

McNeil, G.P., Zhang, X., Genova, G., and Jackson, F.R. (1998). A molecular rhythm mediating circadian clock output in Drosophila. Neuron *20*, 297-303.

Meijer, J.H., van der Zee, E.A., and Dietz, M. (1988). Glutamate phase shifts circadian activity rhythms in hamsters. Neurosci. Lett. *86*, 177-183.

Mertens, I., Vandingenen, A., Johnson, E.C., Shafer, O.T., Li, W., Trigg, J.S., De Loof, A., Schoofs, L., and Taghert, P.H. (2005). PDF receptor signaling in Drosophila contributes to both circadian and geotactic behaviors. Neuron *48*, 213-219.

Metaxakis, A., Oehler, S., Klinakis, A., and Savakis, C. (2005). Minos as a genetic and genomic tool in Drosophila melanogaster. Genetics *171*, 571-581.

Meyer, P., Saez, L., and Young, M.W. (2006). PER-TIM interactions in living Drosophila cells: an interval timer for the circadian clock. Science *311*, 226-229.

Moore, R.Y. (1983).Organization and function of a central nervous system circadian oscillator: the suprachiasmatic hypothalamic nucleus. Fed.Proc. *42*, 2783-2789.

Murad, A., Emery-Le, M., and Emery, P. (2007). A subset of dorsal neurons modulates circadian behavior and light responses in Drosophila. Neuron *53*, 689-701.

Myers, M.P., Wager-Smith, K., Rothenfluh-Hilfiker, A., and Young, M.W. (1996). Light-induced degradation of TIMELESS and entrainment of the Drosophila circadian clock. Science *271,* 1736-1740.

Myers, M.P., Wager-Smith, K., Wesley, C.S., Young, M.W., and Sehgal, A. (1995). Positional cloning and sequence analysis of the Drosophila clock gene, timeless. Science *270,* 805-808.

Newby, L.M., and Jackson, F.R. (1993). A new biological rhythm mutant of Drosophila melanogaster that identifies a gene with an essential embryonic function. Genetics *135,* 1077-1090.

Newby, L.M., and Jackson, F.R. (1991). Drosophila ebony mutants have altered circadian activity rhythms but normal eclosion rhythms. J. Neurogenet. *7,* 85-101.

Newsome, T.P., Asling, B., and Dickson, B.J. (2000). Analysis of Drosophila photoreceptor axon guidance in eye-specific mosaics. Development *127,* 851-860.

Nitabach, M.N. (2005). Circadian rhythms: clock coordination. Nature *438,* 173-175.

Ordway, R.W., Pallanck, L., and Ganetzky, B. (1994). Neurally expressed Drosophila genes encoding homologs of the NSF and SNAP secretory proteins. Proc. Natl. Acad. Sci. U. S. A. *91,* 5715-5719.

Pak, W.L., and Leung, H.T. (2003). Genetic approaches to visual transduction in Drosophila melanogaster. Receptors Channels *9,* 149-167.

Parfitt, K., Reist, N., Li, J., Burgess, R., Deitcher, D., DiAntonio, A., and Schwarz, T.L. (1995). Drosophila genetics and the functions of synaptic proteins. Cold Spring Harb. Symp. Quant. Biol. *60,* 371-377.

Park, J.H., Helfrich-Forster, C., Lee, G., Liu, L., Rosbash, M., and Hall, J.C. (2000). Differential regulation of circadian pacemaker output by separate clock genes in Drosophila. Proc. Natl. Acad. Sci. U. S. A. *97,* 3608-3613.

Peng, Y., Stoleru, D., Levine, J.D., Hall, J.C., and Rosbash, M. (2003). Drosophila free-running rhythms require intercellular communication. PLoS Biol. *1,* E13.

Peschel, N., Chen, K.F., Szabo, G., and Stanewsky, R. (2009). Light-dependent interactions between the Drosophila circadian clock factors cryptochrome, jetlag, and timeless. Curr. Biol. *19,* 241-247.

Peschel, N., Veleri, S., and Stanewsky, R. (2006). Veela defines a molecular link between Cryptochrome and Timeless in the light-input pathway to Drosophila's circadian clock. Proc. Natl. Acad. Sci. U. S. A. *103,* 17313-17318.

Pittendrigh, C.S. (1967). Circadian systems. I. The driving oscillation and its assay in Drosophila pseudoobscura. Proc. Natl. Acad. Sci. U. S. A. *58,* 1762-1767.

Pittendrigh, C.S. (1954). On Temperature Independence in the Clock System Controlling Emergence Time in Drosophila. Proc. Natl. Acad. Sci. U. S. A. *40*, 1018-1029.

Plautz, J.D., Kaneko, M., Hall, J.C., and Kay, S.A. (1997). Independent photoreceptive circadian clocks throughout Drosophila. Science *278*, 1632-1635.

Preitner, N., Damiola, F., Lopez-Molina, L., Zakany, J., Duboule, D., Albrecht, U., and Schibler, U. (2002). The orphan nuclear receptor REV-ERBalpha controls circadian transcription within the positive limb of the mammalian circadian oscillator. Cell *110*, 251-260.

Price, J.L., Blau, J., Rothenfluh, A., Abodeely, M., Kloss, B., and Young, M.W. (1998). double-time is a novel Drosophila clock gene that regulates PERIOD protein accumulation. Cell *94*, 83-95.

Prokopenko, S.N., Brumby, A., O'Keefe, L., Prior, L., He, Y., Saint, R., and Bellen, H.J. (1999). A putative exchange factor for Rho1 GTPase is required for initiation of cytokinesis in Drosophila. Genes Dev. *13*, 2301-2314.

Qin, G., Schwarz, T., Kittel, R.J., Schmid, A., Rasse, T.M., Kappei, D., Ponimaskin, E., Heckmann, M., and Sigrist, S.J. (2005). Four different subunits are essential for expressing the synaptic glutamate receptor at neuromuscular junctions of Drosophila. J. Neurosci. *25*, 3209-3218.

Ralph, M.R., Foster, R.G., Davis, F.C., and Menaker, M. (1990). Transplanted suprachiasmatic nucleus determines circadian period. Science *247*, 975-978.

Reddy, A.B., Karp, N.A., Maywood, E.S., Sage, E.A., Deery, M., O'Neill, J.S., Wong, G.K., Chesham, J., Odell, M., Lilley, K.S., Kyriacou, C.P., and Hastings, M.H. (2006). Circadian orchestration of the hepatic proteome. Curr. Biol. *16*, 1107-1115.

Reddy, P., Zehring, W.A., Wheeler, D.A., Pirrotta, V., Hadfield, C., Hall, J.C., and Rosbash, M. (1984). Molecular analysis of the period locus in Drosophila melanogaster and identification of a transcript involved in biological rhythms. Cell *38*, 701-710.

Renn, S.C., Park, J.H., Rosbash, M., Hall, J.C., and Taghert, P.H. (1999). A pdf neuropeptide gene mutation and ablation of PDF neurons each cause severe abnormalities of behavioral circadian rhythms in Drosophila. Cell *99*, 791-802.

Reppert, S.M., and Weaver, D.R. (2002). Coordination of circadian timing in mammals. Nature *418*, 935-941.

Richier, B., Michard-Vanhee, C., Lamouroux, A., Papin, C., and Rouyer, F. (2008). The clockwork orange Drosophila protein functions as both an activator and a repressor of clock gene expression. J. Biol. Rhythms *23*, 103-116.

Robertson, H.M., Preston, C.R., Phillis, R.W., Johnson-Schlitz, D.M., Benz, W.K., and Engels, W.R. (1988). A stable genomic source of P element transposase in Drosophila melanogaster. Genetics *118,* 461-470.

Rorth, P., Szabo, K., Bailey, A., Laverty, T., Rehm, J., Rubin, G.M., Weigmann, K., Milan, M., Benes, V., Ansorge, W., and Cohen, S.M. (1998). Systematic gain-of-function genetics in Drosophila. Development *125,* 1049-1057.

Rosato, E., Tauber, E., and Kyriacou, C.P. (2006). Molecular genetics of the fruit-fly circadian clock. Eur. J. Hum. Genet. *14,* 729-738.

Roseman, R.R., Johnson, E.A., Rodesch, C.K., Bjerke, M., Nagoshi, R.N., and Geyer, P.K. (1995). A P element containing suppressor of hairy-wing binding regions has novel properties for mutagenesis in Drosophila melanogaster. Genetics *141,* 1061-1074.

Rothenfluh, A., Abodeely, M., and Young, M.W. (2000a). Short-period mutations of per affect a double-time-dependent step in the Drosophila circadian clock. Curr. Biol. *10,* 1399-1402.

Rothenfluh, A., Young, M.W., and Saez, L. (2000b). A TIMELESS-independent function for PERIOD proteins in the Drosophila clock. Neuron *26,* 505-514.

Rutila, J.E., Suri, V., Le, M., So, W.V., Rosbash, M., and Hall, J.C. (1998). CYCLE is a second bHLH-PAS clock protein essential for circadian rhythmicity and transcription of Drosophila period and timeless. Cell *93,* 805-814.

Sandrelli, F., Tauber, E., Pegoraro, M., Mazzotta, G., Cisotto, P., Landskron, J., Stanewsky, R., Piccin, A., Rosato, E., Zordan, M., Costa, R., and Kyriacou, C.P. (2007). A molecular basis for natural selection at the timeless locus in Drosophila melanogaster. Science *316,* 1898-1900.

Sarov-Blat, L., So, W.V., Liu, L., and Rosbash, M. (2000). The Drosophila takeout gene is a novel molecular link between circadian rhythms and feeding behavior. Cell *101,* 647-656.

Sathyanarayanan, S., Zheng, X., Xiao, R., and Sehgal, A. (2004). Posttranslational regulation of Drosophila PERIOD protein by protein phosphatase 2A. Cell *116,* 603-615.

Satoh, A.K., O'Tousa, J.E., Ozaki, K., and Ready, D.F. (2005). Rab11 mediates post-Golgi trafficking of rhodopsin to the photosensitive apical membrane of Drosophila photoreceptors. Development *132,* 1487-1497.

Sehgal, A., Price, J.L., Man, B., and Young, M.W. (1994). Loss of circadian behavioral rhythms and per RNA oscillations in the Drosophila mutant timeless. Science *263,* 1603-1606.

Shafer, O.T., Helfrich-Forster, C., Renn, S.C., and Taghert, P.H. (2006). Reevaluation of Drosophila melanogaster's neuronal circadian pacemakers reveals new neuronal classes. J. Comp. Neurol. *498,* 180-193.

Shafer, O.T., Kim, D.J., Dunbar-Yaffe, R., Nikolaev, V.O., Lohse, M.J., and Taghert, P.H. (2008). Widespread receptivity to neuropeptide PDF throughout the neuronal circadian clock network of Drosophila revealed by real-time cyclic AMP imaging. Neuron *58,* 223-237.

Shafer, O.T., Rosbash, M., and Truman, J.W. (2002). Sequential nuclear accumulation of the clock proteins period and timeless in the pacemaker neurons of Drosophila melanogaster. J. Neurosci. *22,* 5946-5954.

Sharma, V.K., and Chandrashekaran, M.K. (2005). Zeitgebers (time cues) for circadian clocks. Current Science *89,* 1136 – 1146.

Shirakawa, T., and Moore, R.Y. (1994). Glutamate shifts the phase of the circadian neuronal firing rhythm in the rat suprachiasmatic nucleus in vitro. Neurosci. Lett. *178,* 47-50.

Siwicki, K.K., Eastman, C., Petersen, G., Rosbash, M., and Hall, J.C. (1988). Antibodies to the period gene product of Drosophila reveal diverse tissue distribution and rhythmic changes in the visual system. Neuron *1,* 141-150.

Skoulakis, E.M., and Davis, R.L. (1996). Olfactory learning deficits in mutants for leonardo, a Drosophila gene encoding a 14-3-3 protein. Neuron *17,* 931-944.

Stanewsky, R., Kaneko, M., Emery, P., Beretta, B., Wager-Smith, K., Kay, S.A., Rosbash, M., and Hall, J.C. (1998). The cryb mutation identifies cryptochrome as a circadian photoreceptor in Drosophila. Cell *95,* 681-692.

Stoleru, D., Nawathean, P., Fernandez, M.P., Menet, J.S., Ceriani, M.F., and Rosbash, M. (2007). The Drosophila circadian network is a seasonal timer. Cell *129,* 207-219.

Stoleru, D., Peng, Y., Agosto, J., and Rosbash, M. (2004). Coupled oscillators control morning and evening locomotor behaviour of Drosophila. Nature *431,* 862-868.

Stoleru, D., Peng, Y., Nawathean, P., and Rosbash, M. (2005). A resetting signal between Drosophila pacemakers synchronizes morning and evening activity. Nature *438,* 238-242.

Su, T.T., Parry, D.H., Donahoe, B., Chien, C.T., O'Farrell, P.H., and Purdy, A. (2001). Cell cycle roles for two 14-3-3 proteins during Drosophila development. J. Cell. Sci. *114,* 3445-3454.

Sudhof, T.C. (1995). The synaptic vesicle cycle: a cascade of protein-protein interactions. Nature *375,* 645-653.

Sudhof, T.C., Czernik, A.J., Kao, H.T., Takei, K., Johnston, P.A., Horiuchi, A., Kanazir, S.D., Wagner, M.A., Perin, M.S., and De Camilli, P. (1989). Synapsins:

mosaics of shared and individual domains in a family of synaptic vesicle phosphoproteins. Science *245,* 1474-1480.

Taghert, P.H., Hewes, R.S., Park, J.H., O'Brien, M.A., Han, M., and Peck, M.E. (2001). Multiple amidated neuropeptides are required for normal circadian locomotor rhythms in Drosophila. J. Neurosci. *21,* 6673-6686.

Taghert, P.H., and Shafer, O.T. (2006). Mechanisms of clock output in the Drosophila circadian pacemaker system. J. Biol. Rhythms *21,* 445-457.

Tanoue, S., Krishnan, P., Krishnan, B., Dryer, S.E., and Hardin, P.E. (2004). Circadian clocks in antennal neurons are necessary and sufficient for olfaction rhythms in Drosophila. Curr. Biol. *14,* 638-649.

Tayler, T.D., and Garrity, P.A. (2003). Axon targeting in the Drosophila visual system. Curr. Opin. Neurobiol. *13,* 90-95.

Thibault, S.T., Singer, M.A., Miyazaki, W.Y., Milash, B., Dompe, N.A., Singh, C.M., Buchholz, R., Demsky, M., Fawcett, R., Francis-Lang, H.L., *et al.* (2004). A complementary transposon tool kit for Drosophila melanogaster using P and piggyBac. Nat. Genet. *36,* 283-287.

Todo, T. (1999). Functional diversity of the DNA photolyase/blue light receptor family. Mutat. Res. *434,* 89-97.

Toh, K.L., Jones, C.R., He, Y., Eide, E.J., Hinz, W.A., Virshup, D.M., Ptacek, L.J., and Fu, Y.H. (2001). An hPer2 phosphorylation site mutation in familial advanced sleep phase syndrome. Science *291,* 1040-1043.

Tseng, A.S., and Hariharan, I.K. (2002). An overexpression screen in Drosophila for genes that restrict growth or cell-cycle progression in the developing eye. Genetics *162,* 229-243.

Ueda, H.R., Chen, W., Adachi, A., Wakamatsu, H., Hayashi, S., Takasugi, T., Nagano, M., Nakahama, K., Suzuki, Y., Sugano, S., *et al.* (2002a). A transcription factor response element for gene expression during circadian night. Nature *418,* 534-539.

Ueda, H.R., Matsumoto, A., Kawamura, M., Iino, M., Tanimura, T., and Hashimoto, S. (2002b). Genome-wide transcriptional orchestration of circadian rhythms in Drosophila. J. Biol. Chem. *277,* 14048-14052.

Veleri, S., Brandes, C., Helfrich-Forster, C., Hall, J.C., and Stanewsky, R. (2003). A self-sustaining, light-entrainable circadian oscillator in the Drosophila brain. Curr. Biol. *13,* 1758-1767.

Voss, S., and Skerra, A. (1997). Mutagenesis of a flexible loop in streptavidin leads to higher affinity for the Strep-tag II peptide and improved performance in recombinant protein purification. Protein Eng. *10,* 975–982.

Wheeler, D.A., Hamblen-Coyle, M.J., Dushay, M.S., and Hall, J.C. (1993). Behavior in light-dark cycles of Drosophila mutants that are arrhythmic, blind, or both. J. Biol. Rhythms *8,* 67-94.

Wijnen, H., Naef, F., Boothroyd, C., Claridge-Chang, A., and Young, M.W. (2006). Control of daily transcript oscillations in Drosophila by light and the circadian clock. PLoS Genet. *2,* e39.

Williams, J.A., and Sehgal, A. (2001). Molecular components of the circadian system in Drosophila. Annu. Rev. Physiol. *63,* 729-755.

Yamazaki, S., Numano, R., Abe, M., Hida, A., Takahashi, R., Ueda, M., Block, G.D., Sakaki, Y., Menaker, M., and Tei, H. (2000). Resetting central and peripheral circadian oscillators in transgenic rats. Science *288,* 682-685.

Yoo, S.H., Yamazaki, S., Lowrey, P.L., Shimomura, K., Ko, C.H., Buhr, E.D., Siepka, S.M., Hong, H.K., Oh, W.J., Yoo, O.J., Menaker, M., and Takahashi, J.S. (2004). PERIOD2::LUCIFERASE real-time reporting of circadian dynamics reveals persistent circadian oscillations in mouse peripheral tissues. Proc. Natl. Acad. Sci. U. S. A. *101,* 5339-5346.

Young, M.W., and Kay, S.A. (2001). Time zones: a comparative genetics of circadian clocks. Nat. Rev. Genet. *2,* 702-715.

Yoshii, T., Todo, T., Wulbeck, C., Stanewsky, R., and Helfrich-Forster, C. (2008). Cryptochrome is present in the compound eyes and a subset of Drosophila's clock neurons. J. Comp. Neurol. *508,* 952-966.

Yu, Q., Jacquier, A.C., Citri, Y., Hamblen, M., Hall, J.C., and Rosbash, M. (1987). Molecular mapping of point mutations in the period gene that stop or speed up biological clocks in Drosophila melanogaster. Proc. Natl. Acad. Sci. U. S. A. *84,* 784-788.

Yu, W., Zheng, H., Houl, J.H., Dauwalder, B., and Hardin, P.E. (2006). PER-dependent rhythms in CLK phosphorylation and E-box binding regulate circadian transcription. Genes Dev. *20,* 723-733.

Zeng, H., Qian, Z., Myers, M.P., and Rosbash, M. (1996). A light-entrainment mechanism for the Drosophila circadian clock. Nature *380,* 129-135.

Zheng, X., and Sehgal, A. (2008). Probing the relative importance of molecular oscillations in the circadian clock. Genetics *178,* 1147-1155.